UNIVERSIDAD DE LAS PALMAS
DE GRAN CANARIA

Departamento de Física

Tesis Doctoral

ANALYSIS OF THE RAINFALL VARIABILITY IN THE SUBTROPICAL NORTH ATLANTIC REGION: BERMUDA, CANARY ISLANDS, MADEIRA AND AZORES

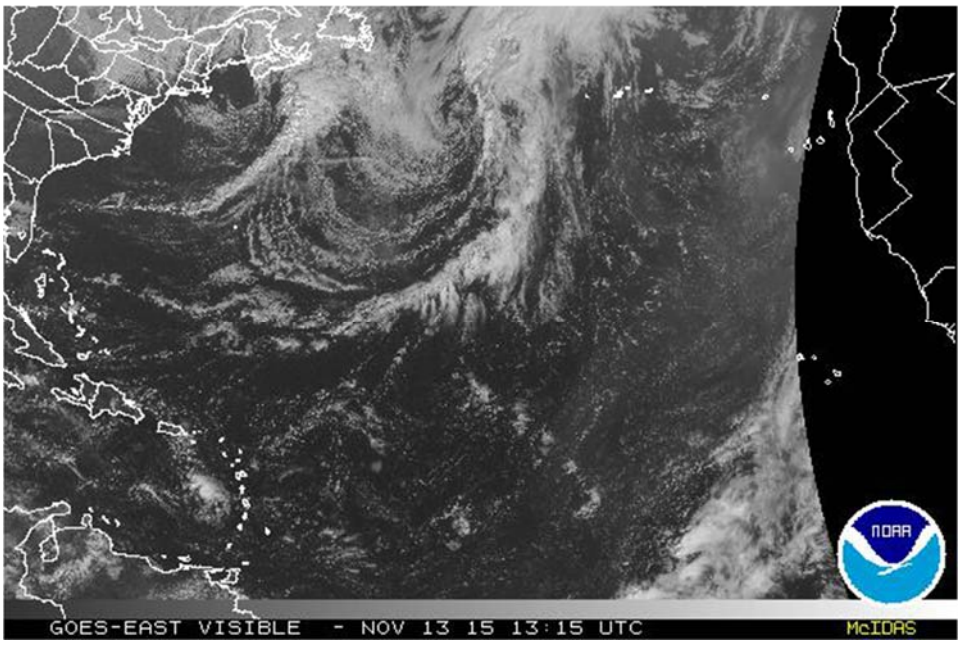

Irene Peñate de la Rosa

Las Palmas de Gran Canaria

Noviembre de 2015

Dª MARIA DE LOS ÁNGELES MARRERO DÍAZ, SECRETARIA DEL DEPARTAMENTO DE FÍSICA DE LA UNIVERSIDAD DE LAS PALMAS DE GRAN CANARIA,

CERTIFICA,

Que el Consejo de Doctores del Departamento en su sesión de fecha 17 de noviembre de noviembre de 2015 tomó el acuerdo de dar el consentimiento para su tramitación, a la tesis doctoral titulada " ANALYSIS OF THE RAINFALL VARIABILITY IN THE SUBTROPICAL NORTH ATLANTIC REGION: BERMUDA, CANARY ISLANDS, MADEIRA AND AZORES" presentada por la doctoranda Dª. Irene Peñate de la Rosa y dirigida por los Doctores D. Juan Manuel Martín González y D. Germán Rodríguez Rodríguez.

Y para que así conste, y a efectos de lo previsto en el Artº 6 del Reglamento para la elaboración, defensa, tribunal y evaluación de tesis doctorales de la Universidad de Las Palmas de Gran Canaria, firmo la presente en Las Palmas de Gran Canaria, a 17 de noviembre de dos mil quince.

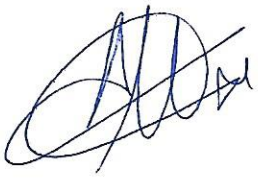

UNIVERSIDAD DE LAS PALMAS
DE GRAN CANARIA

UNIVERSIDAD DE LAS PALMAS DE GRAN CANARIA

Programa de doctorado Física Fundamental y Aplicada

Departamento de Física

ANALYSIS OF THE RAINFALL VARIABILITY IN THE SUBTROPICAL NORTH ATLANTIC REGION: BERMUDA, CANARY ISLANDS, MADEIRA AND THE AZORES

Tesis Doctoral presentada por D" Irene Peñate de la Rosa

Dirigida por el Dr. D. Juan Manuel Martin González y

Codirigida por el Dr. D. Germán Rodríguez Rodríguez

El Director,

(firma)

El Codirector,

(firma)

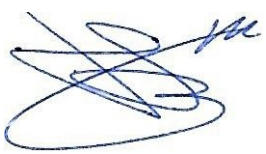

La Doctoranda,

(firma)

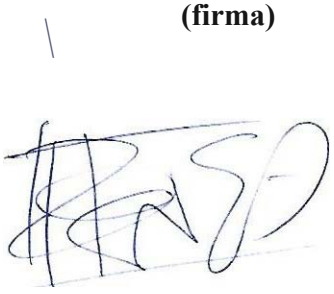

Las Palmas de Gran Canaria, a 17 de noviembre de 2015

UNIVERSIDAD DE LAS PALMAS
DE GRAN CANARIA

DEPARTAMENTO DE FÍSICA

PROGRAMA DE DOCTORADO: FÍSICA FUNDAMENTAL Y APLICADA

TESIS DOCTORAL

ANALYSIS OF THE RAINFALL VARIABILITY IN THE SUBTROPICAL NORTH ATLANTIC REGION: BERMUDA, CANARY ISLANDS, MADEIRA AND AZORES

PRESENTADA POR: IRENE PEÑATE DE LA ROSA

DIRIGA POR EL DR. D. JUAN MANUEL MARTÍN GONZÁLEZ

CODIRIGIDA POR EL DR. D. GERMÁN RODRÍGUEZ RODRÍGUEZ

LAS PALMAS DE GRAN CANARIA, 2015

Para Pedro y Ángela (mis padres),

Andrés, Alejandra y Jorge

Irene

ACKNOWLEDGEMENTS

This thesis has been carried out within the framework of a research collaboration between the Spanish Agency of Meteorology (AEMET) and the Bermuda Weather Service (BWS), such cooperative efforts have been very successful in accomplishing my meteorological training and research objectives. I would like to acknowledge the support to both institutions, especially to Mark Guishard (BWS) for his passionate discussions and by way of his outstanding knowledge about contemporary scientific theories relevant to tropical cyclone forecasting, including case studies of local events. It was a real pleasure learning from him during my stay at Bermuda Weather Service having a great experience in training in the above mentioned field.

I would like to acknowledge the Government of Bermuda Department of Airport Operations (DAO), BAS-Serco Ltd. and The Bermuda Institute of Ocean Sciences (BIOS) for making possible this cooperation. I also want to thank to the Bermuda Weather staff, particularly to James Dodgson for his helpful comments and Ian Currie for his support mainly with questions related to data inquiries.

Furthermore, I would like to acknowledge the collaboration and support of Agencia Estatal de Meteorología (AEMET) in particular to Manolo Palomares for making possible this cooperation, Juana Arolo, Juan Manzano, Sonia Ripado and the Spanish Weather Service staff in the Canary Islands, especially to Orlando Pazos, Pino Domínguez and Ricardo Sanz for their support with data sources and climate reports and to Ignacio Egea Ureña (observer in Lanzarote airport).

I must also acknowledge the support of the the IPMA (Instituto Portugues do Mar e Atmosfera) for the development of this thesis. In particular to Álvaro Pimpão Silva, Fátima Espírito Santo Fátima Coelho and Luís F. Nunes.

The data used in this study has been kindly provided by the Bermuda Weather Service (BWS), Spanish Agency of Meteorology (AEMET) and Consejo Insular de Aguas de Gran Canaria and IPMA (Instituto Portugues do Mar e Atmosfera).

I gratefully acknowledge the input and suggestions of my colleagues at ULPGC (University of Las Palmas of Gran Canaria) in the preparation of this work, especially I would like to express my sincere gratitude to my thesis director Dr. Juan Manuel Martín González and also to my co-director Dr. Germán Rodríguez Rodríguez and to M. C. Cabrera-Santana and A. Rodríguez-González (GEOVOL Group Research Department of Physics) for providing topographic maps.

I also want to thank A. Mazzarella, Paul E. Roundy and another anonymous reviewers for their helpful comments. I cannot conclude without to extend my sincere thanks to my fellows Candy and Daniel Sandoval and J.L. Gonçalves Teixeira for reading preliminary versions of this dissertation.

Finally, I would like to give thanks to my entire family for their unconditional support and especially to my husband, Andrés.

Irene

ABSTRACT

This study presents an analysis of the rainfall in the subtropical North Atlantic region, proceeding as a reference the archipelagos of Bermuda, Canary Islands, Madeira and Azores. The spatial and seasonal variability and the annual cycle of the rainfall, on the basis of daily rainfall data records in the past decades with particular emphasis on the normal period 1981-2010, have been the main focus of this work. Particular importance has been given to the annual pattern, due to its crucial role in freshwater resources management. Geographical and topographical features, such as relief, orientation or proximity to the sea are some of the factors that influence rainfall regime which define the different areas considered in this study. In general, the rainfall in the Canary Islands and Madeira both follow a similar pattern, which is different from the one that characterizes the Bermuda and Azores archipelagos. Non-linear models have been a suitable framework for this characterization. It stresses the random nature of the rainfall distribution over Bermuda and Azores where the duration of dry periods follows an exponential adjustment close to a discrete Poisson model more accurately than a Power Law or scale-free behaviour. However, the rainfall in Madeira and more markedly in The Canary Islands has a more complex character, which can be treated through an analysis of scale or a fractal point of view. Even though the Azores anticyclone is the common synoptic situation dominating this region almost throughout the year, a marked spatial-temporal variability was found when analysing the different time series from the selected weather stations. The analysis of the wind direction and speed has been a helpful tool in describing the different seasonal rainfall patterns, and to differentiate between frontal and convective rainfall types. Investigation of the inter-annual rainfall variability in Bermuda indicates preliminary results as an increasing trend in winter rainfall days, a decreasing one in rainfall rate and a potential relationship with certain modes of atmospheric

variability such as the North Atlantic Oscillation Index (NAO). The findings from this study have allowed a better knowledge on the climate within this biogeographical region, which is considered as of a great scientific interest.

ABSTRACT IN SPANISH

Este estudio presenta un análisis de la precipitación en la región subtropical del Atlántico Norte, tomando como referencia los archipiélagos de Bermudas, Canarias, Madeira y Azores. La variabilidad espacial y estacional, así como el ciclo anual de la lluvia en las pasadas décadas con particular énfasis en el periodo normal 1981-2010 han supuesto el centro de atención del mismo. Particular énfasis se ha dado también a la tendencia anual debido al papel crucial que tiene en la gestión de los recursos hídricos.

Las características geográficas y topográficas como el relieve, la orientación o la proximidad al mar son algunos factores que influyen en el régimen pluviométrico que define las distintas zonas consideradas en este estudio. En general, la precipitación en las islas Canarias y Madeira sigue un patrón similar el cual es diferente al que caracteriza a los archipiélagos de Bermudas y Azores. Los modelos no lineales han supuesto un marco adecuado para esta caracterización. Destaca el carácter aleatorio de la lluvia en Bermudas y Azores donde la distribución de la duración de periodos secos sigue un ajuste exponencial propio de un modelo de Poisson más que un comportamiento de escala o Power Law. Por el contrario, dicha distribución en Madeira y más marcadamente en Canarias posee un carácter más complejo pudiendo ser caracterizada a través de un análisis de escala o desde un punto de vista fractal. A pesar de que el anticiclón de Azores domina esta región prácticamente todo el año, una marcada variabilidad espacio-temporal es encontrada al analizar las diferentes series temporales de precipitación seleccionadas.

El análisis de la dirección y la intensidad del viento han sido útiles en la descripción de los distintos patrones estacionales de la variable de estudio y para diferenciar entre precipitación frontal y convectiva. El análisis de la variabilidad interanual en Bermudas indica, como resultado preliminar, una tendencia hacia el aumento del número de días lluviosos, una disminución en la tasa de precipitación y una

relación potencial con modos de variabilidad atmosférica como la NAO (North Atlantic Oscillation Index). Los resultados derivados de este estudio han servido para profundizar en el conocimiento de la climatología en esta región biogeográfica la cual es considerada de gran interés científico.

INDEX

INDEX

INDEX

INDEX

INDEX

INDEX

INDEX

INDEX

1. Introduction

INTRODUCTION

1. Introduction

Life on Earth critically depends on freshwater availability; in particular, human life, settlement, and any of its activities restricted by the existence of such a vital resource. This fact is particularly evident in desert, arid, and semi-arid zones, where prolonged droughts are commonly related to health problems, soil erosion and massive population displacements. Hence, mankind largely depends upon precipitation, the primary mechanism transporting water from the atmosphere to the planet surface, as a part of the water cycle, and a driving agent of many other processes.

Rainfall climatology in a given area is of great importance to assess precipitation effects on a wide range of natural phenomena; thus, positive or negative anomalies in precipitation regimes have severe impacts on freshwater availability for consumption, agriculture, terrain stability, desertification processes, etc. (Potter & Colman 2003). These effects are also reflected in the variety of flora, landscapes, and natural resources. All these factors form a system in a highly fragile equilibrium which involves unpredictable consequences for the population, related to possible global or local climate changes. Consequently, temporal and spatial variability of precipitation over various scales is the most essential intrinsic property of precipitation and constitutes an issue for general concern. Adequate characterization of local rainfall climatology plays a relevant role in hydrology, ecology and agriculture. The characterization distribution of the rainfall events can help decide which measures should be taken in order to prevent problems related to water management. Furthermore, rainfall variability may cause meteorological effects like floods or droughts, depending on the duration and intensity. Both have consequences in a variety of areas, such as the ones cited above, as well as in human activities and infrastructure (Coates 1996).

INTRODUCTION

Identifying the nature and patterns of the interannual variability of precipitation can be crucial because these fluctuations exert a long-term effect on water resources, affect plant growth and the biogeochemical cycle, and modulate extreme events, such as floods and prolonged dry periods. For instance, several studies suggested that the variability of annual precipitation can be important for the temporal dynamics of aboveground primary production and thus for global vegetation biogeography (Fang et al. 2001, Knapp & Smith 2001, Wiegand & A Moloney 2004, Yang et al. 2008).

Naturally, freshwater availability depends on rainfall variability and influences the development of human life (Potter & Colman 2003). As a consequence, methods like water conservation, wastewater treatment, and reuse to irrigation or water desalination have been developed in many areas to improve freshwater resources. Brazil, Barbados, Jamaica, Honduras, Chile and Canaries are examples where such methods are employed in different sectors.

Bermuda represents a case where government encourages people to follow plans based on a water strategy policy, including the development of water catchment and distribution, guaranteeing water supply to the islands. For instance, Public Health (Water Storage) Regulations of 1951 legally outline the collection and storage of rain water for domestic purposes in the islands. There are no rivers, streams or lakes in Bermuda, so rain water constitutes the main supply of freshwater, being the source of drinking water. To this end, one of the systems used for collecting and storing water is rainwater harvesting, which is considered a good option in areas of significant rainfall when space-time variability allows meeting the water needs (Rowe 2011). This system is employed in most of Latin American, the Caribbean and African countries (Tanzania, Botswana). In particular, the collection and storage of rainwater from roofs, land surfaces, or rock

catchments is also used in Tokyo (Japan), Berlin (Germany), Thailand, Indonesia, Philippines, Bangladesh, Hawaii and the Virgin Islands. This practice is based on three basic elements: a collection area, a transportation system, and appropriate storage. Furthermore, this system can avoid many environmental problems often caused by conventional large-scale projects.

Drinking water has been a concern in Bermuda ever since it was settled by humans in the 1600s. The residents collected rainwater from the roof of the houses made by limestone to make easier the filtering of the rain water that diverted into vertical structures and usually was stored in underground reservoirs or tanks. Nowadays, 50% of all the potable water consumed in Bermuda comes from this system and regulations require that new buildings have the requirements to collect adequately the rainfall needed for human use annually. Bermuda was thought to have no ground water, but freshwater lens formations were discovered in the 1920s and 1930s. Since then, groundwater extraction provides a supplement to rainwater. Drinking water has a good quality because limestone neutralizes acids. Today, the increase of the demands on fresh water resources lead to the development of technologies like desalination and reverse osmosis, providing potable water to several major tourist facilities and industries.

On the contrary, the Canary Islands are an example where the hydraulic resources directly derived from rainfall are scarce. In historical terms, The Canary Islands have always been characterized by high population mobility rates as a consequence of its geo-strategic position between three continents. Agriculture and fishing were the main economic resources in the islands before the sixties. The limited economic resources-mainly in the field of agriculture, unequal distribution of lands, water properties, and high competition from American and African markets led the population to a fleeing poverty.

INTRODUCTION

Economic decline, droughts, diseases, and famine were the most significant causes of the substantial emigration avalanches from the Canaries to America; mainly to Cuba and Venezuela.

The general low annual pluviometry, essential for the development of the primary sector, made fresh water insufficient for the development of human life in the islands. Appropriation, use and distribution of the surface water were serious problems that the social system had to cope with in the past. Water extraction from groundwater aquifers was overexploited rapidly (Custodio 2002). Social conflicts caused by the concept of private ownership of water were continuous until the 19th century. Hydric conditions worsened with demographic increase. Moreover, in more recent times -post 1950- the development of tourism allowed the economy in the islands to flourish. This new local industry, which required large amounts of water, had its heyday in the sixties and currently attracts between 9 and 12 millions of tourists per year. Tourism put end to the growth of emigration and the Canary Islands became an immigration destination, witnessing an important increase of the population since then.

The lack of freshwater was partially alleviated by a change in mentality, since the notion of water as common property or social assets was considered, combined with the use of new technologies through the construction of water reservoirs and a great development in sea and brackish water desalination (Veza 2001). Nowadays, there are many water reservoirs: cisterns, ponds and dams distributed all over the islands. They have been built to collect and store rainwater, especially in Gran Canaria where in the mid of the 20th century (around 1950), covering a surface of about 1558 Km2 , 69 water reservoirs and dams of more than 15 meters in height and with a capacity of 100.000 m3 were built. The capacity of such reservoirs ranges from 780.000 to 1.300.000 m3. In fact,

it is one of the places in the world with more dams per square meter. However, these new methods to reduce the water scarcity entail new risks such as atmospheric pollution and aquifer deterioration (Aguilera-Klink et al. 2000).

Not all the islands suffer equally from the scarcity of fresh water. In fact, the western islands are wetter than the eastern ones. Nevertheless, rainfalls are irregular in temporal and spatial distribution with occasionally-long dry periods. Summarizing it up, climatology has always determined the economy as those activities that depend on the water.

The atmosphere is a highly non-linear system; hence, as with many others meteorological phenomena, rainfall is characterised by very complex dynamics exhibiting wide variability over a broad range of time and space scales. The turbulent nature of atmospheric flows could play a relevant role in the physical process behind rainfall. The prevailing tendency rainfall pattern affecting the Canary Islands are mostly influenced by local factors like relief and geographical location.

Because of the high complexity of atmospheric processes, conventional statistical methods have proved to be quite inefficient to describe the statistical structure of phenomena such as rainfall over a wide range of scales. However, it has been shown that many complex processes occurring in Earth's atmosphere exhibit fractal or power law scaling (Dickman 2004), particularly rainfall occurrences (Mazzarella & Diodato 2002). That is, statistical properties of a given process are similarly related to each other over a wide range of scales. Thus, exploration of invariance properties across scales offers an alternative approach to quantify the variability of rainfall process.

In spite of the fact that model performance regarding prediction has improved significantly over the last few years, the complexity of some phenomena, especially non-

linear ones, makes it difficult to understand the underlying dynamic of such events. Linear methods are not considered adequate to analyse rainfall processes due to their non-stationary character (Santos et al. 2001). Time does not follow a uniform pattern in rainfall events, but there are others different in terms of time ranges. These temporal asymmetries indicate that rainfall behaviour has a non-linear nature and operates interacting at a range of scales (Morata et al. 2006). Thus, it is necessary to develop a specific framework for examining it. In this sense, the use of statistical methods like Poisson model and the scaling framework or Power Law helps characterize the rainfall behaviour in the studied region.

Heavy rainfall events, are natural phenomena, related to the atmospheric dynamics, which under some conditions can turn into natural catastrophes (De 2004). Such events have been identified among the rare occurrences that should be taken into account due to their socio economic impact and harmful effect on the population. Thus, these atmospheric phenomena can be considered, in some occasions, as natural hazards.

Floods are at world scale the natural disaster that affects a larger fraction of the population. Its effects can affect to the surrounding areas of the hydrographic network (basins, rivers, dams) and the coast line (Pires et al. 2010).

Accordingly to USA FEMA (Federal Emergency Management Agency) flood can be defined as: "A general and temporary condition of partial or complete inundation of two or more acres of normally dry land area or of two or more properties from: Overflow of inland or tidal waters; Unusual and rapid accumulation or runoff of surface waters from any source; Mudflow; Collapse or subsidence of land along the shore of a lake or similar body of water as a result of erosion or undermining caused by waves or currents of water exceeding anticipated cyclical levels that result in a flood as defined above." A flash flood

is the result of intense and long duration of continuous precipitation and can result in dead casualties. The speed and strength of the floods either localized or over large areas, results in enormous social impacts either by the loss of human lives and or the devastating damage to the landscape and human infrastructures (Pires et al. 2010). Torrential rains, showers, thunderstorms and strong winds associated to severe weather can cause disasters such as flooding or power outages and significant damages to agricultural, vegetation, utilities, homes, roofs and even human fatalities. Sometimes these events are accompanied by significant swells and surf observing large battering waves producing coastal inundations and damages to ships.

The large precipitation occurrences either more intense precipitation in a short period or less intense precipitation during a larger period can have as consequence land movement may affect geological phenomena. Although flood episodes depend on the topography and hydrological capacity of the terrains, the human intervention plays an important role. Particularly in activities such as deforestation, dams, change of water fluxes, and the waterproofing of the terrain surface. The risk of floods should be address based not only on the knowledge of both meteorological and hydrogeological factors. In order to avoid significant socio-economical losses caused by flood occurrences (Pires et al., 2010).

Rainfall, as considered as a natural phenomenon associated with extreme variability as above mentioned, have been described as scale-invariant processes, which is the main characteristic of fractal sets. Thus, it has been shown that many complex processes occurring in Earth's atmosphere exhibit fractal or power law scaling (Dickman 2004). The natural phenomena such as earthquakes (Smalley et al. 1987, Turcotte & Greene 1993, Chen 2003) or floods (Turcotte & Greene 1993, Mazzarella 1998) has been

studied as fractal processes. In addition, some meteorology phenomena such as clouds and radiative transfer (Lovejoy et al. 1987) or the phenomenon of El Niño (Mazzarella & Giuliacci 2009). Particularly rainfall occurrences are considered scale invariant processes and they might be characterized as fractal objects (Olsson et al. 1992, Olsson et al. 1993, Mazzarella & Diodato 2002, Izzo et al. 2004).

Statistical properties of a given process are similarly related to each other over a wide range of scales. Thus, exploration of invariance properties across scales offers an alternative approach to quantify the variability of rainfall and desert dust emission processes. Since the occurrence of natural disasters is not absolutely avoidable, examining the properties of such processes at shorter time scales and their temporal and spatial variability could contribute to their understanding. Owing to their highly complex nature, these processes are not fully understood and deserve further study. These are the main reasons to analyse rainfall variability in this work.

Building on the aforementioned, the rainfall trend in the North Atlantic subtropical region focused on Bermuda constitute the subject matters of this study. Precipitation in these islands depends both of local and large-scale environments.

This paper also analyses the presence of strong regional rainfall patterns in Bermuda that aim to identify them with cycles corresponding to climate modes. Large changes in winter atmospheric circulation over the North Atlantic are linked with the North Atlantic Oscillation (NAO). Which is the dominant mode of mid-latitude atmospheric variation on monthly to decadal scales (Hurrell 1995, Hurrell et al. 2003, Hurrell & Deser 2010). The NAO index provides the winter Mean Sea-Level Pressures (MSLP) variability in the North Atlantic region. Accordingly, NAO index can be defined as the difference between the standardised December–March MSLP at the Azores High

and the Icelandic Low and describes the steepness of a north-south atmospheric pressure gradient across the North Atlantic Ocean (Rogers 1984).

Changes in winter modes of atmospheric and oceanic variability throughout the North Atlantic basin have been affected historically by NAO (Rogers & Van Loon 1979, Hurrell & Van Loon 1997, Hurrell & Deser 2010). Thus, the weather and hydrology in this region are influenced by this significant pattern of climate, affecting atmospheric variables such as surface air temperature, precipitation, storminess, wind speed and direction, atmospheric heat and moisture flux and convergence (Hurrell 1995, Dickson et al. 2000, Hurrell et al. 2003, Trigo et al. 2004, Hurrell & Deser 2010). Between the years of the strongest positive NAO phase periods (1988- 1989 and 1994-1995), northern Europe (north of 45ºN) experienced mild and wetter winters and greater precipitation than normal at regions in the path of the prevailing westerlies and with abrupt orography (e.g. western and northern Scotland and southern Norway; Jones & Conway 1997). In the subpolar region, during periods of positive NAO index precipitation, storminess and wave heights tend to enhance (Beersma et al. 1997, Bijl et al. 1999, Alexandersson et al. 2000, Alexander et al. 2005). Some studies have argued that positive NAO index winters are associated with a north-eastward shift in Atlantic storms (Hurrell & Van Loon 1997, Trigo et al. 2002). Strong eastward air flow between the Iceland Low and Azores High carries storms from North America towards Western Europe. Moreover, a northward shift of the mean position of The Gulf Stream is experienced such like above (Taylor et al. 1998, Taylor & Stephens 1998, Weisse et al. 2005).Westerlies that usually prevail in the region between Florida and Cape Hatteras (west of the Azores High) weaken. As a result, the associated reduced wind stress and heat exchange lead to the development of warm temperature anomalies in the subtropical gyre (Bjerknes 1964, Cayan 1992). Negative

NAO in winter favours easterly winds and cold weather over Europe (Hirschi & Sinha 2007). Nevertheless, a negative NAO index favours storm tracks to shift southward (Bjerknes 1964, Cayan 1992, Rodwell et al. 1999). In winter season such a situation favours outbreaks of cold air from North America crossing the Sargasso Sea (Zhang et al. 1996, Davies et al. 1997, Jones & Thorncroft 1998).

The NAO also controls ocean properties (Visbeck et al. 2003) like fluctuations in SST, salinity, vertical mixing, ocean heat content, ocean currents and their related heat transport, circulation patterns and ice formation (Sutton & Hodson 2003). An example is the inverse relationship between temperature and biogeochemical properties in the Sargasso Sea linked to NAO variability (Bates 2001). Marine ecosystems (Drinkwater et al. 2003) can be also affected (Bates 2007) by NAO.

Therefore, the characterisation of the NAO temporal structure is relevant to understand the physical processes affecting both the ocean and the atmosphere (Hurrell & Deser 2004). There is not a single time scale of variability for the NAO. However, large changes occur from one winter to the next and from one decade to the next (Hurrell & Deser 2010). Some studies have been debated that the NAO is associated to long-term trends and show large variability at quasi-biennial and decadal time (Hurrell & Van Loon 1997).

In terms of global significance, another important pattern is the El Niño Southern Oscillation (ENSO) which affects large-scale weather and climate variability worldwide. This phenomenon is known to cause climate variability on interannual and decadal time-scales in both the North Pacific and North Atlantic Oceans (Holton et al. 1989, Lau et al. 1992, Enfield & Mayer 1997, Hurrell & Deser 2001). El Niño is a climate cycle that occurs during several year periods. As a consequence, a shift of warm surface water

across the tropical Pacific from west to east is caused by the relaxation of the trade winds. The Gulf Stream position shifts northwards after the El Niño events and during NAO positive phases with a lag of 2 years (Taylor et al. 1998, Taylor & Stephens 1998). Warming in the tropical North Atlantic, Caribbean Sea and the SE subtropical gyre is observed after roughly 4-12 months of El Niño in the Pacific Ocean (Zhang et al. 1996, Bojariu 1997, Penland & Matrosova 1998). This favours a more stable Atlantic atmosphere (Zhang et al. 1996, Davies et al. 1997, Jones & Thorncroft 1998). Furthermore, NAO could greatly reduce ENSO effects or vice versa (Lee et al. 2008). Effects of El Niño in the Sargasso Sea can also be found in several climatological studies (Zhang et al. 1996, Bojariu 1997, Penland & Matrosova 1998).

Interannual hydrographic and biogeochemical variability in Bermuda seems to be modulated by NAO and ENSO. However, such correlation is poor with the Southern Oscillation Index (SOI) (Bates 2001). Several authors have studied the influence of ENSO on the tropical Caribbean Sea and western Atlantic Ocean. The relationships between ENSO and the frequency of hurricanes in the North Atlantic basin (Elsner et al. 1999) stands out as well.

The NAO acts throughout the year (Marshall et al. 2001) but exerts a dominant influence in the winter months. The two areas most affected by the weather activity are the low pressure over Iceland and the sub-tropical high pressure located over Azores. Thus, most comparisons presented in this paper related to the influence of NAO on rainfall variability in Bermuda are focussed in winter when the atmosphere is more active dynamically and perturbations exhibit their largest amplitudes (Hurrell & Van Loon 1997, Cassou 2010). However, it should be taken into account that some studies over the Sargasso Sea area have shown that interannual variability of some oceanic parameters

during summer (June–September) and fall (October–December) were correlated to (NAO) and strongly influenced by wind events (Bates 2007). In fact, fluctuations of surface pressure, temperature, cloudiness and precipitation occur throughout the year over the North Atlantic, and decadal and longer-term variability is not confined to winter.

1.1 Previous rainfall studies in the research area

The rainfall studies found in the literature come generally from the national meteorological centres in each respective country. These reports mainly consist on the description of the statistics (maxima, minima and average values of the existing time-series) for a normal period (30 years). In Bermuda, rainfall studies over the islands are scarce (Macky 1946, 1957), not updated and based on short data bases. Nowadays, the Bermuda weather service has available a web site (*http://www.weather.bm/climate.asp*) to retrieve monthly reports. In addition, the hydrogeology of Bermuda, including the geologic control of freshwater lens, has received considerable attention (Vacher & Wallis 1992, Vacher & Rowe 1997, 2004). At the Canaries and the Portuguese archipelagos, we can highlight the recent publication of a Climatic atlas where the main statistical values of temperatures and rainfall are shown for each island of the three archipelagos. Previous to that, the National Institute of Meteorology in Spain (INM) published a description of the Canary weather (Font Tullot 1956) and the historical rainfall records and its variability for Spain (Almarza et al. 1996). Sequentially, the INM publishes the rainfall statistics on the normal periods such as 1961- 1990 (Almarza et al. 1996), 1971- 2000 (Servicio de desarrollo climatológico 2002), 1981- 2010 (Guijarro & Jiménez de Mingo. 2013).

Regarding the analysis of the water resources, Saenz-Oiza (1975) is found in the literature for Canary Islands, as well as Guerra (1989) that is the official document for the Canary Islands hydrologic plan. Similarly, the hydrogeology of Madeira was studied by

Prada (2000) in her doctoral thesis, whereas a description of Azores Weather can be found in Bettencourt (1979). Additionally, a study based on the results from a local climatic model in Azores was presented by de Azevedo et al. (1999).

There are some studies referred to particular heavy rainfall events which caused severe damages or particular locations where eventually heavy rainfall occurred. For instance, rains and flooding in the city of Las Palmas by Máyer (2003). A case of study on heavy rainfall in Santa Cruz de Tenerife on 31st March 2002 was addressed by the National Institute of Meteorology in Spain (Elizaga et al. 2003). The storm "Delta" and its extratropical transition through Canary Islands was also studied as a particular case of study (Martin et al. 2007). It was also emphasized the situations of heavy rainfall and strong winds during winter 2010 in the Canary Islands. In particular the first situation occurred specifically between 1st and 3rd of February with episodes of heavy rainfall (Martín 2010, Carretero et al. 2011) and the second between 17th and 18th February (Martín 2010), corresponding to an explosive cyclogenesis where intense winds with hurricane force were observed. At the Portuguese archipelago, there are also some studies focused on particular weather situations or particular places. The climatic characterization of the winter season of 2009 and 2010 and the study of floods occurrence episode of February 2010 with particular incidence on 2nd and 20th in the Madeira Island has been analysed (Miranda et al. 2010, Pires et al. 2010). Likewise, Fragoso et al. (2012) investigated the flash flood in Madeira Island in autumn 2012 and the landslides occurrences on 05 November 2012 were studied by Couto et al. (2013) and Teixeira et al. (2014). A case study on the Azores archipelago could also be found in Kleissl et al. (2007).

Some authors investigated the rainfall trends as well as the relationship between rainfall variability and the atmospheric climates modes such as the North Atlantic Oscillation (NAO). García-Herrera et al. (2001) studied the relationship between the rainfall in the Canary Islands and NAO and concluded an increasing during the negative NAO phase. Similar analysis were carried out by Puyol et al. (2002, 2004), adding the southern Oscillation in the analysis. In Bermuda, There is a preliminary analysis of Bermuda historical weather data (Gaurin 2008) where winter NAO index is compared with temperature, rainfall and sea level pressure at Bermuda. Only a few studies about rainfall trends has been found in the literature. García-Herrera et al. (2003) searched the relationship between the rainfall trends in Canary Islands and the NAO, however they found that stronger influence in the trends was consequence of the heavy rainfall events. Similarly, Campos et al. (2011) found no significance in the analysis of the precipitation trends based on a radiosonde study on the subtropical region. Finally, a fractal analysis on the Madeira rainfall resulted in exhibiting the complex nature of these processes (De Lima & De Lima 2009).

1.2 Objectives

The purpose of this study is to perform an analysis of observed daily rainfall records that provides insight into the evolution and significance of rainfall trends in the North Atlantic subtropical region including Bermuda, Canary, and Madeira and Azores archipelagos in order to gain a better understanding of the climate of this region. Samples cover an average of fifty years, however emphasis was made in the common normal period 1981-2010.

A special attention is being made on rain the annual pattern as a key element to define measures to support the sustainable development of the areas of study, which is

essential for freshwater resources management. Wind speed and wind direction trends are examined since they are linked to the temporal variability of the annual cycle of rainfall.

Taking into account the extremely complex nature and non-stationary character that rainfall presents, this study explores its temporal variability to provide insight into the climate of this region from a contemporary perspective undertaking a rainfall statistical analysis. Non lineal models are considered an adequate framework to such purpose. This work intends firstly to analyse if rainfall data over this area can be modelled by a Poisson distribution resulting from the assumption of a random behaviour considering firstly only the occurrence or not occurrence of the phenomenon. Moreover, other goal of the study is to examine if the analysis of the distributions of the series show temporal scaling properties and Power-law behaviour. In this case the intensity of precipitation amounts are taking into account. Complex patterns through fractal analysis are also examined to improve the understanding of this phenomenon.

In relation to the seasonal analysis, another aim of this work is to investigate if the seasonality index (SI) proposed by Walsh & Lawler (1981) and Peña-Arencibia et al. (2010) describe adequately the rainfall regimen in these archipelagos immerse in relative different geographical and climatic environments.

Other purpose of the work is to prove if the wavelet analysis is a suitable tool for the analysis of rainfall over Bermuda in order to understand their temporal scales of variability and see if this process responds to a multi-scale structure and non-stationary behaviour. Lisbon and Gibraltar NAO winter index time series is also analysed using this tool.

This paper also pretends to give insight into the variability of Bermuda's rainfall following as aim to compare rainfall at Bermuda with NAO index and to analyse if the

results could help to bring light to recognize the presence of strong regional patterns that could be identified with cycles corresponding to climate modes. Particularly, the exploration of if the annual number of rainy days (NRD) correlates with the NAO index will be one subject of focus of this work. This investigation also includes the analysis of the long-range dependence of the rainfall process.

Summarising, the main objectives are:

1. Description of the behavior duration - intensity of the rainfall events in the study area.
2. Temporal distribution and quantification of their clustering.
3. Suitability of nonlinear models for the rainfall characterization.
4. For the Canary Islands, comparison with the desert dust intrusions.
5. Analysis of the spatial, seasonal and interannual rainfall variability over the archipelagos forming part of this region.
6. Study of the relationship between the NAO index and rainfall events in Bermuda.
7. Determination of the degree of randomness of the analyzed Time series and zone differentiation based on the rainfall.

2. Area of study

2. Area of study

This work is related to the different locations within the subtropical area which cover a geographic and climatic zone located approximately 23.5° north of the Tropic of Cancer (Fig.1).This subtropical climate is temperate and warm averaging an annual temperature above 18 ºC.

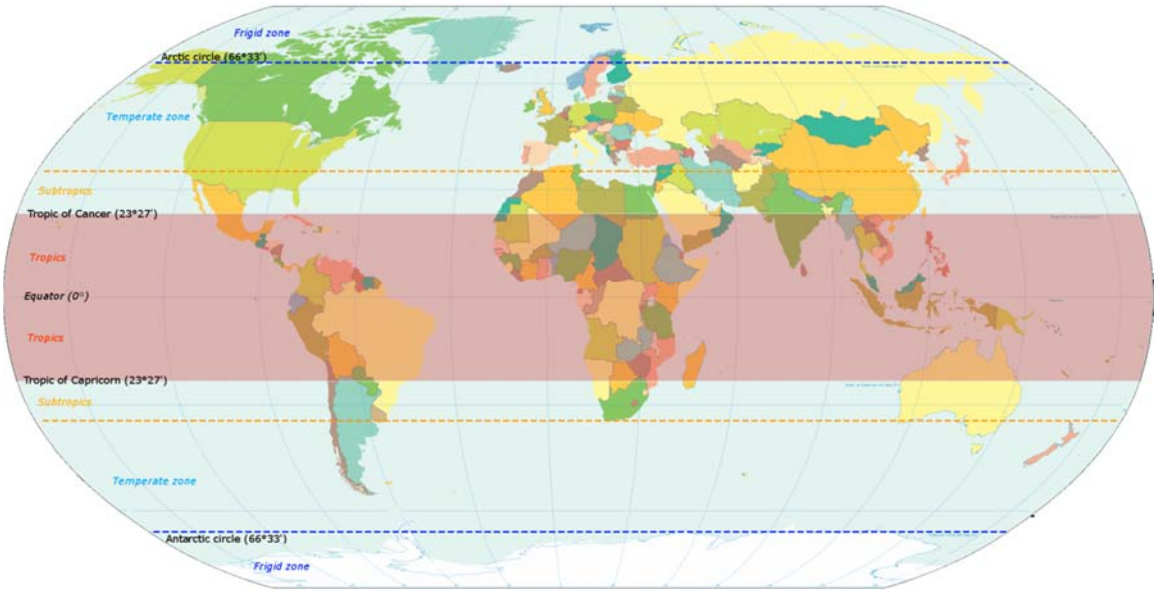

Fig.1. Location of the subtropical area

(https://upload.wikimedia.org/wikipedia/commons/b/b0/World_map_indicating_tropics_and_subtropics.png)

This area of study is also affected by the Subtropical Jet: a belt of zonal winds located approximately between 11.000 and 13.000 m.

Rainfall in the Bermuda archipelago is broadly studied in this work, this area is considered representative of the subtropical climate due to its geographical location. A comparison with the Canary archipelago is made, given their location at similar latitude around 30ºN within the Atlantic subtropical belt and affected by the Bermuda-Azores High. Most of the geographical sites considered in the analysis of the rainfall trends in this work are located at the Canary Islands. A brief comparison of the precipitation variability in this area with the rainfall regimen has been made with the closest

archipelagos of Azores and Madeira. The geographic, topographic and climatic features of these islands are very similar to those of the Canaries since all of them form part of the Macaronesia, by having a volcanic origin, oceanic climate and located in the subtropical area. Naturally, the Canary archipelago is more exposed to influence from the African continent and less affected by the Atlantic perturbations than the Portuguese islands, which present a higher annual rainfall particularly the Azorean archipelago.

Furthermore, another purpose of this study is to compare the fractal behaviour between rainfall and dust events that hover the Canary Islands stemming from the Sahara desert.

2.1. Bermuda

2.1.1. Geographic and topographic features

Bermuda is a tiny isolated archipelago close to 35 km long from tip to tip with an area of about 55 km^2. The mean width is approximately of 1.5 km and the maximum one of 3 km. It is located in the western North Atlantic Ocean, east of the eastern coast of the United States at 32.3° N 64.8° W; approximately 1130 km east-southeast of Cape Hatteras (North Carolina, USA), 1222 km southeast of New York City and 1574 km from Jacksonville, Florida (Vandever & Pearson 1994) and 1330 km northeast from the Bahamas (Coates et al. 2013). The archipelago consists of approximately 123 islands in close proximity, including Bermuda, St. George's, St. David's and Somerset that are joined by bridges and some other islands and islets (Coates et al. 2013). The landscape orography is very flat. The elevation of most of the land mass is less than 30 m a.s.l., rising to a maximum of less than 100 m. The highest point, *Town Hill,* rises about 79 meters (Vacher & Rowe 1997, Elsner & Kara 1999). The Bermuda topographic geographic map and the location of the archipelago in the North Atlantic Ocean are shown in Fig.2.

AREA OF STUDY

The islands are of volcanic origin. The topography is dominated by Quaternary carbonate cemented dunes (Rowe & Bristow 2012). The permeability of the limestone cap to which they belong does not allow the presence of rivers, streams or freshwater lakes (Coates et al. 2013). The hydrogeology of Bermuda is discussed in detail in several papers (Ayer & Vacher 1983, Thomson 1989, Vacher & Rowe 1997, 2004, Rowe 2011).

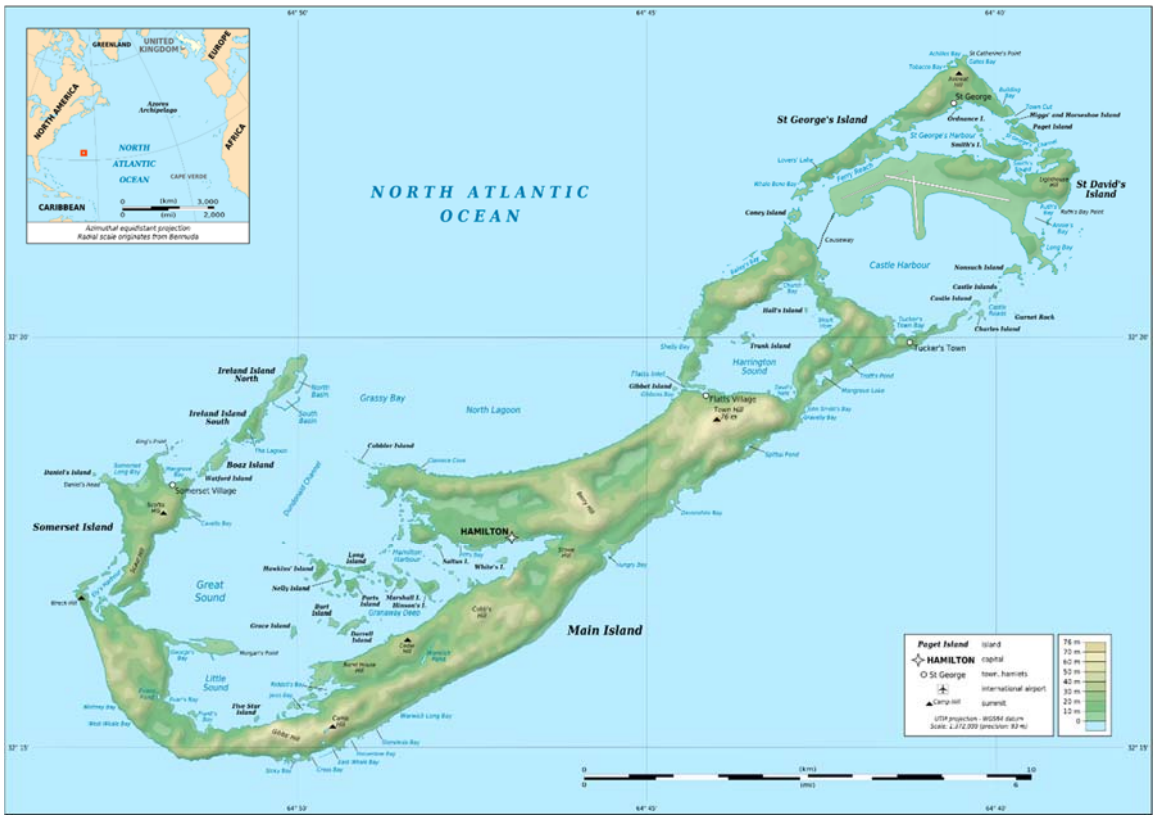

Fig.2. Bermuda topographic map. Inset indicates geographic location of the archipelago in the North Atlantic Ocean (Eric Gaba-Wikipedia Commons) (http://mapsof.net/map/bermuda-topographic-map)

In spite of its location at such high latitude, the proximity to the warm Gulf Stream makes coral growth possible (Yost et al. 2012) and due to the surrounding reefs it is considered the most northerly group of coral islands in the world.

2.1.2. Climatic characterization

Located in the Sargasso Sea of the subtropical North Atlantic Ocean, Bermuda can be characterized by a subtropical climate (Rowe 2011). Hence, the archipelago is frost, snow and ice-free, except for rare occurrences of hail (Vandever & Pearson 1994).

2.1.2.1. Temperature

The air temperature is moderate owing to the maritime climate of the islands and it is practically unaffected by the topography. The surrounding sea is the main factor regulating temperature. Contrary to the islands that make up the Macaronesia, Bermuda has little topographic contrast affecting the air temperature. The average monthly temperatures range from 17 to 27 ºC with little diurnal variation (Vacher & Ayers 1980, Rowe 1984). The annual average temperature is 21 ºC, the annual average maximum 32 ºC and the annual average minimum 8 ºC (Macky 1948). Extreme temperatures are not frequent. From June to August temperatures average approximately 25-27 °C, with past record daily temperatures having reached 35 °C (*BWS2014 http://weather.bm/climate.asp*).

August is the warmest month with a temperature average about 27 ºC. From January to March is the coldest period and March the coldest month with mean temperature that can reach 18 ºC. The coldest temperatures can reach values of about 6 ºC in winter (Vandever & Pearson 1994). The annual average sunshine is 2588 hours with an average daily of 7 hours. The lowest values of monthly sunshine are observed in December and the highest in July (Macky 1952).

2.1.2.2. Humidity and cloudiness

Humidity is high year round due to the maritime influence of the North Atlantic Ocean which acts as moisture source. Due to the small size of the islands and their low

elevation cloudiness is not retained by the orography. A particular cloudiness formation known as *Morgan's cloud* is observed as a band over the islands when east north easterly wind or a west-south westerly wind prevail. Even in a relatively dry air mass, cumulus clouds and associated showers can be observed over the islands (BWS Glossary).

2.1.2.3. Precipitation

Most of the rainfall events are associated with frontal activity, mainly observed in winter (Rowe 2011). Rain showers are the most common type of precipitation during summer. Cold front passages can produce large 24 hour rainfall totals, but generally mesoscale events providing short lived rainfall events, are responsible for the heaviest precipitation rate in the archipelago. Frontal systems are characterized by reduced visibility by rain and changes in temperature gradient across the front. The intensity and amount of precipitation depends on the sharpness of the frontal trough. The rainfall persistence is a function of the speed of the front. Local or short lived thunder-storms associated with convective showers provide heavy rain over the archipelago and can be related to tropical systems sporadically (Macky 1946). No month is free from the possibility of thunderstorms over Bermuda. However the maximum activity is observed in late summer and winter seasons. The late summer maximum in rainfall amounts is observed in October and is due to the moist unstable maritime tropical air and the second maximum occurs because of the frontal passages being frontal lifting the most common cause of thunderstorm activity (Vandever & Pearson 1994). Spring in the driest season. Local weather like the *Morgan's Cloud* explained in the previous section can produce heavy showers and even thunderstorms in summer time (BWS (Bermuda Weather Service) Glossary).The average annual rainfall of about 1464 mm is distributed

throughout the year (Macky 1957). The archipelago is frost, snow and ice-free, except for rare occurrences of hail (Vandever & Pearson 1994).

2.1.2.4. Surface winds

The Bermuda-Azores High regulates the surface wind flow. In summer southerlies prevail over the area. In late summer and fall, an easterly circulation at low levels is mainly observed. In winter and spring, westerly winds are the most frequent. Winter storms produce gale force (17-21 m s^{-1}) winds over the island.

2.1.2.5. Visibility

The main phenomenon that reduces visibility is precipitation. Fog, mist or and haze are all infrequently reported by the Bermuda Weather Service (BWS). Salt spray due to strong winds in winter can cause also reduction of visibility (Vandever & Pearson 1994).

2.1.2.6. Dynamic climatology. Typical synoptic situations

The Gulf Stream is an important factor that modifies any air mass passing west of Bermuda. Frontal systems moving South and East off the North American coast that reach the islands experience changes in their displacement across the Gulf Stream and Western Sargasso Sea, giving quite mild winters (Macky 1946). Nevertheless, the Bermuda-Azores High regulates the surface wind flow. From May to October the High is well established, where very few migratory highs pressure systems can reach the area (Vandever & Pearson 1994). In summer, it is located east of Bermuda and when it becomes elongated extends westward over the north eastern United States, when the islands are under the influence of persistent troughs; the surface circulation may vary between west and south.

AREA OF STUDY

The typical synoptic pattern and tropical air mass source regions favours convective precipitation during the summer. During the autumn season, the Bermuda-Azores High weakens and moves southward, allowing cold fronts to approach the islands but hardly ever penetrates into the tropics favouring an easterly flow. Frontal systems are typically more strongly defined during winter and generally extended into the tropics. Cold fronts affecting the archipelago can be followed by both cold continental or maritime polar air masses. Under winter synoptic pattern, overcast and squally conditions can be frequent. The typical winter synoptic situation is characterized by low pressures moving eastward from North America and passing south of Nova Scotia favouring a south westerly surface wind (see Fig.3).

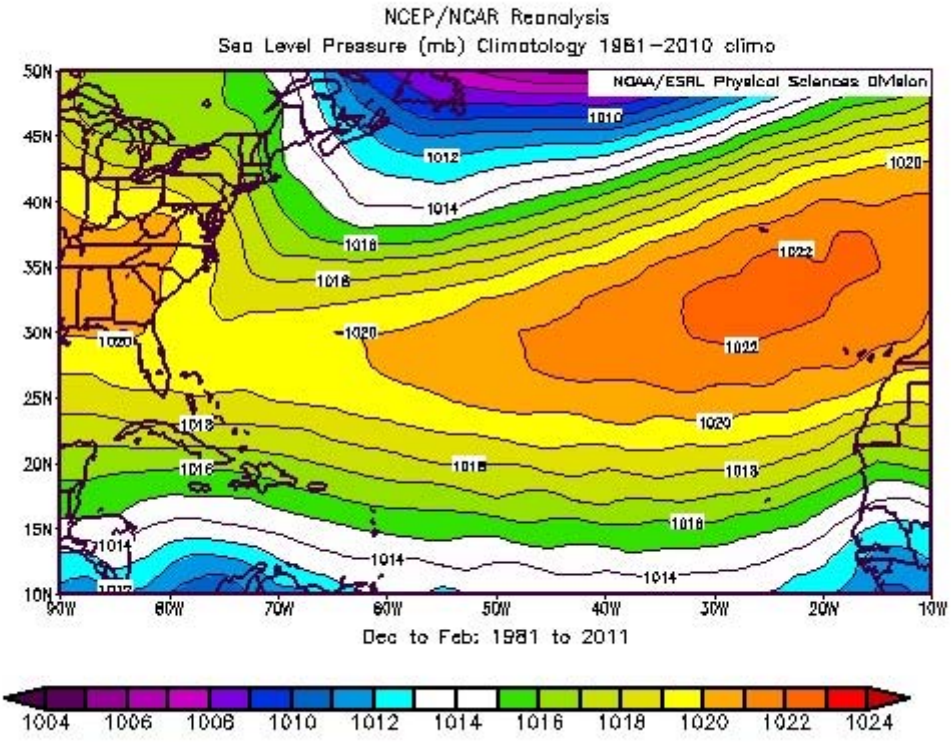

Fig. 3. Sea level pressure (mb) Dec-Jan-Feb composite mean for the winters in the recent climate (1981-2010) representing typical winter synoptic situation over Bermuda (NCEP (National Center for Environmental Prediction) /NCAR (National Center for Atmospheric Research) reanalysis).

By the end of March, the Bermuda High begins to migrate northward, blocking cold fronts as they move off the East Coast. This situation favours the development of intense systems of low pressures from Cuba or the Bahamas moving north-northeast. Strong winds and short lived rainfall, responsible for sporadic heavy rainfall events, can be observed over the islands during the spring. Warm air, brought in a moderate south westerly circulation. In May there is an increasing tendency for Bermuda to come under the influence of a light easterly circulation in the lower levels as the stronger belt of a westerly´s move northward. Such situation favouring strong winds and heavy rainfall can be observed over the archipelago. Severe convective storms and tornadoes are sometimes associated with these conditions. Warm air, brought in a moderate south westerly circulation. In May there is an increasing tendency for Bermuda to come under the influence of a light easterly circulation in the lower levels as the stronger belt of a westerly´s move northward. Such situation favouring strong winds and heavy rainfall can be observed over the archipelago. Severe convective storms and tornadoes are sometimes associated with these conditions.

It is possible to distinguish different synoptic situations responding to different frontal behaviour:

A. Fronts

A1. Winter fronts

A1.1. Cold fronts followed by a deep cold continental polar air mass.

Thunderstorm activity with gale force winds is commonly observed with them.

A1.2. Fast moving cold fronts followed by a maritime polar air mass. As the front approaches, surface southerly winds rapidly increase. Heavy rains with thunderstorms are witnessed just prior to a frontal passage.

A2. Fall fronts

A2.1. Cold fronts passing the area

A2.2 Cold fronts that dissipate when they approach the islands. They are associated with high pressure systems moving into the south-eastern U.S. weak as they move of the eastern coast of U.S. Under this situation the general flow becomes more zonal (west-east).

A. 2.3. Stationary fronts located south of Bermuda. If the cold front is oriented northeast-southwest it usually moves slowly southward. This movement is blocked by the Bermuda-Azores High and the front becomes stationary near 30 degrees north. A surface easterly flow is generated since the High moves slowly eastward to pass north of Bermuda.

A2.4. Cold fronts that turn into warm ones. They are favoured by the formation of a stable wave and/or low in the Gulf of Mexico or off the East Coast of Florida moving to the northeast.

B. Cyclones

The islands are mainly affected by convective precipitation and frontal systems (Government of Bermuda 2005 *http://www.conservation.bm/publications/projects-reports/state_of_the_environment_2005.pdf).* However, four types of cyclones affect Bermuda's weather: the Texas (lows formed west of New Orleans) West Gulf (formed in the western Gulf of Mexico or east Texas), East Gulf (lows that favour quasi-stationary front in the eastern Gulf of Mexico) and South Atlantic or Hatteras Low type (storms that form in the south western region of the North Atlantic with the exception of Tropical Cyclones). The first and second types are spring and winter situations. The third cyclone

type is a typical winter related to snowstorms in the south eastern states. When these storms travel considerably further south of their normal track, they will occasionally pass south of Bermuda (Vandever & Pearson 1994).

Bermuda is in the path of some of the Atlantic basin hurricanes. Such location, near the northern limit of the normal Atlantic tropical cyclone re-curvature band, favours tropical systems approaching from the south (Elsner & Kara 1999) and strong winds or moderate showers affect the area. These hybrid storms, such as the subtropical cyclones, are formed in close proximity south of the islands and track northward. The presence of warm water near Bermuda due to the influence of the Gulf Stream, located more than 1046 km off the coast of the Carolinas, supports the maintenance of hurricanes as they pass through the region, and the formation of subtropical cyclones.

The tropical season extends from June through November. Nevertheless, September and October followed by August are the months of higher occurrence of tropical disturbances in this area (Guishard et al. 2007). Large daily rainfall accumulations are occasionally observed over the islands resulting from stalled tropical systems, for example: tropical storm Bertha (WMO 2009; *http://www.wmo.int/pages/prog/www/tcp/Meetings/HC31/documents/Doc.4.2.9_Bermuda.doc*). Bermuda occasionally suffers a direct hurricane hit during the tropical cyclone. The archipelago experiences longer duration gales from winter storm systems than from tropical cyclones (Tucker 1972, 1982). Additionally, easterly waves associated with severe weather are anomalous phenomena over this area.

2.1.3. Oceanographic conditions

The North Equatorial Current located at the southern latitudes of the North Atlantic flows westward dividing into two branches, one affecting the Caribbean and the

other one Cuba, which is known as the Antilles Current. The Antilles Current flows northwest and joins the Florida current, where both of them flow northward as the Gulf Stream (Vandever & Pearson 1994). Owing to its location southwest of the Gulf Stream (see Fig.4) lies Bermuda in the warm waters of the Sargasso Sea which are especially effective at modifying SST since its temporal variations are associated with cyclone development and lateral water movements (Li et al. 2002). The area does not experience strong temperature gradients. SST (Surface Sea Temperature) has a seasonal variation of 8-10 ºC (Michaels et al. 1994). The annual average SST varies from 15- 19 degrees Celsius from January through April compared to 27-29 degrees during August and September, when it is more likely to observe tropical systems affecting Bermuda. These warm waters extend west and north to the Gulf Stream and prevent cold air masses from the American continent (Macky 1948).

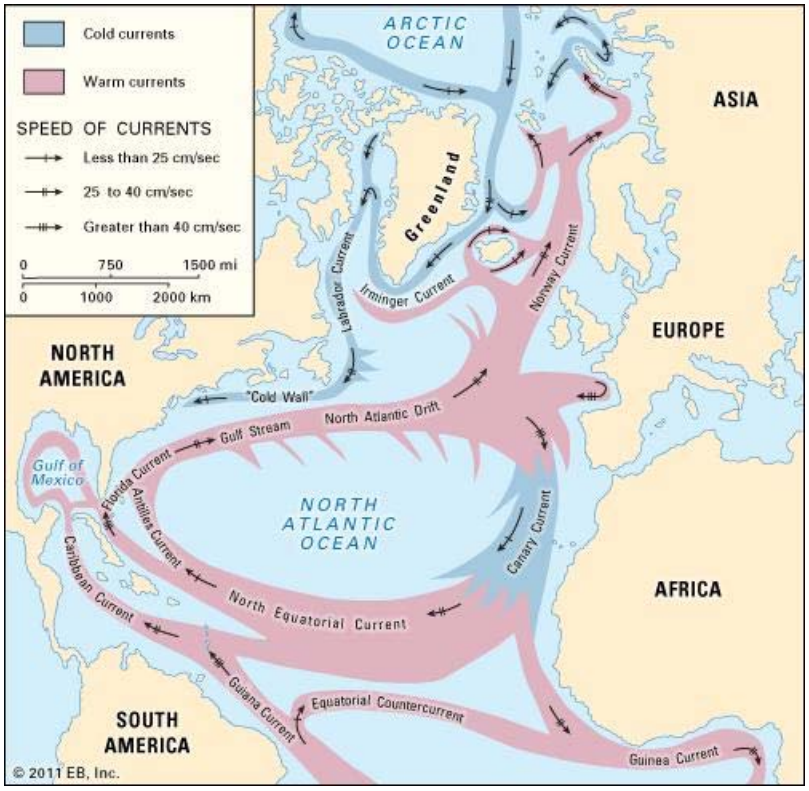

Fig.4. Location of the warm and cold currents in the North Atlantic Ocean (https://www.britannica.com/place/Gulf-Stream/images-videos)

2.2. The Macaronesia

The Canary Islands, Azores and Madeira, together with the Savage Islands (Portugal) and Cape Verde Islands form part of the Macaronesia, a concept introduced by the botanist P. Barker-Webb in the 19th century who considered this group of islands as a bio geographical unit (Masseti 2010). The Location of the Azores, Madeira and Canary archipelagos is shown in Fig. 5.

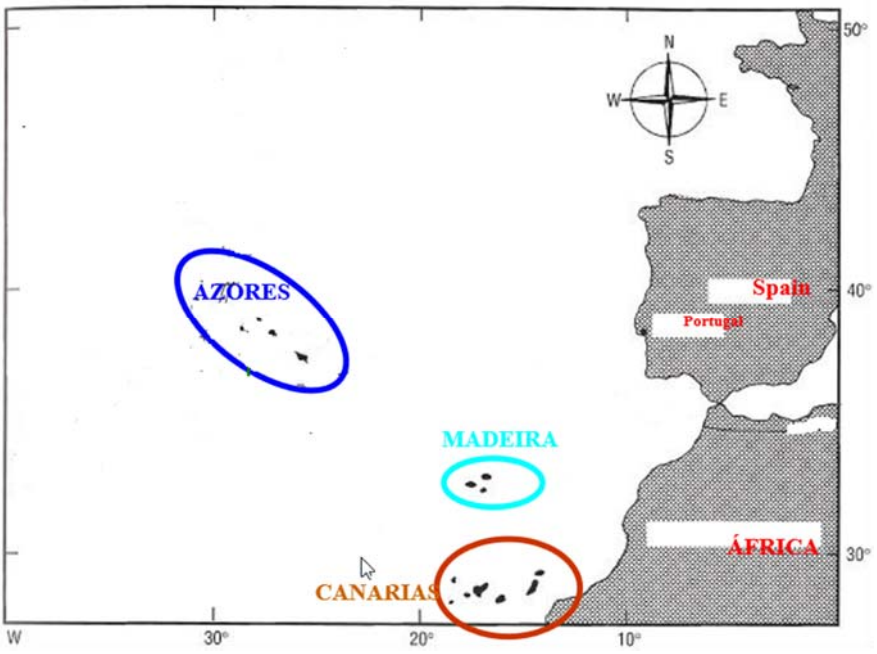

Fig. 5. Location of the Azores, Madeira and Canary archipelagos (Morton, B., et. al., 1998)

According to the worldwide Köppen Climate Classification (Koppen 1936) different types of climate can be found in this group of islands:

A. Dry Climates-Type B

A1.BWh (hot desert), is in Lanzarote and Fuerteventura and in the south of Gran Canaria, Tenerife, La Gomera and El Hierro at low levels.

A2.BWk (cold desert), is in the southwest of Tenerife and La Gomera,

A3.BSh (hot steppe) and BSk (cold steppe), both are present in the Canaries, as altitude increases. In Madeira the BSh climate is observed in Porto Santo.

B. Temperate Climates-Type C

B1. Csa (temperate with hot and dry summer), is in the Canary, Madeira and Azores islands.

B2 .Csc (temperate with dry and cool summers), is solely at higher altitudes: *Pico Del Teide* (Canary Islands) and *Pico Ruivo* and *Pico do Areiro* (Madeira). This variety of climate is not observed in the Azores.

B3. Cfa (temperate with no dry season and with hot summer), is only observed in coastal areas of Azores.

B4. Cfb (temperate with no dry season with a mild summer), is only in coastal areas of Azores.

B5. Cfc (temperate with no dry season with a short and cool summer), is solely in Azores.

B6. Dfc (cold without a dry season and a fresh summer), is merely in the highest central areas of Tenerife, from an altitude of 2900 m.

B7. ET (tundra), only in the Azores, in *Mount Pico* (Island of Pico) from an altitude of about 1600 metres (Agencia Estatal de Meteorología de España & Instituto Meteorología de Portugal 2012).

2.2.1. The Canary Islands

The eastern Atlantic archipelago of the Canary Islands (Spain) offers a mild climate and distinctive flora and fauna. The Canary archipelago is constituted by seven main inhabited islands named from east to west: Lanzarote, Fuerteventura, Gran Canaria,

Tenerife, La Palma, La Gomera, and El Hierro, plus six islets. The first three mentioned are considered the eastern islands and the rest the western (see Fig.6).

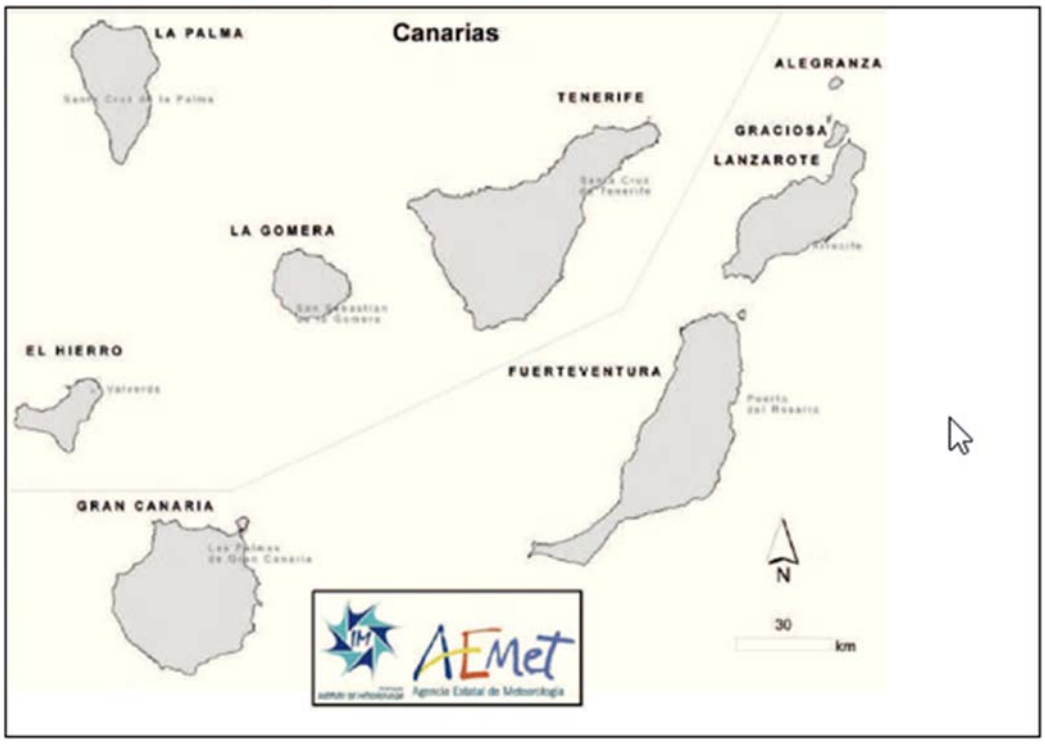

Fig.6. Layout of the archipelago of The Canary Islands (AEMET & IPMA 2012)

The western islands are green; however moving eastwards through the archipelago, the landscape become increasingly more arid.

The proximity to the Saharan desert, the influence of the Azores High, the Atlantic lows and the subtropical situations that from time to time reach this area, make the islands a strategical site. This densely populated oceanic archipelago has a combination of subtropical, semi-arid and semi-humid conditions (Sperling et al. 2004) with strong orographic, topographic, meteorological and ecological contrasts. The existence of four national parks on the islands and the declaration of Lanzarote, El Hierro and La Palma as an UNESCO biosphere reserves demonstrate such variety. It highlights the *National Park Garajonay*, on the island of La Gomera which offers the lushness of the *Laurisilva* forest.

It has been also suggested that the Canary flora is a relic of a subtropical Tertiary flora (Vargas 2007).

The climatology that joins with the abrupt relief have a marked effect over the vegetation distribution over the islands ranging from succulent plants at sea level to forests at the higher altitudes. The different elevation levels found in the islands are four. The first one is the surface from 0 to 200 meters, the second between 200 and 600 meters, the third is a medium altitude between 600 and 1000 meters and the last one is the high altitude between 1000 and 2371 meters. These levels have a narrow relationship with the main vegetation zones. In such a way that they can be identified respectively with zone of xerophytic shrub, zone of thermophile forest, zone of humid forest, zones of pines and zones of high mountains.

Furthermore, the existence, of two astronomical observatories El Roque de los Muchachos (ORM) in La Palma and El Teide (OT) (Teide Observatory) in Tenerife, both located at an altitude around 2390 m above the sea level , reveals the presence of clear skies with excellent air quality. The OT is situated at 16º30'35" West and 28º18'00" North. The ORM is situated on the edge of the Caldera de Taburiente National Park, with geographical coordinates 17º52´34" West and 28º45´34" North (Varela et al. 2008). The observations made from them have been monitored over several decades. The Carlsberg Meridian Telescope (CMT) at the ORM provides nightly values of atmospheric observations since 1984. Various studies have been performed with data obtained at this observatory (Varela et al. 2004, Varela et al. 2008, Sicard et al. 2010).

2.2.1.1. Geographic and topographic features

This archipelago is a Spanish autonomous community and an outermost region of the European Union. It is located in the Atlantic Ocean, northwest of African coast,

bounded by 27º37' and 29º30' N latitudes and 13º30' and 18º10' W longitudes. Their geographic position reaches about 1250 km from Mainland Europe. The difference in heights, the irregular layout of the ravines, the orientation of the mountain peaks are crucial factors that determine the rainfall, cloudiness and temperature distribution, giving rise to micro-climates between isles and in even different sectors of an island. All this is generated as the result of volcanic activity on the African continental shelf where these islands form a chain with a roughly linear arrangement extending about 500 km in the longitudinal direction. The geological history of the islands is characterized by different volcanic eruptions throughout the various phases of formation. The chronological transition, in the emissions of different types of materials during the volcanic eruptions, has highly conditioned the current landscape of the isles. Its eastern edge lies only 100 km from the Saharan coast. The orography and topography of the islands are highly variable, with sharp differences between them. The relief presents a high altitude compared to a small surface. The peaks rise towards the centre of the islands which are criss-crossed by a dense network of ravines in radial disposition. Elevation changes from a maximum height of about 3718 m.a.s.l., in Tenerife, to elevations rarely above 600 m in the eastern islands (Lanzarote and Fuerteventura).

Table 1: Surfaces of the Canary Islands in km and maximum altitude (m)

Island	Surface (km^2)	Maximum Altitude (m)
Lanzarote	845,94	671 (Peñas del Chache)
Fuerteventura	1659,74	807 (Jandía)
Gran Canaria	1560,10	1949 (Pico de las Nieves)
Tenerife	2034,38	3718 (El Teide)
Gomera	369,76	1487 (Garajonay)
La Palma	708,32	2423 (El Roque de los Muchachos)
El Hierro	268,71	1501 (Malpaso)

La Palma, Gran Canaria, El Hierro and La Gomera, also exhibit high elevations, close to 2400, 1950, 1500, and 1490 m, respectively. In general, the islands' orography is very rugged, except in the flat eastern islands. Table 1 summarizes the surface of the Canary Islands in km and maximum altitude (m) for each island.

Their almost latitudinal disposition and abrupt topography induce disturbances in the Canary Current and the North Atlantic trade winds persistent flow in which they are immersed.

2.2.1.2. Climatic characterization

Due to their position in the Atlantic subtropical belt, which is being dominated almost all year by the Bermuda-Azores High preventing transient disturbances as Atlantic lows, while producing a typical weather in the Canaries considered as stable and dry.

The islands are located about 4º from the Tropic of Cancer and influenced by the Intertropical Convergence Zone (ITCZ) known as meteorological Equator that nearly encircles the planet, oscillating between the Tropics of Cancer and Capricorn. The ITCZ is formed by the combination of heating and convergence forces aloft. It is identified by bands of clouds associated with the convergence of winds along the equator. The winds converging on the equatorial low-pressure trough are known generally as the trade winds, or trades. The northeast trade winds blow in the Northern Hemisphere from the Bermuda-Azores High and the southeast trade winds in the Southern Hemisphere from the S. Elena High. The first are displaced from the Canary and Cape Verde islands to the Antilles and the second are divided into two branches: the western one which feed the ZCIT and the eastern one that returns in order to penetrate into Africa, where it is absorbed by the Saharan Low. The seasonal migration of the ITCZ is represented in Fig.7. The trade winds pick up large quantities of moisture as they return through the Hadley circulation cell for

another cycle of uplift and condensation. The circulation pattern consist in winds rising along the ITCZ, moving northward and southward into the subtropics, descending to the surface, and returning to the ITCZ as the trade winds. During summer, a marked wet season accompanies the shifting ITCZ over various regions. In January, this zone crosses northern Australia and dips southward in eastern Africa and South America.

Fig. 7. Seasonal migration of the Inter-Tropical Convergence Zone (ITCZ).

(*http://www.geography.hunter.cuny.edu/~tbw/wc.notes/15.climates.veg/climate/A/seasonal.migration.ITCZ.jpg*)

The seasonal cycle of dust is directly linked to meteorological processes in the monsoon (Marticorena & Cairo 2006).The summer monsoon onset in western Africa is related with the displacement of the ITCZ to 10º N that takes place every year between the months of July and August (Sultan & Janicot 2003), being then when the Sahel receives considerable precipitation coinciding with the monsoon station in the northern hemisphere (*http://www.lodyc.jussieu.fr/~bslod/index.html*). The northern limit of the south-westerly winds of the monsoon is called the Intertropical Front (ITF). The monsoon winds are controlled by the gradient of pressure between the thermal low centred along the ITF and the high oceanic pressures governed by the anticyclone of Santa Helena. Such

thermal low is characterized by a maximum of positive vorticity and the confluence of humidity between the monsoon humid winds from the SW and the dry Harmanttan winds from the NE that are normally loaded with dust round 15º N in the ITF. Dust transport, from source regions, is directly related to the shift of the ITF (Sultan & Janicot 2003). The deep convection in the ITCZ is located southern of the thermal low, limited to middle and low levels of the troposphere. The establishment of the ITF corresponds to the monsoon pre-onset, contributing with humidity through isolated convective systems developed in the region Sudan-Sahel. The humidity in the middle troposphere and the strong winds in low levels are induced by the AEJ (African Easterly Jet) which also favours the duration of the convective systems in the region.

The area is affected by both coastal upwelling and Saharan mineral dust eolian inputs, which strongly influences their climate. Each island has a distinctive feature. An example is Gran Canaria Island with a central location in the archipelago. Severe weather is not frequent at the islands, but sometimes they are affected by high temperatures, dust events, strong winds and waves, heavy rains, hail or thunderstorms.

2.2.1.2.1. Temperature and sunshine

This is characterised by a low annual thermal oscillation in coasts and in the middle mountain region, approximately between 700 and 1500 m. The monthly average temperature of the coldest month (January) ranging from 6 ºC to 18 ºC and the monthly average temperature of the warmest month (August and September) exceeds 22 ºC (normal values for the period 1971-2000, AEMET) (Campos et al. 2011). Temperature is affected by cloudiness, altitude and orientation (Font-Tullot 1956). Annual temperature range is about 6 ºC to 7 ºC in coastal areas (Departamento de producción de AEMET & Departamento de Meteorología e Clima de IMP 2012). In spring it is dry, with about 26-

29 dry days on average and about an average daily of 7 or 9 hours of sunshine. With their oceanic climate, the islands are slightly warmer in spring than in winter. However, the daily average maximum temperature rises by May. During the summer months, the Canaries are hot, dry and very sunny and daytime average temperatures reach 29° C throughout the season. In summer, the average dry days are about 30 and the hours of sunshine are 11. The autumn brings a slow decrease of average maximum temperatures that are still about 24° C. By November, the islands are much wetter, with 21 dry days on average and also a reduction in the number of average sunshine hours to about six per day. In winter, the islands show an average maximum temperatures of 21° C coupled with about six hours of sunshine.

A spatial variability in annual temperatures among the islands is also noted mainly due to the orographic contrast. The warmest annual average temperatures are recorded in southern coasts where the annual mean is about 24 ºC. This is generally observed in Lanzarote and Fuerteventura, the flattest and driest islands where the maximum average daily temperature reaches 28 ºC. In the rest of the archipelago as the altitude rises the annual average temperature decreases reaching between 14 ºC and 9 ºC. In the *Cañadas del Teide* (Tenerife), the mean value is about 5 ºC. In some areas of La Palma Island the annual average temperatures are found bellow 10 ºC. Moreover, in the eastern islands the annual average temperatures are in general slightly higher than in the western ones. The annual average daily minimum temperature in the islands is roughly 18 ºC (Departamento de producción de AEMET & Departamento de Meteorología e Clima de IMP 2012).

2.2.1.2.2. Humidity and cloudiness. Inversion layer

The proximity to the Sahara desert converts the archipelago into a very complex scenario. A subsidence inversion approximately between 700 and 1500 m often exists.

The presence of this inversion layer is crucial in the air mass flows that reach the islands (Varela et al. 2008). Above the inversion layer, the air is dry and clear. A temperature inversion occurs when the normal temperature decreases with altitude (normal lapse rate) and begins to increase with a certain altitude. This can happen at any point from ground level to several thousand meters. The normal profile permits warmer less dense air at the surface to rise, but the warm air inversion prevents the rise of cooler denser air underneath. The trade-wind inversion layer separates two very different air masses: the maritime mixing layer (MML) and the free TL (Troposphere Layer) (Torres et al. 2001). Below the inversion layer, the presence of a fresh and humid boundary layer explains the marked contrast between the windward side with green valleys in the north and the leeward side of the islands with sandy beaches. Vegetation zones can be classified into humid and semi-arid types (Juan et al. 2000). Moisture is condensed when prevailing trade winds reach the higher islands bringing cloudiness, humidity and at times rain to the northern sectors. Hence, northern locations are generally dull, wet and cloudy, while the southern ones are characterised by dry clear days with sunshine. Rain is a consequence of this inversion layer rupture, and then convection is present.

2.2.1.2.3. Precipitation

The main feature of the rainfall regime in the Canaries is its irregularity. The location of the islands, far from the belt of low pressures in the medium latitudes, explains the low rate of precipitation throughout the islands. However, the combined effect of the trade winds and the abrupt relief makes some places in these islands much wetter than the normal pattern at this latitude. The average precipitation regime shows a strong seasonality with maximum monthly rainfall during autumn and winter, with January and February the rainiest month, and dry or rainless months in spring and summer being July

and August the driest ones. The rainy season ranges from October to April, when the high centres of pressure move towards the north allowing some disturbances to reach the area.

Most of the North Atlantic cyclonic activity is restricted to the high latitudes between 50º and 70º N. Surface low centres located at 30º northward of the Canary Islands latitude hardly ever affect the area directly, especially at low levels. The average surface low number over the influence area is only about 12 disturbances per year with a central averaged pressure greater than 1006 h Pa (García-Herrera et al. 2001). Rainfall is generally low throughout the islands. Rain events only happen when disturbances break the inversion layer, either at the surface when Atlantic lows reach the area or at upper levels with the influence of troughs.

The relief is one of the critical variables controlling the local rainfall distribution. In general, precipitation increases across the archipelago from east to west. Frontal tails associated with surface (Vacher & Rowe 1997, Elsner & Kara 1999)the eastern islands are characterised by dry and stable meteorological conditions almost all year round and are quite arid (García-Herrera et al. 2001, García-Herrera et al. 2003). The common characteristic of the western islands is high elevations, which amplifies any atmospheric disturbance, making these islands very sensitive to weather variations. By the contrary the eastern ones, where the relief is not a triggering factor, require deeper disturbances in order to witness precipitation. It preferably rains at the northern sides. The south of the islands tends to be hotter and drier, though rainfall is generally low throughout the islands. It can be observed maximum average annual rainfall values exceeding 1000 mm in high altitudes of the island of La Palma. The lowest values, less than 100 mm, occur on the southern coasts of the main islands. The average annual number of rain days (with precipitation greater than or equal to 0.1 mm) increases with elevation with more than 50

days. However, the lowest annual mean of rain days is less than 10 days per year, relates to the southern coast of Gran Canaria (Departamento de producción de AEMET & Departamento de Meteorología e Clima de IMP 2012).

Heavy rainfall in the islands is due mainly to the presence of cut-off lows. These perturbations often begin as a trough in the upper levels that becomes a closed circulation that extends to the surface. A branch or closed circulation can be separated and isolated from the subtropical jet when it becomes sharply undulate. As a result of this process closed circulations are generated. Such depressions are formed at high levels within their own circulation losing contact with those associated within the subtropical jet moving independently. Then, cut-off lows have a characteristic cycle of life. They generate at high levels associating with a process of undulation, separation, and break with the subtropical jet. Behaving as isolated and cyclonic systems reflected in high and medium levels (300 and 500 hPa). These disturbances retain some of the characteristics of the circulation that originates them: at the left side a core of cold air is present at middle levels, while on the right side the air is warmer (Martín-León 2003).

In sporadic occasions, large amounts of rainfall that land on the islands are associated with tropical systems. Nevertheless, most of the rainfall affecting the islands is due to the pass of Atlantic lows with cold or warm associated fronts.

Snow and ice is only present in the peaks of Tenerife, La Palma and rarely Gran Canaria and can be observed in winter and rarely in October and April. Hail is hardly ever observed but can be observed throughout the archipelago.

2.2.1.2.4. Surface winds

The predominant wind pattern is from the NE, known as the trade winds, which are blowing over the Atlantic from the northeast for almost the whole year and driving one of the major coastal upwelling ecosystems in the world along the NW African coast (Fernandopullé 1976). The trade winds blow mainly during summer to the north side of the islands, adverting wet and fresh air, dominating the area at a frequency of 95% during the summer, mainly in June and July, and at about 50% the rest of the year.

There at the upper levels the circulation flows NW at 700 hPa and W-NW at 500 hPa from November to June.

2.2.1.2.5. Visibility

Because of their geographical location, being so close to the western African coast, dust outbreaks streaming from the Saharan Desert at times will also affect the islands air visibility.

2.2.1.2.6. Dynamic climatology. Typical synoptic situations

The climate of the Canary Islands is basically modulated by the Azores High. The permanent north-easterly surface flow is the main feature during the summer, occurring from mid-May to the beginning of October when trade winds blow with the highest intensity of the year. The stable anticyclone of the Azores Islands and a relative system of low pressures in the north of Africa allow such situation. In summer, the Azores High moves north-west preventing low pressure systems associated with rainfall affecting the area. A typical synoptic pattern affecting both archipelagos the Canaries and Bermuda during the summer is shown in Fig.8.

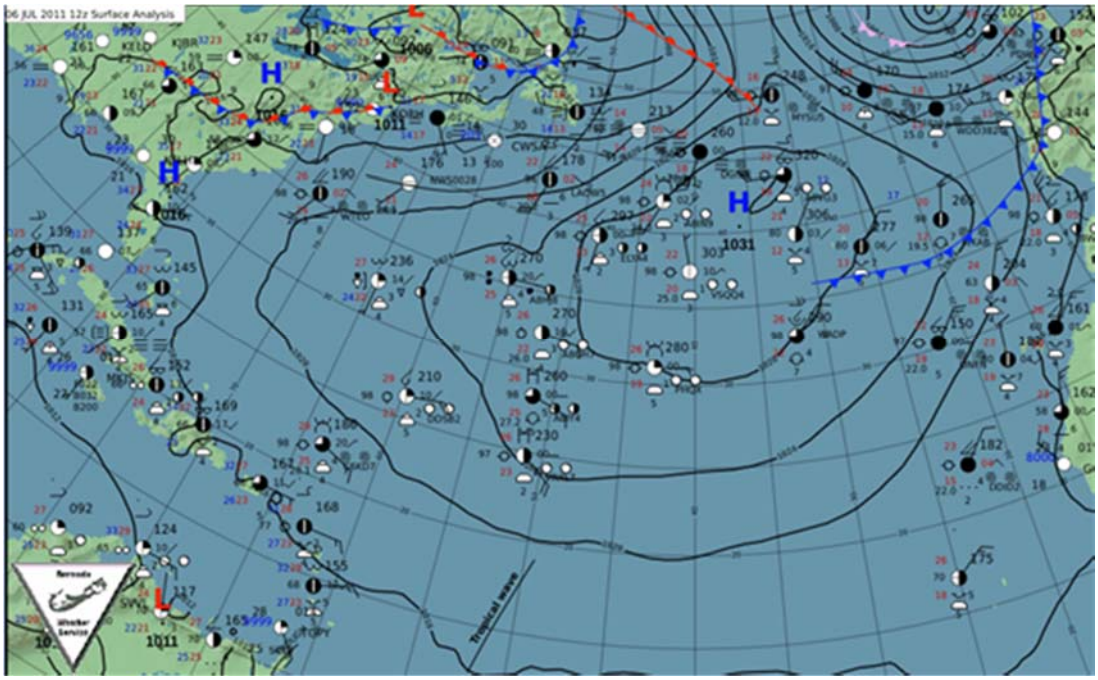

Fig.8. Typical synoptic pattern for the Canary Islands and Bermuda during the summer. 06 July 2011. Surface Analysis (BWS)

This favours some lows from the North of Africa entering towards the islands. Extreme weather conditions such as heat waves occasionally affect the archipelago mainly during August. In autumn, from the beginning of October to middle December, the Azores High moves lightly towards southern latitudes allowing some perturbations to affect the islands. The frequency of the trade winds drops and its intensity weakens. High pressures accompanied by maritime polar air prevail in the islands. However, some systems of low pressure from the Southern Atlantic area or cut-off lows reach the archipelago. Tropical perturbations can be rarely observed in this season. Low frequency continental air irruptions can be also observed.

During wintertime (from mid of December to beginning of March) the Azores High moves towards southern latitudes reaching around February the parallel 35° north latitude and cold frontal systems associated with cold depressions affect the Canaries. The sub polar low pressure belt descends also towards the southern latitudes. Although

anticyclonic circulation dominates when compared to the cyclonic one, the frequency of north-easterly surface flow is the lowest of the year. However, Atlantic lows affect the area and cut-off lows are frequent from November to January. Such perturbations bring surface circulation from the fourth quadrant. Irruptions of cold air from northern latitudes, maritime south western air and tropical air are present in winter.

During spring season, from the beginning of March to the end of May, some perturbed situations affect the islands as low intense maritime polar air mass which is present from February to May. In April the Azores High begins to migrate north-western, then surface flow from the western and north western sectors prevails.

The following typical synoptic situations can be considered as characteristic weather types in the Canaries:

A. Non-perturbed situations:

A1. Trade winds

A2. Islands between two systems of low pressures

A3. Saharan invasions

B. Perturbed situations:

B1. Cold depressions

B1.1. Situated in the N, NE or E of the Canary Islands

B1.2. Situated in the SW, W or NW of the Canary Islands

B2. Mobil trough with fronts

B3. Mobil trough without fronts (irregular situations)

B4. Cut-off lows

B5. Subtropical depressions

B6. AEW (African Easterly Waves)

Apart from these typical synoptic situations, maritime polar air mass commonly passes the archipelago except during the summer.

A. Non-perturbed situations. Among the non-perturbed situations are: the trade winds regimen, islands between two systems of low pressures and Saharan invasions.

A1. Trade winds: On the surface, a very stable system of high pressures appears close to The Azores Islands and relative low pressures in the north of Africa. It stands up, mainly during the summer, an orographic dipole in Africa, near the Atlas Mountains. At high levels, there is often a ridge at the west side of the islands, as the dominant wind blows from the NW and subsidence prevails over the area.

•**Surface wind pattern:** Normally, regular and not gusty winds dominate the region. The privileged direction is NNE with intensity between 8 and 10 m s^{-1} during the day and from 5 to 8 m s^{-1} at night.

•**Cloudiness and precipitation:** There is a remarkable stability associated with a semi-permanent thermal inversion with a base between 900 m and 1600 m. Temperature increases across this layer up to 6 ºC (42.8º F), acting as a lid that obstructs any convective development. Water vapour is condensed at low levels, under the inversion layer, developing no precipitating thin clouds, which are called *sea of clouds* (Font Tullot 1956) when viewed from higher elevations of the clouds. The cloud base is stable at nearly 600 or 900 m, being lower at night and rising during the daytime due to warming. The subsidence inversion limits a superficial wet layer in which develops a layer of stratocumulus by turbulence. Under these weather conditions, there is an absence of significant precipitation. The typical cloudiness comes from N-NE due to the trade winds.

•**Visibility:** In general, it is good. Sometimes slightly reduced by brume or haze of dust when the air has a continental trajectory.

Trade winds prevail during the summer with a frequency higher than 90%, thus being considered as the normal weather in the archipelago.

A2. Islands between two systems of low pressures, low height gradient.

This is frequent during winter. It is characteristic of a breeze regimen. In a synoptic situation with a lot of clouds calms and changeable low winds prevail.

A3. Saharan invasions. These are situations that may occur year round. However, they affect in winter the low levels and in summer the middle and high elevations. Its durations may be from a few days or even up to two weeks. In high levels, usually there is a ridge over North Africa, Western Europe and the Mediterranean Sea. Normally a trough is situated at the NW of the Canary Islands while on surface the anticyclone is reflected, displaced towards Western Europe reaching, at times, the Mediterranean Sea and North Africa. The African low pressures move towards Saharan and North Mauritania and even to the Atlantic Ocean. It established an easterly flux over the Canary Islands with a continental origin. The mass of air penetrates with winds of the 2nd quadrant from the Saharan desert. The eastern islands are mostly affected by Saharan dust invasions, but they can occasionally reach the western ones. In summer, the Bermuda-Azores High moves to the NW allowing some systems of low pressure from the North of Africa affect the islands. Air masses in both low and medium levels are generated over the continent as a consequence of significant warming over the African continent due to convection. Then dust stemming from the Saharan desert is transported reaching the higher elevations of islands. However, during the winter the anticyclone of the Azores experiences a weakening and it is displaced from its normal position (Díaz et al. 2001). Along with this situation, together with the establishment of a system of low thermal pressures close to the western African coast affecting the Canaries and high pressures over northern or

north-eastern Africa in all favour dust outbreaks over the islands at low levels.

The synoptic configuration, which induces the strongest entries of dust at low levels, responds to the location of a strong anticyclone affecting northern or north-western Africa located at western Algeria, southern Morocco, Western Sahara or northern Mauritania. This system is often accompanied by a depression in the vicinity of the archipelago, preferably situated at the south or southwest of the islands. Such situation generates south-easterly winds favouring the dust invasion over the archipelago. Winter temperatures over the continent are lower than in summer and African air masses are generated in low levels without convection towards medium levels. This explains that the dust advection affecting the islands was forced by the wind reaching lower elevations.

•**Surface wind pattern:** Normally, irregular and gusty winds are characteristic of this synoptic situation. The privileged direction is E-SE with an average speed of 5-8 m s^{-1} during the day and 3-6 m s^{-1} at night.

•**Temperature and stability:** Firstly, they are present between 500 and 1000 meters above sea level and are propagated towards the surface while the superficial wet layer is removed. These situations are associated with strong warm advections which reinforce thermally the trade inversion. At 850 hPa temperatures may be higher than 28 ºC during the summer although under 1000 ft (304m), without reaching the surface, it can reach temperatures near to 40 ºC. In some occasions, the African flux doesn't replace the wet layer over the sea, rising above it. Then the rises in temperatures are not perceptible in the surface. During the winter, the air stemming from the E or SE is dry and relatively fresh.

•**Cloudiness and precipitation:** There is absence of low clouds. However, frequently high and medium clouds are observed. It scarcely rains, but occasionally there may be

dry storms when a trough in high levels is situated in the W of the archipelago with a diffluent flux over the islands.

•**Visibility:** Is reduced by haze or suspended dust, often between 5 and 10 km. Sometimes, lower visibilities of about 3-5 km and rarely lower than 1000 m may also be observed. It used to be worst during the central hours of the day, probably caused by a high molecular agitation or a wide light dispersion.

B. Perturbed situations. They take place when the ridges at high levels make way for troughs or isolated lows (cut-off lows), by perturbing the atmosphere and breaking the thermal inversion that inhibits the convection. This is quite a frequent occurrence between the months of October and March being more usual from November to February.

B1. Cold depressions. Most of them are derived from the rupture of the polar front and also accompanied of a cold frontal system. Heavy rainfall and strong winds enhanced by the orography factor are associated in these situations.

B1.1. Situated in the N, NE or E of the Canary Islands. This is the most common perturbed situation affecting the islands. They occur from November to February and last only a few days. In high levels, there is a close depression with temperature at 500 h Pa between -16 and -24 ºC. On the surface the isobars show a cyclonic gyre at the N or NE of the islands.

•**Surface wind pattern**: Prevailing winds blow from the NW or N. They are in general weak or moderate.

•**Cloudiness and precipitation:** They are Cumulus and Cumulonimbus, isolated in general and with high bases (usually above 600 m). The convective activity stands out at dusk, being less evident during the day. Weak showers of short duration and some storms are the more usual ways of precipitation.

•**Visibility:** In general is good, except at intervals of 5000 meters due to showers during a short period of time.

B1.2. Situated in the SW, W or NW of the Islands. These are the situations which provide the most intense and widest precipitations over the islands. At high levels, a low is observed centred in the W, NW or SW with a cold core between -16 ºC and 24 ºC in 500 h pa. On the surface, it is reflected as a closed low slightly ahead of the position of the perturbation at high levels. There is a strong instability, organized convection and wide precipitations. Organized lines of storms sweep the islands from SW to NE. Fronts hardly ever occur.

•**Surface wind pattern:** The synoptic flux is S in all levels, being wet and warm at lower levels with enough thermal forcing. Winds are moderate but with strong variations and gusts.

•**Cloudiness and precipitation:** Are frequent, with wide Cumulus and Cumulonimbus, characterized by bases no lower than 500 ft. (152 m) occasionally strong showers and storms are observed.

•**Visibility:** In general is good, except at intervals of 5000 metros due to showers, and occasionally at 1000 m during the most intense precipitations.

B2. Mobil trough with fronts. Related to maritime irruptions of polar air. At high levels a trough is observed moving quickly from the W. On the surface, a closed low is located at the north of the islands, generating a north-westerly flow with a cold front associated. The islands remain in a region of dynamic forcing under the cold advection. Such irruptions are often associated with anticyclone systems.

•**Temperature:** Drops significantly in upper levels and the inversion layer weakens.

•**Surface wind pattern:** The general synoptic flux is W or NW, weak or moderate.

•**Cloudiness and precipitation:** There are frequent Nimbostratus and Cumulonimbus with bases between 500 and 800 m. Continuous precipitations are observed. Rainfall favoured by the orography can be heavy.

•**Visibility:** It is in general about 8 km during the precipitations, being only 4000 or 5000 m during moderate or strong showers.

B3. Mobil trough without fronts. Here we can considerer all those situations which have in common the presence of a shortwave trough in high levels which produces a notable forcing and instability. On the surface the situation can be extremely variable.

B4. Cut-off lows. The cut off lows affecting the islands are more frequent from November to January.

B5. Extra or Subtropical depressions. Hardly ever, the Canary Islands are affected by the perturbations generated in the ZCIT which at the end of the summer is in its more northern position. Such disturbances can move towards the islands immerse in the eastern circulation. Then the subtropical anticyclone is displaced from its normal position and in upper levels the African High dominates and a trough from the North Atlantic reaches the islands. An example is the extra tropical depression Delta (27th -29th November 2005) with strong winds associated (maximum surface wind gusts in 1-minute of 200 km/h in the Izaña observatory (Tenerife island) with an elevation of 2371 m. (Martiín et al. 2007).

These violent winds resulted in additional widespread tree, utility, structural and property damage. There were some reports of considerable injury to homes, roofs, vegetation and ships. Power outages telephones and power cut were also associated with this storm. The track of this storm forecasted by The NHC (National Hurricane Centre) is show in Fig.9.

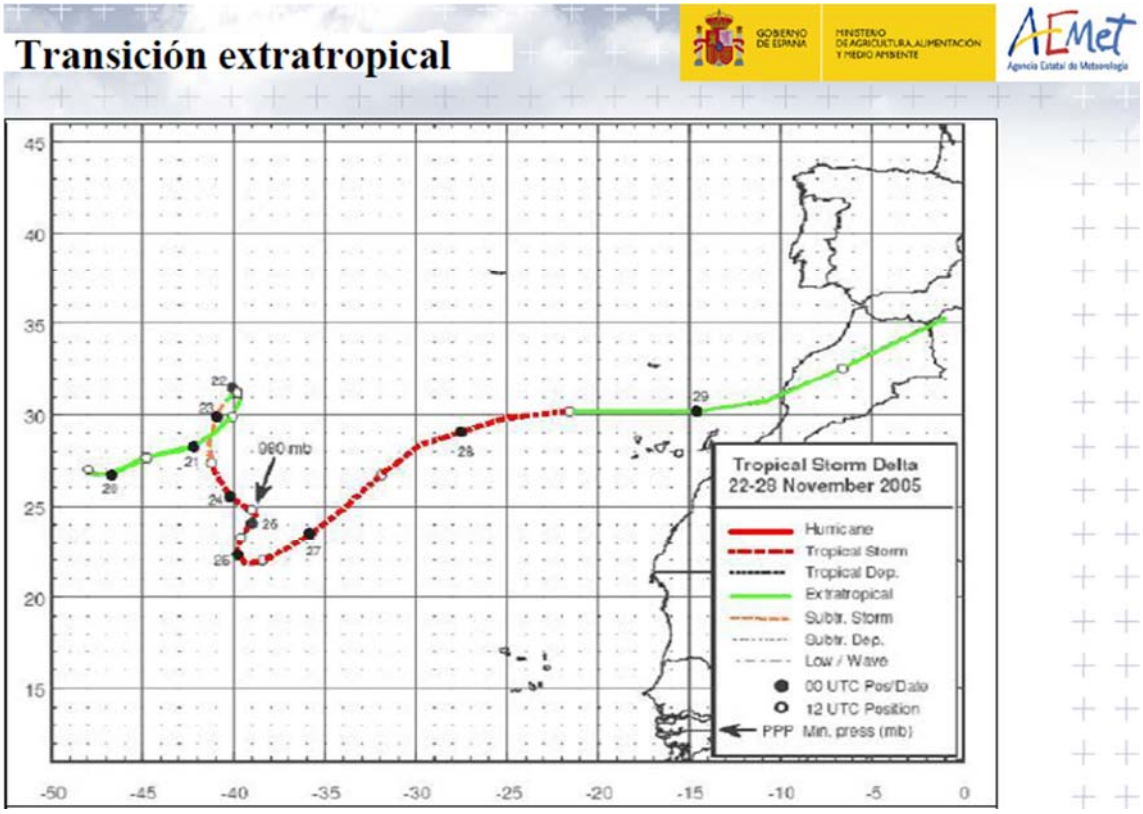

Fig.9. Track of the extra tropical depression Delta (27th -29th November 2005) (Best Track NHC)

Another example is the hybrid system which suffered a transition from extra tropical to subtropical cyclone and affected the islands between 26th January and 4th February 2010 followed by heavy rain and significant thunderstorm activity affecting the area. The abrupt orography helped to increase the efficiency of the convective rain and severe weather was witnessed in the area. A total amount of precipitation of 610 mm/m^2 was recorded in 72 hrs. on the Gran Canaria Island. This pattern characterized by interactions between subtropical lows and baroclinic lows associated with strong winds over the Canaries have been observed in other situations, for instance on 13th -15th December 1975.

B6. AEW (African Easterly Waves). Some synoptic configurations related to Saharan dust and observed during the summer are determined for the establishment of a general eastern current that corresponds to the circulation in the meridian side of a wide

anticyclone. They are located between southern Europe and northern Africa, its central region extends from Western Europe to the Atlantic Ocean, reaching the longitude 30º W (Font Tullot 1956). Sometimes the Canaries are affected by an eastern flow related to the southern part of this anticyclone. Such eastern currents are associated with tropical disturbances known as *AEW* (*African Easterly Wave*) (Prospero et al. 2005), characterized by a deformation in the isobaric field appearing troughs more or less defined, that move from the east to the west. They play an important role in the convection over western Africa and responsible for the transport of dust from the continent towards the Atlantic Ocean, this occurrence is found between May and October, generally in August and September being concomitant with the station of greater precipitation in the *Sahel* (Fontaine et al. 1995). Such disturbances consists in systems of low pressure that move horizontally reaching its maximum amplitude at 750 hPa and are originated from the presence of a jet in the middle troposphere in the African region about 16ºN and between 700 and 650 h Pa., causing the instability associated with the AEJ (*African Easterly Jet*) favouring its energetic source to the development of these. A trough in the AEJ (approximately around 0º W) can represent a vortex in the southern side of the *Easterly Wave.* The shift of such waves is produced above the line of 15º N and the ones that pass southern of it transport humidity and generate convection inducing precipitation. During the summer season, a layer of air located at 500 h Pa over Africa, associated with these waves moves forward to the west from the north-western Africa, being intercepted by the maritime mixing layer turning into the named SAL *(Saharan Air Layer) (Dunion & Velden 2004)*. Once it reaches the ocean its base is about 900 to 1800 and its top is about 5000 meters (Diaz et al. 1976). The frequency and quantity of precipitation over the *Sahel* is often regulated by the pass of these waves that propagate towards the west closely

related to the AEJ (Lare & Nicholson 1994). Its presence towards the south plays an important role in the occurrence of a late summer monsoon and in the hurricanes genesis. However, those that pass 15º N provide dry and warm air from the Sahara transporting tons of dust while traveling westward with the trade winds. In approximately one week such waves can transport dust to the Gulf of Mexico and Florida having a life from 3 to 4 days (Carlson 1969). Such perturbations are often present with the establishment of an orographic dipole over the Atlas Mountains and convergent of a wind over the African coast which favours the dust entry over the Canary archipelago. While the disturbance is over the African continent, they are very effective in raising lots of dust that can be transported towards the islands by easterly winds. An example of this type of situations was observed between 31st of July and 03rd of August 2000. Easterlies surface winds between 20-28 km/h were observe and the visibility reduced to 3000 metres. Such situations can also produce heavy rainfall, strong winds and thunder storms. In conclusion, Canaries constitute a unique and highly complex environment to explore space and time properties of processes related to the atmospheric dynamics.

2.2.1.3. Oceanographic conditions

The oceanographic conditions affecting the islands are mainly determined by three factors: the cooler Canary Current, the eastern influence of North Atlantic subtropical gyre and the upwelling off Northwest Africa.

Their oceanic position plays an important role in the temperature conditions, the sea acts as a thermo-regulator and as a source of humidity and as well as in the wind conditions. In fact, in absence of a gradient and with enough sunshine, a marine breeze rises as a consequence of the thermal difference between the air above the sea and the land. Firstly, the cooler Canary Current that flows along the African coast from north to south between

30° N and 10° N and offshore to 20° W (Fedoseev 1970). It reaches its maximum intensity during summer and the coldest waters are in the most eastern longitudes. Among other important factors, this current is responsible for inducing atmospheric stability. Therefore, it reduces the probability of subtropical system development and the occurrence of heavy winds or rainfall.

In addition, the Azores Current, reaching Madeira in the north and flowing southward along the African coast also contributes to understand the oceanographic dynamic of the area (Wooster et al. 1976). Secondly, eastern influence of North Atlantic subtropical gyre and thirdly the upwelling off Northwest Africa. Cold waters near the Sahara coast show nutrient enrichment detected by high chlorophyll values. Summer SST (Sea Surface Temperature) ranges from 22° C to 24° C and winter from 17° C to 19° C, where these values are considered lower than might be expected for a subtropical region, principally due to the cold upwelling (Fernandopullé 1976) increased by the trade winds regimen during summer (Wooster et al. 1976, Van Camp et al. 1991).

The large and permanent upwelling and the broad continental shelf make the Saharan Bank (West Africa, between 21º N and 26º N latitude) (Balguerías et al. 2000) one of the richest fishing grounds in the world.

2.2.2. Madeira

2.2.2.1. Geographic and topographic features

This archipelago is located in the North Atlantic Ocean, at 33º10´ to 32º20´ north latitude and 17º20´ to 16º10´ west longitude, about 980 km from Portugal and 100 km from Africa. It is composed by two main islands (Madeira which covers an area of 728 km^2 and Porto Santo Island with 42 km^2 and groups of very small inhabited islands (Sundseth 2009). Elevations change from the main island which has a steep topography

with a maximum height of 1862 m a.s.l. (*Pico Ruivo*) to lesser heights at islands such as Porto Santo with peaks about 500 m a.s.l. The constitution of the archipelago of Madeira is shown in the bottom-left corner of Fig. 10.

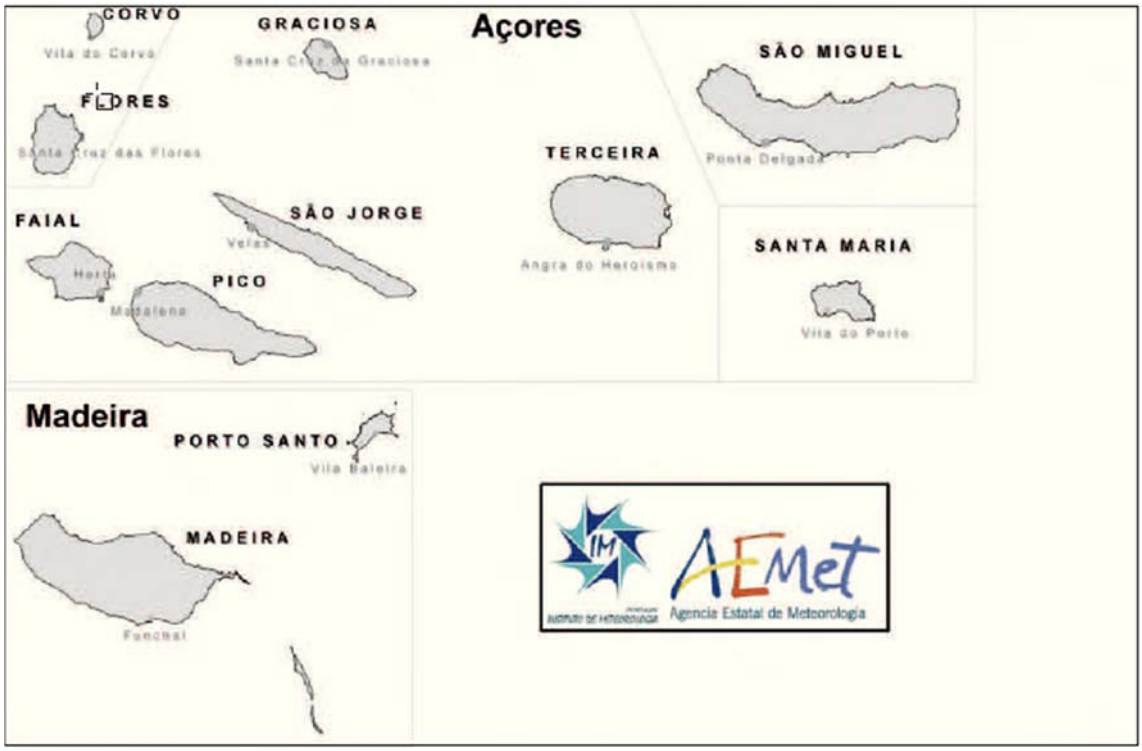

Fig.10. Layout of the archipelago of the Madeira and Azores Islands. (AEMET & IPMA 2012)

2.2.2.2. Climatic characterization

2.2.2.2.1. Temperature

Madeira is characterized by a mild climate. Mean annual air temperature varies between 8 ºC and 12 ºC at the highest altitudes and between 14 ºC and 18 ºC in the coastal regions. February is the coldest month and August the warmest one. The maximum air temperature values in summer oscillate between 17 ºC at high elevations and 26 ºC in coastal areas. The annual ranges of the averaged minima temperatures are between 4 °C and 8 ºC (Departamento de producción de AEMET & Departamento de Meteorología e Clima de IMP 2012).

2.2.2.2.2. Precipitation

As in Canaries, the northern and western sectors are much wetter than the southern and eastern ones where a larger amount of precipitation at higher altitudes can also be observed. Madeira is the rainiest island, since precipitation is strongly influenced by orography observed as an annual average of about 590 mm in Funchal. December and January are the wettest months. The dry period is short, covering only the month of July, whereas during the summer (June to August) the values of the average rainfall are low. The greatest number of rain days is observed at high elevations of Madeira (188 rain days per year) (Departamento de producción de AEMET & Departamento de Meteorología e Clima de IMPA 2012). The archipelago is snow and ice-free. Hail is rarely observed. During autumn and winter the precipitation regime in Madeira is caused by the passage of mid-latitudes systems, such as extratropical cyclones and frontal systems (Couto et al. 2013).

2.2.2.2.3. Surface winds

North is the most frequent wind direction at low levels due to the influence of the Azores high pressure system during the whole year. The westerly surface flow also affects the islands associated with the Atlantic lows (De Lima & De Lima 2009).

2.2.2.2.4. Dynamic climatology. Typical synoptic situations

The High pressure of the Azores dominates the North Atlantic (subtropical) Ocean (mainly during the summer), except when some Atlantic depressions reach the islands.

2.2.2.3. Oceanic conditions

The SST (Sea Surface Temperature) in Madeira is influenced by The Gulf Stream oscillating between 17 ºC in winter and 22 ºC in summer (Báez & Sanchez-Pinto 1983).

2.2.3 The Azores Islands

2.2.3.1. Geographic and topographic features

The Azores Islands are located between the latitude 37º to 40º N and the longitude 25º to 31º W and they have a total geographical area of about 2330 km^2. The nine islands that constitute the Azorean archipelago are from the biggest to the smallest: São Miguel (with 746.79 km^2), Pico (with an area of 436 km^2), Terceria, São Jorge, Faial, Flores, Santa Maria, Graciosa and Corvo (17.12 km^2). These islands are relatively distant from the others, and they are the most occidental territories of Portugal and Europe. The eastern islands are Santa Maria and São Miguel. Terceira, Graciosa, São Jorge, Pico and Faial have a central location in the archipelago and Flores and Corvo are the western ones. The topography is relatively gentle with undulating hills and peaks. Due to the islands volcanic origin, their landscapes are dominated by calderas with volcanoes and lagoons. In Pico Island stands out a volcano that reaches a height of 2351 m., as well as in Faial where its central caldera reaches 1043 m. The layout of the archipelago of Azores is shown in the above Fig. 10.

2.2.3.2. Climatic characterization

2.2.3.2.1. Temperature and sunshine

Winters are mild, with average values similar to Madeira. Temperatures rarely fall below 0 °C only at high elevations (The Pico Island). The average temperature is about 14 °C in January or February (the coldest months) and in coastal areas between 4 ºC and 8 ºC at higher altitudes. The mean temperature in August, the warmest month, is about 22 ºC in lower regions. In summer the average maximum air temperature ranges between 18 ºC in higher regions and 24 °C in the lower ones. The mean annual minimum temperature varies between 4 °C and 8 ºC at higher altitudes, and decreases below 0 °C in Mount Pico,

with values above 12 ºC in low regions (Departamento de producción de AEMET & Departamento de Meteorología e Clima de IMP 2012). The hours of daily and annual sunshine are short (Báez & Sanchez-Pinto 1983).

2.2.3.2.2. Precipitation

As in the Canaries, the distribution rainfall in Azores increases from low to high altitudes and from eastern to western regions. Azores is the wettest archipelago in the Macaronesia, where they have a numerous amounts of lakes, pools, temporary ponds and mountain streams (Sundseth 2009). The highest average annual rainfall value has been registered at Flores Island (1665.6 mm) and the lowest at Santa Maria Island (729.5 mm). The Pico Island is the rainiest one with locations, where annual rain values greater than 4000 mm have been recorded. November, December and January, are the wettest months where June to August are the driest ones. As in Madeira the dry summer season is very short. In some of these western islands there are no dry seasons. The number of rainy days is high. The highest number has been recorded on Flores Island with roughly 120 days per year (Departamento de producción de AEMET & Departamento de Meteorología e Clima de IMPA 2012). Snow is only observed at the highest peaks.

2.2.3.2.3. Surface winds

Trade winds affect mainly the eastern islands while central and western ones are more influenced by a south westerly surface flow (Báez & Sanchez-Pinto 1983).

2.2.3.2.4. Dynamic climatology. Typical synoptic situations

2.2.3.3. Oceanic conditions

The bathymetry is very irregular with submarine volcanoes and abrupt slopes. The SST varies between 16 ºC in winter and 23 ºC in summer (Báez & Sanchez-Pinto 1983).

A more detailed description of the climatic characteristics of the Macaronesia can be found at the following website:

(*http://www.aemet.es/es/conocermas/publicaciones/detalles/segundoAtlas_climatologic*)

3. Data sets

3. Data sets

To describe the rainfall variability in the North Atlantic subtropical area, the rainfall data sets from Bermuda and the Macaronesian area have been analysed. The weather stations used are represented in figure 11 which can be also found in the Annexe I. The whole North Atlantic Ocean with the stations located at Bermuda, Madeira, Azores and the Canary Islands is shown in figure 11A and the Canary Islands (Lanzarote, Fuerteventura, Gran Canaria, Tenerife, La Palma, La Gomera and El Hierro) with the selected stations are represented in more detail in figure 11B.

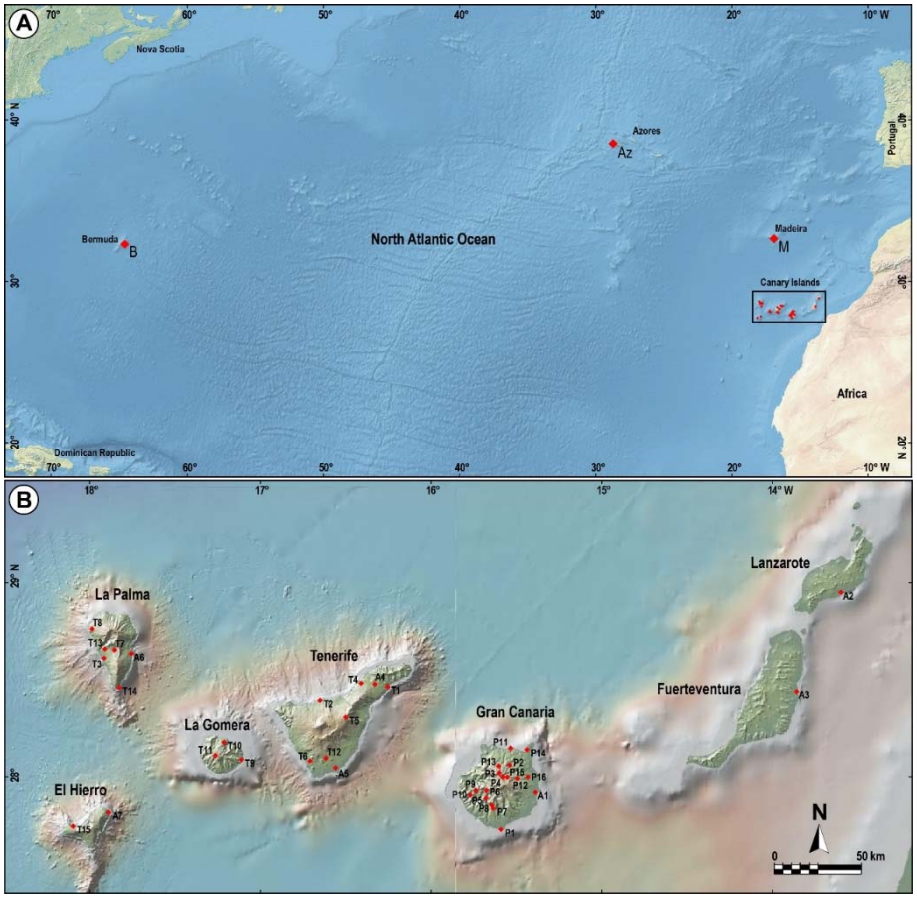

Fig.11. Weather stations used for this study. A) North Atlantic Ocean (Bermuda, Madeira, Azores and the Canary Islands) and B) The Canary Islands (Lanzarote, Fuerteventura, Gran Canaria, Tenerife, La Palma, La Gomera and El Hierro) (This figure can be found in a larger size in the Annexe I).

Data sets of Bermuda have been provided by BWS (Bermuda Weather Service) (*http://www.weather.bm/)*, of the Canary Island by AEMET (Agencia Española de

Meteorología) in Spain (http://www.aemet.es/) and Consejo Insular de Aguas de Gran Canaria (http://www.aguasgrancanaria.com/). Data of Madeira and Azores have been given by IPMA (Instituto Portugues do Mar e Atmosfera) (*https://www.ipma.pt*).

Samples cover an average of fifty years, however emphasis was made in the common normal period 1981-2010.

3.1. Bermuda

Daily and hourly rainfall values recorded in four different weather stations are used to carry out the analysis of the rainfall in Bermuda. The locations of the rainfall gauges are represented in Fig.12. Observations of daily rainfall are nominally made at 9 am local time and measuring the total precipitation for the preceding 24 hours. The minimum amount of rainfall recorded was 0.254 mm.

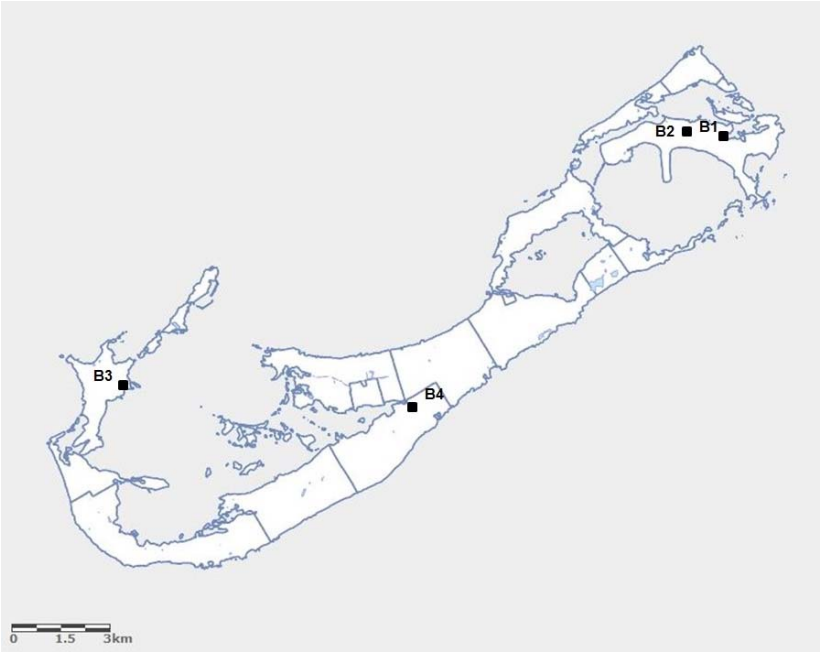

Fig.12. Weather stations on Bermuda used for this study: .B1 (Naval Air Station), B2 (Bermuda Airport), B3 (Somerset Village) and B4 (Dept. of Agriculture and Fisheries)

The recording periods, geographical locations, as well as codes used to designate each gauge are given in Table 2.

Table 2. Weather stations selected for the rainfall analysis in Bermuda. Sta. code (station code used in this work), Sta. name (Station name), Acr. (Acronym used in the study), Elev. (Station elevation in m), Loc. (Location), geographical coordinates (Lat.N and Log.W: Latitude North and Longitude W respectively in sexagesimal format), Period (recording periods of measurement stations). Stations: Naval Air St. (Naval Air Station), Bermuda A. (Bermuda Airport), Somerset V. (Somerset Village) and D. Agric. & Fish. (Department of Agriculture and Fisheries).

Sta. code	Sta.name	Acr.	Elev.(m)	Loc.	Lat.(N)	Lon.(W)	Period
B1	Naval Air St.	NAS	7	NE	32 21 50	64 40 09	01/01/1949-28/05/1995
B2	Bermuda A.	BA	36	NE	32 22 01	64 40 38	31/05/1995-31/12/2011
B3	Somerset V.	SV	25	NW	32 17 44	64 51 45	01/01/1974-29/06/2011
B4	D.Agr. & Fish.	A&F	23	C	32 17 34	64 45 44	01/01/1968-31/06/1970

Two of the daily rainfall time series are relatively short (BA: 16 years and 4 months, and A&F: 2 years and 6 months), and have been used just to complete and extend the longest available sequences (NAS: 46 years and 5 months), due to their spatial proximity. In this sense, it is particularly noteworthy that the distance between stations is less than 20 km and the altitude differences is lower than 30 meters. This is especially true for stations located at Main and St. George islands; in this case distances are less than 15 km and the altitudes do not vary more than 13 m. Hence, taking into account the dimensions and flatness of the islands, it is reasonable to expect a very similar rainfall patterns at the various stations of measurement, as well as over the entire archipelago.

As in any other field of earth sciences, the completeness and length of rainfall records is of the utmost importance to perform studies of variability on annual and inter-annual scales. Hence, characterization of rainfall regime at a given area requires complete time series spanning over long periods. Frequently, to meet these requirements, it is mandatory to refill eventual gaps and enlarge data sets as much as possible. A variety of methods can be employed for filling data gaps. However, the recommended approach for

this, and to extend data series, is to use data from nearby stations and rescale it in attempting to match various statistical characteristics.

The longest time series with a north-eastern position at the archipelago is from the Naval Air Station (NAS) covering 46 years from 1st January 1949 to 28th May 1995, where the gauge was initially placed approximately at 32°21'50.43"N, 64°40'0.95"W. From the end of May 1995 the gauge was moved to Bermuda's International Airport (BA) at 32°22'1.40"N, 64°40'38.87"W. It has remained at that location, to the present day.

These two datasets of daily rainfall accumulation (NAS and BA) have been merged for the following reasons:

1) The sites are only separated by 1.04 km (horizontal) and 29m (vertical) distance.

2) They were both used by the operators of the Bermuda Weather Service, as operated successively by the US Naval Air Station up to 1995 and Serco & BAS-Serco, a company established in 1997 between Bermuda Aviation Services (BAS) and Serco Management Services Inc. thereafter *(http://www.bas-serco.bm/).*

3) These sites both formed the basis for the record of rainfall at the Bermuda International Airport.

However, it has a gap of about two years and half, between 1st of January 1968 to 30th of June 1970. The missing daily data in those two and a half years are filled by the observations A&F station, located in the central part of Bermuda. Data from BA station covering 16 years from 31st of May 1995 to 31 of December 2011 have been used to increase the NAS series duration in several years, thus conforming a unique complete sequence of daily precipitation values of sixty-three years spanning from 1949 to 2011 named in this study BER1 (Time series1). Table 3 resumes the time series used in this work.

DATA SETS

Reports regarding daily rainfall data from the Department of Agriculture and Fisheries (A&F) were considered as another source of rainfall data that the BWS holds because of the relative proximity of the stations and the absence of important orographic effects in the islands. In the past (since 1852) different sites were considered as official observations. Thus diverse sources of data (St. George's, Prospect, Fort George, Hamilton and Ireland Islands) were used in calculating averages of rainfall (Macky 1957). Comparisons of the daily rainfall time series from the A&F (from 1961 to 1972) and BA stations were carried out through a summary of temperature and rainfall data 1961-1972 compiled by I.W: Hugues, M. Douglas and D. Hooper and the viability of using data from A&F station to refill the gap in NAS time series has been confirmed.

Extension of NAS time series with data from BA station has been made by simple transposition, without needing to rescale, because relocation of the gauge between these two similar topographic settings has not caused noticeable changes of the surroundings. Therefore, as expected, no significant changes, other than that related to the natural variability of the process, have been observed between the original and the extended series.

The second time series consist of daily precipitation data collected at a privately owned and operated weather station placed in the Somerset Village (see Fig.12) and is named as SOM (Time series 2). It represents a relatively long data set, 37 years and 6 months, from 1st of January of 1974 to 29th of June 2011 of similar quality to that of NAS and BA, which has been used to explore spatial homogeneity of precipitation patterns over the archipelago and, as a consequence, providing support and strengthening the viability of characterizing Bermuda rainfall regime from the reconstructed long time series.

The third time series used in this work is based on hourly data and has been extracted from two sources: NAS and BWS. The first one provided two sets of observations: Airways reports from 1st January 1942 to 31st January 1980 and METeorological Aerodrome Reports (METAR) from 1st February 1980 to 31st December 1995. Data from Bermuda airport were extracted from 1st of November 1996 to 31st December 2011 provided by BWS. Therefore, there is a data gap not refilled between 1st January 1996 and 31st October 1996 and another between 1st July 1970 and 31st December 1972. Hourly data from such sources are called BER2 (Time series 3) and it is considered representative of Bermuda airport. For the initial selection of the rainfall events, data with visibility equal or less than 5 km is considered.

Table 3. Time series from Bermuda used in the study. N (number of station in the work), Source (weather stations that provide the data), Period and N.yr. (Number of years considered in the data analysis) and Obs. (Type of observation: D (Daily) or/and H (Hourly)).

N	TS.Code	Source	Period	N. yr	Obs.
1	BER1	B1/B2	1949-2011	63	D
2	SOM	B3	1974-2011	37	D
3	BER2	B1/B2	1942-2011	70	H

The parameters analysed were: rainfall (mm), wind direction (angular degrees), wind speed (kt) and present weather observations.

For the analysis of the wind direction and speed frequency and comparison when frontal and convective rain occurrences, (section 5.5.2.3.2.) rainfall events extracted from METARs. The studied period was 1942-2011.

3.2. The Canary Islands

Due to the heterogeneous topography of the Canary Islands, data from various representative measurement points of this area has been used in this work. Rainfall time

series have been extracted from archives provided by AEMET. Only rainfall greater than or equal to 0.1 mm was considered. A single station, N 22, Lomo Ahorradero (P15), is from another source: Consejo Insular de Aguas de Gran Canaria. This site was included given the quality and length of the archive data.

Nomenclature used to denote each measurement station is described below. The islands are divided into two provinces: Las Palmas (LP) and Sta. Cruz de Tenerife (TF). The aerodromes of reference are named by the following acronyms G. Canaria airport (A1), Lanzarote airport (A2), Fuerteventura airport (A3), Tenerife North airport (A4), Tenerife South airport (A5), La Palma airport (A6) and El Hierro airport (A7). The corresponding airport codes are G. Canaria A. (GCLP), Lanzarote A. (GCRR), Fuerteventura A. (GCFV), Tenerife north A. (GCXO), Tenerife south A. (GCTS), La Palma A. (GCLA) and El Hierro A. (GCHI).

The main part of the stations considered in this work are located at Gran Canaria (Fig.13) which is the most suitable island for this study, because of its relative central position in the archipelago and its medium elevations. The locations of the weather stations of the province of Las Palmas (LP) are depicted in Fig. 11B and Fig.13 (in more detail) and goes from P1 to P16. Those for the province of Sta. Cruz de Tenerife (TF) are represented in Fig.11B and are so-called from T1 to T15.

Stations located at the surface (0-200 meters) were: A1, A2, A3, A5, A6, A7, P1, P11, P14, P16,T1, T2, T6 and T9; between 200 and 600 meters: P7, P10, P12, T3, T4, T13, T14 and T15; situated at medium altitudes between 600 and 1000 meters: P2, P5, P8, P9, P13, T7, T8, T10 and T12 and at high altitudes (between 1000 and 2000 meters): P3, P4, P6, P15 and T11. The highest point is Izaña (T5) with an elevation 2371 m. The average period considered was 48 years, from January 1965 to December 2012.

For the analysis of dry periods between rainfall events (section 5.2.2) and the application of theories of the Permutation Entropy (PE) and Kolmogorov complexity (KC) (section 5.9) the following 18 weather stations for the Canaries were considered: A1, A2, A5, A7, P2, P5, P11, P12, P13, P14, P16, T1, T2, T5, T12, T13, T14 and T15. This selection responds to the different orientations and elevations of the sites where the rain gauges are located. The results were compared with those achieved for BER1 (Bermuda), M (Madeira) and Az. (Azores). The studied normal period was 1981-2010.

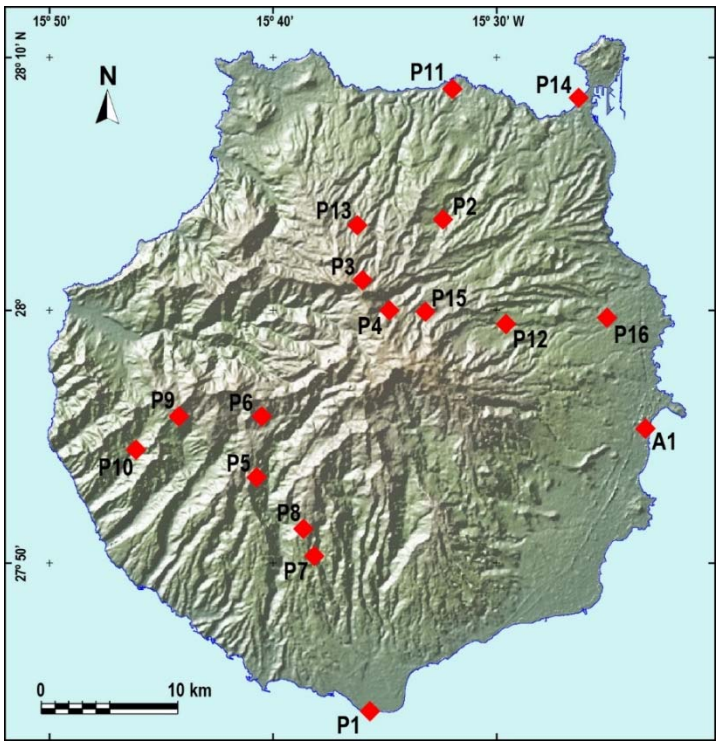

Fig. 13. Topographic map and geographic location of measurement stations in Gran Canaria.

Furthermore, METeorological Aerodrome Reports (METARs) from four aerodromes of reference have been used. Such reports contain encoded information in METAR data format on atmospheric parameters and are made by trained certified weather observers who review and encode the observations. This procedure is developed following a protocol regulated by the World Meteorological Organization (WMO, 1995), in consort with the International Civil Aviation Organization (ICAO), and using a general

standard format. The parameters extracted from METARs to be used in this study are visibility (km), rainfall (mmm^{-2}), wind direction (angular degrees) and wind speed (kmh^{-1}).

A rainfall event was considered when some of these descriptors were included in the METAR: RA (rain), SHRA (shower), TS (thunder storm) or DZ (drizzle).

Data from METARs from G.Can. A (A1) were used in the investigation of the duration of dry periods between rainy events (section 5.2.2.) and from G.Can. A (A1), Fuert. A. (A3) and La Palma A. (A6) for the study of the fractal characteristics of the rainfall in Canaries (Section 5.4.).

For the analysis of the wind direction and speed frequency and comparison when frontal and convective rain occurrences, rainfall events extracted from METARs from G.Can. A (A1), La Palma A. (A6) and Lanz. A. (A2) were considered (5.5.2.3.3). The studied period was 1942-2011.

To explore the fractal behaviour (section 5.4.2) and regional differences of rainfall, data from rain gauges from the stations named from P1 to P10 for LP and from T1 to T11 for TF were used. For the comparison between fractal behaviour of rainfall events and desert mineral dust incursions affecting the Canary Islands, (section 5.4.1.1) the aerodromes chosen as reference were Gran Canaria (A1), Fuerteventura (A3) and La Palma (A6) (Fig. 11B). These weather stations were selected based on availability of long data sets and representativeness. Gran Canaria airport, located at 27.93 N and 15.3 W, with an elevation of 24 m, an international high density traffic airport operational 24 h a day provides a good quality METARs based data set. Fuerteventura airport situated at 28.45 N and 13.86 W, with an elevation of 26 m and placed at the eastern edge of the archipelago, gives appropriate measurements of dust incursions affecting the islands, due to its proximity to the Sahara. Finally, La Palma airport, in the western side, sited at 28.62

N and 17.76 W and at 33 m a.s.l. was also selected being affected by heavy precipitation when Atlantic lows affect the archipelago. Data acquisition was semi-hourly and only diurnal observations from 06:00 to 21:00 UTC were considered. Analysed records cover a period of twenty two years, from January 1989 to December 2010. For La Palma, less observations than in the others airports were available because they were hourly until the end of March 2002 and semi-hourly from the beginning of April 2002 up to date.

As a criterion for the referred study, a dust event duration has been defined as the number of dusty days, considering a day dusty when during a 24 h period a dust observation with visibility equal to, or lower than, 8 km was reported. The intensity of the dust event was estimated by the minor visibility recorded. For the selection of dust events, visibility data were considered only if the METAR included one of the following phenomena: haze (HZ), widespread dust in suspension in the air (DU), drifting dust raised by wind at or near the station at the time of observation (DRDU), dust storm (DS) or blowing dust (BLDU).

For the study of the seasonal and inter-annual rainfall variability (section 5.5**)** only 15 weather stations where considered for Canaries. For Gran Canaria, P5, P11 and P12 were not taking into account in the calculations of the daily maxima rainfall because of the inclusion of - 4 in the data base (see Table C in Annexe I). However this analysis was focussed in only four sites for Canaries (Lanzarote A. (A2), El Hierro A. (A7), L. Canteras (P14) and S.C. of Tenerife (T1) due to the quality and completeness of the measurement and in the normal period 1981-2010. All these weather stations are located at coastal areas avoiding the difficulties when comparing sites with different elevations. Finally, for the study of episodes of heavy rainfall, (section 5.6) all the available weather stations within AEMET were taken into account.

3.3. Madeira and Azores

For the Portuguese Atlantic archipelagos only two time series were employed. For Madeira, datasets were taken from the Funchal Obs. (M) and for Azores from the Horta Obs. (Az). A normal period (1981-2010) was selected.

Since other studies investigating the fractality of precipitation in Madeira have been already conducted (De Lima & De Lima 2009); data from this archipelago and Azores were not used for such analysis.

The study for these Portuguese islands was about the frequency of dry periods, seasonal and inter-annual rainfall variability and analysis of complexity. A comparison with Bermuda and the Canary Islands was made. The locations of the weather stations used is shown in Fig.10. The geographical coordinates and characteristics of these sites are found in table 4.

For the analysis of the wind direction and speed frequency and comparison when frontal and convective rain occurrences, rainfall events extracted from METARs from Horta and Funchal airports (Horta A. and Funch. A.) (Section 5.5.2.3.3) were used. The studied period was 2003-2014.

3.4. Data availability and quality

The forty one weather stations selected for the record analysis used in this study (rainfall and dust events), identifiers and characteristics are indicated in table 4 such as: number of station in the work, station code, station name, province: LP (Las Palmas) and TF (Sta. Cruz de Tenerife), acronym used in the study, station elevation in m., location, geographical coordinates in sexagesimal format, period, number of years considered in the data analysis and type of observation.

Table 4. Weather stations selected for the analysis of all the records used in this study. N (number of station in the work), Ind. (station code), St. Name (station name), Prov. (province: LP (Las Palmas) and TF (Sta. Cruz de Tenerife)), Acr. (Acronym used in the study), Elev. (station elevation in m), Loc. (location), geographical coordinates (Lat.N and Log.W: latitude North and longitude W respectively in sexagesimal format), Period, N.yr (number of years considered in the data analysis) and Obs. (type of observation: D (daily) or/and H (hourly)).

N	Ind.	St. name	Prov.	Acr.	Elev.(m)	Loc.	Lat.N	Long.W	Period	N.yr.	Obs.
1	C649I	G. Can. A.	LP	A1	24	E	27 55 21	15 23 22	1951-2012	62	D/H
2	C029O	Lanz. A.	LP	A2	14	SE	28 57 07	13 36 01	1972-2012	41	D/H
3	C249I	Fuert. A.	LP	A3	25	E	28 26 41	13 51 47	1969-2012	46	D/H
4	C447A	Ten. N. A.	TF	A4	632	NE	28 28 39	16 19 46	1960-2012	62	D/H
5	C429I	Ten. S. A.	TF	A5	64	S	28 02 51	16 33 39	1980-2012	33	D/H
6	C139E	La Palma A	TF	A6	33	E	28 37 59	17 45 18	1970-2012	43	D/H
7	C929I	El Hierro A.	TF	A7	32	NE	27 49 08	17 53 20	1973-2012	40	D/H
8	C689E	Masp.	LP	P1	6	SW	27 44 08	15 35 53	1997-2012	16	D
9	C656U	Teror Dom.	LP	P2	630	N	28 03 59	15 32 38	1963-2012	50	D
10	C662I	Valleseco R.	LP	P3	1400	N	28 01 44	15 36 12	1965-2012	48	D
11	C654Q	S. Mat. Lag.	LP	P4	1160	C	28 00 18	15 34 49	1965-2012	48	D
12	C626E	Mogán B A.	LP	P5	715	SW	27 53 35	15 40 45	1964-2012	49	D
13	C624E	Tejeda V.Ñ.	LP	P6	1040	C	27 55 55	15 40 30	1964-2010	47	D
14	C637A	S.B. Tir. P.	LP	P7	570	S	27 50 20	15 38 10	1965-2012	48	D
15	C625O	S.B.Tir.L.P.A.	LP	P8	806	S	27 51 24	15 38 41	1965-2012	48	D
16	C625A	Mogán Inag.	LP	P9	950	W	27 55 52	15 4415	1952-2010	59	D
17	C627A	S. Nic. T.T.	LP	P10	420	SW	27 55 12	15 45 47	1965-2009	45	D
18	C669A	Arucas Bañ.	LP	P11	50	N	28 08 47	15 32 01	1965-2012	48	D
19	C647O	Valseq. G.R.	LP	P12	540	C	27 59 30	15 29 38	1965-2012	48	D
20	C665L	Moya Font. C.	LP	P13	950	N	28 03 25	15 36 15	1965-2012	48	D
21	C659Q	L. Canteras	LP	P14	15	N	28 08 26	15 26 02	1965-2012	48	D
22		L. Alhorr.	LP	P15	1100	C	27 59 57	15 33 13	1924-2012	89	D
23	C649U	Telde - LL.	LP	P16	150	E	27 59 43	15 25 09	1965-2012	48	D
24	C449C	S.C. Ten.	TF	T1	35	NE	28 27 47	16 1519	1960-2012	62	D
25	C469A	S.J. Rambla	TF	T2	106	N	28 23 38	16 39 02	1948-2012	62	D
26	C129C	Tazac. M.T.	TF	T3	274	W	28 36 42	17 54 54	1984-2012	29	D
27	C457C	Tacoronte	TF	T4	564	NE	28 28 55	16 24 35	1945-2012	62	D
28	C430E	Izaña	TF	T5	2371	C	28 18 32	16 29 58	1933-2012	62	D
29	C419X	Adeje Cal. B	TF	T6	130	SW	28 04 53	16 42 39	1988-2011	23	D

N	Ind.	St. name	Prov.	Acr.	Elev.(m)	Loc.	Lat.N	Long.W	Period	N.yr.	Obs.
30	C126A	El Paso C.F.	TF	T7	844	W	28 39 14	17 51 11	1986-2012	27	D
31	C117A	Puntagorda	TF	T8	684	NW	28 45 38	17 59 08	1986-2012	27	D
32	C329Z	S. S. Gomera	TF	T9	15	E	28 05 23	17 06 41	1995-2012	18	D
33	C317B	Agulo J.B.	TF	T10	765	NW	28 10 44	17 12 47	1986-2012	27	D
34	C315P	Valleher. Ch.	TF	T11	1242	W	28 06 38	17 15 47	1986-2012	27	D
35	C427E	S. M. Abona	TF	T12	642	S	28 05 48	16 36 57	1952-2012	61	D
36	C128B	Ll. Arid. B	TF	T13	410	W	28 39 32	17 54 37	1978-2012	35	D
37	C127U	Fuenc. Cal.	TF	T14	498	S	28 29 42	17 49 43	1946-2012	67	D
38	C939U	Sabinosa	TF	T15	299	W	27 44 51	18 05 45	1978-2012	35	D
39		Berm. A.		BER1	7	NE	32 21 50	64 40 01	1949-2011	63	D
40	505	Horta Obs.		Az.	45	SE	38 31 16	28 42 50	1970-2011	42	D
41	522	Funch. Obs.		M	58	S	32 38 51	16 5 333	1970-2011	42	D

Some abbreviations used for the weather stations are: A. (Airport), Obs. (observatorio) G.Can. (Gran Canaria), Fuert. (Fuerteventura), Lanz. (Lanzarote), Ten. N. (Tenerife Norte), Ten. S. (Tenerife Sur aeropuerto), Masp. (Maspalomas), Teror Dom. (Teror-Dominicas), Valleseco R. (Valleseco-La Retamilla), S. Mat. Lag. (San Mateo-Las Lagunetas), Mogán B. A. (Mogán- Barranquillo Andrés), Tejeda V. Ñ. (Tejeda-Vivero de Ñameritas), S.B. Tir. P. (San Bartolomé de Tirajana-Palomas), S.B. Tir. L.P.A. (San Bartolomé de Tirajana-Lomo Pedro Alfonso), Mogán Inag. (Mogán (Inagua)), S. Nic. T.T. (San Nicolás de Tolentino-Tasarte), Arucas Bañ. (Arucas (Bañaderos)), Valseq. G.R. (Valsequillo-Granja Las Rosas), Moya Font. C. (Moya-Fontanales Cisterna), L. Canteras (Las Palmas de G.C.-Las Canteras), L. Alhorr. (Lomo Alhorradero), Telde-LL. (Telde Los Llanos), S.C. Ten. (Santa Cruz de Tenerife), S.J. Rambla (San Juan de La Rambla), Tazac. M.T. (Tazacorte-Mña Todoque), Adeje Cal. B (Adeje-Caldera B), S. S. Gomera (San Sebastián de La Gomera), Agulo J.B. (Agulo-Juego Bolas), Valleher. Ch. (Vallerhermoso-Chipude C.F.), S. M. Abona (San Miguel de Abona), Ll. Arid. B (Llanos

de Aridane B), Fuenc. Cal. (Fuencaliente-Caletas), Berm. (Bermuda) and Funch. (Funchal).

These points have been selected due to their geographical position, altitude and orientation. These factors contribute in explaining the rainfall regimen affecting the studied area. Even though the coverage of time varies between stations, the average recording period, around 48 years, is considered suitable for the purpose of this study. It should be taken into account that this period can change according to the objective of the investigation as will be explained in the result section. The comparison between the conclusions extracted from the analysis of the different stations must be in some cases interpreted cautiously because of the absence of a whole common period for all the analysis made.

Due to the absence of orographic effects in Bermuda, an advantage in the analysis of the rainfall is to consider a single station as representative of the entire archipelago. Although some other stations are currently being operated in Bermuda, (Commissioner's P., St. David's and F. Prospect) the time series records are quite short to be compared with the rest of the observations sets.

However, for the rest of the sites within this subtropical region, the practical limitation when analysing data from many stations has been found. The rainfall data availability for the Canary Islands in AEMET is shown in Fig.14 as the distribution of the rainfall Time series in La Palma (LPa), La Gomera (G), El Hierro (EH), Tenerife (Ten), Gran Canaria (GC) Lanzarote (Lz) and Fuerteventura (Fv) throughout the number of years of measurements. In light blue is shown for periods of 0 to less than 30 years and in dark blue for periods equal or more than 30 years (Fig.14a) or equal to 30 years (Fig.14b). The rainfall data coverages for the periods 1951-2012 and 1981-2010 are represented at the top and in the the central part of the figure respectively (Fig.14a and

14b). The percentage of the number of stations according to its quality can be found at the bottom (Fig.14c).

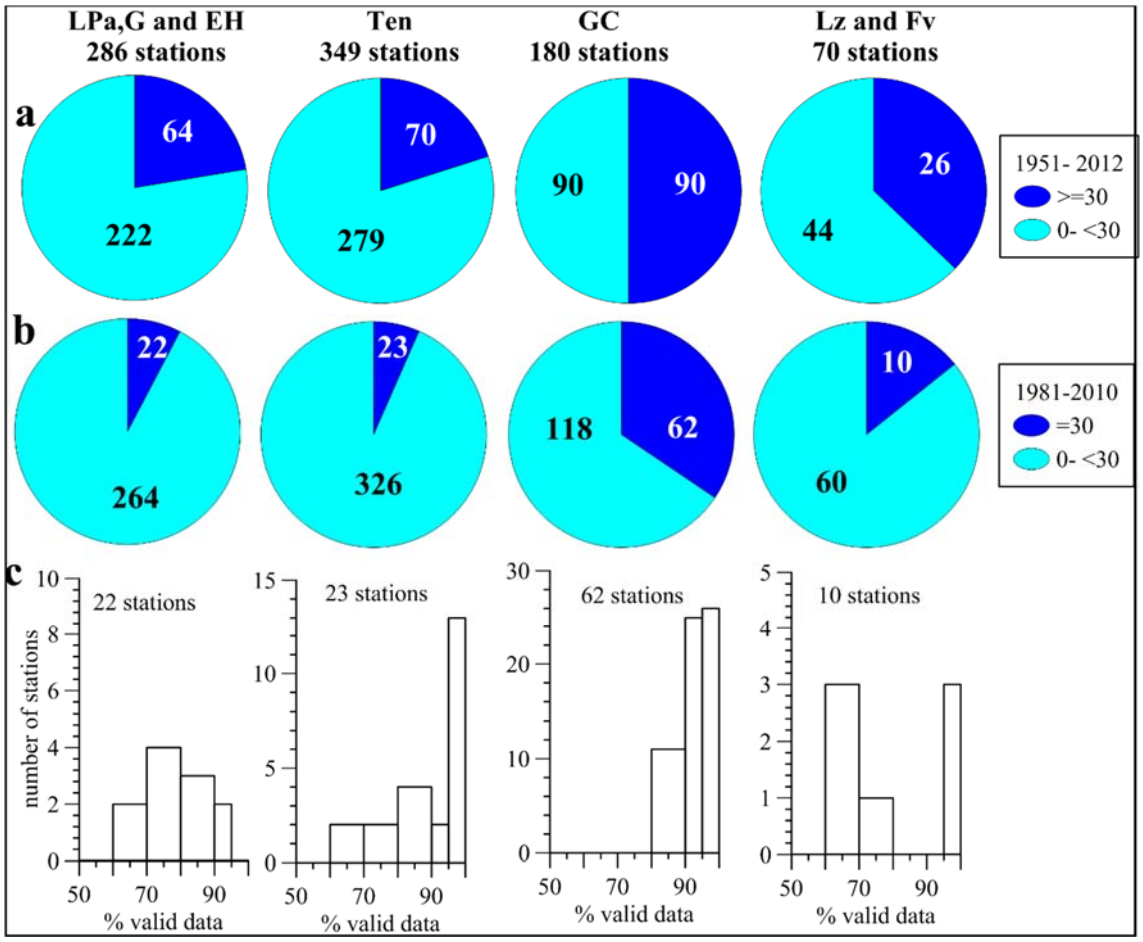

Fig. 14. Distribution of the rainfall Time series in La Palma (LPa), La Gomera (G) , El Hierro (EH), Tenerife (Ten), Gran Canaria (GC) Lanzarote (Lz) and Fuerteventura (Fv) through the number of years. (a) Rainfall data coverage for the period 1951-2012. Light blue for 0 to less than 30 years and dark blue for 30 or more years. (b) Rainfall data coverage for the period 1981-2010. Light blue for 0 to less than 30 years and dark blue for 30 years. (c) The percentage of the number of station according to its quality.

The selection of the weather stations for most of the analysis made in this work responds to the availability of Time series of 30 years of high quality.

High quality or 100% of valid data is considered when the time series have not gaps or a -4 coded value on a specific date. The -4 code value means that no rainfall amounts were register on this date, and is being accumulated towards the next registered date. This problem is found in a large number of weather stations in the Canaries located

at medium or high altitudes because they are not easy to reach to make the observations. Negligible rainfall, less than 1mm is coded by -3 and corresponds to a value less than 0.1 mm. In this work such values have been computed as 0.05 mm.

The largest number of the stations with rainfall measurements during 30 consecutive years in the period 1981-2010 is in Gran Canaria (GC), a percentage of 34.4%, followed by the most eastern islands with 14.3%, the most western ones with 7 % and Tenerife with 6.6 % (Fig.14b). Moreover, the highest percentage of valid data (80%) is found in Gran Canaria (Fig.14c) .This is one of the reasons, apart from its central location in the archipelago, why the rainfall trend in Gran Canaria has been deeply studied.

In Annexe I, table A shows the statistical of data availability with a percentage higher than 95% from the weather stations within AEMET during the period 1981-2010 in La Palma (LPa), La Gomera (G) and El Hierro (EH); table B in Tenerife (Ten), table C in Gran Canaria (GC) and table D in Lanzarote (Lz) and Fuerteventura (Fv). These 4 tables include the code of each station (Ind.), the station name (St.name), the orientation (North N (1) /South S (2)) , the elevation in m (Elev.(m), the latitude in degrees (Lat.(deg.)), the longitude in degrees (Lon.(deg.)), the number of dates with -4 (N(-4)), the number of dates with negligible rainfall (N(-3)), the number of zeros (N(0)), the number of values higher than zero (N(>0)), the number of data coded by -9999 or not data (N(-9999)), the number of blank spaces or no data (N (B)), the number of real data (N R), the percentage of data (data %), the initial year (Ini.yr.), the last year (Last yr.) and the total number of years (N.yrs.).

For Madeira, data from the Funchal Obs (M) were considered because of its appropriate length. Data from the Horta Obs. (Az) were also chosen because it serves as a reference for the numeric models (ECMWF) (European Centre for Medium-Range

Weather Forecasts). Several problems like data homogeneity, changes in instrumentation and the lack of long time series should be considered in the interpretation of the results obtained from this analysis. The worst quality of the rainfall measurements is usually found in the rainiest locations where the gaps are frequent or the accumulation of several rainfall days is registered in one single day. This practice hinders the analysis of the daily rainfall data which could be very interesting in detecting the extreme events.

3.5. Numerical models

Synoptic weather conditions favouring rainfall events over the islands have been extracted by using analysis from atmospheric numeric models in order to verify the occurrence of heavy rainfall events. To such end, compositions of geopotential height, wind, temperature and humidity fields in different pressure levels were examined. Most synoptic charts used come from the ERA 40 reanalysis developed by the ECMWF (European Centre for Medium-Range Weather Forecasts) and included in the Meteorological Archival and Retrieval System (MARS). Additionally, these synoptic data were compared with reanalyses from the National Centre for Environmental Prediction (NCEP) and a counterpart of NOAA's Earth System Research Laboratory (ESRL), the National Center for Atmospheric Research (NCAR), which is supported by the National Science Foundation (NSF). *http://www.cdc.noaa.gov/Composites/printpage.pl*). Several results from the Spanish stations were compared with HIRLAM (High Resolution Limited Area Modelling) analysis.

Satellite images represent a basic support to carry out this study. Among others, these images provided by NOAA and NASA (*http://www.nhc.noaa.gov http://rapidfire.sci.gsfc.nasa.gov/gallery*) were used to analyse some specific situations. METEOSAT images were provided by the AEMET (Agencia Española de Meteorología). Dust Aerosol Column Optical Depth (AOD) from AERONET (AErosol

RObotic NETwork) and NASA MODIS (Terra and Aqua) were downloaded from (*http://disc.sci.gsfc.nasa.gov/giovanni*). SeaWIFS (Sea-viewing Wide Field-of-view Sensor) images provided by the CREPAD (Centro de Recepción, Proceso, Archivo y Distribución de Datos de Observación de la Tierra) within the INTA (Instituto Nacional de Técnica Aeroespacial) were also considered as useful tools.

Winter NAO indexes (from December through March) based on standardised sea-level pressure differences between Lisbon, Portugal and Stykkisholmur, Iceland (Hurrell 1995) and compiled by the Climate and Global Dynamics (CGD) division at NCAR (*http://www.cgd.ucar.edu/cas/climind/*) were also analysed.

4. Methodology

4. Methodology

A standard practice recommended by World Meteorological Organization (WMO 1984) to adequately characterize the rainfall regime in a specific area is to choose a thirty-year period of a given variable in order to define its normal climatology. In particular, this concept has been commonly used in defining normal rainfall regime (Pryor & Schoof 2008). This criterion has been adopted to examine the spatial homogeneity between stations, the comparison of the seasonal and inter-annual rainfall variability in Bermuda with other stations and the calculation of the probability density function in terms of frequency of annual total rainfall. The rest of the analysis has been performed by considering the whole available, sixty-three years, data set. Before graphically representing the data, statistical techniques have been used such as moving average smoothing, exponential smoothing and running medians smoothing. The missing rainfall data were filled in with those from other data sources by simple transposition, without needing to rescale, because of similar location of the gauges. Thus, time series were not interpolated by adjusting some sort of mathematical function or by values obtained by statistical procedures. Initially in this work, conventional statistical methods have been used to describe inter-annual and seasonal variability of the meteorological variables studied. These statistical techniques include correlation analysis, descriptive statistics, Mann-Kendall's rank correlation tests, the test of Chow, bar charts and the least square linear fitting the linear regression model. All of the correlation statistics and their significance (p values) have been computed with classic statistical tests (Wilks 2006). Jarque-Bera (J-B) and Lilliefors normality tests were used to confirm the behaviour of the yearly accumulated rainfall applied to the analysis over the studied areas estimated by histograms.

Regularities in the time series behaviour over time were also investigated, like the tendency, general direction of a variable for long time periods, possible periodic fluctuations, the rises or falls on the data and even the possible randomness of the process, irregular movements determined by chance, etc. A key issue in the time series analysed in this study was to determine its stationarity. A series is considered stationary if its statistical values (such as mean or standard deviation) do not change with time.

Nevertheless, because of the high complexity of rainfall processes, the procedures above mentioned have been considered to be quite insufficient to describe properly the statistical structure of the analysed phenomena and non-linear methods were also employed. The existence of a power-law frequency statistical behaviour and fractal properties have been shown to be an efficient approach in order to describe them. Therefore, rainfall events have been studied deeply in this work under theories based on the Power Law (P.L.) scaling and the fractal dimension. Both are related to the scale-invariant properties of time series distributions. The frequency of dry periods between rain events and the daily rainfall intensity have been analysed by the PL concept. The clustering of the rainfall and dust incursions patterns has been analysed by the fractal framework according to different ranges of time. The long-range dependence and the analysis of the complexity comparing rainfall patterns between the different archipelagos considered in this study were examined by the Kolmogorov complexity (KC) and the Permutation Entropy (PE) methods. The seasonality index, the long-term mean index of seasonality and the Chi-square test were used to identify the seasonal patterns.

Furthermore, mathematical tools as wavelet analysis to decompose energy in the time series across different time scales were very useful in obtaining the spectral time decomposition of the rainfall time series. Initially a Discrete Wavelet Transform (DWT), with a Daubechies (Db8) type base function was used to analyse the temporal variation

of the monthly rainfall. The variability of the number of rainfall days (NRD) comparing to the NAO index for different time scale ranges was also analysed by the DWT. The Continuous Wavelet Transform (CWT) was used to identify the dominant time scales in the daily rainfall time series. The Cross Wavelet Power (CWP) was employed to analyse the relationship between the standardized NAO index and both the NRD and the annual rainfall rate (the annual accumulated rainfall per NRD).

Data were processed using specific programs designed in MATLAB (MATrix LABoratory), 2010 (The Math Works, USA) and IDL (Interactive Data Language) programming language software packages. A brief explanation of the statistical methods used in this work is given in the next subsections.

4.1. Statistical methods

4.1.1. Poisson model

The generalized Poisson distribution has been found useful in fitting over or under dispersed data (Consul & Famoye 1992, Tuenter 2000). A Poisson process can be defined as a stochastic counting process with independent increment. The number of events in a time interval follows a Poisson distribution. However, the waiting time between occurrences are exponentially distributed (Dalelane & Deutschländer 2013). In this work a subject of investigation is if the distribution of dry periods obtained from the time series of daily rainfall over Bermuda can be modelled by a Poisson distribution resulting from the assumption of a random behaviour.

The Poisson distribution is a discrete probability distribution used to model the number of events occurring within a given time interval T.

$$p(x;\lambda) = \frac{e^{-\lambda}\lambda^{x}}{x!} \tag{1}$$

Where p(x,λ) is the probability of observing *x* events in a given time interval ΔT, (in this work the probability to find dry days between rain events) and λ is expressed as:

$$\lambda=\mu\Delta T \quad (2)$$

Where μ is the rate of events per unit of time (rain events per the number of total days during the studied period).

The time interval between events dt or time between arrivals in a Poisson process follows an exponential distribution

$p(dt) = \mu e^{-\mu dt}$ (3) which only depends on the parameter μ .

It can be easily detectable in a semi-log plot and it is the slope of the linear adjustment representing the inverse of the mean of the dry events. This indicates that a Poisson process has no memory; the probability of observing an event is independent of the occurrence of the previous one.

For this analysis, the histogram of the number of dry days between successive rainfall events is represented. Semi logarithmic of time intervals between dry periods is also shown.

It is well known that a problem in rainfall analysis is the lack of rainfall records long enough. In these circumstances, the use of the Poisson model for understanding the rain behaviour was successful. Its validity, was confirmed not only for describing general rain properties but also as a basis for predicting the most severe rain characteristics observed in a given period of time. The probability distribution of these characteristics provides satisfactory predictions according to the observed records.

The Poisson distribution, with two μ parameters has been also obtained as a limiting form of the generalized negative binomial distribution (Consul & Jain 1973). To investigate the random behaviour of the daily rainfall at Bermuda, only the observation or not observation of the event is taking into account to analysing the

probability to find dry days (P(x)) between rainy ones. To such end, the histogram of the number of dry days between successive rainfall events is represented.

Semi logarithmic of time intervals between dry periods is also shown. Some meteorological processes including extreme events have been explained by a Poisson model. Several studies reveal the suitability to this random framework to analyse time series of temperature (Onof et al. 2000, Abaurrea & Cebrián 2002, Cebrián & Abaurrea 2006, Brown et al. 2008, Tomassini & Jacob 2009, Radermacher & Tomassini 2012, Dalelane & Deutschländer 2013).

4.1.2. Non-linear methods

4.1.2.1. Power Law frequency statistics. Scaling properties

The Scaling or Power Law (PL) distributions play an important role in describing non-linear complex systems. They are often used to describe many natural and social phenomena and specifically to analyse both the intensity and the intervals between environmental disturbances. Rainfall in Bermuda has been also study in this work under PL scaling concept which is related to the scale-invariance of the time series distribution. A time series present scaling behaviour if its parameters are similarly related over a wide range of sizes or scales exhibiting the same statistical characteristics. In this case the intensity of precipitation amounts are taking into account. The Scaling, Power Law o Pareto distributions play an important role in describing non-linear complex systems.

Scaling or Power Law relationships arise commonly as probability or frequency-size distributions (in this study probability of reaching certain thresholds of rainfall intensity or observing certain daily accumulated rainfall (mmd^{-1})), and are characterized by the form

$$f(x) = C \times \alpha \qquad (3)$$

Where C is a constant and the value f(x) is proportional to some power of the input x (accumulated daily rain) (White et al. 2008). In this case accumulated daily rain. The logarithmic transformation of this function becomes a line and the slope of the resultant straight line gives an estimation of the scale exponent α (White et al. 2008). This behaviour occurs for values of the variable x higher than a given threshold that are in the tail of the distribution. The presence of a cross over or break point in a PL suggests the existence of possible critical phenomena associated with transition phases (McGarry et al. 2002, Sornette 2006, Scheffer et al. 2009) where environmental properties of a certain phenomenon are probably changing rapidly (Olsson et al. 1993). The change in some parameter can modify the properties of the whole system.

Scaling framework allows the comparison of analogous phenomena and the characterization of regions over a similar environment. A time series present scaling behaviour if its parameters are similarly related over a wide range of sizes or scales exhibiting the same statistical characteristics at any scale and are not associated with a particular one. Thus, the presence of scaling invariance in a given process, is a characteristic associated with PL distributions (Sornette 2004, Newman et al. 2006). Such process is scale free, considering scale as the spatial and temporal dimension of the phenomenon. In other words, a change in scale does not alter the statistical behaviour of the system. Furthermore, systems that behaves as PL evolve far from equilibrium and are frequently high dissipative.

Several methods have been proposed to prove this PL behaviour mainly at the end of the tails distributions and when, as in this study, the length of the time series is not enough long. Due to its heavy-tail, the PL distribution suggests that extremely large values occur at higher frequency than in other distributions, such as the normal or exponential. This indicates that commonly, small events are not qualitatively different

from large, extreme events (Stumpf & Porter 2012). Therefore, a PL at the end, *long tail distribution*, indicates that the frequencies or probabilities to find extreme phenomena or rare events, far away from average values are higher than those ones obtained from the classic statistics. A Power Law behaviour also suggests the presence of a non-linear complex system (Savaglio & Carbone 2000) where different processes occur simultaneously, showing several behaviour degrees. The whole behaviour of the system is function of all the elements which conform it and have a strong non-linear relationship (Goodwin 1994, Amaral & Ottino 2004).

In recent years it has been shown that a wide number of nature phenomena follow PL distributions (Schroeder 1991, Newman 2005). Even in extreme natural hazards e.g. earthquakes (Mega et al. 2003), floods (Mega et al. 2003, Malamud & Turcotte 2006), landslides (Li et al. 2011) or forest fires (Weiguo et al. 2006). Many atmospheric variables, like rainfall, also follows a power law distribution, at least in the tails of the distributions. The presence of power laws has also been suggested as the fingerprint of systems that show self-organized criticality (SOC) (Bak 1996). A P.L behaviour in the empirical data values or in the time interval between them may show the existence of rare underlying mechanisms or processes like feedback loops, random network, self-organization or phase transitions (West et al. 1997, Barabási & Albert 1999, Newman 2005, Newman et al. 2006).

One important limitation of this tool related to the occurrence of the power–law behaviour at the tail of the distribution (Stumpf & Porter 2012) where increases the uncertainty on the exponent value estimation. On the other hand, other distributions that sometimes offer a best data fit than scaling laws are the lognormal (Mitzenmacher 2004), the stretched exponential (Laherrere & Sornette 1998) and other truncated PL (Burroughs 2001, Tsallis 2009). However, one advantage of the use of PL tools is the simplicity of

the analysis. This is quite consistent with much of the literature on scaling in ecologic, geophysics or economics systems. Furthermore, recently scaling laws have been shown to be present over a large range of scales (Virkar & Clauset 2012, Clauset 2009). In spite of the fact that model performance regarding to prediction has improved significantly over the last few years, the complexity of some phenomena, extraordinarily non-linear ones. This makes the understanding of the underlying dynamics of such events much more difficult.

In this study a histogram of the daily accumulated rainfall and a log-log plot were performed on the numerical series obtained from differences between daily rainfall intensity.

4.1.2.2. Fractal properties. Dust Cantor method

Some phenomena in nature have properties of self-similarity showing a fractal structure; this is a characteristic of objects that show the same structure at all scales. In other words, small sections of a time series related to such processes cannot be distinguished from the whole signal, after been accurately scaled (Schroeder 1991, Boettcher & Paczuski 1996). The fractal geometry is a suitable tool to study natural non-equilibrium systems. The fractal dimension concept provides information at different scales of the time series related to such phenomena (Malamud & Turcotte 2006). Many algorithms to estimate the fractal dimension have been proposed, each one with its advantages and drawbacks. The box-counting method is the oldest and more commonly used because it is intuitive and easy to apply (Lovejoy et al. 1987, Olsson et al. 1992, Olsson et al. 1993).

In this study, we try to characterize rainfall events over the North Atlantic subtropical area. To this end, the intervals or clusters of the rainfall events which can be considered as natural punctual processes, are analysed. A kind of fractal analysis known

as the *Cantor Dust method* has been applied. This technique has been successfully used on different natural processes like earthquakes (Smalley et al. 1987, Chen et al. 2003), desert storms (Mayer 1992), floods (Turcotte & Greene 1993, Mazzarella 1998, Mazzarella & Rapetti 2004), volcanology (Dubois & Cheminee 1991), El Niño events (Mazzarella & Giuliacci 2009), rainfall (Olsson et al. 1992, Olsson et al. 1993, Izzo et al. 2004, De Lima & De Lima 2009) and eolian dust deposits on desert alluvial terraces (Mazzarella & Diodato 2002, Pelletier 2007).

This method consists in a box-counting algorithm (Mandelbrot 1983, Takayasu 1990, Turcotte 1997), which tests whether the time series are distributed in time according to a fractal pattern, even within a limited range of scales. The box-counting methods use boxes to cover an object to find the fractal dimension (Olsson et al. 1992, Olsson et al. 1993, De Lima & De Lima 2009). The total length of the time series is represented by the space of observation and the time intervals by the boxes.

The *Cantor dust* method is based on dividing the space of observation, the time interval, T , into n non-overlapping segments or boxes of smaller intervals and of characteristic size, s, such that

s =T/n with n= 2, 3, 4,…

Computing the number *N(s)* of intervals of length *s* occupied by at least one event, if the distribution of occurrences has a fractal structure then

$$N(s) = Cs^{D} \quad (4)$$

The slope D of the regression line of log (N(s)) on log (s) provides the fractal or box –counting dimension D = abs(D) = |D|, which describes the strength of the rainfall or dust events gathered and can be used as a measure of the nature of the phenomenon, since it quantifies the scale-invariant clustering of the time series (Mazzarella 1998, Mazzarella & Diodato 2002). If D approaches to zero clustering increases, the smaller values of D

represent the more isolated clusters. So the smaller fractal dimensions are related to clusters formed by occurrences sparsely distributed in time. (Mazzarella 1998, Luongo & Mazzarella 2003, Izzo et al. 2004). If *D* is close to *1*, the events are randomly or arbitrarily spaced in time. It means that they obey to a denser or uniform distribution and not time gathering or clustering. The signal is partitioned into boxes of various sizes and the amount of non-empty squares is counted. A log–log plot of the number of boxes versus the size of the boxes is done. Signal binarization, i.e. whether a box is occupied or not, implies a limitation of the method, thus the box-counting technique doesn't take into account the data numbers in the frequency with which boxes are filled, that means that the distribution of the events is not considered. (Olsson et al. 1992, Olsson et al. 1993, De Lima & De Lima 2009).

In this work, only a mono-fractal analysis is developed, which deals merely with the occurrence or no occurrence of the phenomenon in each temporal box. However, the study of the intensity of the phenomena, according to other authors, can be studied throughout a multi-scaling (Olsson et al. 1993) or multifractal (De Lima & De Lima 2009) analysis.

Non-equilibrium phenomena following power laws verify general scaling relations and are, by definition, self-similar (Schroeder 1991, Boettcher & Paczuski 1996). Self- similarity is a key concept in the scaling properties exploration because it means that small sections of a time series cannot be distinguished from the whole signal after being properly scaled. That is, self-similar time series have a fractal structure. Thus, knowledge of its fractal dimension provides a way to relate information at different scales (Malamud & Turcotte 2006). The box-counting method is the oldest and more commonly used because it is intuitive and easy to apply (Lovejoy et al. 1987, Olsson et al. 1992,

Olsson et al. 1993). The method employed in this study to estimate the fractal dimension of dust and rain events is known as the Cantor dust method considered by other authors as a proper framework for non-linear analysis like the fractal behaviour of rainfall occurrence (Mazzarella & Diodato 2002). It is in fact a box-counting algorithm in which the space of observation represents the total length of the time series and the boxes correspond to the time intervals. The intervals or clusters of dust or rain events are taken as natural point processes (Mandelbrot 1983, Takayasu 1990, Turcotte 1997).

4.1.2.3. Long-range dependence

A linear relationship on a log- log plot with slope α indicates the presence of scaling (self-similarity). Applied to scaling process if the spectral density function Sx is a power Law for frequencies near to zero, the process can be considered as long memory (LM) or a long range dependent (LRD) (Barbosa et al. 2006).

$$\lim_{f \to 0} S_x(f) = C \mid f \mid^{\alpha} \tag{5}$$

where C and α (the scaling exponent) are constant and C > 0 and -1< α < 0. The slope of the wavelet

Spectrum β is related to α by: $\alpha = -\beta - 1$ (6)

The long memory (LM) parameter, d, is related to α by $d = \frac{\beta + 1}{2}$ (7)

4.1.2.4. Analysis of the complexity

4.1.2.4.1 Kolmogorov complexity (KC)

The Kolmogorov complexity was introduced by Kolmogorov (1903-1987). This is a method of analysis for binary combination that allows to determine the degree of complexity of a time series. Its magnitude is defined as the lowest value in bits that an

information needs to describe a particular object (Charpentier et al. 2007, Durand & Zvonkin 2007).

This measure was the basis in developing an algorithm to calculate the index of complexity c (n) which is an approximation of Kolmogorov complexity that estimates the degree of randomness in a time series (Lempel & Ziv 1976). This measure allows the characterization of spatial-temporal patterns in non-linear systems (Kilby et al. 2014). Similar patterns in a time series are detected through this algorithm. The information can be compressed and as result a shorter time series is obtained when repeated patterns are found.

The complexity index c (n) measures the number of different patterns in a given time series. According to the Lempel-Ziv (LZC) algorithm, the complexity of a time series {Xi}, i = 1, 2, 3, 4... n, is calculated as follows:

1. In a first step, the original series is encoded.

2. The complexity index c (n) is a function of the length of the sequence N. The values of c (n), approaching a maximum value b (n) when N approaches infinity. For instance:

$$c(n) = O\big(b(N)\big), b(N) = \frac{log_2 n}{n} \qquad (18)$$

3. The measurement of standardized information is calculated and defined by:

$$C(n) = \frac{c(n)}{b(n)} = c(n)\frac{log_2 n}{n} \qquad (19)$$

A high value of C (n) indicates increased randomness and a lower level of predictability (Kilby et al. 2014).

Binary series 0 and 1, are often used to facilitate the understanding of this method.

The corresponding complexity measure c (n) is obtained by normalization.

A detail description of the Kolmogorov complexity can be found in Durand & Zvonkin (2007) and Ferbus-Zanda & Grigorieff (2010).

4.1.2.4.1 Permutation Entropy (PE)

This concept was introduced by Bandt & Pompe (2002) as a complexity measure for time series. Entropy can be approximately defined as the degree of disorder or uncertainty in a system, thus it is an indicator of its state. Statistical equations for entropy have been derived by Boltzmann in physics who links entropy to energy and by Shannon in the field of information theory. Both parameters have an inverse relationship. That is, adding information to the system leads to the more efficient use of energy, and thus lowering entropy (Bailey 2001). Initially, only monotonous self-maps of one-dimensional intervals were considered and the permutation entropy (PE) formulation was made under the framework of dynamical systems. However, this concept has been generalized by the use of ordinal symbols related to arbitrary finite partitions in a dynamical system where the symbols are the labels of the partition sets. These labels are ordinal patterns. Therefore, this theory is related to the measure of the amount of information based on the presence of a pattern which is defined by a natural encoding of the time series into a sequence of symbols (Amigó & Keller 2013).

An ordinal pattern of length L is a vector displaying the rank order of consecutive entries in a random time series. The permutation entropy of order L is defined as the Shannon entropy of the ordinal L-patterns. This is an average measure of uncertainty and related to the average amount of information contained in a random variable. The permutation of the values of a time series is determined by this method and the characterization of the structure of the local order in a time series is a measure of the complexity in dynamic systems.

According to Riedl et al. (2013), the calculation of the PE of a given time series {x} of length N is made by the following method: The permutation order is defined as m which leads to a possible permutation pattern, which is built from 1 to m.

The time series {xi} index is i = 1, ... n where n is the counter for each pattern.

The dynamic representation is presented in Fig. 15 for, m = 3 (Riedl et al. 2013).

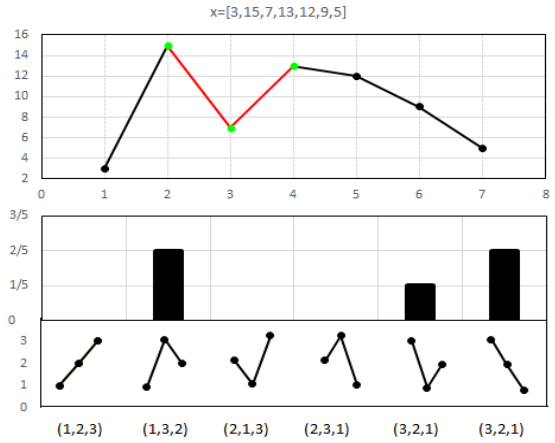

Fig.15. Representation of the permutations for m = 3 and its frequencies in a signal. (Riedl et al. 2013).

The rank of values is calculated following a certain sequence and the resultant values are indexes in ascending order. The natural encoding reflects the rank order of successive components of the time series (xi) in sequences of length n and the permutation entropy is defined by:

$$PE = -\sum_{j=1}^{m!} p'_j \, log_2(p'_j) \qquad (20)$$

Where p'_j represents the permutation or a relative frequency of the possible patterns detected in the sequence of symbols. The permutation per symbol is given by:

$$PEn = -1/(n) - 1 \sum_{j=1}^{m!} p'_j \, log_2(p'_j) \qquad (21)$$

This calculation is necessary for a possible comparison entropy permutation with different values of m. In this work m=4. The highest value of de *Pen* is 1, which indicates that all permutations have the same probability of occurrence. However, if PE is zero, indicates that the time series is very regular. The calculation of PE depends on the choice of the m value. For long time series a PE value higher than 3 is suggested (Ouyang et al. 2013).

The principle of maximum entropy, interpreted as maximum uncertainty, has been used in the analysis of rainfall time series (Tapiador 2007, Lumley et al. 2014). In particular to explain the origin of clustering and persistence of the rainfall occurrence process, (Koutsoyiannis 2006) or to explore temporal changes in the dynamics of El Niño/Southern Oscillation (ENSO) (Saco et al. 2010).This concept has been also applied to the solar wind time series (Suyal et al. 2012).

4.2. Statistical tests

4.2.1. The test of Chow

The test of Chow (1960) is used in this work to analyse similarities between fitted straight segments or coefficients in the resultant linear regressions of the plot-plot representation. Chow Test examines whether parameters of one group of the data are equal to those of other groups.

The Chow Test formula is:

$$F_{(k,N_1+N_2-2k)} = \frac{[SSE_p - (SSE_1 + SSE_2)]/k}{(SSE_1 + SSE_2)/(N_1 + N_2 - 2k)} \quad (8)$$

where SSEp = sum of squared error term for pooled model

SSE1= sum of squared error term for group 1

SSE2= sum of squared error term for group 2

k is the number or estimated parameters and N1 and N2 are the number of observations in each group. For a great online description of the Chow test (Lütkepohl 2005) and (http://www.stata.com/support/faqs/stat/chow.html)

4.2.2. The Mann-Kendall's test

The Mann-Kendall (MK) statistical trend test (Mann 1945, Kendall 1975) was applied to explore the existence of long-term trends in the annual precipitation regime

through the survey period. This kind of non-parametric test allows comparing each consecutive element of a time series with all previous values. The comparison of the relative magnitudes of data is made without assuming any particular distribution Apart from its widespread use another reason for choosing this method is its low sensitivity to abrupt breaks due to inhomogeneous time series (Jaagus 2006, Tabari et al. 2011a, Tabari et al. 2011b). Significant variations over time or trend in the sample data is examined by a hypothesis testing process. The null hypothesis means that there is no trend. Each test is based on certain parameters for accepting or rejecting such hypothesis. Failure to reject it is not sufficient to conclude with a specified level of confidence that a trend exists. The robustness of the Mann-Kendall's rank correlation test has been broadly demonstrated, e.g. NNSMP National Nonpoint Source Monitoring Programme, (Meals DW 2011).

4.2.3. The Jarque-Bera and Lilliefors tests

The Jarque-Bera (J-B) test is a two-sided goodness-of-fit test based on the null hypothesis that a sample follows a normal distribution with an unknown mean and variance. It is used to check a hypothesis about if a given sample behaves as a normal random variable. On large sample sizes, the statistical test has a Chi-square distribution with two degrees of freedom. The J-B test uses a table of critical values computed by using a Monte-Carlo simulation for sample sizes less than 2000 and significance levels between 0.001 and 0.50. Critical values for the J-B test are computed by interpolating, using the Chi-square approximation only when extrapolating for larger sample sizes (Jarque & Bera 1987, Deb & Sefton 1996).

In this work, this test is applied to evaluate the normality in annual rainfall distributions using the MATLAB (The Math Works, USA) program.

As input argument, the significance level of the hypothesis test (*alpha*) is employed as a scalar value in the range (0, 1).

The test returns the following outputs arguments:

1. – The value *h* which is equal to 1 if the null hypothesis is rejected at the 5% significance level, and h is equal to 0 if accepted.

2. - The by *p-value*, which is a scalar in the range (0, 1). Small p-values put in doubt the validity of the null hypothesis.

3. – The statistical test (*stat*) which returned as a nonnegative scalar value.

4. - The critical value (*critval*) for the alpha significance level is also returned as a nonnegative scalar value. If alpha is in the range (0.001, 0.50) and the sample size is less than or equal to 2000, the test looks up the critical value in a table of precomputed values. The critical value can also be calculated using a Monte Carlo simulation. The null hypothesis is rejected when *stat* is greater than *critval.*

An analogous test named Lilliefors is used for small samples. The Lilliefors test uses a similar table of critical values than the J-B tests with the same significance levels, whereas the sample sizes are less than 1000 (Lilliefors 1967, 1969, Conover 1980).

4.3. Seasonality index

Several indexes, different in mathematical formulation but strongly correlated among themselves, have been used to characterize the seasonal variation of precipitation (Fatichi et al. 2012). The most common approach to characterize it was suggested by Walsh & Lawler (1981). These authors proposed a relative Seasonality Index (SI) based on the differences between observed monthly precipitation and that expected under the hypothesis of precipitation uniformly distributed throughout the year. That is, for a given year, y, SI is given by

$$SI_y = \frac{1}{P_y}\sum_{m=1}^{12}\left|P_{my} - \frac{P_y}{12}\right| \qquad (9)$$

where P_y is the annual total precipitation and P_{my} represents monthly total precipitation observed during the *m*-th month of year *y*. Such as suggested by these authors when the study is extended over a long period it is possible to derive a global average index of seasonality by replacing annual and monthly amounts by average values over the considered period. That is,

$$SI = \frac{1}{\bar{P}} \sum_{m=1}^{12} \left| \bar{P}_m - \frac{\bar{P}}{12} \right| \quad (10)$$

where $\bar{P}_m$ is the mean precipitation for month m during the overall period under analysis and $\bar{P}$ is the overall mean annual rainfall.

It results easy to show that this index ranges between 0 and 1.83 and that these limits correspond to situations with precipitation uniformly distributed over the 12 months of the year, in other words all months have the same rainfall, and when all annual precipitation takes place in a single month, respectively. The authors suggested a classification of rainfall regimes in terms of SI, which is presented in table 5. A condensed version of this classification, clustering various subclasses, have been used by Peña-Arencibia et al. (2010) and is also presented in the same table. In this work the following acronyms are used: very equable (VE), rather seasonal with a short drier season (SSD), equable but with a definite wetter season (EW), seasonal (S), markedly seasonal with a long drier season (MLD), most rain in 3 months or less (3MR), extreme, almost all rain in 1-2 months (E) and short wet season (SW).

Table 5. Classification of rainfall regimes in terms of SI by Walsh and Lawer, 1981 (W&L-1981), and Peña-Arencibia, et al. 2010 (PA-2010) including acronyms used in this work.

SI	W&L-1981	PA-2010
≤ 0.19	Very equable (VE)	Very equable (VE)
0.20-0.39	Equable but with a definite wetter season (EW)	
0.40-0.59	Rather seasonal with a short drier season (SSD)	

0.60-0.79	Seasonal (S)	Seasonal (S)
0.80-0.99	Markedly seasonal with a long drier season (MLD)	
1.00-1.19	Most rain in 3 months or less (3MR)	
≥ 1.20	Extreme, almost all rain in 1-2 months (E)	short wet season (SW)

The average index of seasonality, $\overline{SI}$, by averaging yearly values. That is, the long-term mean value of the seasonality index for a period of N years is estimated as

$$\overline{SI} = \frac{1}{N}\sum_{y=1}^{N} SI_y \quad (11)$$

Taking into account the difference between the global and mean indexes of seasonality, given by Eq. 10 and Eq. 11, respectively, Walsh & Lawler (1981) defined an index of rainfall replicability as the quotient between both parameters, $RI = SI/\overline{SI}$. Note that this parameter is lower or equal than 1, with the equality corresponding to the case in which the rainfall regime every year is equal to the mean regime, and, in such a case, the wettest and dries months are the same every year. Therefore, this index provides information on the variability or deviations of annual rainfall regimes from the mean annual regime. Thus, when the ratio is high the rainiest and driest months tend to be the same each year and the mean rainfall regime is significantly replicable. In the opposite scenario, low values of the index indicate that wettest and driest monthly periods can occur over a wide range of calendar months and regime replicability is low. Some studies have argued that rainfall replicability index is a useful method to quantify mean rainfall regime (Bello 1998, Sumner et al. 2001).

It is important to underline that both seasonality indexes and the chi-square test allow for identification of seasonal patterns, but none of them provide information on

when and how much precipitation occurs. Thus, complementary information on precipitation amount is also needed to fully describe seasonality.

An alternative method for statistical assessment of seasonality in the rainfall time series is based on the Chi-squared test. To apply this test, days of the year are converted to angles as follows (Batschelet 1981).

$$x = \left(\frac{360}{365}\right) d, \quad d = 1, \cdots, 365 \tag{12}$$

The circle divided in a fixed number of angular bins, N_b, of α degrees each, so that $N_b.\alpha=360^o$. In this study $N_b=12$ and $\alpha=30^o$. Thus, each one of the twelve bins (30º arc) corresponds to a month, approximately. Then, compute the overall monthly mean precipitation by averaging the rainfall associated with every day belonging to each month. Resulting values are empirical frequencies associated with each month.

Whether the same precipitation is expected to occur during any month, expected values for each bin are the overall yearly mean precipitation divided by twelve. That is, precipitation expected during each month is the same. In this case monthly precipitation distribution is uniform. On the contrary, when precipitation during some months is significantly higher than during the rest of the year, it is far from uniformity and seasonality can be statistically accepted.

The χ^2-test can be used to compare empirical and theoretical uniform distributions. The null hypothesis to be assessed is H_0: precipitation is uniformly distributed throughout the year, against the alternative H_1: precipitation is not uniformly distributed. The χ^2-test test statistic is given by the sum of squared differences between observed and expected frequencies divided by the expected frequencies. The corresponding degrees of freedom are 10 because one parameter must be evaluated to compute expected monthly precipitation, which is the yearly average precipitation. Then, for testing the null hypothesis on a 95% confidence level, the critical value is $\chi^2 = 18.31$.

Therefore, when χ^2-statistic is larger than its critical value null hypothesis can be rejected, concluding that there exist significant differences among monthly values of precipitation and uniformity cannot be accepted.

Rainfall seasonality has been broadly studied using the indexes above described some examples are the analysis of precipitation seasonality in Spain (Sumner et al. 2001) or in Greece (Livada & Asimakopoulos 2005).

Other indexes used to explore intra-annual seasonality of precipitation are the Precipitation Concentration Index (PCI) (De Lùis et al. 2000, Fatichi & Caporali 2009), and the Seasonality Concentration Index (SCI) (Fujita 2008) and the Mr for a given year as defined by Davidowitz (2002).

An example of the use of the index seasonality on the annual land surface evaporation in a global circulation model is found in Van den Hurk et al. (2003).

4.4. Wavelet analysis

The spectral analysis is a technique that allows the study of a signal by decomposing the series in different frequency bands and estimates the relative importance of each of these frequencies and contribution to the total variation of the series. A very general mathematical principle based in Fourier theory asserts that any periodic function can be decomposed into the sum of infinite sinusoidal functions of harmonic frequencies of the fundamental frequency. In Fourier analysis each sinusoidal function is defined by a specific amplitude, phase and period. The Fourier transform operates on the time series by moving the variable that is defined in the time domain to the frequency domain. The variance n a time series gives an idea of how the data are scattered; therefore it is a measure of variability of the data. The energy of the signal, or power, is related to the variance. The result of applying the Fourier transform is a graph of the spectral density, which can be interpreted as the total area under the curve equal to the variance of the

process. Then, any peak of the curve represents the contribution of the variance to a specific frequency. Although the spectral density is not exactly the same as the spectrum of a signal, sometimes both terms are used interchangeably. Thus, the Fourier spectrum of frequencies reveals the presence of periodic components and it is useful to investigate the regular variations in a time series. If a time series is completely random, each data is completely independent from the previous, it is often treated as noise.

Nevertheless, the wavelet technique is being increasingly used in data analysis as it offers advantages over the Fourier method (Meyers et al. 1993, Liu & Miller 1996, Emery & Thompson 2001). Wavelets are a family of basic functions that can be used to approximate any given signal (Morata et al. 2006). The main difference between wavelet and Fourier decomposition is in the support of the respective functions. The wavelet transform coefficients are influenced by local events, while the Fourier coefficients are influenced by the function on its entire domain. Furthermore, Fourier transform allows localisation in frequency but not in time; and Wavelets enables both.

The Wavelet transform (WT) is a useful tool for examining variability of a given process in the time-frequency domain, including multi-scale structure and non-stationary behaviour of temporal signals. The spectral analysis through a Wavelet transform was introduced and formulated by Morlet et al. (1982) and Grossmann & Morlet (1984). It can be used to analyse signals at different frequencies and reproduces properly the local behaviour of a time series (Percival & Walden 2000).

The wavelet analysis allows decomposing a non-linear series into time-frequency space and helps to find the dominant mode of variation through a wavelet transform which consist on a series of bandpass filters (Kumar & Foufoula-Georgiou 1997, Mallat 1998, Torrence & Compo 1998, Datsenko et al. 2001, Addison 2002). Thus, wavelet separates a signal into multi resolution components.

The transform has a multiscale nature and the spectrum is divided into intervals of varying widths that can be treated separately. The interval widths are related to the scale of the analysis: small (large) scales are associated with the processing of small (large) intervals.

The wavelet transform can be used to analyse time series that contain no stationary power at many different frequencies. The scalogram (time-frequency or time-scale graphic) of a time series-is the squared modulus of its wavelet transform, $|WT(a, b)|^2$, and represents the signal power distribution in the time-frequency domain. That is, an averaged power spectrum for all the scales or frequencies (wavelet coefficients), similar to a smoothed Fourier power spectrum. By varying the wavelet scale s and translating along the localized time index n, one can construct a picture showing both the amplitude of any features versus the scale and how this amplitude varies with time (Torrence & Compo 1998). The overall power spectrum for all the scales, or frequencies, similar to a smoothed Fourier power spectrum, is obtained by averaging over time for any frequency. The average over a frequency at any instant provides the total local power in the time series. The time average between two given frequencies reveals the contribution of such a frequency band to the signal power at any instant (Torrence & Compo 1998).

Thus, wavelets are appropriate tools to study non-stationary signals by means of the localization in time and frequency (Morata et al. 2006). Details of these methodologies are given in several text books (Mallat 1999, Percival & Walden 2000). A theoretical treatment of the wavelet analysis is given in Daubechies (1992), Farge (1992), Meyers et al. (1993) and Lau & Weng (1999).

Various applications of wavelet transforms to geophysics (Kumar & Foufoula-Georgiou 1997, meteorology or climatology can be found in the literature (Wang & Lu 2010, Yi & Shu 2012, Zhang et al. 2014). For example applied to the analysis of rainfall

variability (Kumar & Foufoula-Georgiou 1993, Westra & Sharma 2006, Johnson et al. 2011). Wavelet Multi-resolution Analysis (WMA), introduced by (Mallat 1989) and (Meyer & Salinger 1992), has also been used in the analysis of the precipitation signals (Kumar & Foufoula-Georgiou 1993, Perica & Foufoula-Georgiou 1996, Labat et al. 2001, Chen & Li 2004, Morata et al. 2006). Another example of the use of the wavelet technique is the analysis of temperature (Gao & Wu 2015), wind (Chen et al. 1995), variability of sea level pressure field (Barbosa et al. 2009, Johnson et al. 2011), cold fronts (Gamage & Blumen 1993), air-sea interface (Meyers et al. 1993, Spedding et al. 1993), aerosols (Pal & Devara 2012), solar activity (Lundstedt et al. 2005, Johnson 2010), the atmospheric boundary layer (Mahrt 1991, Terradellas et al. 2001), convection (Weng & Lau 1994), turbulence (Farge 1992, Gao & Li 1993) and wetness grades in different areas (Jiang et al. 1997). Wavelet decomposition has also been suggested as a possible tool to analyse time of SSTs (Johnson et al. 2011). Another examples of the use of the wavelet technique are the analysis of NAO indexes (Barbosa et al. 2006) or response of ENSO to greenhouse warming (Timmermann 1999).

Wavelet transforms are divided essentially in two distinct varieties: the continuous wavelet transform (CWT) and the discrete wavelet transform (DWT). Both DWT and CWT are continuous-time transforms. However, CWTs operate over every possible scale and translation whereas DWTs use a specific subset of scale and translation values.

In this analysis, we apply both a discrete and a continuous wavelet transform to obtain the spectral time decomposition of the Bermuda rainfall time series.

4.4.1. Discrete Wavelet Transform (DWT)

To explore the different time-scales variability of the rainfall over Bermuda, the Discrete Wavelet Transform (DWT) was used thus it allows a scale-by-scale analysis of the signals (Kumar & Foufoula-Georgiou 1997). The DWT is defined as an orthonormal

transform. The basic idea of the DWT is to filter the data sequence to obtain the wavelet coefficients at different levels. In the DWT scheme, the signal *f* of length *N* is decomposed into both approximation (cA_j), and detailed (cD_j) coefficients by the use of two quadrature mirror filters (quadrature mirror filter bank).

Thus, the DWT analysis is a filtering operation where the high frequency (high pass) component appears in the detail coefficients cDj and the low frequency (low pass) component in the approximation coefficients cAj. In DWT the detail coefficients are not further decomposed, and at each scale, the detail signal is stored and the decomposition continues filtering the approximate signal which will be taken as the input signal for the next scale.

At each decomposition or reference level *J*, the approximation coefficients cA_J and detail coefficients cD_1, cD_2, ,…, cD_J are obtained, and we can reconstruct the approximation signal $A_J(t)$ and the detailed signal $D_j(t)$, j=1…J (Percival & Walden 2000). Therefore, the signal f(t) may be expressed as the sum of a smooth part plus details as follows:

$$f(t) = A_J(t) + \sum_{j=1}^{J} Dj(t) \qquad (13)$$

Where each detail D_j is associated with changes at physical scales of $\tau_j=2^{j-1}$ (j=1….J) and the smooth A_j (or approximation) represents variations over physical scales 2^J and higher. The details D_j represent how the averages (weighted) of the observations change from one time interval to the next and the scale τ_j gives the width of the time interval for which the averages are computed. Thus, detail D_j represents differences in averages over time intervals of 2^{j-1} corresponding to observations time-spaced between 2^j.

Coefficients at larger scales are associated with wider intervals in the spectrum, whereas coefficients at smaller scales are associated with narrower intervals.

The wavelet variance of a process X = Xt, t = 1, . . . , N over all dyadic scales τj = 2j−1 (j = 1, . . . , J) constitutes a second order description of the process through a 'wavelet spectrum', with large values of j corresponding to low frequencies and small values of j corresponding to high frequencies (Barbosa et al. 2006).

To sum up, the wavelet transform can be thought of as a consecutive series of band-pass filters applied to the time series where the wavelet scale is linearly related to the characteristic period of the filter. DWT is useful to rebuild a signal from its wavelet coefficients in order to reduce the information (Terradellas et al. 2001).

A signal can be represented by a minimal number of components or wavelets coefficients. For orthogonal wavelets, the distribution of noise energy is relatively uniform among all dyadic scales (Morata et al. 2006). One drawback of the use of the DWT is that is only applicable to series of dyadic length. In this kind of analysis commonly it highlights that as the resolution decreases, the amplitudes of the coefficients that can be considered as filters for the corresponding scales indicate the intensity of the precipitation fluctuation at every frequency.

Results from these method used by other authors (Morata et al. 2006) show that rainfall can be seen as a multi-resolution response to several atmospheric effects linked to different frequencies.

Wavelet transforms also play an important role in the study of self- similar processes (Morata et al. 2006). In this work the wavelet spectrum is estimated for each index from a level J = 8 on the basis of the Daubechies wavelet filter (Db8).

4.4.2. Continuous Wavelet Transform (CWT)

The algorithm used to apply Continuous Wavelet Transform is described by Torrence & Compo (1998) and based on the most commonly used Morlet wavelet. In the CWT the scale a and translation parameters b assume continuous values, and the |WT (a,

b)|^2 of a time series can be visually represented by an image or a field of isolines. In this work we calculated the CWT employing the Morlet wavelet, which is a modulated Gaussian function that is well localized in both time and frequency. Where ω_0 is a dimensionless frequency that defines the number of cycles of the Morlet wavelet. For large ω_0, the frequency resolution improves, though at the expense of decreased time resolution. For this reason, we used several values of the parameter ω_o, finding that ω_o = 20 was well adjusted to our purposes.

$$\boldsymbol{\psi_0} = \pi^{-1/4}\ e^{iw_0 t} e^{\frac{-1}{2}r^2} \qquad (14)$$

The algorithm used is described by (Torrence & Compo 1998) and based on the most commonly used Morlet wavelet (Chapa et al. 1998, Huang et al. 1998).

The continuous wavelet transform of a discrete time series x_n is defined as the convolution of x_n with a scaled and translated mother wavelet ψ to give

$$W_n(s) = \sum_{n'}^{N-1} x_{n'} \psi^* \left[\frac{(n'-n)\delta t}{s}\right], \qquad (15)$$

Where * indicates the complex conjugate, s is the scale, n= 0, . . . , N - 1 is a localized time index, and δt(1/25 for pentad and 1/4 for monthly) and N(750 for pentad, 120 for monthly) are the time spacing and length of the time series x_n, respectively.

In this study a Continuous Wavelet Transform (CWT) is applied to obtain the time-frequency decomposition of the Bermuda airport rainfall time series and to obtain wavelet-filtered time series between two given scales (frequencies). The algorithm is based on the most commonly used Morlet wavelet. More details of this methodology are given in several text books (Mallat 1999, Percival & Walden 2000).

4.4.3. Cross Wavelet Power (CWP)

When comparing two variables, especially in climate sciences, or when analysing tele-connections, the multivariate analysis applied to wavelet framework is a useful tool that provides information about the scale dependent degree of correlation between two given signals (Onorato et al. 1997, Maraun & Kurths 2004). The cross wavelet analysis was introduced by Hudgins et al. (1993). Some authors have been addressed the application of this method in processes related to NAO like ENSO-North Atlantic Oscillation (NAO) teleconnections (Huang et al. 1998) or the influence of NAO on European surface temperatures (Pozo-Vazquez et al. 2001).

The cross wavelet power of two time series X and Y is defined as $W^{XY=}W^{X}W^{Y}$ * (3) where * denotes complex conjugation. Its complex argument can be interpreted as the local relative phase between both time series in time frequency space (Grinsted et al. 2004). The distribution of the cross wavelet power of two time series with background power spectra PXk and PYk is given in Torrence and Compo, Eq 31, (1998) as:

$$\frac{|W_n^X(s)W_n^{Y}*(s)|}{\sigma X \sigma Y} = \frac{Z_v(p)}{v}\sqrt{P_k^X P_k^Y} \qquad (17)$$

Where σx and σy are the respective standard deviations and Z_v (p) is the confidence level associated with the probability p for a pdf defined by the square root of the product of two Chi-square (χ^2) distributions. This analysis allows discerning if the similarity between the variables analysed by DWT is only a coincidence (Grinsted et al., 2004).

Cross-correlation and cross-spectral were employed in the analysis of relationships between rainfall in Bermuda and NAO. Results extracted from this study are presented in cross scalograms which provide the unfolding of the features of the interaction of two processes in the scale space plane (Kumar and Foufoula-Georgiou,

1997). Similar analysis has been applied to precipitation by other authors (e.g. (Bourodimos & Oguntuase 1974).

5. Results and discussion

5.-Results and discussion

The principal results of spatial variability on rainfall regime over these archipelagos, as well as variability at different time scales, with special emphasis on the distribution throughout the year, are presented in the following sections.

5.1. Spatial homogeneity in Bermuda

The dimension and flat orography of the archipelago are strong indications of the possible homogeneity in rainfall over Bermuda. Then, as a first step towards addressing the study of the rainfall variability through these islands, the comparison of the seasonal rainfall distribution between Bermuda A. (BER1) and

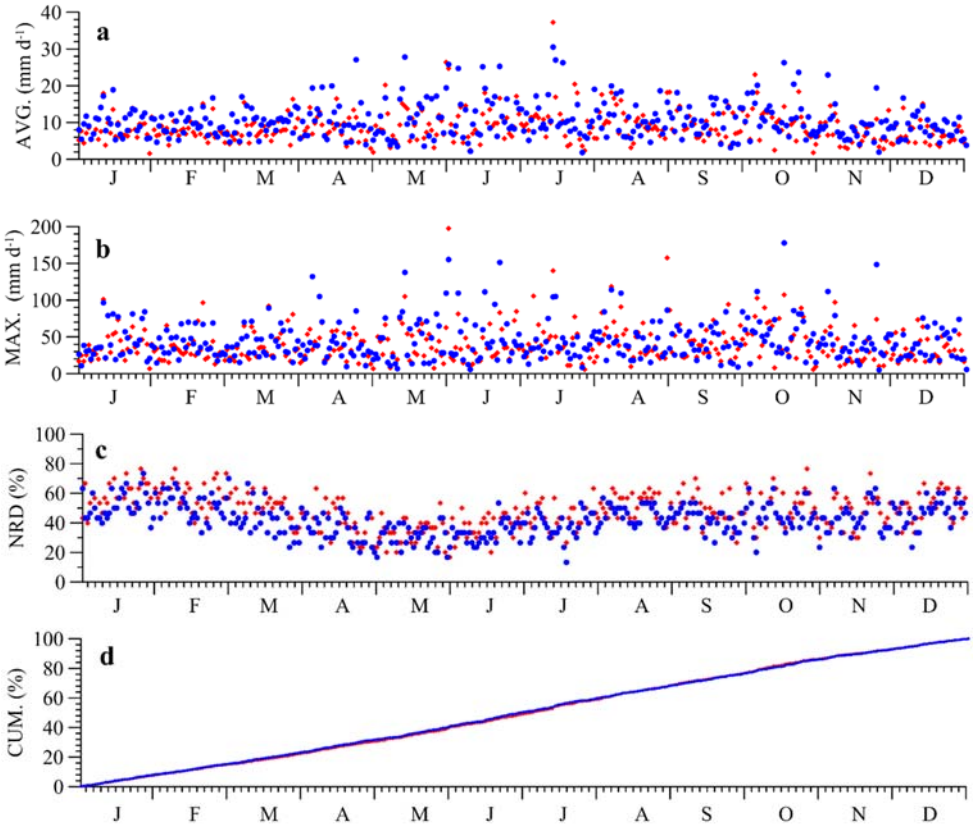

Fig.16. Seasonal distribution of rainfall at Bermuda A. (a) Daily rainfall average for each day of the year in mmd^{-1} (AVG) (b) maximum daily rainfall for each day of the year (MAX) in mmd^{-1} (c), number of rainfall days (NRD) (%) and (d) daily rainfall accumulation (CUM) (%) at Bermuda A. (red dots) and Somerset V. (blue dots). Period 1981-2010. Daily data from BWS.

Somerset V. (SOM), which are placed at almost opposite location within the archipelago, has been examined. Results are depicted in Fig.16, with red dots (BER1) and blue dots (SOM), respectively. The daily average (AVG) and maximum (MAX) rainfall are shown in Fig.16a and 16b, respectively. Pearson correlation coefficients between these signals are r=0.61 and r=0.57 correspondingly. The average rainfall for a specific day is the average of 30 daily values from the normal period (365 days for non-leap year). For instance, the average for the January 1st was estimated using the 30 values from January 1st of each year from the selected period, 1981-2010. Variables represented are estimated for any calendar day during this normal period.

Similarly, Fig. 16b describes the maximum daily rainfall (MAX). It can be observed that the patterns of these parameters are quite similar along the year for both sites, with records of maxima not exceeding in general 100 mmd^{-1}. The maximum amount of rainfall recorded at Bermuda A. was 197 mm on 1st Jun 1996, while at the Somerset V. station 155 mmd^{-1} were registered for that date.

Another variable of interest to check the similarity between rainfall patterns at different places is the number of rainfall days (NRD). In this study, a day has been considered to be rainy if the amount of precipitation is 0.25 mm or greater. The percentage of NRD for any calendar day is represented in Fig.16c and provides information about how many times during the whole period studied it rains each day of the year. Results show that such parameter calculated at both stations exhibits a significant correlation, Pearson coefficient, r =0.72.

The daily average accumulation (CUM) throughout the year is calculated by summing the average daily amounts for January 1st, January 2nd, January 3rd, etc. during the normal period. Results are presented in percentage. In spite of the homogeneity between both time series, rain events take place during approximately the same periods

of time, the value of the daily accumulation rainfall from SOM is approximately 19,4% higher than for BER1 (Fig. not shown). However, accumulation percentages, calculated as the quotient between the daily accumulation and total annual precipitation multiplying by 100, are shown in Fig.16d. This parameter exhibits almost the same behaviour at both locations. This means that although SOM is the station with heavier 3

Results derived from comparing both time series reveal that rainfall regime is virtually the same at both sides of the archipelago. In fact the same exploratory techniques, used to examine rainfall regime in time series at BER1, have been used to examine SOM rainfall patterns, leading to almost the same results, especially when using just the coincident period. This validates the spatial homogeneity hypothesis for rainfall in the region. Therefore, only the BER1 time series will henceforth be used, due to their longer duration and for being considered representative of the rainfall behaviour over the whole archipelago. This fact represents a great advantage to avoid practical limitations that emerges when analysing data from many stations.

However, the complex topographic and orographic features that characterize the rest of the archipelagos included in this work reveal a considerable spatial non-uniform rainfall pattern, being the relief one of the critical variables controlling the local rainfall distribution.

5.2. Frequency of dry periods

5.2.1. Bermuda. Poisson model

The analysis in this section is being focused on the duration of consecutive dry events between rainfall events. The frequency histogram (bin=20) of dry periods as a function of the time intervals in days (Ti; i= 3, 4, 5…) is represented in Fig.17. Results point out that the probability of observing dry periods is not the same for a certain time interval (Eq.1). In other words they are not uniformly distributed.

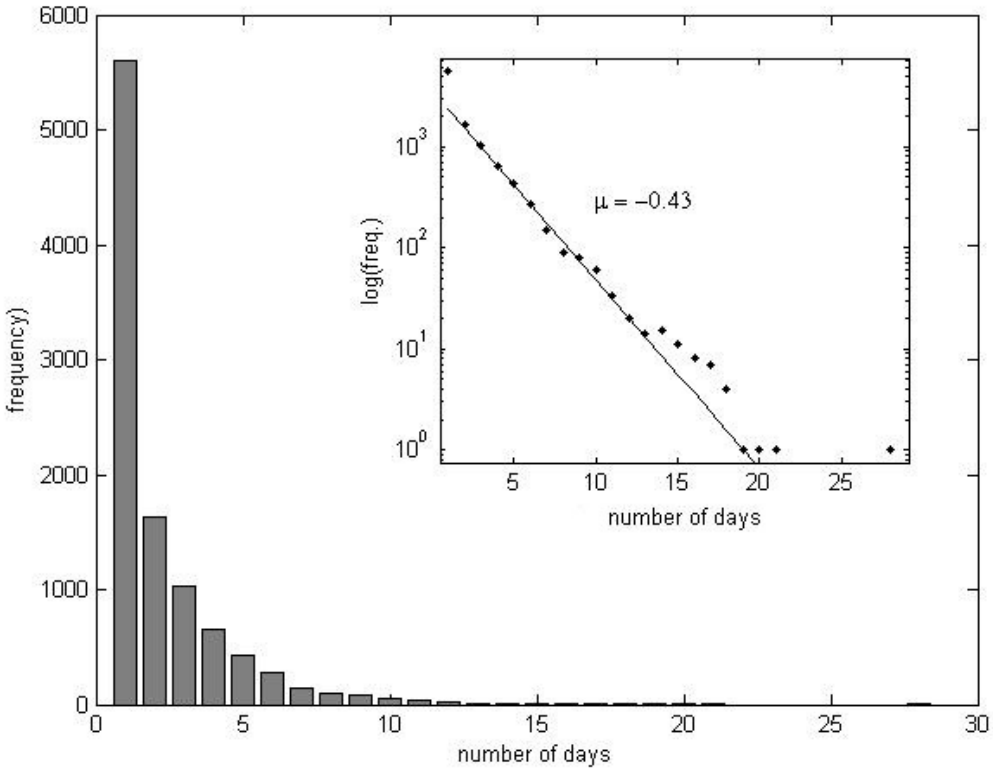

Fig.17. Histogram of the number of dry days between successive rainfall events. Inset figure the semi-log plot of the frequency with fitted straight. Bermuda airport (1949-2011). Daily data from BWS.

The frequency of dry periods declines rapidly with increasing number of days without rain indicating an exponential behaviour with characteristic features of a Poisson process. The distribution shows a peak during a period of one day. That means that in Bermuda the most likely time interval between rain events is 24 hours. Such situation can be predicted with a lower margin of error. However, the probability to find larger dry periods decreases sharply as lower frequency is being observed between 13 and 22 consecutive dry days.

The distribution shows about 28 through 29 days as the maximum duration of a dry period that can be taken as a rare phenomenon.

The exponential decay behaviour of the distribution is tested by taking a semi logarithm of the previous figure and fitting a straight line, obtaining the inset figure. On

the X axis the time differences between rain occurrences is shown and the Y-axis represents the logarithmic scale of the number of dry days (NDD). Two zones can be considered in this representation. The first one extends from 0 to nearly 13 dry days, the second one from 13 to 22 consecutive dry days. It can be inferred that between one and 13 days, the measurements follow a straight line that can be adjusted with slope $\mu = -0.438 \pm -0.04$. This means that it rains a 44% of the days during a year. The μ value or the rainfall average rate is very close to the NRD (Eq.2) average. The time passed between rain events becomes more random and follows a negative exponential distribution. This is a powerful indicator that the rainfall in Bermuda can be modelled as a Poisson process (Dalelane & Deutschländer 2013).

The values fitted to the straight line correspond to those predicted by the model. This behaviour is essential in this model, being the randomness the main characteristic of the sample as is defined in the semi log plot line. This suggests that the duration of certain number of dry periods follows a non-memory behaviour, indicating certain unpredictability. This feature of less memory or evolution without after effects means that an observation of a dry period is independent of the previous one.

The Poisson model shows a high goodness of fit until the value of 13 dry days and then underestimates the duration of dry periods, revealing the loss of non-memory.

In addition, there is a second zone where data seem to be scattered or biased indicating a different nature of this region between 13 to 22 consecutive dry days. This behaviour indicates the breaking of the non-memory state. For values greater than 13 dry days, the Poison model fails while a phenomenon of learning appears. If 13 or more consecutive dry days are observed, the probability of having such a NDD or longer dry spells increases. That is, when more than 13 consecutives dry days are observed, there is a high probability of having 14, 15 or more consecutive dry days. The occurrence of a

given dry day depends on the not observation of rainfall in the previous ones. This process underlies different subjacent mechanisms based on the presence of more or less than 13 consecutive dry days. Furthermore, from the analysis of the last part of the distribution or upper tail, it can be inferred that it is very unlikely to observe approximately 28 consecutive days without rain. Accordingly to these results, it is possible to characterize Bermuda as a region with an annual rainfall pattern with a high rate of rainfall days.

5.2.2. Comparison with Canaries, Madeira and Azores

The duration of dry periods between rainy events in Gran Canaria A. has been analysed by using the long data set derived from METARs, gaining insight on the rainfall time distribution over the Canary archipelago. This station has been selected because of the available long data set and its geographical location. It is important to note that METARs only take into account the occurrence or non-occurrence of rain event but not their intensity. This implies that a light rain is considered as rainfall occurrence in the same way as a heavy one. Hence, dry periods could be even longer than those detected in this study.

The frequency number of dry periods as a function of the number of days is represented in Fig.18. It can be observed that the number of dry events decreases sharply for low and moderate durations, but a small number of notably large events are present in the upper tail, with dry periods between rain events reaching durations of about 5 months. This difference is noticeable when this distribution in Bermuda was analysed in the previous section, where the higher duration of dry periods reaches approximately one month. This indicates a difference in rainfall patterns, obviously the Canaries are much drier than Bermuda.

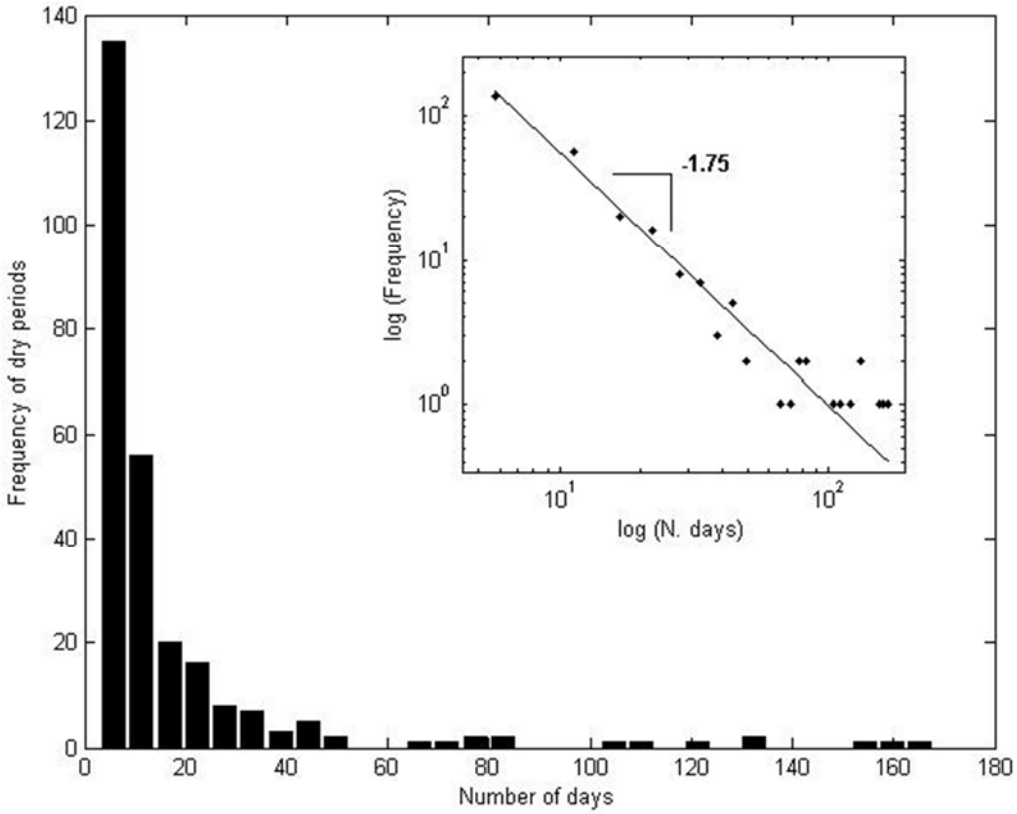

Fig.18. Histogram of time intervals (in days) between rain events for G. Canaria A. and log–log representation with fitted straight line (inset figure). Period 1989-2010. Hourly data (METARs) from AEMET.

Data follow a heavy tail and suggesting a PL behaviour. The log–log plot of the frequency of dry spells versus duration shown in the inset of Fig.18 reveals the existence of a PL with exponent $\beta = -1.75 \pm 0.25$, determination coefficient of linear regression $R^2 = 0.90$ and a root mean square error RMSE = 0.42. As commented previously, it is remarkable that for very large durations, data are scarce and sparse, and therefore this may influence the computed values of the exponent. The scale parameters β in the case of a PL or μ when analysing a Poisson process are equivalent and both give the value slope of the straight line for the linear regression adjustments derived from in the log–log or semi log-log plots used to represent the analysed distributions, respectively.

These results agree with those reported in other studies (Mazzarella 1999, Izzo et al. 2004). In general, the presence of long tails is an indicator of the absence of some

statistics like the mean or the variance, in particular for absolute values of the exponent β (|β|) less than 3, as most of the values found in this analysis. When analysing dry spell frequencies presented in this section, such statistics could be interpreted as infinite. This kind of pattern reveals the possibility of natural hazards (Cello & Malamud 2006) and also suggests the existence of scale-invariant properties underlying critical phenomena (Sornette 2004). Occurrences of both dry or rain events following PL laws might point out the existence of self-organised criticality (SOC).

A low |β| does not imply fewer annual rainfall events, but a higher clustered pattern and longer dry periods. These distributions over different locations in the north subtropical area including Bermuda (BER1), Funch. Obs. (M), Horta Obs.(Az.), Lanzarote A. (A2), El Hierro A. (A7), S. C.Ten. (T1) and L.Canteras (P14) for the normal period 1981-2011 have been also analysed similarly and the frequencies of dry periods have been represented versus the number of consecutive dry days between rain events.

In general dry periods of a short duration are more probable, whereas long ones are rare, which may correspond to extreme events or droughts. The goodness of fit to the straight lines obtained in the log–log representations shows |β| values and different statistical estimators and the greatest NDD for Bermuda (BER1), Funch. Obs. (M), Horta Obs. (Az.) and 18 weather stations within the Canary Islands for the normal period 1981-2010 are presented from lower to greater |β| value in Table 6. The p-value was close to zero for all them. For Gran Canaria A. (A1) there is a certain difference between |β| when calculated from METARs observations than from data obtained from weather stations. It should be taken into account that METARs observations are hourly while rainfall is measured from a gauge daily. The relative difference of the length of the studied period: 1989-2010 for the METARs and 1981-2010 for A1 and the confidence intervals (IC) for

all the stations should be also considered. The error variance (δ^2) quantifies the variance of the distinct values represented around the regression line.

Table 6. Acronyms for the selected weather stations, St. Name (station name), Elev. (station elevation in m), Loc. (location), exponent |β| confidence interval (C.I.), determination coefficient of linear regression R^2 , error variance (δ^2) and the greatest number of annual dry days (NDD (dyr^{-1})) for Bermuda (BER1), Funch. Obs. (M), Horta Obs. (Az.) and 18 weather stations within the Canary Islands from lower to greater |β| value. Period 1981-2011. Daily data from BWS, AEMET and IPMA.

St.Name	Acron.	Elev.(m)	Loc.	|β|	C.I.	R2	δ2	NDD
S. M. Abona	T12	642	S	1.45	0.33	0.85	0.35	275
Ten. S. A.	A5	64	S	1.89	0.20	0.96	0.12	181
Mogán B A.	P5	715	SW	1.90	0.28	0.92	0.28	226
Ll. Arid. B	T13	274	W	1.91	0.22	0.95	0.16	168
Fuenc. Cal.	T14	410	S	1.97	0.24	0.95	0.18	160
Izaña	T5	2371	C	1.99	0.54	0.95	0.33	138
Arucas Bañ.	P11	50	N	2.05	0.26	0.94	0.23	159
Lanz. A.	A2	14	SE	2.07	0.20	0.97	0.11	123
El Hierro A.	A7	32	NE	2.07	0.33	0.93	0.31	234
G. Can. A.	A1	24	E	2.11	0.26	0.95	0.23	150
L. Canteras	P14	15	N	2.12	0.22	0.96	0.15	148
Telde - LL.	P16	150	E	2.18	0.25	0.96	0.17	84
Valseq. G.R.	P12	540	C	2.21	0.26	0.96	0.19	113
Sabinosa	T15	299	W	2.23	0.18	0.97	0.11	103
Teror Dom.	P2	630	N	2.23	0.27	0.95	0.22	83
S.J. Rambla	T2	106	NW	2.26	0.24	0.96	0.17	89
Moya Font. C.	P13	950	N	2.28	0.63	0.91	0.58	93
S.C. Ten.	T1	35	NE	2.36	0.22	0.97	0.13	97
Funch. Obs	M	58	S	2.39	0.28	0.96	0.21	123
Berm. A.	BER1	7	NE	2.97	0.39	0.95	0.28	17
Horta Obs	Az	45	S	3.46	0.42	0.96	0.28	18

For all the weather stations examined values of δ^2 were less than 1, then the represented points in figures (frequency of the number of dry periods as a function of the

number of days) fits the lines plotted. Furthermore, due to the confidence intervals (I.C.) values, the results achieved from Moya Font. C. (P13) and Izaña (T5) should be approached with caution. Moreover, samples for these two stations and S. J. Rambla (T2) and S.M. Abona (T12) contained some gaps which do not affect the results obtained in this analysis.

A high |β| value may involve some truncation in the distribution, and therefore a low probability of long dry periods (longer than one year). These results reveal the presence of a PL relationship between the frequency of the occurrence dry spells and their duration almost in all the weather stations analysed (except Horta Obs. (Az.) and Bermuda A. (BER1)). The highest values of |β| (>3) are found in Horta Obs. (Az.) (3.46) followed by Bermuda A. (BER1) (2.97). The distributions of the number of dry spells between rain events in Horta Obs. (Az.) and Bermuda A. (BER1) follow an exponential adjustment more accurately than a PL, which indicates that this process behaves as a discrete Poisson process or a random one. It rains almost half of the days of the year, besides the lowest annual number of dry days (NDD) is 18 for Az. and 17 for BER1.

Considering the exponential adjustment and the confidence intervals (C.I) the |β| for (2.97±0.39) is very close to 3 and therefore the variance is well defined. This process is limited, then the probability of extreme events is low.

The rest of the weather stations analysed, as above mentioned, follows a PL. The parameter |β| is between 1 and 3, then the variance is not well defined and there is a high probability of extreme events. It is noteworthy that through the slope of the PL exponent |β| different areas within the islands can be characterized. These results agree with the general pattern of the rainfall in the islands which is enhanced by the relief. Below the inversion layer, located approximately between 700 and 1500 m, the presence of fresh and humid air explains the high rainfall occurrence in the windward sides of the northern

sectors. The southern coasts of the islands are drier. Furthermore, the occurrence of rainfall events increases from east to west. Thus, Atlantic disturbances affect predominately the western and higher islands, which are wetter.

Funch. Obs. (M) and S.C. Ten. (T1), located at southern and north-eastern sectors, respectively, present both high |β| parameter taken into account its lower altitudes. The geographical location of Funch. Obs. (M) (in a higher latitude than Canaries) and the northern position of T1 in Tenerife Island affected by local factors can explain this behaviour. The longest dry period observed in Fuch. Obs. (M) is 123 dry days, whereas that period may be extended to as much as 97 days in S.C. Ten. (T1).

Values around 2.2 are found in Canaries at stations located in general in the northern or western sectors and in general at medium altitudes between 100 and 950 meters like Teror Dom. (P2), Valseq. G.R. (P12) and Moya Font. C. (P13) in Gran Canaria or Sabinosa (T15) in the most western island. For them, the greatest number of days per year without rain is between 83 and 113.

Sometimes local effects are the responsible of heavy rainfall over some locations where normally the rainfall rate is relatively low (3.4mmd^{-1}) low due to its location. An example is P16, in an eastern zone and at 150 m, where sporadically heavy rainfall is observed. An example was the rainfall episode observed on 23th October 2015 with a maximum daily rainfall of 110 mmd^{-1} causing damage due to flooding. The previous day heavy rainfall (110 mmd^{-1}) was also observed in the east of Gran Canaria (Jinamar). Observed. The maximum daily rainfall for this weather station for the normal period 1981-2010 was 178mmd^{-1}.

Stations with a northern or eastern location and with elevations lower than 50 m like L. Canteras (P14), El Hierro A. (A7) and P11 present in general an intermediate |β| value (between 2.05 and 2.12). The annual number of dry days (NDD) is greater than for

the stations mentioned previously, and ranges between 123 and 234. It seems that in A7 in a western island and P11 in a norther sector the number of annual dry days is high, however mainly in El Hierro the accumulated yearly rainfall stands out, the maximum daily rainfall can reach 280 mmd^{-1}, whereas the yearly NRD is in average 50, lower than the most of the analysed stations. Then rainfall in some cases is more clustered.

Izaña (T5), the highest station with an elevation of 2.371m could belong to this group because its location above the inversion layer generally doesn't favour the rainfall occurrence. However sometimes relief enhances it. It should be noted that gaps were found in the sample when the rainfall analysis of this station was made.

Lower $|\beta|$ values (less than 2) are found in stations located in southern sectors although with elevations between approximately 640 to 700 m, they are not influenced by the trade winds which brings cloudiness and sometimes rain to the islands. In these cases the absence of some statistics like the mean or the variance could be inferred due to the presence of long upper tails at the end of the distribution which indicates a greater likelihood of drought. Among the analysed stations the lowest $|\beta|$ values are found in Mogán B.A. (P5), Ten. S.A. (A5) and S.M. Abona (T12). The greatest annual number of dry days (NDD) are between 160 and 275. This responds to arid or semi-arid areas. In other words, there may be years when it hardly rains. Such behaviour may be also suggested for Ll. Arid. B (T13) and Fuenc. Cal. (T14) both of all them in leeward sides.

Given that rainfall greater than or equal to 0.1 mm has been initially considered, to better understand this process, the behaviour of the dry periods distribution is again analysed by removing rainfall data lower than 1 mmd^{-1} and 5 mmd^{-1}. A rainfall event is considered light when the daily accumulated rainfall is less than 2 mmd^{-1} and moderate if it ranges between 2 and 10 mmd^{-1}.

The log-log plots of the dry events distributions and the |β| values of the slopes of the linear fits are given for each case in the figures represented below and table 6, respectively. Circles represent daily rainfall distribution when values are greater than or equal to 0.1 mmd^{-1}, red crosses when values are greater than 1 mmd^{-1} and red dots when only rainfall records greater than 5 mmd^{-1} are taken into account.

Results from this analysis for S.C. Ten. (T1), Ten. S.A. (A5), Bermuda A. (BER1) and Horta Obs. (Az.) representing the log–log plots with fitted straight lines of the frequency of dry periods versus the number of consecutive dry days between rain events when values of daily rainfall are greater than or equal to 0.1 mmd^{-1} (circles), greater than 1 mmd^{-1} (red crosses) and greater than 5 mmd^{-1} (red dots) for the period 1989-2010 are shown in Fig.19.

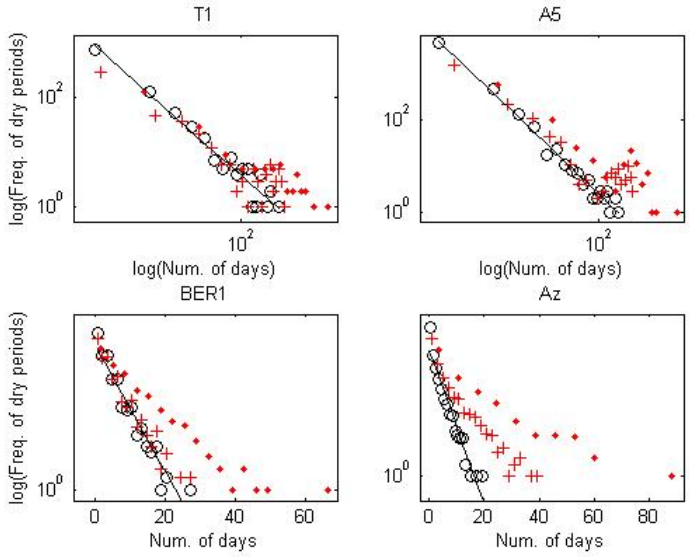

Fig. 19. Log–log plot with fitted straight line of the frequency of dry periods versus the number of consecutive dry days between rain events when values of daily rainfall are greater than or equal to 0.1 mmd^{-1} (circles), greater than 1 mmd^{-1} (red crosses) and greater than 5 mmd^{-1} (red dots) the frequency of dry periods versus the number of days for S.C. Ten. (T1), Ten. S. (A5), Bermuda A. (BER1) and Horta Obs. (Az.). Period 1989-2010. Daily data from AEMET, BWS and IMPA.

As rainfall records lower than 1mmd^{-1} and 5mmd^{-1} are removed, obtaining graphs with crosses and dots, respectively, the NDD increases (see right side of the figures). The

dry periods are often observed near or between rainfall events. Obviously, the probability of long dry periods between rain events (greater than 150 days) increases significantly. when considering rainfall records greater than or equal to 0.1 mm (circles). Not only observing longer dry periods is more likely, but the probability of dry spells increases considerably. This behaviour is clearly observed at the end of the tails as is depicted in Fig.19 with red crosses and dots.

As mentioned above, the distributions of dry periods in Bermuda A. (BER1) and Horta Obs. (Az.) are completely different from the others weather selected stations, The average value of the number of dry days between rain events increases, but the dry periods are evenly distributed, which is characteristic of Poisson processes. A higher average number of dry days between rainfall days is observed. However, they are not concentrated as in the previous cases at the end of the distribution increasing the relative size of its tail. Therefore, the statistical probability of an increase of the number of dry spells between rain events for a given year is low.

5.3. Rainfall intensity in Bermuda. Power Law behaviour

The histogram shown in Fig. 20 represents the frequency of the daily accumulated rainfall in mmd^{-1} for Bermuda and the inset figure depicts the log-log plot. It is observed that the distribution of the daily rainfall intensity in general is not homogeneous. The adjustment of the histogram shows a maximum in rainfall intensity frequency when light rainfall events (<2 mmd^{-1}), decreasing sharply from moderate (2-10 mmd^{-1}) to heavier (10-50 mmd^{-1}) ones. For larger accumulations a possible behaviour of a long tail is shown. A few number of violent or very heavy rain with intensity of about 200 mmd^{-1} is also present in the upper tail of the distribution. For violent rainfall occurrences, data are scarce and sparse and this may influence on the values of the exponents. This kind of

distribution is inherent to scaling properties and the PL behaviour which is verified by the log-log plot in the inset of Fig.20.

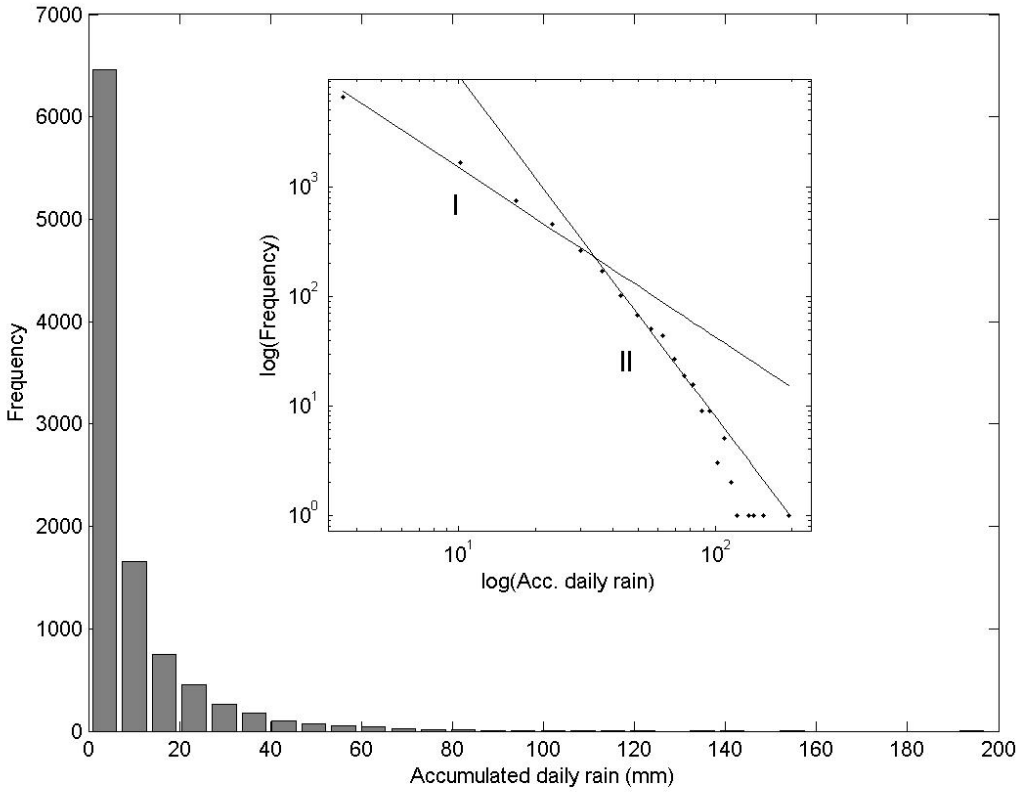

Fig.20. Histogram of daily rainfall intensity or daily accumulated rainfall (mmd^{-1}) and log-log representation with fitted straight (inset figure).Bermuda airport. Period 1949-2011. Daily data from BWS.

Two straight lines or scaling regions indicated with Roman numbers I and II and different slopes separated by a crossover are shown. This break point, close to

30 mmd^{-1}, represents an interruption in the rainfall trend and a transition phase. Between these segments the environmental properties of rainfall are probably changing rapidly. The regression line I presents a slope or PL exponent $\beta = -1.53 \pm 0.2$, determination coefficient of linear regression $R^2 = 0.990$, p-value 0.00 and a variance error 0.02. The number II characterizes heavier rain with slope $\beta = -3.09 \pm 0.33$, $R^2 = 0.98$; p-value 0.00 and a variance error 0.019. This segment, steeper than segment I, unveils a

dense and uniform organisation of rainfall. The test of Chow (Chow & Denning 1993) used to analyse similarities between fitted straight segments from the log-log representation (Eq.8) shows F= 55.93 and p-value = 0.000. Therefore it confirms that each straight line represents a different process.

These results can be interpreted as a certain threshold of daily accumulated rainfall that favours changes in the structure of the rainfall distribution. The crossover means the presence of different laws governing the rainfall behaviour. Rainfall occurrences associated with minor than 30 mmd^{-1} follow an almost homogenous annual pattern mostly marked in winter with a maximum in January and a minimum in spring. However, those related to intensities greater than 30 mmd^{-1} are more common in summer with a maximum in October. Probably, the first ones are associated with frontal passages more common in winter season and the second ones could be generated by thunderstorm activity associated with moist unstable maritime tropical air, most frequent during the late summer or the tropical season (Vandever & Pearson 1994). In fact, cold front passages can produce large 24 hour rainfall totals, but generally mesoscale events associated with convection processes providing short lived rainfall events are responsible for the heaviest precipitation rate in the archipelago. The results gained in this section are similar to those from other studies about rainfall (Mazzarella 1999, Izzo et al. 2004).

5.4. Fractal characteristics. The Canary Islands.

Fractal behaviour of the rainfall occurrence regime has been examined by using time series extracted from METARs. To this end, semi-hourly data from three reference aerodromes have been considered. Furthermore, the fractal dimension of a set of long daily rainfall time series has been analysed to gain a better understanding of the spatial distribution of rainfall occurrences over the archipelago. For this analysis, data were recorded from automatic and manual weather stations located at the points depicted in

Figs. 11B and Fig.13. For this purpose, the Cantor dust method has been used. Results are presented in the following subsections.

5.4.1. Rainfall events extracted from METARs

Results of the fractal analysis for rainfall events in Gran Canaria A. (A1) are shown in the Fig. 21 (asterisks) The number N(s) of intervals of length is containing at least one rain event as a function of the interval length are plotted in a bi-logarithmic graph. Straight-line segments fitted by regression are constructed over different scale intervals. The smallest time interval chosen was approximately half an hour and gradually increased by a factor of 2. The fractal dimension, derived from the slope, D = |D|, ranges from 0 to 1.

The non-overlapping segments of a characteristic size, s (hour), in which the time interval is divided versus the number N(s) of intervals of length s (hour) is occupied by the rainfall events being represented in Fig. 21. It reveals the existence of segments (timescales) with different behaviour separated by crossovers or cut-offs. These break points can be interpreted as characteristic time periods when changes in the temporal structure of the phenomena distribution take place (Olsson et al. 1993) or as a combination between scale-invariant clustering and random occurrence of events (Smalley et al. 1987). Between two segments or scaling regions there are transitions where the environmental properties are probably changing rapidly.

Segments at each side of these transitional zones have been indicated with Roman numbers I and II. The first segment (I) corresponds to a box-size interval from 1 h to 6 days, and is characterised by a D = 0.38, revealing a similar scaling pattern within this time range. This D value indicates a scaling regime and an irregular distribution of the rainfall at this timescale. In this time interval, rain events can be closely gathered while long dry episodes are observed between them. Consequently, on average, precipitation is

not evenly spread throughout this time interval. Following a conviction common to many existing studies (Mazzarella & Giuliacci 2009), a regular time distribution of events produces a rise in D up to the limiting value D =1.

For time increments above 6 days the slope of the curve approaches −1 (segment II). Rainfall events occurring for time increments exceeding two months represent the saturation of the process (D = 1). In a statistical sense, this means that rainfall events have a similar frequency of occurrence for time increments greater than two months. Results obtained by applying the Cantor Dust method suggest that each segment is related to a different underlying process that explains the occurrence of the rainfall events according to each range of time. Regarding analogous observations taken in other aerodromes of reference, La Palma A. was chosen to represent the wettest islands, building upon the influence of the Atlantic low-pressure systems that affect the western part of the archipelago mainly during the winter season. On the other hand, Fuerteventura airport, was selected due to its proximity to African coast being the driest one.

General results, from the other two reference aerodromes, Fuerteventura A. (A3) and La Palma A. (A6), are summarised in Table 7 which includes the scaling range (SR), the box-counting fractal dimensions (D) from the analysis of rain data series, as well as the root mean square error (RMSE).

Table 7. Results of the box-counting analysis (scaling range, SR; fractal dimension, D; and associated RMSE) of the rain events in reference aerodromes. (Scaling range is given in hours, h and days, d). Period 1989–2010. Hourly surface data from METARS (AEMET).

Station	SR	D	RMSE
A1	1h–6 d	0.38	±0.027
A3	1h–6d	0.27	±0.027
A6	1h–6d	0.41	±0.036

The coefficient of determination for A. and La Palma A. is 0.98, and 0.99 in Gran Canaria A. Results show that at a time increase of about one week, the steepest gradient and the highest D value (0.41) rainfall in Fuerteventura correspond to La Palma, the rainiest island. In contrast, the lowest D value (0.27) is found in Fuerteventura, which is flat, evidently showing a strong clustering behaviour, since rain occurrences are scarce and irregularly distributed in time. In this case the dry periods are longer than the episodes of rain. For periods of time, between one day and one week, La Palma and Gran Canaria present a high D; thus rain occurrences are uniformly spread over this period of time and shorter dry episodes are observed. La Palma offers a relatively high fractal dimension for the rainfall analysis, D, value (0.41) and thus is more affected by rain due to its geographical location and influence of Atlantic lows.

5.4.1.1. Comparison with desert mineral aerosol incursions

Fractal behaviour of other meteorological variables like dust intrusions stemming from the Saharan desert affecting the Canary Islands has been also found (Peñate et al. 2013). In the mentioned study, the dust occurrence regime was examined by using time series extracted from METARs (semi-hourly data). For this purpose, the Cantor dust method was also used. As a criterion for this work, a dust event duration has been defined as the number of dusty days, considering a day dusty when during a 24 h period a dust observation with visibility equal to, or lower than, 8 km is reported. The intensity of the dust event is estimated by the minor visibility recorded. For the selection of dust events, visibility data were considered only if the METAR included one of the following phenomena: haze (HZ), widespread dust in suspension in the air (DU), drifting dust raised by wind at or near the station at the time of observation (DRDU), dust storm (DS) or blowing dust (BLDU).

Aerodromes chosen as reference are those from Gran Canaria (A1), Fuerteventura (A3) and La Palma (A6) (Fig. 11B). These weather stations were selected based on availability of long data sets and representativeness. Gran Canaria airport, with an elevation of 24 m, an international high density traffic airport operational 24 h a day provides a good quality METARs based data set. Fuerteventura airport placed at the eastern edge of the archipelago, gives appropriate measurements of dust incursions affecting the islands, due to its proximity to the western African coast with the Sahara Desert as the main aerosol source. Finally, La Palma airport, in the western side, was also selected being affected rarely by desert mineral aerosols.

The box-counting log–log plots and slopes, D are represented in Fig.21 for the rainfall (asterisks) and dust event (dots) data series at Gran Canaria A. (A1)

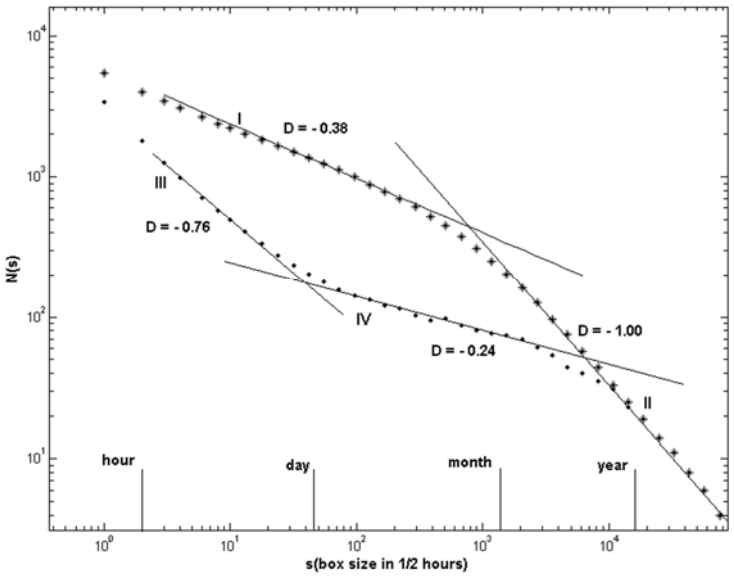

Fig. 21. Box-counting log–log plots and slopes, D, for the rainfall (asterisks) and dust event (dots) data series at Gran Canaria airport. The non-overlapping segments of a characteristic size, s, (1/2h) in which the time interval is divided versus the number N(s) of intervals of length s (1/2 hour) occupied by the rain or dust events. Data from METARs for the period 1989–2010.AEMET.

The non-overlapping segments of a characteristic size, s, (1/2h) in which the time interval is divided versus the number N(s) of intervals of length s (1/2 h) occupied by the dust events.

Results from the Dust Cantor method applied to G.Can. A. (A1) shows a regression line for timescales ranging from 1 to nearly 8 h. The fractal dimension is D =−0.76. (segment III). This steep slope unveils a dense and uniform organisation of dust events in the time domain. This corresponds to a distribution of dust cells poorly clustered for a shorter period than one day. The break, close to one day, may indicate periods of good visibility in terms of mineral outbreaks over the islands between dust events. A segment appears close to the time interval between 8 -10 h and approximately two days, representing a transition phase. Other scaling region can be observed at timescales ranging from two to approximately sixty days (segment IV) for which the fractal dimension is D = 0.24. The slope of this intermediate segment, comparatively small, evidences that dust events are organised in clusters dispersed over this timescale. Another transition phase is found between 2 months and roughly seven months, when the saturation is reached for the dust events, represented by the straight (segment II) with a slope close to 1. This implies that, on average, at least one dust event occurs over this Atlantic area for time periods exceeding seven months.

Results suggest that each segment is related to a different underlying process that explains the occurrence of the dust events according to each range of time. Comparing these results with other aerodromes of reference, for a scaling range of 1-8 h D value was equal to 0.76 for both G.Can.A. (A1) and Fuert. A. (A3) and of 0.79 for La Palma A. (A6). For a period between 2 days and 2 months D value was equal to 0.24 for A1, 0.30 for A3 and 0.29 for A6. The D values obtained from the analysis of the dust events are

very close. This is because the timing of dust events is the same for all the islands and consequently the resulting clustering pattern is very similar.

Comparing both phenomena, dust and rain events over the islands, it is observed that for Fuerteventura the dry periods are longer than the episodes of rain. For periods of time, between one day and one week, La Palma and Gran Canaria present higher D for rainfall than for dust events. At this scale time, the dust event time pattern in Fuerteventura shows a value of D slightly higher than for rain occurrences, such as corresponds to a more arid climate. Results derived from this study reveals that in general, for a timescale of about one day, dust or haze events (HZ) are more closely distributed than rainfall ones. In other words, dust is more persistent than rainfall throughout the day. This implies that they are affected by meteorological processes acting at different timescales.

5.4.2. Rainfall events extracted from rain gauges

Rainfall occurrences affecting the islands are generally associated with typical synoptic unstable situations such as cold depressions (located at N, NE and E or at SW, W and NW of the islands) and mobile troughs with or without fronts (irregular situations). These disturbances are usually accompanied by an intensified advection which occurs south of the low cores, breaking the inversion layer and providing abundant wet air or by the effect of frontal tails associated with North Atlantic low-pressure systems.

The annual number of rainfall days (NRD), total accumulated rainfall per year (CUM) in mm yr^{-1} and daily maximum rainfall (MAX) in mmd^{-1} over the Canary Islands from daily data from weather stations are depicted in table 8. These results were assessed throughout the year excluding the months from June to August.

Table 8. Acronyms for the selected weather stations, annual number of rainfall days (NRD), total accumulated rainfall per year (CUM) in mm yr^{-1} and daily maximum rainfall (MAX) in mmd^{-1}. Period 1969-2010. Daily data from AEMET.

Acr.	NRD yr^{-1}	CUM (mm yr^{-1})	MAX (mm d^{-1})
A1	1.896	7.978	116
A3	1.001	4.089	91
A6	2.385	13.632	149
A2	1.319	3.896	58
A4	4.219	26.196	172
A5	698	4.021	135
T1	2.885	11.656	231
P1	274	11.02	70
T5	3.083	28.862	428
A7	1.271	6.921	280
P2	3.398	22.783	200
P3	3.314	36.958	199
P4	3.259	25.090	217
P6	1.465	17.578	145
P8	1.006	8.960	123
T3	821	7.615	85
T4	4.740	37.589	152
T2	2.601	16.508	134
P7	977	8.322	106
P5	1.184	13.766	207

Table 9 shows the fractal dimension estimates based on the altitude, location of the stations and the percentage of the NRD.

Table 9. Acronyms for the weather stations used in the study (Acr.), fractal dimensions (D), station elevation in m (Elev.), location (Loc.) and percentage of the annual number of rainfall days (NRD yr^{-1} (%). Period 1969-2010. Daily rainfall data from automated and not automated stations. AEMET.

Acr.	D	Elev.(m)	Loc.	NRD yr^{-1} (%)
T6	0.29	130	SW	17
P1	0.312	25	S	21
A5	0.319	64	S	23
A3	0.337	25	E	25
P7	0.338	570	S	23
T9	0.34	15	E	31
P8	0.345	806	S	23
T10	0.36	765	NW	38
P5	0.365	715	SW	26
P9	0.37	950	W	29
T2	0.375	106	NW	47
T3	0.383	274	W	33
A1	0.387	24	E	35
A2	0.388	14	E	37
A7	0.394	32	NE	35
P6	0.397	1040	C	34
T5	0.418	2371	C	42
T7	0.43	844	W	44
P10	0.44	318	SW	32
T11	0.45	1242	W	45
T8	0.47	684	NW	46
T4	0.47	564	N	75
P2	0.486	630	N	76
A6	0.51	33	E	62
T1	0.518	35	NE	60
P3	0.54	1400	N	76
P4	0.563	1160	N	80
A4	0.593	632	N	94

These results are summarising in table 10. A high D does not necessarily imply a high total accumulated or maximum rainfall. It is worth noting that in the Canary Islands the daily maximum rainfall in some weather stations like in T5 (Izaña), which is the highest one, doubles more than Bermuda.

Table 10. Fractal dimensions (D), station elevation in m (Elev.), location (Loc.) and percentage of the annual number of rainfall days (NRD yr-1 (%). Period 1969-2010. Daily rainfall data from automated and not automated stations. AEMET.

D	Elev. (m)	Loc.	NRD yr-1 (%)
0.20–035	15–806	S/SE	17–31
0.36–0.40	106–950	W/NW C	26–47
0.41–0.45	1040–2371	N/NE	34–42

The main results of the analysis of precipitation are summarize in Fig.22 which displays the D estimates by rainfall amounts (circles with different sizes and colours), which are pictured on the Canary archipelago map according to their locations. In particular, the results demonstrate the variability of the rainfall fractal dimension with latitude, altitude and longitude.

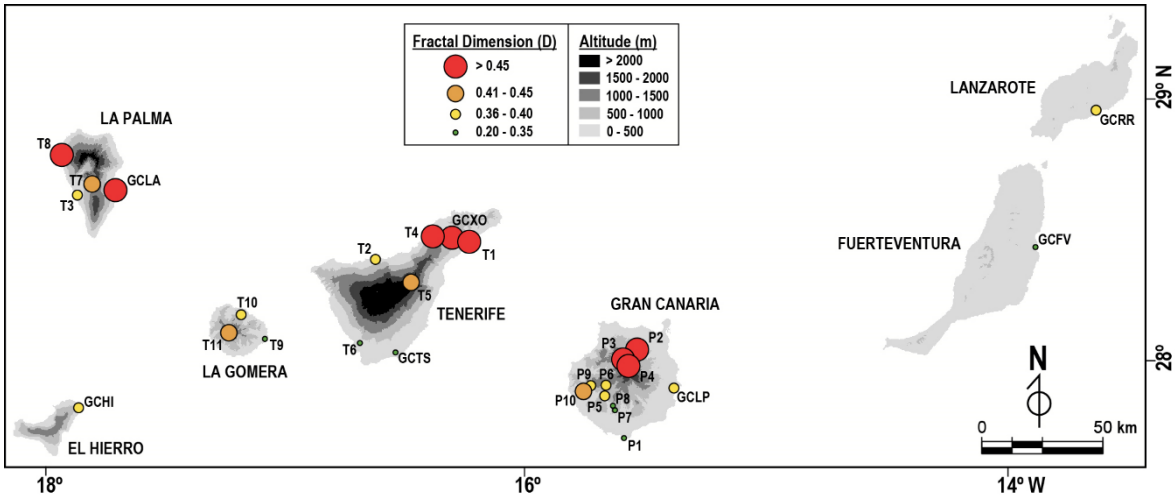

Fig.22. Spatial variability of rainfall fractal dimension over the Canaries. Daily data from AEMET.

As result, the greater D values were estimated in the northern (Ten.N.A. (A4), Valleseco R. (P3)) and central S. Mat.Lag. (P4) sectors of the islands (0.54 and 0.56, respectively) compared to those located at the southern and eastern sides (from 0.20 to 0.35). This explains why the majority of rainfall events are observed at northern sites (windward sides of the islands).

A further factor that clearly influences precipitation over the islands is the relief. This factor also modifies the fractal behaviour of the rain trend. The higher stations (with elevations between 1000 and 2370 m) located at the central area of the islands (Tejeda V.Ñ. (P6) and Izaña (T5)) also presented values of D near 0.4. In most cases these values are greater than those estimated at flatter locations, but with some exceptions. For instance, El Paso C.F. (T7) and Valler. Ch. (T11), with medium elevations between 840 and 1200 m, exhibit a relatively high D between 0.43 and 0.45. These stations, in spite of having a leeward position, are very affected by low-pressure systems. In contrast, Puntagorda (T8) at a lower altitude shows a greater D value (0.47) because of its northern location. This station is more affected by the frontal tails linked to North Atlantic lows.

There is an evident gradual increase of D in the archipelago from east to west. Another result is that among the eastern islands there are examples of southern or eastern flatter sites, like Masp. (P1) or Fuert. A. (A3), which are strongly influenced by the Sahara, showing low D values between 0.31 and 0.33. On the other hand, western stations on the western islands (El Paso C.F. (T7), Valleher.Ch. (T11) and Puntagorda (T8)) show a greater D value than those in eastern or central islands, such as Mogán B.A. (P5), Mogán Inag. (P9) or Tejeda V.Ñ. (P6). It should be noted that a low D does not necessarily imply fewer annual rainfall events, but a higher clustered pattern and consequently longer dry periods. Nevertheless, results show as a general pattern that stations with a large number of annual rainfall days present a relatively high D value (Table 10).

Due to its central location in the archipelago, topographic structure, and the influence of different synoptic situations, the precipitation regime properties of Gran Canaria have been analysed in more detail. The special relief of this island allows clear differentiation between windward and leeward sides determined by the thermal inversion layer located between approximately 900 and 1500 m. Fractal dimension for northern Gran Canaria locations (Teror Dom. (P2), Valleseco R. (P3) and S. Mat. Lag. (P4)) ranges from D = 0.48 to D = 0.56. In general, points located at the thermal inversion layer level (P4) show larger D values (0.56) than those situated below (P2) or above (P3) this level. However, fractal dimension for southern locations (Masp. (P1), S. B. Tir.P. (P7), S. B. Tir.L.P.A. (P8) and Mogán B.A. (P5)) ranges from 0.31 to 0.36. The flatter point (P1) presents the lower value among all the studied stations. This lower D value reveals desert-like precipitation behaviour. Eastern stations (G.Can.A. (A1)) also present lower D values than the northern ones. An exception is S.Nic. T.T. (P10), a station located in the west southwest of Gran Canaria with a relatively high D. This is due to the major influence of systems of low pressures affecting the SW sectors of the islands, which provide abundant wet air and rainfall.

Summary it up, results obtained from this analysis attest to a clear change of the fractal behaviour between islands as a function of the geographical features (elevation and geographical orientation). Even on a given island, there is a noticeable change in the clustering regime as a result of the orientation and elevation of the stations where the phenomenon is measured. These findings agree this those extracted in 5.2.2., where the duration of dry periods between rainy events for the Canary Islands under the scaling concept was studied.

5.4.3. Comparison with Madeira

It is worth mentioning that analyses carried out in Madeira (De Lima and De Lima, 2009) reveal a similar general pattern to that found in the present study, with larger D values at northern or central locations and lower values in southern sectors. Absolute values of the fractal dimension for a given geographical sector are lower in the Canaries.

In Madeira D values are approximately 0.71 at northern locations and close to 0.75 in central highlands and to 0.53–0.56 for southern sectors (De Lima and De Lima, 2009). In the Canaries D values are, in general, lower and widely scattered and range between 0.29 and 0.59. Only some northern stations like Ten.N.A. (A4), or those of a higher altitude than 1100 m like Valleseco R. (P3) and S.Mat. Lag. (P4), show similar D to the stations of Madeira, reaching a D between 0.54 and 0.59. Differences in fractal properties at both archipelagos can be explained in terms of geographic and topographic features. Naturally, the Canaries are more exposed to influence from the African continent and less affected by the Atlantic lows than the Portuguese islands, which present a greater annual rainfall.

Studies developed in regions with a pluviometry regime defined by longer periods of rain, such as the city of Lund in Sweden (Olsson et al. 1993) or in Madeira (De Lima & De Lima 2009), reveal that the saturation of the process occurs for roughly one week, showing a rain pattern evenly distributed over the year with small changes between seasons (Olsson et al. 1993). The saturation for periods longer than a week implies inherent deficiencies of applying the box-counting method to study rainfall events, mainly when time series of a relatively small size are used (De Lima & De Lima 2009). Hence, for example, for time intervals exceeding roughly two months, an isolated rain event will be found in an interval filling a box. This may incorrectly indicate a pattern which does not fully describe the nature of the phenomenon. For this reason, analysis of the dry

periods between the aforementioned rain events is developed in this work to provide a better understanding of the scale analysis of rainfall events over this region.

5.5. Seasonal and inter-annual rainfall variability

5.5.1. General description

5.5.1.1. Bermuda

A summary of the main results of the seasonal and inter-annual and seasonal variability of rainfall analysis in Bermuda is given in Fig.23 where the daily rainfall data (Ra) evolution at different time scales is found. Values of this variable corresponding to a certain day of a given year and its intensity have been represented in a colour map form in mmd^{-1} (Fig.23a). The inter-annual and the seasonal variability of rainfall accumulated (anomaly) are represented in Fig.23b and Fig.23c, respectively.

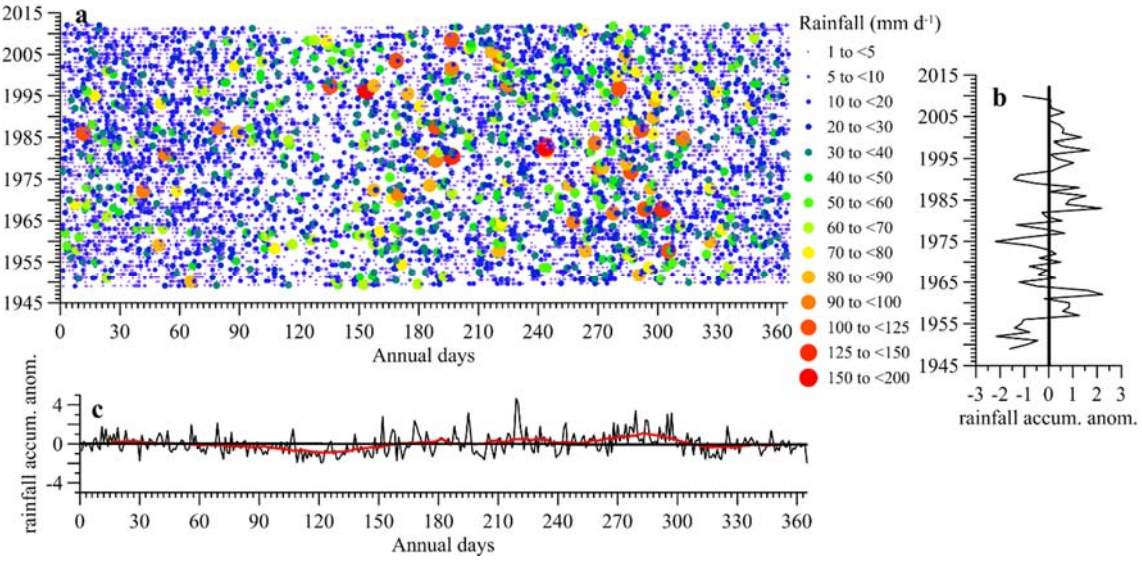

Fig.23. Seasonal and inter-annual variability of rainfall in Bermuda (a) Daily rainfall corresponding to a certain day of a given year and its intensity given by a colour indicated in a colour-bar in mmd^{-1} .(b) Inter-annual variability of accumulated rainfall (anomaly) (c) Seasonal variability of rainfall accumulated (anomaly) and 31 days- running mean in red line. Bermuda A. Period 1949-2011. Daily data from BWS.

Daily rainfall values have been considered as elements of a matrix containing a number of rows equal to the total number of years analysed which are 63. The number of columns represents the days per year (365). In leap years, the data corresponding to 29th

of February have been removed, assuming that February months have only 28 days. The resulting matrix can be expressed as Ra (y, d), where the indexes y and d stand for year and day of the year, respectively. Index d corresponds to the abscissa axis, index y to the ordinate axis, and each pixel in the figure represents the rainfall recorded on a certain day of a given year, and its intensity (in mmd^{-1}) is given by circles with different sizes and colours.

According to the inter-annual variability of rainfall accumulated (anomaly), the highest value is observed in 1962 and the lowest one 1975 (Fig.23b).

The monthly daily rainfall accumulations are represented in Fig.23c. Red lines are the running means calculated for 31 days. The greatest monthly rainfall totals are observed around October and the lower ones in spring.

Very heavy rainfall events over Bermuda are episodic and observed mainly in summer. Analysis of the colour map evidences that, in general, rainfall events are highly intermittent and of relatively low intensity, with a maximum daily event of 197 mmd^{-1} recorded on June 1st 1996 and other of 157 mmd^{-1} on August 31st 1982.

The minimum values were recorded in 1952 (37 mmd^{-1}) and in 2011 (52 mmd^{-1}).

This geographical area exhibits a distinct tropical cyclone season which extends from June through November. However, the contribution of tropical cyclones to average annual rainfall accumulation over the islands is sporadic. Thus, it may be deemed as insignificant over the selected period, when compared to the contributions of frontal or broadly convective precipitation. However, there are some exceptions and individual tropical cyclones, for example Bertha, may contribute significantly to daily or monthly accumulations in a given year. Therefore, in order to explore features of the annual pattern of rainfall occurrences over Bermuda, the standard criteria for the delimitation of the seasons has been considered and the tropical one is not taken into account.

5.5.1.2. Comparison with Canaries, Madeira and Azores

The seasonal and inter-annual rainfall variability with a similar representation to the previous subsection in order to compare with Bermuda is made for the weather selected stations (El Hierro A. (A7), S.C. Ten (T1), L. Canteras (P14), Lanz A. (A2), Berm. A. (BERM1) Horta Obs. (Az.) and Funch. Obs. (M)) and shown in Fig. 24. The analysis of these colour maps shows that in Bermuda there is clearly no dry season. The rainfall occurrences are almost uniformly distributed throughout the year with a wetter period during the summer. In Azores the dry season is very short, being July the driest month. On the contrary, in Canaries and Madeira there is a dry season in summer from June to August, markedly in Canaries, when rainfall occurrences are sporadic and of low intensity.

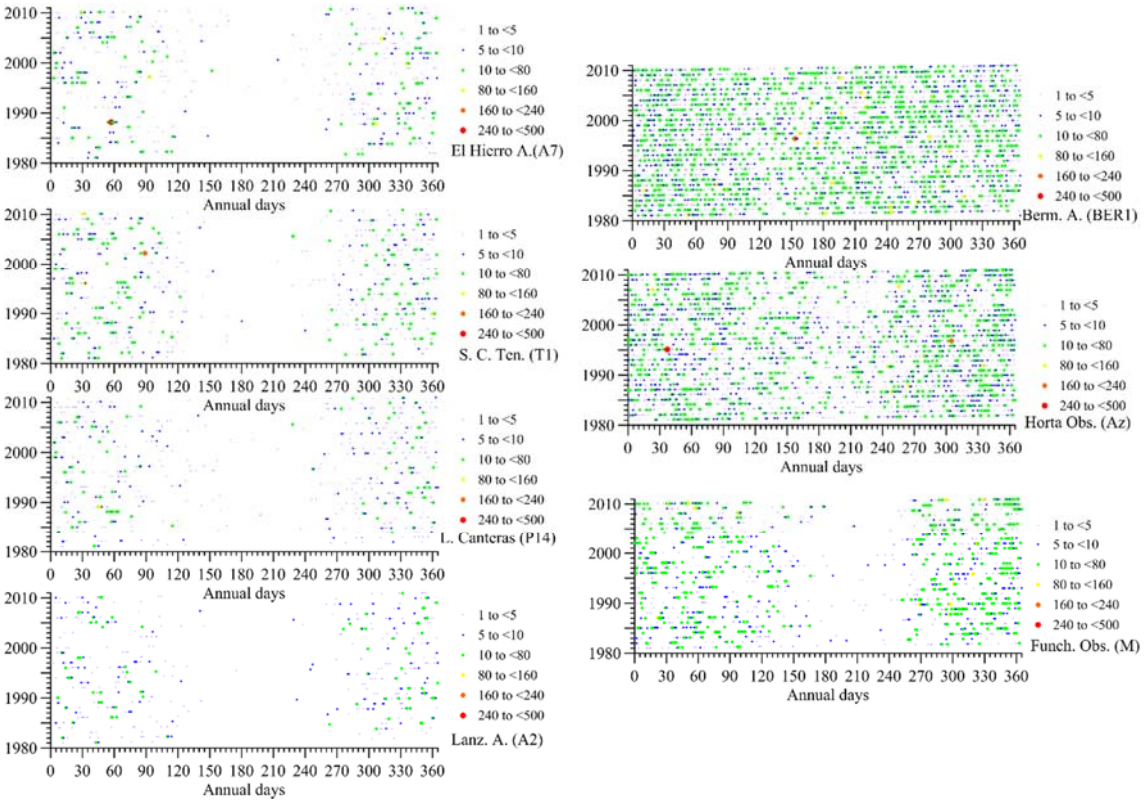

Fig. 24. Seasonal variability of daily rainfall corresponding to a certain day of a given year and its intensity given by a colour indicated in a colour-bar in mmd^{-1}. El Hierro A. (A6), S.C. Ten (T1), L. Canteras (P14), Lanz.A. (A2), Berm. A. (BER1), Horta Obs. (Az.) and Funch. Obs. (M). Period 1981-2010. Daily data from AEMET, BWS and IPMA.

The results extracted from this section confirm the ones achieved by other authors derived for normal period 1971-2000 (Departamento de producción de AEMET & Departamento de Meteorología e Clima de IMPA 2012).

Table 11. Acronyms for the selected weather stations, total accumulated daily rainfall (CUM) in mm, average rainfall (AVR) in mm, standard deviation (STD) in mm, daily maxima (MAX) in mmd^{-1}, number of rainfall days (NRD) in d, the rainfall rate (Rate) in mm and the total number of data (Ndata) for the whole period 1981-2010. Daily rainfall data from BWS, AEMET & IPMA.

Acr.	CUM mm	AVR mm	STD mm	MAX mmd^{-1}	NRD d	Rate mm	N.Date
A1	4438	0.41	2.90	85	1746	2.54	10957
A2	3322	0.30	2.00	55	1617	2.05	10957
A5	3978	0.36	3.06	136	945	4.21	10957
A7	6173	0.56	5.12	280	1496	4.13	10957
P2	14833	1.37	5.20	115	2338	6.34	10864
P13	18198	1.65	11.78	166	2587	6.64	10434
P14	3687	0.34	2.16	112	1268	2.91	10957
P16	6717	0.62	4.06	178	1971	3.40	10865
T1	6770	0.62	4.13	233	2485	2.72	10957
T2	8779	0.81	3.71	87	2141	4.10	10834
T5	10479	0.52	22.87	337	1455	3.77	10439
T12	6695	0.63	4.68	130	447	14.97	10681
T13	11980	1.10	5.85	123	1175	10.20	10895
T14	15240	1.41	7.23	162	1235	12.32	10834
T15	10659	0.99	5.47	285	2303	4.63	10772
M	18539	1.70	6.72	159	2544	7.29	10877
Az	30741	2.81	8.35	391	6584	4.67	10957
BER1	44493	4.06	10.14	197	5081	8.76	10957

The seasonal and inter-variability of the rainfall is also studied when considering 16 selected weather stations for the Canary Islands, Funch. Obs. (M) and Horta Obs.

(Az.). Results for 15 of them, except P16, can be found in tables E, F and G for the NRD, accumulated rainfall and daily maxima respectively (Annexe I).

Table 11 shows the total daily accumulated rainfall (CUM) in mm, the average rainfall (AVR) in mm (calculated as the CUM per number of data (NDate)) , the standard deviation (STD) , the daily maxima (MAX) in mmd^{-1}, the number of rainfall days (NRD) in d, the rainfall rate (Rate) (calculated as the CUM divided by the/NRD in mm) and the total number of data (Ndata) for the whole period 1981-2010. Results of the daily rainfall maxima from the stations Mogán B.A. (P5), Arucas Bañ. (P11) and Valseq. G.R. (P12) in Gran Canaria Island are not included because of the inclusion of some – 4 in the data base (see Table C in Annexe I).

The heaviest daily rainfall among the selected stations was 391 mmd^{-1} recorded in Azores (Horta Obs.) on 7th February 1995. The second extreme record was recorded in the Canary Islands where the average maximum daily rainfall value was 165 mmd^{-1} and the extreme value was 337 mmd^{-1} recorded on 17th March 1993 in Izaña (T5) followed by 285 mmd^{-1} on 8th November 2004 in Sabinosa (T15) and 280 mmd^{-1} on 27th February 1988 in El Hierro A. (A7). Highlighting the only weather station with heavy rainfall during the summer in Bermuda, with a maximum daily rainfall record of 197 mmd^{-1} in June. The lowest daily maximum value was 55 mmd^{-1} recorded in Lanz. A. (A2) observed in February.

5.5.2. Seasonal variability

5.5.2.1. Seasonal variability of the rainfall events in Bermuda

The analysis of the average monthly rainfall in Bermuda during the 63 year period of observations depicted at the red line in Fig.25. Dash blue lines are the 99% confidence intervals and the green line represents the expected total rainfall considering the same amount of rainfall that is recorded for each month. According to these results, the summer

average monthly rainfall presents an increasing trend with major peaks in October and August and secondary peaks are found in June and January.

The significance of the thunderstorm development and fronts are strongly defined as they pass close to Bermuda in late September and October producing a peak in the precipitation amount. This is mainly due to the moist unstable maritime tropical air but not usually associated directly with tropical systems. Then, the amount of rainfall decreases towards November-December and a minor peak is observed around January when winter fronts are active in the area. After this, precipitation diminishes again and reaches the minimum annual mean between April-May and drops again in November.

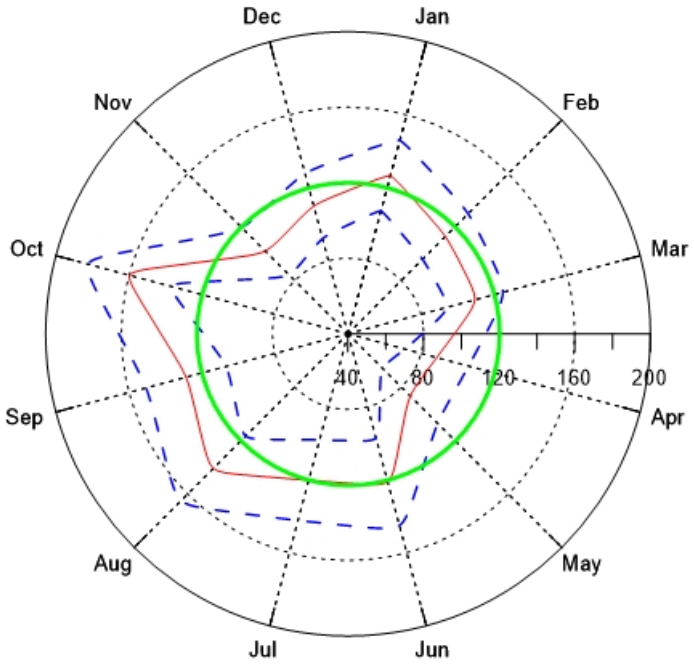

Fig.25. Variability of monthly average daily rainfall in mmd^{-1} (red line) with the 99% confidence intervals (dash blue lines) and the expected total rainfall in mm considering uniform rainfall through the year (green line). Bermuda A. Period 1949-2011. Daily data from BWS.

The monthly rainfall over Bermuda shows a maximum in monthly variability in 1973 and a minimum in 2006 (Fig.26). A minimum in April and a maximum in July are marked for both years, whereas the first one is clearly much deeper during 1973. The

peak in summer is similar for both time series, but only in 1973 there is another in October. In winter the amount of rainfall decreases.

The monthly distribution from daily rainfall data for the period 1981-2010 for Bermuda A. (rainfall ≥ 0.25 mm) of the NRD, accumulated rainfall and the rainfall maxima are given in the tables E, F and G respectively, included in the Annexe I. Tables with the same parameters for the weather stations in Canaries, Madeira and Azores are also included in the same annexe.

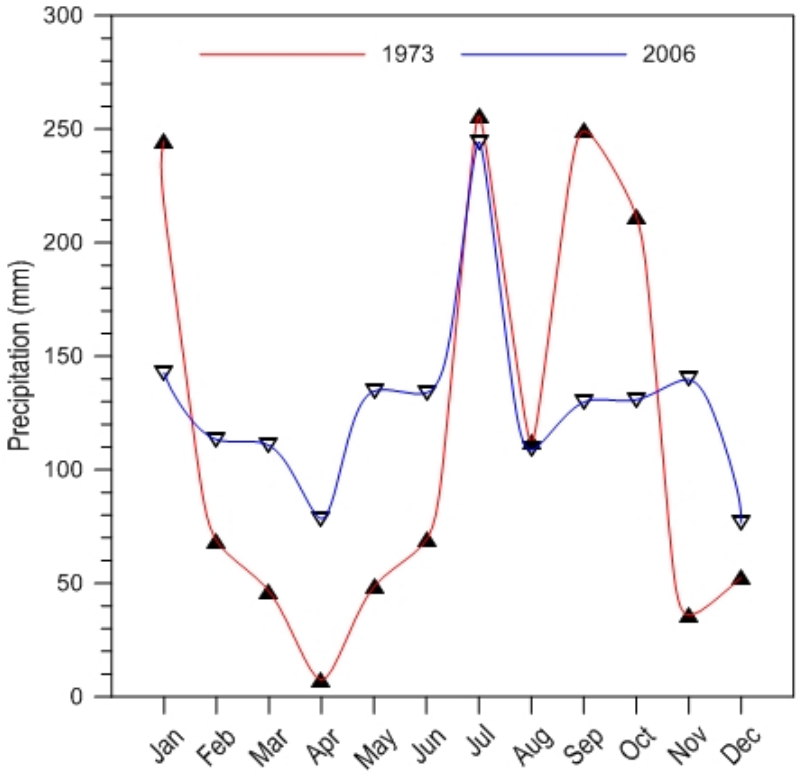

Fig.26. Monthly average of daily rainfall variability in mmd^{-1} comparing for the year 1973 (red line) and for the year 2006 (blue line). Bermuda A. Period 1949-2011. Daily data from BWS.

Summarising it up, the rainfall daily average follows a bimodal pattern. These results are in line with other studies about the Bermuda rainfall (Macky 1957).

5.5.2.2. Comparison with Canaries, Madeira and Azores

The rainfall frequency of the occurrences in this subtropical region is modulated by the Azores High which dominates the area almost all year long, except when some Atlantic depressions reach the islands. In general, the rainy season starts in October when the centres of high pressure move north allowing some perturbations to reach the area. The permanent north-easterly surface flow associated with dry weather is the main feature during the summer, occurring from mid-May to the beginning of October.

Results from the seasonal rainfall distribution comparison with the rest of the archipelagos considered in this work, are depicted in Fig.27.

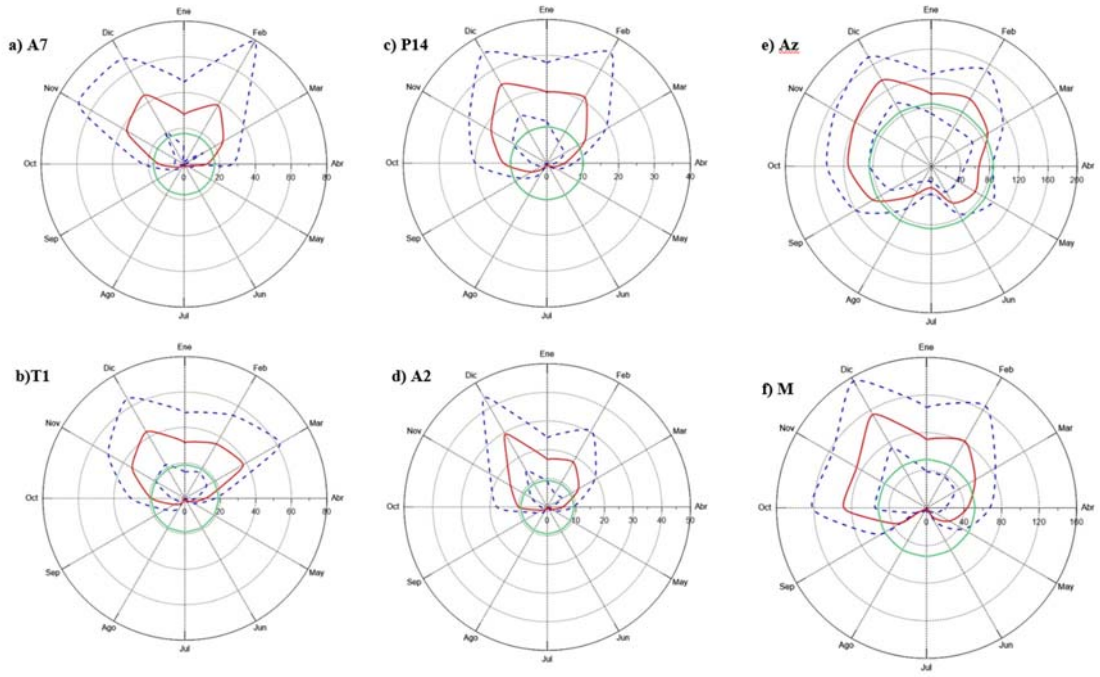

Fig.27. Monthly average of daily rainfall variability in mmd^{-1} (red line) with the 99% confidence intervals (dash blue lines) and the expected total rainfall in mm considering uniform rainfall through the year (green line). Horta Obs. (Az), Funch. Obs. (M), El Hierro A. (A6), S.C. Ten (T1), L. Canteras (P14) and Lanz. A. (A2). Period 1981-2010. Daily data from AEMET and IPMA.

The results show that for Canaries the greatest monthly averages of daily rainfall are observed from November to March (Fig.27a, b, c and d). High values are detected in December for all the stations and in February except in T1 (S.C. Ten.) where the second

maximum is observed in March. (Fig.27b). Only in A7 (El Hierro A.) there is a marked maximum in November (Fig.27a).On the contrary, the lowest values are found from June to August for all then. The greatest ones in Funch. Obs. (M) are observed from October to February with the maximum in December and the minima in July and August (Fig.27f). In Azores it rains like in Bermuda throughout the year, only July can be considered a dry month. The maximum average values are observed in December (Fig. 27e).

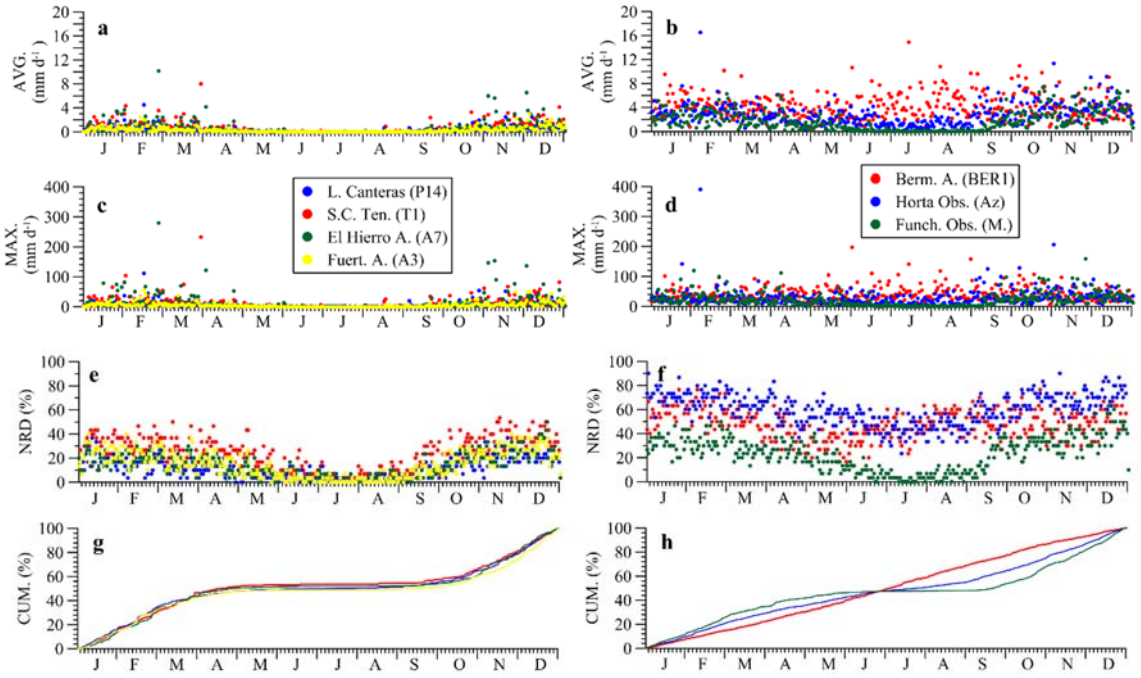

Fig.28. Comparison of the seasonal distribution of rainfall in the Canary Islands (Las Canteras (blue), S. C. Ten. (red), El Hierro A. (green) and Fuer. A. (yellow) on the left side with Berm. A. (red), Horta Obs. (Az.) (blue) and Funch. Obs. (M) (green) on the right side. (a /b) Daily rainfall average for each day of the year in mmd^{-1} (AVG); (c/d) maximum daily rainfall for each day of the year in mmd^{-1}(MAX); (e/f) number of rainfall days (NRD) (%) and (g/h) daily rainfall accumulation (%) (CUM). Period 1981-2010. Daily data from AEMET, BWS and IPMA.

Similar analysis is found in Fig.28 where the daily average rainfall for a specific day of the year (from 1 to 365) is calculated for the normal period (1981-2010) as explained above in section 5.1.The daily rainfall averages for each day of the year in mmd^{-1} (AVG) are in Fig.28a and b. Maximum daily rainfall for each day of the year in mmd^{-1} (MAX) are in Fig.28 c and d. The number of rainfall days (NRD) is shown in

Fig.28 e and f. Finally, the daily rainfall accumulation (CUM) is in Fig.28 g and h, both are in percentage. On the left side, results for the Canary Islands (Las Canteras (P14 in blue dots), Sta. Cruz de Tenerife (T1 in red dots), El Hierro A. (A7 in green dots) and Fuerteventura A. (A3 in yellow dots) are represented. On the right side, those for Bermuda (BERM1 in red dots), Horta Obs. (Az. in blue dots) and Funch. Obs. (M. in green dots). All the parameters are normal for the period 1981-2010.

The NRD in Bermuda (BER1) is observed from the highest to the lowest in January, August, October, December and March. Nevertheless, the lowest are detected in May followed by June, April, July, November and September. This behaviour can also be observed in Fig.16c.

The largest accumulated rainfall is recorded in August, followed by October, January, July, September, February, June, March, December, April, November, being May the driest month. The highest daily maxima are observed in June followed by August, July, October, May and January. However, the lower are witnessed in April followed by December, March, September, February and November.

The highest values, of the average daily rainfall for a specific day, are detected in winter reaching in Bermuda 8 mmd^{-1}, followed by Horta Obs. (Az.) here some exceptional values of about 16 mm d^{-1} are also found (Fig.28b). Whereas they are generally lower than 6 mmd^{-1} in the Canary Islands (Fig.28a) and Funch. Obs. (M) with peaks of about 8 mmd^{-1} in autumn and winter and at some specific day 10 mm d^{-1} in El Hierro. In summer, this parameter shows values reaching 12 mmd^{-1} in Bermuda with some out layers reaching 16 mmd^{-1}. In Horta Obs. they are between 4 and 6 mmd^{-1} mainly in June and in September, while for the Canaries and these values are lower than 2 mmd^{-1} (Fig. 28 a and b).

The results from the analysed weather stations reveal that for the Canary archipelago the greatest daily maximum values are observed from November to March. On the contrary, the lower daily maxima are witnessed from June to August (Fig.28c). Only in Bermuda the maximum daily annual rainfall is observed in summer, exhibiting peaks from June to August and October. The minima are observed in December, March and April (Fig. 28d). The highest maxima daily rainfall in Funch.Obs. (M) are observed in February, April and November; the minima in July and August. In Horta Obs. (Az.) the maximum values are observed in November and in January and the minimum in July and in April (Fig. 28d).

Table 12 shows the lower and greater monthly daily maxima rainfall for the period 1981-2010 and the station names. See also table G in Annexe I.

Table 12. Month, lower annual daily maxima rainfall (Max (mmd^{-1})), greater annual daily maxima rainfall, acronyms for the weather stations used in the analysis (Acr.), and station names (St. name). Period 1981-2010. Daily rainfall data from AEMET, BWS and IPMA.

	Lower daily Max			Greater daily Max		
Month	Max (mmd^{-1})	Acr.	St.name	Max (mmd^{-1})	Acr.	St.name
Jan.	22	A2	Lanz.A.	166	P13	Moya Font. C.
Feb.	55	A2	Lanz.A.	391	Az	Horta Obs.
Mar.	33	P14	L.Canteras	337	T5	Izaña
Abr.	16	A2	Lanz.A.	121	A7	El Hierro A.
May	5	A1/A5	G.Can.A./TenS.A.	105	BERM1	Berm.A.
Jun.	1	A2/A5	Lanz.A./TenS.A.	197	BERM1	Berm.A.
Jul.	0	A2	Lanz.A.	118	BERM1	Berm.A.
Aug.	4	A1/A5	G.Can.A./TenS.A.	157	BERM1	Berm.A.
Sep.	11	A2	Lanz.A.	125	Az	Horta Obs.
Oct.	24	A2	Lanz.A.	128	Az	Horta Obs
Nov.	39	A1/A5	G.Can.A./TenS.A.	285	T15	Sabinosa
Dec.	33	P14	L.Canteras	138	T14	Fuenc.Cal.

In April the Azores High begins to migrate north-western. During the spring season (from the end of March to April), low intense maritime polar air mass is present over the region. The daily maximum rainfall during this season for the selected period 1981-2010 was recorded at Izaña (T5) the highest station and in the western island (El Hierro A. (A7)).

In late spring and summer (from May to August) the highest number of extreme rainfall daily events were observed at Bermuda when the Azores High extends westward. Nevertheless, summer is the dry season for the rest of the archipelagos investigated, thus the High moves north-west preventing low pressure systems associated with rainfall affecting the area.

In late summer and autumn (from September to October) an anticyclonic circulation prevails, although Azores High moves slightly towards the southern latitudes and some systems of low pressure or cut-off lows reach the archipelagos within the Macaronesia which are frequent from November to January. In this period Horta Obs. (Az.) registers the highest daily rainfall maxima. The extreme rainfall daily values were recorded in El Hierro (Sabinosa (T15)) and La Palma (Fuenc.Cal. (T14)).

Finally, during the winter (from the end of December to March) the (High moves towards the southern latitudes and cold frontal systems associated with cold depressions affect the Canaries. Then, the absolute daily maxima are observed in these islands, except in February when they are recorded at Horta Obs. (Az.).

The rainfall regime in the Canary Islands related to the NRD with an average of 1702 rainfall days per year for the 19 selected stations (Fig.28e) is similar than Funch.Obs.(M) and quite different from Bermuda (Fig. 28f).

The seasonal variability of rainfall of the NRD (anomaly) for Bermuda (BER1), Horta Obs. (Az.), Funch. Obs. (M), El Hierro A. (A7), S.C. Ten (T1), L. Canteras (P14)

and Lanz. A. (A2) for the period 1981-2010 is found on right side of Fig.29 and it is compared with the seasonal variability daily average on the left side. Red lines are the running means calculated for 31 days.

The pattern of the rainfall daily average exhibits a maximum around October in Bermuda. However, the highest monthly NRD are observed from January to March, with a secondary peak in October. The trend in the average of the NRD decreases lightly during summer when precipitation is getting heavier. Both parameters drop in spring. These features can be seen at the top of Fig.29.

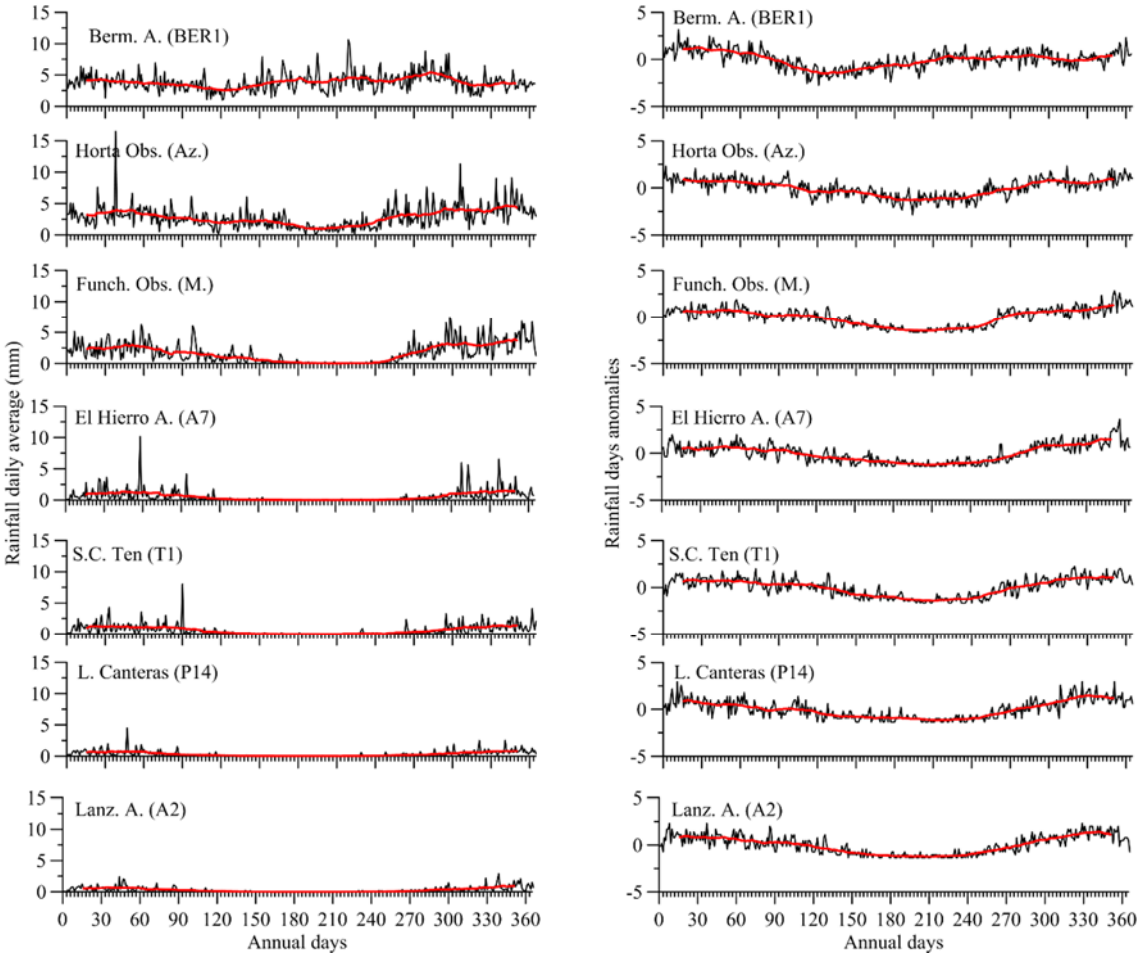

Fig.29. On left side, seasonal variability of rainfall daily average (mm) and 31 days- running mean in red line. On the right side, seasonal variability of number of rain days (anomaly) and 31 days- running mean in red line. Bermuda (BER1), Horta Obs. (Az), Funch. Obs. (M), El Hierro A. (A6), S.C. Ten (T1), L. Canteras (P14) and Lanz. A. (A2). Period 1981-2010. Daily data from AEMET, BWS and IPMA.

Among the sites selected, the NRD from highest to lowest are observed at Az. (Horta Obs.), (BER1 (Berm. A.), P13 (Moya Font.C.), M (Fuch. Obs.), T1 (S.C.Ten.), P2 (Teror Dom.), P15 (L. Alhorr.), T15 (Sabinosa), P12 (Valseq. G.R.) , T2 (S.J. Rambla), P16 (Telde Ll.), A1 (G.Can. A.), A2 (Lanz.A.), A7 (El Hierro A.), P11 (Arucas Bañ.), T5 (Izaña), P14 (L. Canteras), T14 (Fuenc. Cal.), T13 (Ll. Arid.B.), P5 (Mogán B. A.), A5 (Ten. S. A.) and T12 (S.M.Abona).

Some locations with a southern (Mogán B.A., (P5)), eastern ((Telde Ll. (P16)) or north-eastern (El Hierro A. (A7)) position or high altitudes like, Izaña (T5) experience extreme but sporadic rainfall events thus the annual NRD observed is not very high.

According to the NRD, only in Bermuda and Horta Obs. (Az.) rainfall is present in a relative high percentage (between 40 and 60%) during the summer. Whereas, in the rest of the archipelagos less than the 20% of NRD are observed in this season (Fig. 28 f and e).

The accumulation percentages show similar behaviour for the Canaries and Funch. Obs. (M), intermediate for Horta Obs. (Az.) and completely different in Bermuda where it rains almost homogenously throughout the year (Fig.28 g and h).

In the Canary Islands, the highest monthly NRD and largest daily accumulated rainfall are observed in December. This behaviour is found in Fig.28e and g respectively. The second NRD maximum values are found in November and January both in a similar percentage and the following in February. In November larger NRD are witnessed but the amount of daily rainfall total recorded is generally larger in February. July is the driest month, with the lowest NRD and daily rainfall totals; followed by August and June for the NRD and June and August for the total daily rainfall. Funch. Obs (M) follows a similar seasonal variability in NRD and total rainfall than Canaries. In Horta Obs. (Az.) the percentage is higher (Fig. 28f) and the second month with highest NRD is January

followed by October. However, the anomalies of NRD are negative during the summer being similar to Canaries. The only station with positive NRD anomalies during this season is Bermuda. The patterns for the NRD for each selected weather station can be found on the right side of Fig.29.

In Canaries for the 19 selected stations the average NRD is 1702 rainfall days per year and the average of the accumulated rainfall 9158 $mmyr^{-1}$ for the whole period 1981-2010.

The weather station among the selected ones with largest daily accumulated rainfall is BER1 (Berm. A.) followed by Az. (Horta Obs.), M. (Fuch. Obs.), P13 (Moya Font.C.), P15 (L. Alhorr.), T14 (Fuenc. Cal.), P2 (Teror Dom.), T13 (Ll. Arid.B.), P12 (Valseq. G.R.), T15 (Sabinosa), T5 (Izaña), P5 (Mogán B. A.), T2 (S.J. Rambla), T1 (S.C.Ten.), P16 (Telde Ll.), T12 (S.M. Abona), A7 (El Hierro A.), P11 (Arucas Bañ.), A1 (G.Can.A.), A5 (Ten. S. A.), P14 (L. Canteras) and A2 (Lanz.A.) See table 11. The only weather station with a marked rainfall pattern in summer is Bermuda which is found in all the analysed variables.

Results extracted from this work confirm those ones achieved by other authors derived for the normal period 1971-2000 (Departamento de producción de AEMET & Departamento de Meteorología e Clima de IMP 2012).

5.5.2.3. Seasonal wind direction and speed variability. Relationship with rainfall

5.5.2.3.1. Variability of wind direction in Bermuda

The analysis of wind direction is made through hourly observation (METAR), the resultant wind roses for Bermuda A. are shown in Fig.30. The main circulation feature over Bermuda area is clearly westerly and southerly surface winds both in nearly the same percentage followed by easterlies. The lowest frequency is observed when wind direction

occurred between the northwest and northeast sectors. The high presence of southerly or south-westerly circulation during the summer (from May to August) (Fig.30c) is the main generator of precipitation in these islands, when the Bermuda-Azores High extends westward. In late summer (September), as the high becomes more elongated; the surface wind will pick up also a south-westerly flow although easterly is also present while the southerly diminishes.

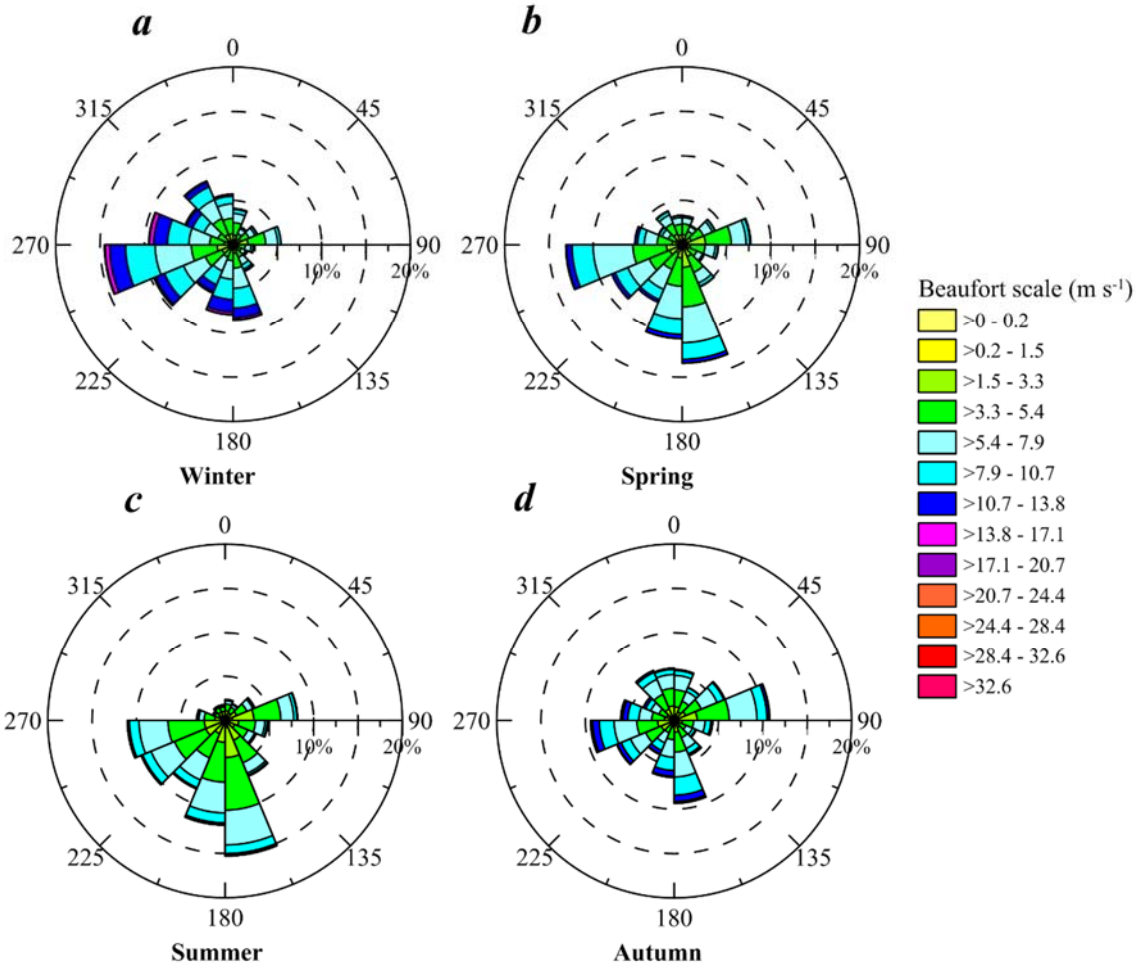

Fig.30. Wind roses representing seasonal wind direction (Wnd. Dir.) and wind speed (Wnd. Sp.) during a) winter b) spring c) summer and d) autumn. Bermuda A. Period 1942-2011. Hourly data from BWS.

However, the easterlies blow with the highest frequency in autumn (between October and November) (Fig.30d) (Fig.30a). Such situation responds to the pass of lows moving eastward and passing well to the south of Nova Scotia associated with cold fronts

followed by a deeps cold continental polar air mass. Although westerlies and southerlies are also present in similar percentage than easterlies. Results show that the prevailing wind direction during wintertime and early spring (from December to April) is westerly and south-westerly, followed by westerly-north-westerly and south-easterly. The Sea Level Pressure (mb) (December-January-February composite mean for the winters in the recent climate (1981-2010) over Bermuda from NCEP/NCAR reanalysis is illustrated in Fig.3. The predominance of westerlies in the region between Florida and Cape Hatteras (west of the Azores High) during winter can be inferred from this representation.

Surface southerly winds are observed over Bermuda during wintertime in presence of highs moving eastward over the Gulf and fast moving cold fronts followed by a maritime polar air mass. Following the frontal passage, winds shift to northwest. By the end of March, the Bermuda High begins to migrate northward and during April and May although the archipelago remains under westerly and southerly flow in low levels, there is a light influence of easterly circulation. Then, it becomes clear that the beginning of the spring is the less wet season, albeit there is not any month completely dry. During this period the Bermuda-Azores High begins to ridge over the island and marks the end of the passage of the winter fronts.

The analysis of the atmospheric variables such as the wind direction in the area of Bermuda is linked to the ocean conditions in the surroundings. For instance, southerly and south westerly winds tend to strengthen surface currents in the Gulf Stream, while north easterly winds weaken them and generate south westward flows along the shelf (Li et al. 2002).

Inter-annual wind direction variability analysis reveals that in general surface winds from the third quadrant prevail throughout the study period with lower frequency between 1963-1969, 1978-1980, 1993- 1996 and 2005- 2007. North-easterly is the least

common wind direction over Bermuda. North-westerlies are present in a low frequency and easterly is rarely present over the selected period.

From 1942 to 1963 westerlies and southerlies prevail being observed in similar percentage. From 1963 to 1970 south-westerlies and north-westerlies are the dominant winds. From 1970 to 1972 data no were provided. From 1974 to 1993 south-westerly and southerly wind directions prevail. The period with lowest frequency of westerlies is from 1993 to 1996 while between 1990 and 1995 north-easterly wind direction is observed in a relative higher frequency. Westerlies occurrence raises again between 1997 and 2005. South-westerlies prevail from 2000 to 2010.

5.5.2.3.2. Wind direction and speed frequency comparison when frontal and convective rain occurrences in Bermuda. Rainfall events extracted from METARs

The analysis of wind direction and speed frequency made through the wind roses for Bermuda A. by comparison when frontal rain (RA) and convective rain associated with thunderstorms (TS) is shown in Fig.31a and 31b respectively. Such events were considered only if in the hourly observation (METAR), the descriptors: RA (rain) or TS (thunderstorm) were included as present weather observations.

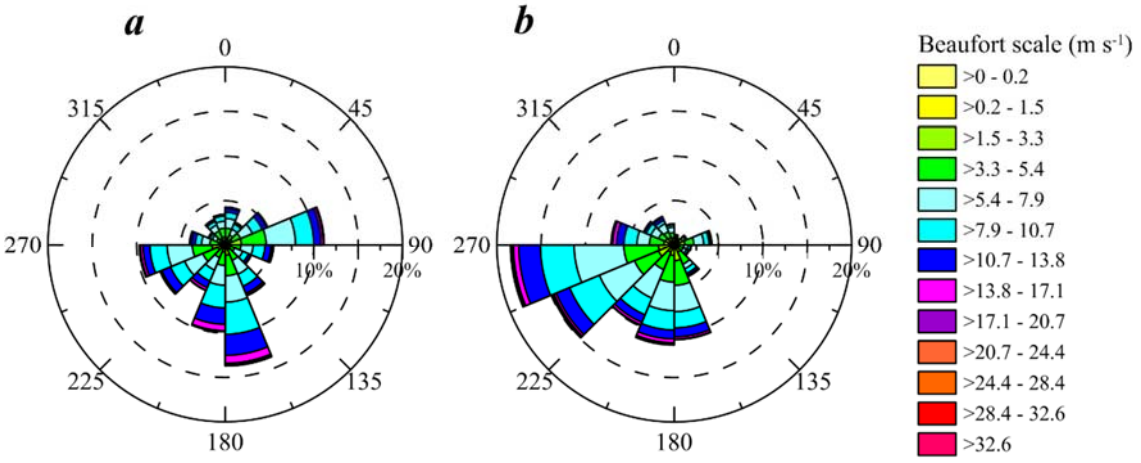

Fig.31. Wind roses representing wind direction (Wnd. Dir.) and wind speed (Wnd. Sp.) when a) frontal rain (RA) and b) convective rain (TS) .Bermuda A., Period. 1942-2011. Hourly data from BWS.

As a result of this analysis, southerly and easterly wind direction seems to be the most common when frontal rain and the westerlies when the convective rain due to thunderstorms occur, being this mainly present in the occasions when wind blows from west direction during the summer. Results show that in a percentage of 46%, the METARS observations including TS (thunderstorm) are found in summer (being September the stormiest month) followed by spring and winter in a similar percentage observing in late winter–beginning of spring a relative peak. Autumn is the month with less occurrences of thunderstorms. Such outcome is supported by some study about Bermuda's Climatology (Vandever & Pearson 1994) which proposes two yearly maxima in thunderstorm activity, the first one in late summer and a second one in late winter. No month is free from the possibility of thunderstorm activity. The most common type of precipitation in the winter is still rain showers although some frontal systems bring continuous rain.

Sufficient lifting for thunderstorm activity occurs either by diurnal cooling or by frontal action. The most common cause of thunderstorm activity is frontal lifting. The remaining small number of thunderstorms are caused by various situations such as

convection in a converging flow of maritime tropical air, instability from a tropical storm, the advection of cooler air over warmer water or stronger than normal diurnal cooling over the warm ocean.

Results from the analysis of monthly wind speed following the Beaufort scale, indicate that Gentle Breeze (4-5 m s^{-1}) is the most frequent wind speed in Bermuda, being mainly observed during the summer then followed by Moderate Breeze (6-8 m s^{-1}). The frequency of Near Gale (14-17 m s^{-1}) and Gale (17-21 m s^{-1}) can be observed throughout the year but mainly in winter in a lower percentage. Hurricane force (≥33ms^{-1}) is hardly ever present from June to November.

The winter months are characterized by higher wind speeds followed by the fall season. However, during the summer months, lower wind speeds are observed. These findings are in line with previous investigations (Bates 2007) defending that the long-term increase in wind speed are not uniformly distributed along the seasons. The wind speed intensification observed near Bermuda in the western North Atlantic Ocean during the fall and winter has also been experienced at marginal seas in the North Atlantic (Greenland and Labrador Seas) and Europe (e.g., North Sea, Mediterranean Sea, Baltic Sea, Bay of Biscay) (Pirazzoli & Tomasin 2003, Pirazzoli 2005). Wind speed at the Bermuda A. is significantly more intense, reaching Near Gale to Gale force (between 15 and 18 m s^{1}) from December to February when westerlies are the most common wind direction. Winds within a typical front may be 8 to 10 m s^{-1} with gusts to 15 m s^{-1}. The explosive development of winter storms moving over the Gulf Stream produce Gale force winds over the island at least three to four times each winter (Vandever & Pearson 1994).

Table 13. Records of maximum sustained wind speed over Bermuda A. Mean Sea Level Pressure (MSLP) (hPa), wind direction (Wind. Dir.), sustained wind speed (Wnd. Spd.) (km/h), wind gust (Wnd. Gust) and type of tropical system. (Hurricane (HR).Period (1942-2011). Daily data BWS.

Date	MSLP (hPa)	Wnd. Dir.	Wnd. Spd. (km/h)	Wnd. Gust (Km/h)	Tropical system
13/09/1948	993,6	180	161.12		HR (Cat. 3-4)
05/09/2003	964,7	190	194.46	240.76	Fabian (HR Cat. 3)
06/09/2003	997	260	157.42	194.46	Fabian (HR. Cat. 3)

From March to April wind intensity decreases in an average, mainly in April to 13-15 m s^{-1} (Near Gale to Strong Breeze) when the westerlies remain at a higher frequency. In summer (from May to August) when southerlies prevail, Fresh Breeze to Strong Breeze are the higher force over the area falling in late summer. The lightest winds occur in August. South-westerly surface flow prevails in September and easterly one from October to November when wind force decreases. Table 13 shows the records of maximum sustained wind speed over Bermuda A. from 1942 to 2011. These results reinforce the earlier ones about surface wind in Bermuda (Macky 1947, 1956).

The lowest MSLP (Mean Sea Level Pressure) value for the period 1942-2011 corresponds to the pass of the hurricane Fabian in November 2003. The second greatest record was due to the Hurricane -4 6 of Cat.3-4 passing Bermuda in 1948 with sustained winds of 161.12 km/hr. The tracks for this tropical systems can be found at the following links:

(http://weather.unisys.com/hurricane/atlantic/2003H/FABIAN/track.dat)

(http://weather.unisys.com/hurricane/atlantic/1948/6/track.gif

http://weather.unisys.com/hurricane/atlantic/1948/6/track.dat

http://weather.unisys.com/hurricane/atlantic/1948/index.php)

The wind speed frequency distribution when rain and rain shower associated with thunderstorms is similar. Moderate breeze (6-8 m s^{-1}) is lightly more frequent with the

presence of thunderstorms. Near gale (14-17 m s^{-1}) can be observed during all year long but in a low percentage. Gale (17-21 m s^{-1}) to Hurricane force (≥33ms^{-1}) are also present but in low frequency.

5.5.2.3.3. Comparison with Canaries, Madeira and Azores

For the archipelagos within the Macaronesia referred to in this study, the westerly surface flow associated with the Atlantic lows causes the heaviest rainfall. However rainfall of less intensity can also occur with trades winds associated with abundant stratified clouds.

Wind roses and wind speed when (a) frontal rain (RA) and (b) convective rain (TS) for Lanz. A., G.Can. A. and La Palma A. are shown in Fig.32; for Horta airport (Horta A.) and Funchal airport (Funchal A.) in Fig.33. The period investigated was 1998-2014 for the Canary Islands and 2003-2014 for the Portuguese islands.

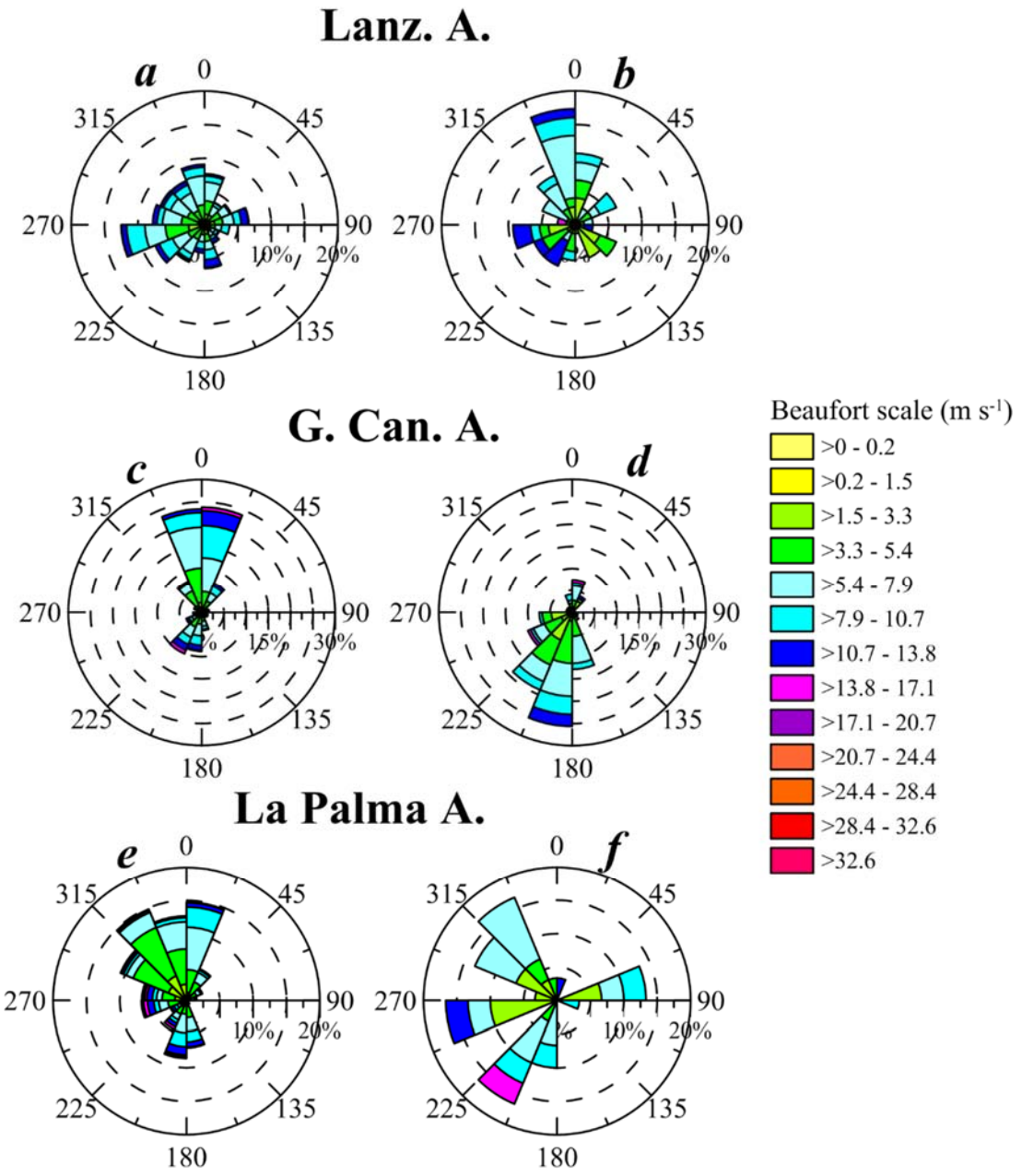

Fig.32. Wind roses representing wind direction (Wnd. Dir.) and wind speed (Wnd. Sp.) when a) frontal rain (RA) and b) convective rain (TS). Lanz. A., G.Can. A. and La Palma A. Period. 1998-2014. Hourly data from AEMET.

Results derived from this analysis show that for G. Can. A. (A1) and La Palma (A6) northerly wind direction is the most frequent when frontal rainfall. Trade winds are often enough to cause rainfall over these islands. However, in Lanzarote A. (A2) when rainfall has a frontal character, the wind blows preferably from the fourth quadrant with certain predominance of the western component. The flatness of this islands could be the reason that makes that rainfall due to trade winds was not as efficient like in G.Can A. (A1) and

La Palma A. (A6), therefore rainfall is generally associated with systems of low pressures that favour westerlies in Lanz. A. (A2).

South-westerly wind direction is the most common in G.Can. A (A1) and south-westerlies, westerlies and north-westerlies prevail in La Palma A. (A6) when convective rainfall. Thunderstorms are mainly present during the autumn following by winter due to the passage of Atlantic lows or cut-off close to the islands. In some occasions heavy convective rainfall is associated with lows of medium latitudes or extra-tropical depressions as Delta in November 2005 (Martin et al. 2007), hybrid systems, extratropical transitions or subtropical systems as the perturbation that affected the islands on February 2010 (Carretero et al. 2011).

The heavy rainfall at Lanzarote A. (A2) is caused by systems of low pressure affecting the islands in autumn and winter. North-westerly wind direction prevails when convective rain is present. South-westerlies and westerlies are present in a lower percentage but with high intensity. In late summer and early autumn, this airport can be affected by storms, often dry ones, with origin in the African continent related to the inter-tropical convergence zone or thermal lows producing abundant medium clouds and rainfall but not of significant amounts.

These results should be taken with caution thus weather stations network were not equipped with lightning sensors during the whole investigated period. Wind roses representing wind direction (Wnd. Dir.) and wind speed (Wnd. Sp.) when a) frontal rain (RA) and b) convective rain (TS) for Horta and Funchal airport for the period 2003-2013 are viewed in Fig.33.

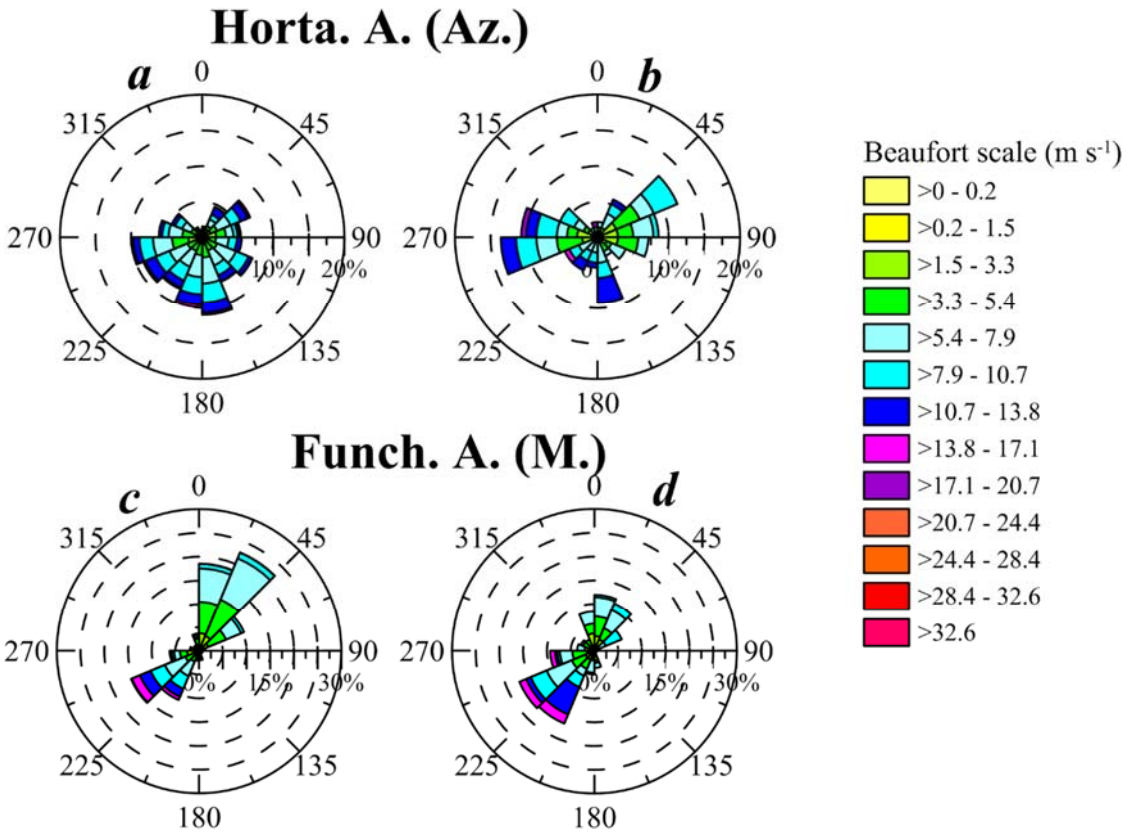

Fig. 33. Wind roses representing wind direction (Wnd. Dir.) and wind speed (Wnd. Sp.) when a) frontal rain (RA) and b) convective rain (TS). Horta airport and Funchal airport. Period. 2003-2014. Hourly data from IMPA.

In Horta A. (Az.) like in Bermuda the most common wind direction when frontal rain is from the third quadrant and when convective rain is present westerlies prevail. In this aerodrome the presence of easterlies is less frequent than in Bermuda when frontal rain and more frequent when convective one.

In Funch. Obs. (M) similar behaviour than in Canaries (G.Can. A (A1) and La Palma A. (A6)) is found.

According to results from METARs thunderstorms occur in Canaries and Madeira preferably in autumn in percentages of 52%, 53%, 61% and 40% in La Palma A. (A6), Lanzarote A. (A2), G. Can. A. (A1) and Funch.Obs.(M), respectively, being November the stormiest month. In Horta Obs. (Az.), similarly than to Bermuda summer is the stormiest season in a percentage of about 42% with the higher number of thunderstorm

occurrences also in September. However followed by autumn (24%) spring (18%) and winter (13%).

The similar behaviour found between Canaries and Madeira is due to their similar location being affected by similar synoptic situations. On the other hand, the more relative western location of Azores could be in part explain its similitude to Bermuda , both could be affected in some occasions by systems with a relative common origin and characteristics such as the tropical ones.

5.5.3. Inter-annual rainfall variability.

5.5.3.1. Bermuda

The inter-annual daily rainfall variability over Bermuda A. is shown in Fig.34 which includes (a) the annual accumulated rainfall ($mmyr^{-1}$), (b) the NRD (number of rainfall days) per year, (c) the maxima daily rainfall in mmd^{-1} and (d) the rainfall rate (annual accumulated rainfall / NRD) rainfall in mmd^{-1}.

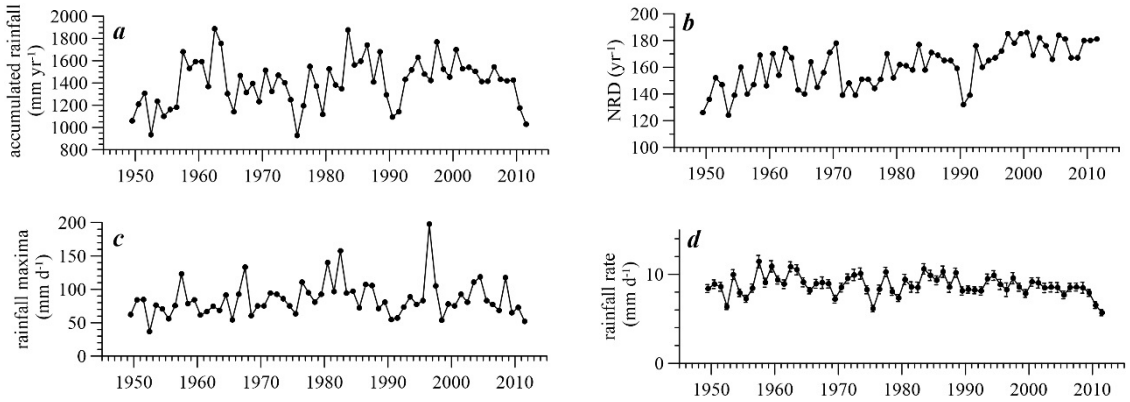

Fig.34. Inter-annual daily rainfall variability. (a) Annual accumulated rainfall (mm yr^{-1}), (b) NRD (number of rainfall days) per year. (c) Maxima daily rainfall in mmd^{-1}. (d) Rainfall rate (annual accumulated rainfall / NRD) in mmd^{-1}. Bermuda A. Period 1949-2011. Daily data from BWS.

Time evolution of the annual accumulated rainfall during the study period makes evident significant changes in total rainfall per annum. The linear trend of accumulated rainfall increases lightly annually, this trend for the average rainfall decreases lightly

(figure not shown) and there is apparently no trend for the rainfall maximum. The increasing linear trend of the RND per year with time stands out. Irrelevant differences between the two main time series analysed in Bermuda (Bermuda A. (BER1) and Somerset V. (SOM) are shown when the annual accumulated anomaly is represented. However, there is a relative greater annual maximum rainfall rates in (SOM) (Figure not shown).

The highest accumulated daily rainfall is observed in 1962 followed by 1983 1997 and 2000. The lowest value was recorded in 1975 followed by 1952, 2011 and 1990 (See Fig.34a). Similar results can be also seen in anomalies in Fig.23b. Differences in total rainfall between successive years have been calculated to quantify these changes. Maximum negative and positive differences are -454.4 mm and 530 mm, respectively. Median value is -29.2 mm and first and third quartiles are -156.9 mm and 147.32 mm, respectively. That is, 50% of annual rainfall differences from one year to the next are smaller than 160 mm. However, transitions as large as 530 mm have been observed.

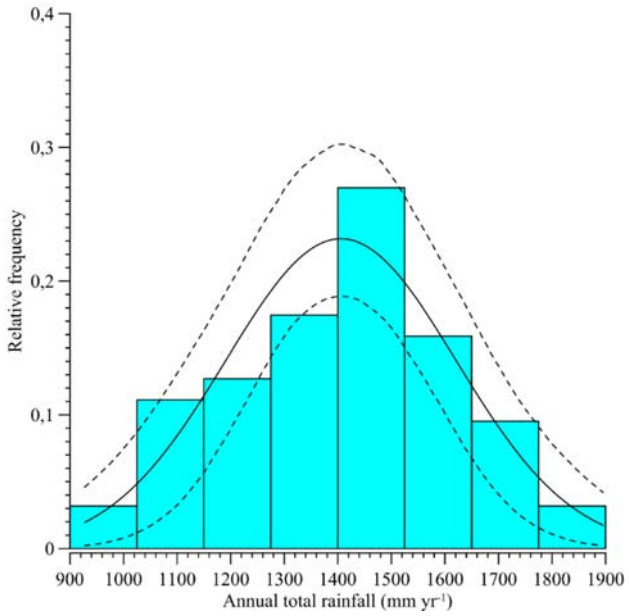

Fig. 35. Associated empirical probability density function in terms of relative frequency of annual total rainfall (mmy-1). Bermuda A. Period 1949-2011. Daily data from BWS.

The empirical probability density function of yearly accumulated rainfall has been estimated in the form of a histogram with fitted normal distribution and associated with a 95% confidence intervals shown in Fig.35. At first glance, annual rainfall histogram seems to resemble a normal distribution. This fact has been statistically confirmed by means of the Jarque-Bera & Anderson-Darling tests of normality, according to which the normality hypothesis can be accepted at 95% of statistical significance.

For this, total rainfall accumulated by year has been grouped in equal size bins ranging between minimum (927mmyr^{-1}) and maximum (1895mmyr^{-1}) observed values, and the relative frequency associated with each bin estimated. Mean accumulated annual rainfall is 1406 mmyr^{-1} while the standard deviation is 217 mmyr^{-1}.

The highest daily maximum is observed in 1996 (a rainfall amount of 197 mmd^{-1}) followed by 1982 and 1980. However, the lower ones are witnessed in 1952, 2011, 1998 and 1990. (Fig.34c).

The inter-annual distribution from daily rainfall data for the normal period 1981-2010 for Bermuda A. (rainfall $\geq$ 0.25 mm) of the NRD, accumulated rainfall and rainfall maxima are given in tables H, I and J respectively, included in Annexe I.

The following is a more detailed explanation of the interannual variability of the the NRD (number of rainfall days) per year and the rainfall rate calculated as the annual rainfall totals (or the amount of rain that falls annually) per number of rain days

(mm d^{-1}).

5.5.3.1.1. Rainfall variability of NRD (Number of rainfall days) and rainfall rate

As a measure of intensity, the rainfall rate anomaly (blue bars) and tendency (dotted line) is represented in Fig.36 versus the NRD per year anomaly (red bars) and tendency (solid line) in terms of variability across time in Bermuda. Daily rainfall rate

pattern follows a parallel sinusoidal behaviour than the NRD from the beginning of the survey period to approximately 1975 (see dotted black line) with relatively greater values around 1960. During this period both signals are in phase. Close to 1990 the pattern of both processes changes noticeably and they reverse their signs.

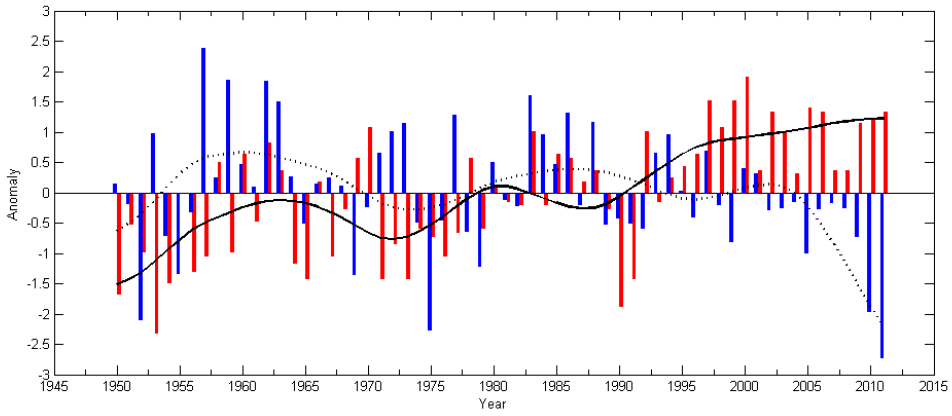

Fig. 36. NRD (Number of Rain Days) anomaly per year (red bars) and tendency (solid line) vs. the annual rainfall rate (annual rainfall totals per number of rain days in mmd^{-1}) anomaly (blue bars) and tendency (dotted line). Bermuda A. Period 1949-2011. Daily data from BWS.

When concerning the inter-annual variability, the main result extracted from Bermuda is that the annual number of rainfall days have increased during the period 1993 to 2011 while the rainfall rate has dropped. Some important changes have occurred in the parameters of atmospheric circulation around 1990 since the frequency of winter storms observed in the sub polar region of the North Atlantic, enhanced from 1980 to 1995 owing to a positive NAO phase (Beersma et al. 1997, Bijl et al. 1999, Alexandersson et al. 2000, Alexander et al. 2005, Bates 2007) seems to have decreased significantly since the mid-1990s (Weisse et al. 2005, Bates 2007). This drop around 1990 is detected in rainfall rate while the NRD increases. However in general there is an increase in the rainfall pattern between 1996 and 2000.

The peak in NRD is achieved in 2000 with 191 rainfall days followed by 1999, 1997 and 2005. Nevertheless, the dips are detected in 1953 followed by 1949, 1990 and 1991. This behaviour is also shown in Fig.34b. The highest annual rainfall rates are observed in 1957, 1959, 1962 and the lowest in 2011, 1975 and 1952, also represented in Fig.34d.

The overall results of this section show the inter-annual rainfall variability in Bermuda. The main statistics from this analysis for de survey period are summarized in Table 14. The average annual rainfall 1406.77 mm yr^{-1} is spread out fairly evenly throughout the year. This value agrees with the results derived from other studies (Macky 1946, Vandever & Pearson 1994) which estimated 1403.60 $mmyr^{-1}$ and 1475.74yr^{-1} mm respectively.

Table 14. Range (RNG), minimum (MIN), maximum (MAX), average (AVG), standard error (SE) and 95% confidence interval (CI) of total daily accumulated rainfall (CUM), ($mmyr^{-1}$), daily average rainfall (AVG) (mmd^{-1}) , daily maxima rainfall (MAX) (mmd^{-1}) and number of rain days (NRD) (dyr^{-1}). Bermuda A. Period 1949-2011. Daily rainfall data from BWS.

	CUM ($mmyr^{-1}$)	**AVG (mmd^{-1})**	**MAX (mmd^{-1})**	**NRD (dyr^{-1})**
Years	63	63	63	63
RNG	928-1888	2.5-5.2	37-197	124-186
MIN/MAX ,year	1975/1962	1975/1962	1952/1996	1953/2000
AVG	1406	3.84	85	161
SE	27.3	0.1	3.3	2
95% CI	54.6	0.15	6.7	4

5..5.3.1.2. Daily precipitation as annual, bi-annual, five years period and decadal normal accumulated rainfall.

The accumulation of daily rainfall over years of investigation was calculated as annual, bi-annual, five-year and ten-year period (decadal). This parameter is calculated by adding sequentially to a rainfall record for a specific day of the year the rainfall accumulated in the following one, two, five or ten years.

Results are depicted in Fig.37. The base period for the calculation was set between 1949 and 2011. Firstly, it seems that low frequency of rain variability prevails. At low resolution (long periods) time the distribution shows a sinusoidal behaviour. At first glance, four cycles could be distinguished: the first of roughly 17 years between 1950 and 1967 with a maximum around 1957, the second of six years between 1967 and 1973, which is flat, the third of 14 years between 1973 and 1987 with maximum accumulations approximately during the period 1976 and 1980 and the last between 1987 to the end of the distribution with a relative maximum around 1997.

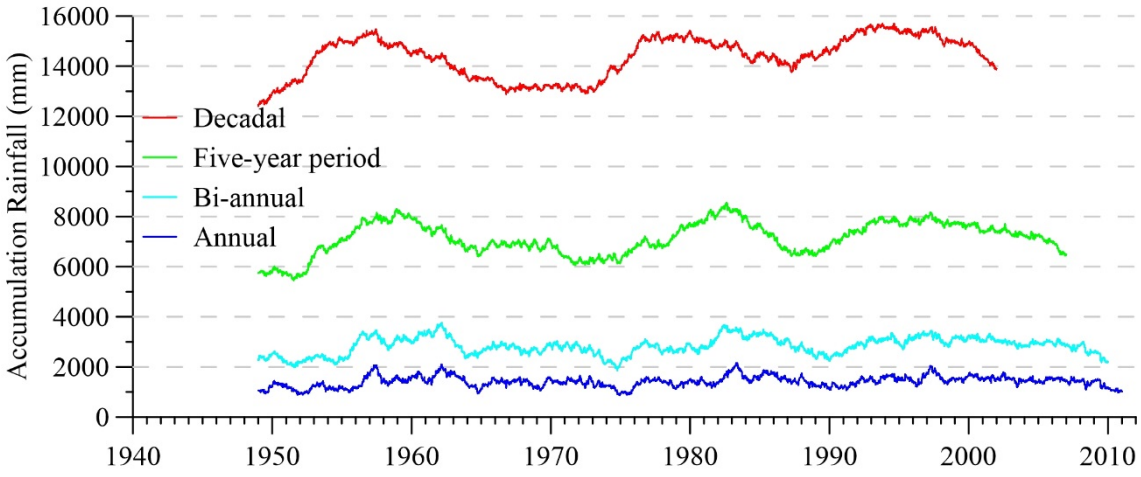

Fig. 37. Accumulation rainfall in annual, bi-annual, five-year period and ten-year period (decadal). Bermuda A. Period 1949-2011. Daily data from BWS.

This last cycle has a medium duration of 15 years for the 10-year rainfall accumulation period and 20 years for the 5-year one. Drops in the annual distribution of the accumulation rainfall are viewed around 1967 and 1973 and another minimum is found between 1987 and 1990. This pattern is clearer for the decadal and the five-year

period analysis. The biannual analysis follows a relative similar behaviour whereas for the annual one is not detectable. Moreover, if a linear regression analysis was made, an increase of the accumulated decadal rainfall linear trend could be suggested.

In the following subsection a comparison of the inter-annual rainfall variability in Bermuda with other archipelagos within the North-Atlantic Ocean is presented by including the analysis of the accumulation rainfall only for a 5-year period and for the normal period 1981-2010, thus only using the second half of the third cycle and the entire fourth one.

The inter-annual distribution from daily rainfall data (rainfall ≥ 0.05 mm) on this normal period for the same weather stations used in the seasonal analysis of the NRD, accumulated rainfall and rainfall daily maxima are given in tables H, I and J respectively, included in Annexe I.

5.5.3.2 Comparison with Canaries, Madeira and Azores

The inter-annual variability of the yearly accumulated rainfall in $mmyr^{-1}$ and the NRD (number of rainfall days) (dyr^{-1}) are represented on the left and right sides of Fig.38 respectively, for Horta Obs. (Az.), Funch. Obs. (M) and Canaries (El Hierro A. (A7), S. C. Ten. (T1), L.Canteras (P14) and Lanzarote A. (A2) compared with Bermuda (BER1) for the period 1981-2010.

The largest accumulated rainfall in BER1 (Bermuda A.) for the normal period 1981-2010 was recorded in 1983. The driest year was 1990. During this period, the largest record in M. (Funch. Obs.) was observed in 2010 when a relative maximum is also found in El Hierro A. (A7) and Horta Obs. (Az). The lowest value in M. was detected in 1986. For Horta Obs. (Az.), the highest annual accumulated rainfall was recorded in 1987, the lowest in 2000. The largest accumulated rainfall in Canaries (average of the 15 weather

stations taken into account in table I Annexe I) was recorded in 1989. The driest year was 1994. The maximum peak in El Hierro A. (A7) in 1988 is also present in Bermuda A.

In particular, the year 2010 was characterized by a climate framework (moderate-high *El Niño*, a negative NAO (North Atlantic Oscillation) and AO (Artic Oscillation) favourable to heavy rainfall occurrences. Results derived from this work assert these arguments. The accumulated rainfall, analysed on the left side of Fig. 38, was in general high in 2010 for all the stations. Some exceptions are BER1, and P14. Though, it was not the rainiest year of the studied period among the investigated stations. The rainiest period was 1987-1989). The analysis of the inter-annual rainfall variability at the selected weather stations adding to them the average values from the 15 stations for the Canary Islands included in the table I Annexe I, is summarised in table 15 by several statistics calculated throughout the yearly values during the normal period 1981-2011.

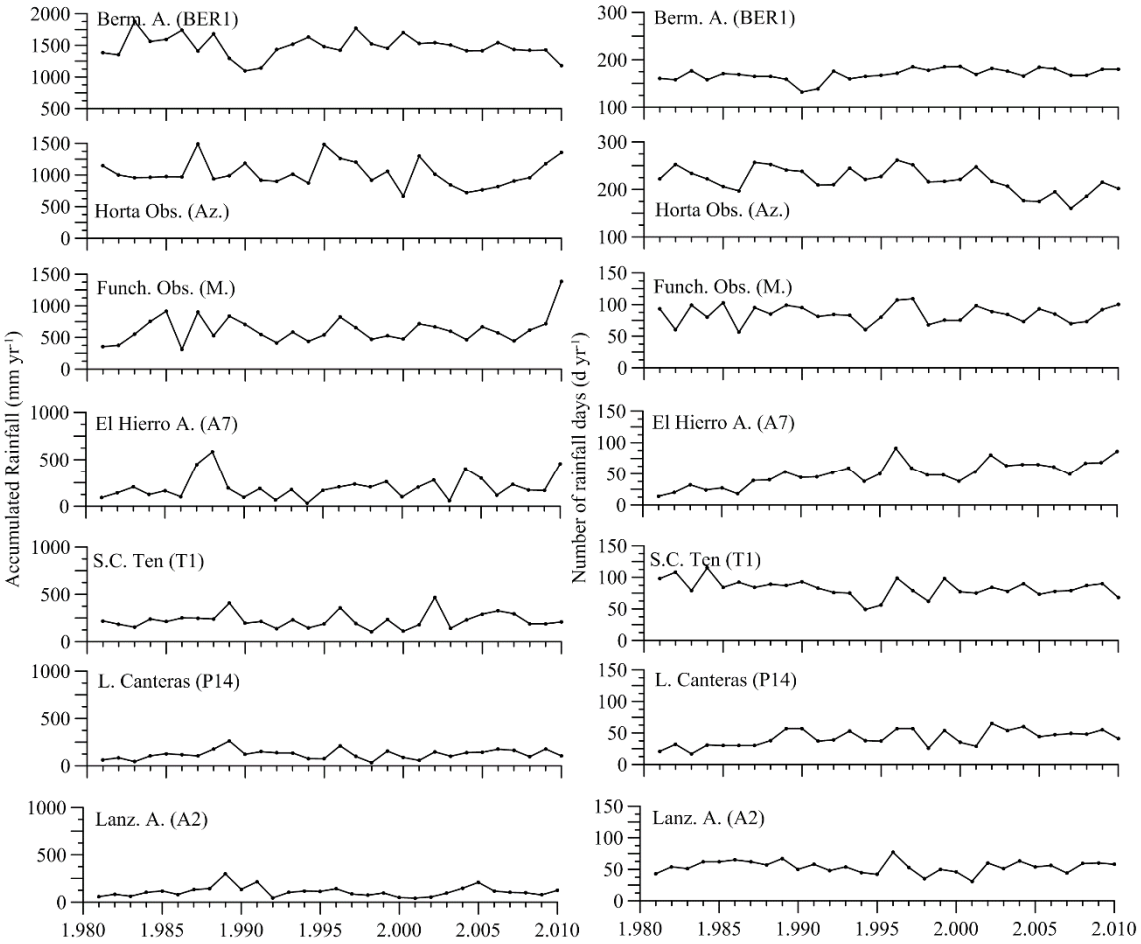

Fig.38. On the left side Inter-annual variability of annual accumulated rainfall ($mmyr^{-1}$). On the right side Inter-annual variability of number of rain days (NRD) (dyr^{-1}). Bermuda (BER1), Horta Obs. (Az), Funch. Obs. (M), El Hierro A. (A6), S.C. Ten (T1), L. Canteras (P14) and Lanz. A. (A2).Period 1981-2010. Daily data from AEMET, BWS and IPMA.

The largest average daily accumulations are observed in BER1, with an average of 1483 $mmyr^{-1}$ followed by Horta Obs. (Az.) with 1025 $mmyr^{-1}$. Both respond to a rainfall pattern without a marked seasonality. Funch. Obs. (M) ranks in third place with an average of 618 myr^{-1}. The average annual rainfall is about 300 $mmyr^{-1}$ for the chosen weather stations in the Canaries (an average of 225 $mmyr^{-1}$ was observed in S.C Ten. (T1) and 206 $mmyr^{-1}$ in El Hierro A. (A7)) .These differences in the Canaries are mainly due to its orientation in the archipelago and within each island and the orography. El Hierro A. (A7) (the western one), is more affected by the pass of the fronts associated with the Atlantic lows, thus experiencing the highest total annual rainfalls, with a maximum of

accumulated daily rainfall of 580 $mmyr^{-1}$. The second rainiest is S.C. Ten. (T1) with a northern orientation which is also located at a western positon within the archipelago. Las Canteras (P14), located north-east of Gran Canaria in a central position with respect to the whole archipelago and Lanzarote A. in an eastern location within Lanzarote Island, is the most eastern of the selected weather stations. Both of these eastern islands experience a lower average total accumulated rainfall close to 100 $mmyr^{-1}$.

The minimum total of the annual accumulations are found in Funch.Obs. (M.) and Horta Obs. (Az.) highlights with records of 300 $mmyr^{-1}$ and 600 $mmyr^{-1}$, respectively. This variable is greater in BER1 with minimum totals close to 1000 $mmyr^{-1}$. The seasonal rainfall patterns which describe these stations explain this anomalous minimum. The normal annual range in Bermuda (1095-1877 $mmyr^{-1}$) stands out when comparing to Lanzarote (A2) and Las Canteras (P14) which present the lower normal annual rainfall ranges with values between of 43-298 $mmyr^{-1}$ and 35-263 $mmyr^{-1}$, respectively.

In Canaries the highest daily maximum among the selected stations was observed in 1988 (280 mmd^{-1}) at El Hierro and the minimum in 2003 at the same station. However considering a larger selection this peak is found in 1993 (337 mmd^{-1}) registered at Izaña (T5). At Fuch. Obs. (M.) was recorded the same as the total rainfall in 2010 (159 mmd^{-1}) and the lowest in 1992. In Horta Obs. (Az) the peak was observed in 1995 (391 mmd^{-1}) and the minimum in 2000.

Table 15. Range (RNG), years with minimum (MIN) and maximum (MAX) values, average (AVG), standard deviation (SD) and 95% confidence interval (CI) for the total accumulated daily rainfall in $mmyr^{-1}$ (CUM), daily maxima rainfall in mmd^{-1} (MAX) and number of rainfall days in dyr^{-1} (NRD). Bermuda (BER1), M (Funch. Obs.), Az. (Horta Obs.), CAN (Canaries average values of the 15 stations), A2 (Lanzarote A.), A7 (El Hierro A.), T1 (S. C.Ten.) and P14 (L.Canteras). Period 1981-2011. Daily data from BWS, AEMET and IPMA.

		CUM ($mmyr^{-1}$)	MAX(mmd^{-1})	NRD(dyr^{-1})
BER1	RNG	1095/1877	54/197	132/191
	(MIN/MAX) years	1990/1983	1998/1996	1990/2000
	AVG	1483	90	169
	SD/95% CI	180/67.3	29.7/11	13/4.8
M	RNG	311/1381	30/159	56/109
	(MIN/MAX) years	1986/2010	1992/2010	1986/1997
	AVG	618	67	85
	SD/95% CI	213/79.7	27/10	14/5.2
Az	RNG	666/1490	32/391	160/262
	(MIN/MAX) years	2000/1987	2000/1995	2007/1996
	AVG	1025	83	219
	SD/95% CI	206/77	67.7/25	26/9.7
CAN	RNG	168/497	54/337	41/73
	(MIN/MAX) years	1994/1989	1994/1993	1994/2009
	AVG	314	131.1	57.6
	SD/95% CI	83/31	69/25.7	8.3/3.1
A2	RNG	43/298	6/55	31/77
	(MIN/MAX) years	2001/1989	2000/1989	2001/1996
	AVG	111	24	53.9
	SD/95% CI	55/20.4	12.5/4.6	9.7/3.6
A7	RNG	31/583	6/280	14/91
	(MIN/MAX) years	1994/1988	2003/1988	1981/1996
	AVG	206	60	49.9
	SD/95% CI	127/47.4	58/21.7	19.2/7.2
T1	RNG	105/468	13/233	49/115
	(MIN/MAX) years	1998/2002	1992/2002	1994/1984
	AVG	225.6	48	82.8
	SD/95% CI	82/31	41.4/15.4	14/5.2
P14	RNG	35/263	6/112	17/65
	(MIN/MAX) years	1998/1989	1998/1989	1983/2002
	AVG	123	26	42.2

SD/95% CI	50.2/18.7	19.8/7.4	12.7/4.7

It stands out the maximum daily rainfall of 233 mm in S. C. Ten. (T1, with a north-eastern location in a relative coastal area at 35 m of altitude which constitutes the metropolitan area of Tenerife Island. This record was observed on 31st March 2002. This rainfall episode flooded the town producing considerable property damage to homes and causing human fatalities (Elizaga et al. 2003).

The average highest NRD at Canaries for the selected weather stations was observed in 2009 (73), the lowest in 1994; at Funch. Obs. (M.) was observed in 1997 (109 rainfall days), the lowest in 1986 and at Horta Obs. (Az.) in 1996 (262 rainfall days) the lowest in 2007.

It is important to take into account that the rainiest stations in these archipelagos which are located at the highest altitudes of Canaries in La Palma Island (*caldera de Taburiente*) or El Hierro (*S. Andrés*), Madeira (*Pico Ruivo*) and Azores (Pico and Faial islands) have not been considered in this study mainly due to the absence of completed Time series.

Climatic normal values for rainfall in the archipelagos of the Canary Islands, Madeira and the Azores for the period 1971-2000 are presented in (AEMET & IMP 2012).

Results show that in Canaries the highest values of average annual NRD with rainfall greater than or equal to 30 mm occur at the highest areas of La Palma, in the Madeira Islands in the upper parts of the island of Madeira (Encumeada) and in Azores, at Faial and São Jorge islands. The lowest values occur at the southern coasts of the main islands

The maximum annual average rainfall in the Canary Islands was observed in Vallehermoso-Igualero (La Gomera), values exceeding 1000 mm can be found at high altitudes of the island of La Palma. In Madeira Islands the greatest average rainfall was recorded in Encumeada (Madeira) and in Azores at Lagoa do Caiado (Pico Island). The highest daily maximum rainfall in Canaries was recorded at San Andrés (El Hierro) on 24th February 1988, in Madeira at Encumeada de São Vicente (Madeira) on 9th December 1976 and in Azores at Nordeste (São Miguel) on 19th November 1975 (Departamento de producción de AEMET & Departamento de Meteorología e Clima de IMP 2012).

Histograms of the empirical probability density function of yearly accumulated rainfall for the same weather stations and period than for the analysis of the inter-annual variability are compared with those for Bermuda in Fig.39

The Jarque-Bera (J-B) and Lillie (L) tests of normality have been used to study if the annual rainfall histograms resemble normal distributions. Results are shown in table 16 which includes the parameters derived by MATLAB (The Math Works, USA) program when the tests are applied: h (value related to the test decision for the null hypothesis that the data comes from a normal distribution), the scalar value *p-value* and the non-negative scalar value *kstat as* test statistic.

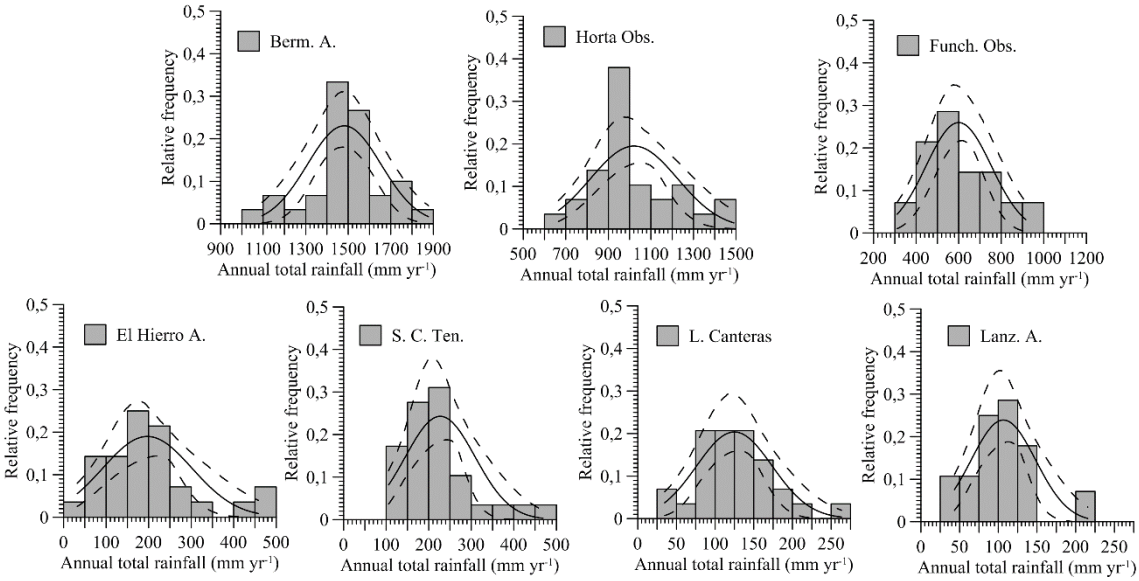

Fig. 39. Associated empirical probability density function in terms of relative frequency of annual total rainfall (mmyr-1) for Bermuda (Berm. A.) Azores (Horta Obs.), Madeira (Funch. Obs.) and Canaries (El Hierro A., S. C. Ten., L.Canteras and Lanzarote A.) Period 1981-2010. Daily data from BWS, AEMET and IPMA.

Table 16. Acronym (Acron.), Station name (St. name), h (value related to the test decision for the null hypothesis that the data comes from a normal distribution), the scalar value *p-value* and the non-negative scalar value *kstat*.for Bermuda A.(BER1), M (Funch. Obs.), Az (Horta Obs.), A2 (Lanzarote A.), A7 (El Hierro A.), T1(S. C.Ten.) and P14 (L.Canteras). Period 1981-2011. Daily data from BWS, AEMET and IPMA.

		Test					
Acr.	**St.name**	**J.Bera**			**Lillie**		
		h	**p-value**	**kstat**	**h**	**p-value**	**kstat**
A2	Lanz.A.	1	0.0019	24.0419	0	0.0594	0.1557
P14	L.Canteras	0	0.1635	2.0361	0	0.5000	0.1025
T1	S.C.Ten.	1	0.0156	8.9771	1	0.0132	0.1807
A7	El Hierro A.	1	0.0112	10.6668	1	0.0026	0.2039
M	Funch.Obs.	1	0.0014	27.2926	0	0.2567	0.1255
Az	Horta Obs.	0	0.1513	2.1279	1	0.0114	0.1829
BER1	Berm.A.	0	0.50	0.0809	0	0.1171	0.1426

The null hypothesis establishes a normal distribution. If the test returns the value h = 1 the null hypothesis is rejected at the 5% significance level which means that the

distribution is not normal. When h = 0, the null hypothesis is accepted and so the normality. According to these results and applying both tests J-B and L., the normality hypothesis can be accepted for the annual rainfall histograms of Berm. A. and L.Canteras. However similar histograms for El Hierro A. and S.C. Ten. do not follow a normal distribution. J-B tests confirms the normality for Horta Obs (Az.), but L. test rejects it. On the contrary, J-B tests rejects the normality for annual rainfall histograms at Funch.Obs. (M) and Lanz. A. (A2) while L. test confirms it.

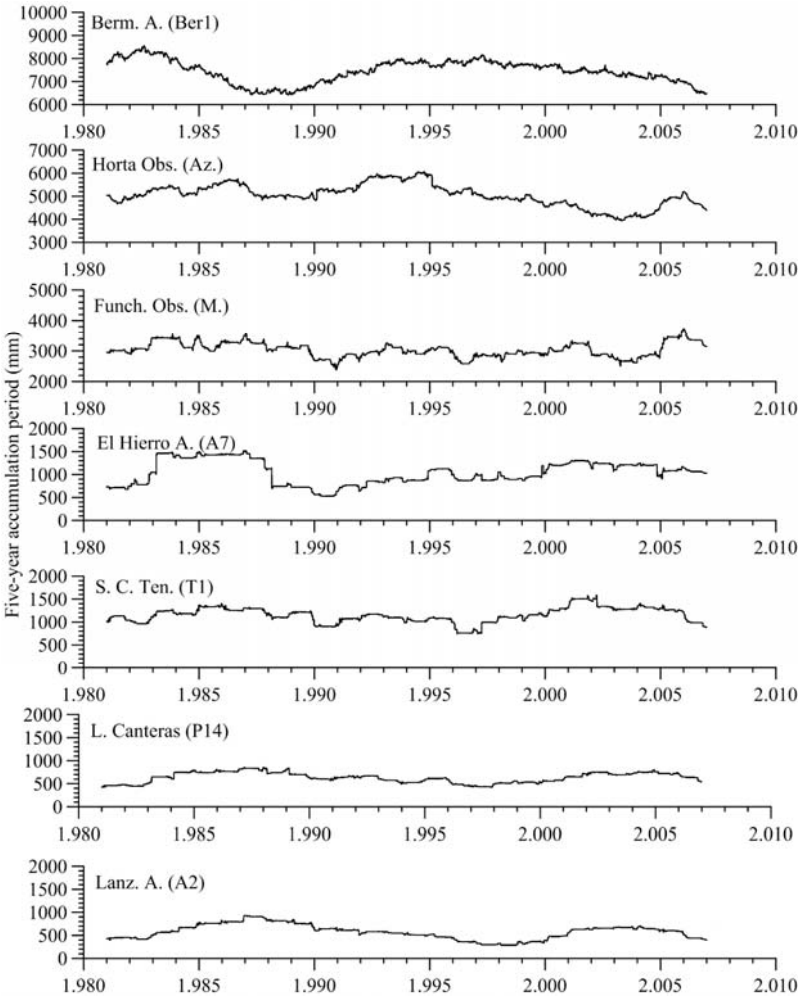

Fig. 40. Five-year period accumulation rainfall (mm). Bermuda (BER1), Horta Obs. (Az), Funch. Obs. (M), El Hierro A. (A7), S.C. Ten (T1), L. Canteras (P14) and Lanz. A. (A2). Period 1949-2011. Daily data from BWS, AEMET and IPMA.

Comparison of distribution of accumulation daily rainfall in mm for a five-year period in Bermuda with Horta Obs. (Az.), Funch. Obs. (M), El Hierro A. (A7), S.C. Ten (T1), L. Canteras (P14) and Lanz. A. (A2) for the period 1981-2010 is shown in Fig.40.

Similarly to the results presented in Fig.37, in Bermuda for the normal period 1981-2010 in this case, two clear sinusoidal cycles can be observed. The first from 1981 to 1987 and the second between 1987 to the end with a relative maximum around 1997. This last cycle has a medium duration of 23 years. The noticeable drop between 1987 and 1990 is also found when the accumulation was calculated for different periods (see Fig.37) and the rainfall variability of NRD (number of rainfall days) was studied (Fig.36).

This trend in the accumulation rainfall is not so clearly distinguishable for the others weather stations. In Horta Obs. (Az.) there is a cycle between 1981 and 1990 and another from 1900 to 2003. It shows a similar pattern than Bermuda A. (BER1) between 1988 and 1995. The ascending trend in accumulations from 1980 to 1984 could be due to more frequency of winter storms in this area enhanced by a positive NAO phase and the Niña of 1983.

The minimum accumulations found in Bermuda (BER1) between 1987 and 1990 is also detected in Horta Obs. (Az.) during roughly the same period and for Funch. Obs. (M), El Hierro A. (A7) and in S.C. Ten. (T1) with a certain lag. As was mentioned above, the frequency of winter storms dropped considerably since the mid-1990s after the previous enhancement during the NAO positive period of 1980 to 1995 (Weisse et al. 2005, Bates 2007), so important changes in the atmospheric circulation occurred around this year.

For Funch. Obs. (M.) cycles for the accumulated rainfall are not clearly defined, but show a close pattern than Horta Obs. (Az.) at the end of the distribution. Between 1982 and 1988 and 1993 and 2002 low variations are found.

The behaviour of this variable at the stations located in the western part of the Canary archipelago, El Hierro A. (A7) and S.C. Ten. (T1), is similar to each other with high accumulations close to 1985, a minimum around 1990 and then a relative ascending pattern until 2002 with certain drop close to 1996. In general in the western part of Canaries, there is an increase in the rainfall accumulated pattern between 1996 and 2002 clearly noticeable in S.C. Ten (T1) less marked in Funch.Obs. (M). However, it descends in this period in Horta Obs. (Az.) and BER1 after a relative maximum in 1997 which may be enhanced by the strong Niño event.

Lanz. A. (A2) and L.Canteras (P14) in Gran Canaria Island show a similar interannual variability pattern with a clear different behaviour from the rest of the analysed weather stations which is explained because of an eastern position of these islands within the archipelago. Two cycles can be distinguished is this pattern. The rainfall rises until 1987 experiencing a drop during the year 1998. S.C. Ten. (T1) is quite similar to them but with another minimum close to 1990.

Spatial variability has been found between archipelagos due to different geographical location and orientation. The western islands in the Canary archipelago show similar behaviour and in at a lesser degree Madeira. They share certain features with Bermuda and Horta like the drop of rainfall accumulations close to 1990 caused by changes in the atmospheric circulation.

5.5.4. Seasonality Index (SI)

5.5.4.1. Bermuda

RESULTS AND DISCUSSION

The global average index of seasonality, estimated by using Eq.10 (see section 4.3) gives a value of SI equal to 0.133 indicating that in average rainfall regime in Bermuda belongs to the very equable class (Walsh & Lawler 1981). In fact, the use of average data conceals inter annual variability details and tends to underestimate seasonality. For this reason, it is recommended to obtain an average index of seasonality $\overline{SI}$ by averaging yearly values. That is, the long-term mean value of the seasonality index during a period of N years is estimated as Eq.11 (see section 4.3)

In this work the following acronyms are used for the classification of rainfall regime in terms of SI, suggested by Walsh & Lawler (1981): very equable (VE), rather seasonal with a short drier season (SSD), equable but with a definite wetter season (EW), seasonal (S), markedly seasonal with a long drier season (MLD), most rain in 3 months or less (3MR), extreme, almost all rain in 1-2 months (E) and short wet season (SW).

In this sense, it is interesting to remark that, even when the index of seasonality estimated by means of Eq.10 indicates that the average rainfall regime in Bermuda belongs to the very equable class, the use of the χ^2-test to assess the null hypothesis of precipitation uniformly distributed throughout the year, gives a value, 40.25, greater than the critical value, 18.31. Therefore, uniformity of the average annual rainfall pattern must be rejected. This result is more coherent with the long-term mean value of 0.408 obtained for the seasonality index derived with Eq.11, by averaging the 63 individual yearly values, and according to which the average rainfall regime in Bermuda belongs to the rather seasonal with a short drier season class.

Global and mean indexes of seasonality for the entire period (1949-2011) are 0.133 and 0.408, respectively, and the corresponding index of rainfall replicability, ($RI = SI/\overline{SI}$) is 0.326.

This low value indicates that wettest and driest monthly periods can occur over a wide range of calendar months and that the rainfall regime is not seasonal. Then, maximum monthly accumulated rainfall, or peak rainfall, may occur in almost any month of the year. The very low seasonality, indicated by the global index, 0.133, can also be a result of the averaging compensation effect of annual significantly seasonal regime, but where the timing of the wetter and drier months varies from year to year.

To display this fact as clear as possible, months of every year have been sorted in order of accumulated rainfall and a weight, ranging from 1, for the driest, to 12, for the rainiest, assigned. Then, any month of a given year has an associated weight indicating its rank in terms of accumulated rainfall within each year. This information is presented in Fig.41 as a colour map where twelve different colour tones represent the rank of each month, from the clearest (driest) to the darkest (rainiest). It is important to remark that there is no month without rain during the studied period.

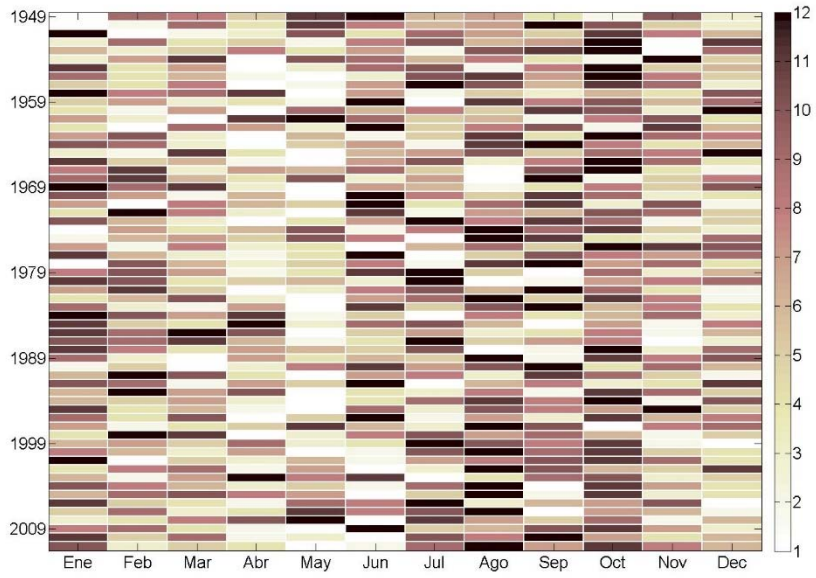

Fig.41. Ranking of months within any year in terms of accumulated rainfall. Lighter (darker) tones correspond to drier (wetter) months. Colour bar legend. Bermuda A. Period 1949-2011. Daily data from BWS.

In agreement with the results presented in Fig.16a and Fig.25, can be recognized that annual average rainfall pattern presents an absolute maximum around October (lighter colours) and a secondary peak around January, as well as two local minima in April-May and November-December, corresponding to the darker colours. Nevertheless, a particularly striking feature is that in the mean pattern previously commented, the rainiest month in average can be, in some years, the driest and inversely, the driest month can become the wettest. This result enables understanding the difference between the global and average indexes of seasonality, defining the replicability index. Thus, the averaging of the values corresponding to a given month and estimating a global average seasonality index, such as in Eq.10, masks the true seasonal structure of precipitation in the study zone.

Additionally, it is interesting to highlight that each one of the calendar months has been, at least once during the year, the rainiest or driest month in the study period. In several years the wettest month is immediately followed by the driest one. However in other years, the reverse situation can be observed, as well as in other periods there is a gradual transition from rainiest to the driest months. Summarizing it up, the timing of the wetter and drier months varies from year to year. Accordingly, there is a considerable variability between individual annual rainfall patterns, which is equivalent to a low replicability and then a no seasonal character of the precipitation regime.

Table 17. The global average Seasonality Index (SI), long-term mean value of the seasonality index ($\overline{SI}$) and index of rainfall replicability *(RI)* according to Walsh & Lawler (1981) for the whole study period 1981-2010 and normal sub-periods for Bermuda A. (BER1). Daily rainfall data from BWS.

Period	SI	$\overline{SI}$	$RI = SI/\overline{SI}$
1949-2011	0.133	0.408	0.326

1949-1978	0.148	0.411	0.360
1966-1975	0.151	0.409	0.368
1982-2011	0.143	0.403	0.355

The long-term mean index of seasonality has also been estimated for three normal overlapped sub-periods (1949-1978; 1966-1975; 1982-2011). Results, given in table 17, are almost the same for each one of these periods, and very similar to that of the overall period under examination. Thus, in average, the rainfall regime in Bermuda can be classified as seasonal with a short a drier seasonal class, in accordance with Walsh & Lawler (1981) or has a clearer seasonal behaviour according to Peña-Arencibia et al. (2010) (see Table 5).

Additionally, global average indexes of seasonality, as well as the corresponding replicability indexes have been computed for the above mentioned three normal sub-periods. Resulting values indicated in columns two and four of table 17, are very similar for any of the thirty sub-period years. However, for both parameters these are slightly greater than those corresponding to the whole period, bringing out the reduction of the cancelling out effect as the number of averaged years diminishes. Accordingly, rainfall regime replicability has remained significantly low and practically unchanged during this study period, indicating that the timing of the wetter and drier months exhibits a considerable annual variability, such as observed in Fig.41.

At first glance, according to these results, Bermuda presents a non-marked seasonal precipitation regime. There is no evident monsoon or rainy season. Rainfall events seem to spread near evenly throughout the year with an increasing trend during the summer.

A subject of a particular practical interest, in the context of inter-annual rainfall variability, is to know if the tendency to have rainfall concentrated in a given month or

season versus others varies over the years. Thus, variability of the annual SI_y during the 63 years of observations is depicted in Fig.42a. A solid line indicates the median value of SI_y, equal to 0.420, while dashed lines indicate first and third quartiles, Q_1=0.349 mmd^{-1} and Q_3=0.475mmd^{-1}, respectively. The minimum value is 0.201mmd-1 for 2006 while the maximum value, 0.705mmd^{-1}, is reached in 1976. The difference between Q_3 and Q_1, named interquartile range, equals 0.26mmd^{-1}. This reveals a moderate inter-annual variability in the rainfall regime. According to these results and following the criterion suggested by Walsh & Lawler (1981), in 52% of the cases rainfall regime corresponds to the class of regime rather seasonal with a short drier season, and 46% to that of equable but with a definite wetter season, while only in 2% of the cases the regime is a seasonal one.

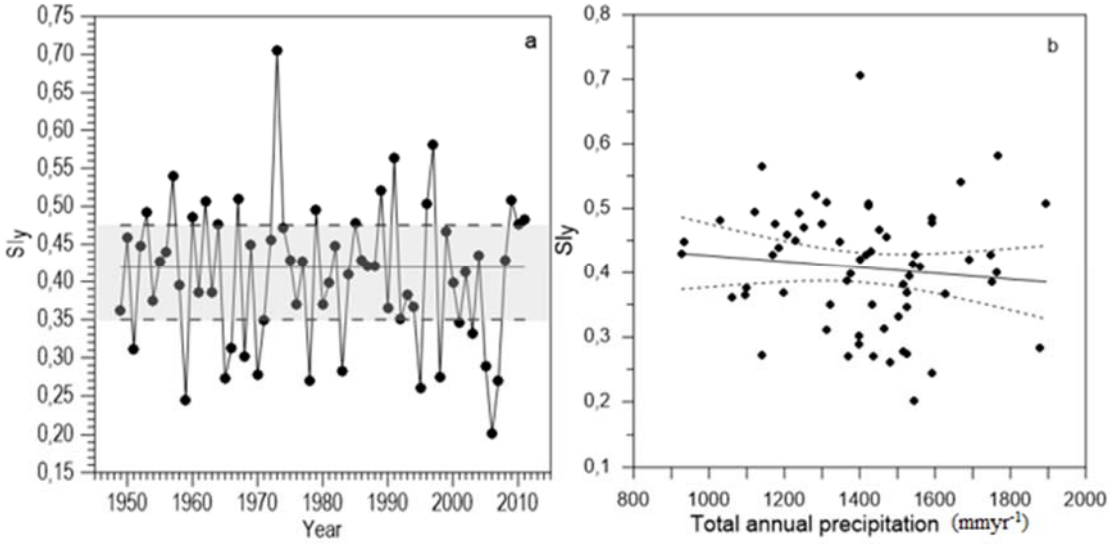

Fig.42 a) Variability of the annual SIy (dots). The median value (solid line) as well as first and third quartiles (dashed lines) are indicated. Interquartile distance is depicted as a shadow area. b) Scatter diagram of SIy versus total annual rainfall ($mmyr^{-1}$), along with best fitted line and 95% confidence intervals. Bermuda A. Period 1949-2011. Daily data from BWS.

However, according to Peña-Arencibia et al. (2010) the 100% of the analysed years present a seasonal rainfall regime (see Table 3). Values of the Chi-square statistical test, applied to assess uniformity, or non-seasonality, for each one of the 63 years are all

considerably greater than the critical value, 18.31. Therefore, the existence of a seasonal pattern in the rainfall regime in any of the analysed years can be accepted with confidence.

Once confirmed that there is a remarkable variability in the seasonal pattern from year to year, other particularly important aspect to be explored is the existence of long-term trends in this annual behaviour through the study period. In this sense, values of seasonality index exhibit considerable variability from year to year (Fig.42a), with local slopes changing from positive to negative, so that a global trend is not apparent. Hence, the modified Mann-Kendall test, including modifications to take into account serial correlations (Hirsch & Slack 1984) has been applied to the sequence of 63 SI_y values to check for possible trends. The test rejects the existence of trends at a 95% confidence level. That is, no statistical significant positive or negative trends in the seasonality index can be inferred from the available information.

Note that changes in the seasonal pattern of precipitation may have many important implications (Pryor & Schoof 2008). Thus, provided that total annual rainfall remains almost the same, a weakening of seasonality entails a more uniform distribution of monthly rainfall through the year while its intensification implies a tendency towards longer dry and shorter rainy periods. Nevertheless, it is important to point out that positive or negative trends in seasonality index do not necessarily entail a change in total annual precipitation. An increase in SI_y means a tendency towards longer dry and shorter wetter seasons, and the reverse, but no a change in annual precipitation. In fact, a relationship analysis of seasonality index against annual rainfall during the whole study period has indicated a lack of statistical significant correlation, either positive or negative, between both variables (Fig.42b). Determination coefficient (R^2) which that there is not linear association between both variables, is 0.011.

In the previous paragraph total annual rainfall has been assumed to remain constant over time. Naturally, it need not necessarily be the case. However, in spite of the results obtained from the Chi-square statistical test and the modified Mann-Kendall test applied to the total annual rainfall time series have shown that there is not enough statistical evidence to support the existence of any significant variations over time in the annual rainfall regime over Bermuda.

5.5.4.2 Comparison with Canaries, Madeira and Azores

The global average and long-term mean seasonality indexes and replicability index for the whole study period (1949-2011) and normal sub-periods for El Hierro A. (A7), S.C. Ten (T1), L. Canteras (P14), Lanz. A. (A2), Horta Obs. (Az.), and Funch. Obs. (M) are viewed in Table 18.

The seasonality Index (SI), the long-term mean value of the seasonality index ($\overline{SI}$) and the index of rainfall replicability *(RI)* for the whole study period 1981-2010 and normal sub-periods for the selected weather stations can be found in Table 19, including acronyms used for the classification of rainfall regime in terms of SI, suggested by Walsh & Lawler (1981). High replicability is denoted by Rep.

Table 18. Global average and long-term mean seasonality indexes, and replicability index for the whole study period (1949-2011) and normal sub-periods for El Hierro A. (A7), S.C. Ten (T1), L. Canteras (P14), Lanz. A. (A2), Horta Obs. (Az.), and Funch. Obs. (M). Daily rainfall data from AEMET, BWS and IPMA.

El Hierro A. (A7)

Periodo	SI	$\overline{SI}$	RI=SI/$\overline{SI}$
1981 – 2010	0,840	1,190	0,706
1981 – 1995	0,926	1,226	0,755
1996 – 2010	0,829	1,153	0,719
1981 – 1990	0,944	1,248	0,756
1991 – 2000	0,807	1,209	0,667
2001 – 2010	0,907	1,111	0,816

S.C. Ten (T1)

Periodo	SI	$\overline{SI}$	RI=SI/ $\overline{SI}$
1981 – 2010	0,781	1,067	0,732
1981 – 1995	0,766	1,079	0,710
1996 – 2010	0,838	1,054	0,795
1981 – 1990	0,746	1,059	0,704
1991 – 2000	0,814	1,052	0,774
2001 – 2010	0,835	1,089	0,767

L. Canteras (P14)

Periodo	SI	$\overline{SI}$	RI=SI/$\overline{SI}$
1981 – 2010	0,773	0,994	0,778
1981 – 1995	0,815	1,082	0,753
1996 – 2010	0,744	0,905	0,822
1981 – 1990	0,804	1,065	0,755
1991 – 2000	0,765	1,045	0,732
2001 – 2010	0,775	0,871	0,890

Lanz.A (A2)

Periodo	SI	$\overline{SI}$	RI=SI/ $\overline{SI}$
1981 – 2010	0,822	1,173	0,701
1981 – 1995	0,841	1,163	0,723
1996 – 2010	0,840	1,182	0,711
1981 – 1990	0,855	1,182	0,723
1991 – 2000	0,838	1,142	0,734
2001 – 2010	0,908	1,195	0,760

Funch. Obs. (M)

Periodo	SI	$\overline{SI}$	RI=SI/ $\overline{SI}$
1981 – 2010	0,628	0,927	0,677
1981 – 1995	0,590	0,928	0,636
1996 – 2010	0,662	0,926	0,715
1981 – 1990	0,577	0,893	0,646
1991 – 2000	0,670	0,986	0,680
2001 – 2010	0,682	0,902	0,756

Horta Obs. (Az)

Periodo	SI	$\overline{SI}$	RI=SI/$\overline{SI}$
1981 – 2010	0,327	0,551	0,593
1981 – 1995	0,359	0,558	0,643
1996 – 2010	0,329	0,545	0,604
1981 – 1990	0,322	0,548	0,588
1991 – 2000	0,342	0,540	0,633
2001 – 2010	0,361	0,565	0,639

The index of seasonality (SI) estimated following Eq.10, by the criterion suggested by Walsh & Lawler (1981) shows that the rainfall regime at the Canary Islands is in general seasonal (S) or has a markedly seasonal with a long drier season (MLD). The rainfall patterns for El Hierro A. (A7) and Lanz. A. (A2) are classified clearly as MLD. In S.C. Ten. (T1) and L. Cant. (P14) it is seasonal (S) for the whole period with MLD regime for some sub-periods.

Table 19. Seasonality Index (SI), long-term mean value of the seasonality index ($\overline{SI}$) and index of rainfall replicability *(RI)* according to (Walsh & Lawler 1981) for the whole study period 1981-2010 and normal sub-periods for El Hierro A. (A7), S.C. Ten (T1), L. Canteras (P14), Lanz. A. (A2), Funch. Obs. (M) and Horta Obs. (Az.). Daily rainfall data from AEMET and IPMA.

	Period	SI	$\widetilde{SI}$	$RI = SI/\widetilde{SI}$
A7	1981- 2010		3MR	
	1981- 1995			
	1996- 2010			
	1981- 1990	MLD	E	Rep
	1991-2000			
	2001- 2010			
T1	1981- 2010	S		
	1981- 1995	S		
	1996- 2010	MLD	3RM	
	1981-1990	S		Rep
	1991- 2000	MLD		
	2001- 2010	MLD		
P14	1981- 2010	S	MLD	
	1981- 1995	MLD	3MR	
	1996- 2010	S	MLD	Rep
	1981-1990	MLD	3MR	
	1991- 2000	S	3MR	
	2001- 2010	S	MLD	
A2	1981- 2010			
	1981- 1995			
	1996- 2010			
	1981-1990	MLD	3MR	Rep
	1991- 2000			
	2001- 2010			
M	1981- 2010	S		
	1981- 1995	SSD		
	1996- 2010	S		
	1981-1990	SSD	MLD	Rep
	1991- 2000	S		
	2001- 2010	S		
Az	1981- 2010			

	Period	SI	$\overline{SI}$	$RI = SI/\overline{SI}$
	1981- 1995			
	1996- 2010			
	1981-1990	EW	SSD	Rep
	1991- 2000			
	2001- 2010			

However, Funch. Obs. (M) shows generally a seasonal rainfall regime (S) but behaves in some sub-periods as rather seasonal with a short drier season (SSD).

Finally the rainfall regime in Horta Obs. (Az.) is characterized as equable but with a definite wetter season (EW).

Related to the long-term mean value of the seasonality index ($\overline{SI}$), the Canaries present in general the most rain in 3 months or less (3MR), for all the studied sub-periods in T1 and A2. This feature is also observed in El Hierro A. (A7) and L. Canteras (P14). The first one also presents an extreme rainfall regime with almost all rain in 1-2 months (E) in some sub-periods. P14 presents MLD for the whole period. Rainfall in Funch.Obs. (M) is characterized as MLD and in Horta Obs. (Az.) as SSD.

Following the criteria of (Peña-Arencibia et al. 2010) seasonal regime (S) prevails in all the weather stations by analyzing both SI and $\overline{SI}$. Only El Hierro A. (A7) according to the last one shows a SW (short wet season) for certain sub-periods.

Finally, taken into account the index of rainfall replicability (RI), in all the weather stations the rainfall regime presents a high replicability and then a seasonal behaviour. The Canary Islands show greater values and Las Canteras (P14) the highest one, and then S.C.Ten. (T1), El Hierro (A7) and Lanz. A. (A2) for the period 1981-2010. Funch. Obs. (M) presents a lower RI (0.677) and the lowest one is found at Horta Obs. (Az.) with 0.593. No differences were found when analysing results from the rest of the

sub-periods. As a result according to this parameter, the Portuguese islands (mainly Azores) have a similar rainfall pattern to Bermuda.

Following PA-2010 in all cases seasonal rainfall regime prevails, except for A7 during the sub-periods 1981-1995, 1981-1990 and 1991-2000 in which the rainfall regime is classified as SW (short wet season).

Table 20. St. name (station name), Acr. (Acronyms), and Chi^2 value for Bermuda A. (BER1), M (Funch. Obs.), Az. (Horta Obs.), A2 (Lanzarote A.), A7 (El Hierro A.), T1 (S. C.Ten.) and P14 (L.Canteras). Period 1981-2011. Daily data from BWS, AEMET and IPMA.

St. Name	Acr.	Chi^2
El Hierro A.	A7	174.60
S.C. Ten	T1	159.08
L. Canteras	P14	87.84
Lanz. A.	A2	101.92
Horta Obs.	Az	133.46
Funch. Obs.	M	307.18
Berm.A.	BER1	40.25

Values of the Chi-square statistical test, for each one of the 30 years applied to the selected stations are resumed in table 20. They are greater than Chi^2-crit (18.31).Therefore, the null hypothesis is rejected just like in Bermuda. In conclusion data are not uniformly distributed for any station, so generally the rainfall pattern in this area should be rather seasonal.

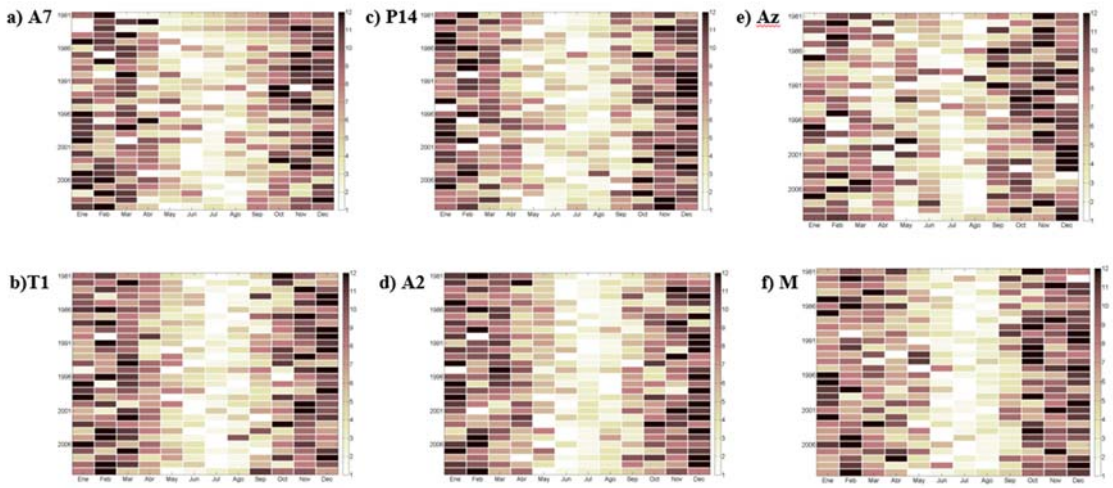

Fig.43. Ranking of months within any year in terms of accumulated rainfall. .Lighter (darker) tones correspond to drier (wetter) months. Colour bar legend. a) El Hierro A. (A7), (b) S.C. Ten (T1), (c) L. Canteras (P14), (d) Lanz. A. (A2), (e) Horta Obs. (Az.), and (f) Funch. Obs. (M). Period 1981-2010. Daily data from AEMET and IPMA.

Taking into account the importance to remark the difference between the relative seasonality (relative contrast between rainfall throughout the year) and absolute seasonality (the length of dry and wet seasons) (Walsh & Lawler 1981), the monthly rankings within any year in terms of accumulated rainfall for a) El Hierro A. (A7), b) S.C. Ten (T1), c) L. Canteras (P14), d) Lanz. A. (A2), e) Horta Obs. (Az.), and f) Funch. Obs. (M) and for the period 1981-2010 has been analysed and they are shown in Fig.43. Similarly to Bermuda, lighter tones correspond to drier months whereas darker wetter ones.

By comparing with the rest of the studied stations, the only one with a marked rainfall pattern in summer is Bermuda with the maximum normal total accumulated monthly rainfall value for the period 1981-2010 in August (4898 mm), and then Oct., Jan., Jul., and Sep. being May the month with lower value (2668 mm). For the Canary and the Portuguese islands winter and autumn are the rainy seasons and summer the dry one.

Results from Fig.43 confirm those achieved when the seasonal variability of the rainfall events was analysed (section 5.5.2. 2.). Table F in Annexe I resumes the monthly accumulated rainfall for the studied period for the normal period 1981- 2010.

The shorter dry season is found in Horta Obs. (Az.) and El Hierro (A7) being July to August the driest period and July the driest month. Funch.Obs. (M) has also a shorter dry season where July and August are almost equally dry. June is relatively dry with sporadic rainfall events. Lanz. A. (A2) has the longer dry season being June in this station drier than in the rest sites analysed.

Results extracted from this work confirm those achieved by other authors derived for the normal period 1971-2000 (Departamento de producción de AEMET & Departamento de Meteorología e Clima de IMP 2012).

Contrary to the results obtained for Bermuda, in Canaries in general and Madeira, there is a rather normal gradual transition from the rainiest to the driest months. The timing of the wetter and drier months is not too variable from year to year. There is a considerable homogeneity between individual annual rainfall patterns, which is equivalent to a high replicability and seasonality of the precipitation regime.

The percentages which correspond to each class of rainfall regime in terms of the values of the SI_y (Seasonality Index (SI) for a given year) according to (Walsh & Lawler 1981), the determination coefficients (R^2) of the SI_y versus the total annual rainfall, the years with minimum and maximum (MIN/MAX) interquartile values and the interquartile range (RNG) for El Hierro A. (A7), S.C. Ten (T1), L. Canteras (P14), Lanz. A. (A2), Horta Obs. (Az.), Funch. Obs. (M) and Bermuda A. (BER1) are represented in Table 21.

The values derived from the SI_y (Seasonality Index (SI) for a given year) given in table 21 are in agreement with long-term mean values of the seasonality index ($\overline{SI}$) (see table 19) following the criterion suggested by Walsh and Lawer (1981) and they are quite different from the global average index of seasonality (SI). Only for L. Canteras (P14) both indexes suggested a markedly seasonal with a long drier season (MLD) rainfall regimen in a relative high percentage. These differences when each index is used are due to the fact that the SI gives information about a relative seasonality which is referred to the seasonal contrast in rainfall amounts rather than whether months are dry or wet in an absolute sense.

Table 21. Percentages corresponding to each class rainfall regime in terms of the values of the SI_y (Seasonality Index (SI) for a given year) according to Walsh & Lawler (1981):very equable (VE), rather seasonal with a short drier season (SSD), equable but with a definite wetter season (EW), seasonal (S), markedly seasonal with a long drier season (MLD), most rain in 3 months or less (3MR), extreme, almost all rain in 1-2 months (E) or short wet season (SW), the determination coefficients (R^2) of the SI_y versus the total annual rainfall, the interquartile SI_y range (RNG), the years with minimum and maximum (SI_y MIN. IQ/SI_yMAX. IQ.) interquartile values and for El Hierro A. (A7), (b) S.C. Ten (T1), (c) L. Canteras (P14), (d) Lanz. A. (A2), (e) Horta Obs. (Az.), and (f) Funch. Obs. (M). Period 1981-2010. Daily rainfall data from BWS, AEMET and IPMA.

Acr.	VE (%)	EW (%)	SSD (%)	S (%)	MLD (%)	3MR (%)	E (%)	R2	SI_y RNG	SI_y MIN.IQ/Yr SI_y MAX.IQ/Yr
A7					17	33	50	0.023	0.283	0.822/1994 1.489/1981
T1					36	42	17	0.071	0.223	0.811/2000 1.339/2001
P14			10	4	36	30	20	0.001	0.222	0.410/2010 1.350/1983
A2					14	50	36	0.021	0.202	0.892/1993 1.558/2001
M					53	33	14	0.244	0.176	0.650/2007 1.182/2000
Az			67	33				0.136	0.118	0.403/2001 0.728/2003

BER1	47	53		0.040	0.121	0.201/2006 0.581/1997

The long-term mean values of the seasonality index ($\overline{SI}$) quantifies this contrasts and it is more sensitive to changes in the rainfall regimes reflecting differences in rainfall concentration (Walsh & Lawler, 1981). These authors proposed a relative (SI) named SI_y. based on the differences between observed monthly precipitation and that expected under the hypothesis of precipitation uniformly distributed throughout the year that for a given year. Accordingly to the SI_y, in Funch.Obs. (M) and L. Canteras (P14) a markedly seasonal with a long drier season (MLD) rainfall regime is found, with a relative high percentage as well of regime with most rain in 3 months or less (3MR). The dry season goes from May to August. For Horta Obs. (Az.) and Bermuda A. (BER1) the class rather seasonal with a short drier season (SSD) regimen is dominant.

Table 22. Monthly annual rainfall rate (annual rainfall totals per number of rain days (NRD) in mmd^{-1}) for El Hierro A. (A7), (b) S.C. Ten (T1), (c) L. Canteras (P14), (d) Lanz. A. (A2), (e) Horta Obs. (Az.), and (f) Funch. Obs. (M). Period 1981-2010. Daily rainfall data from BWS, AEMET and IPMA.

month	**A2**	**A7**	**P14**	**T1**	**Az**	**M**	**BERM1**
Jan.	0.5	0.9	0.6	1.0	3.2	2.3	4.5
Feb.	0.6	1.3	0.8	1.3	3.8	2.9	4.3
Mar.	0.4	0.8	0.4	1.2	2.9	1.9	3.8
Abr.	0.2	0.4	0.2	0.4	2.2	1.4	3.5
May	0.1	0.1	0.1	0.1	2.2	0.9	2.9
Jun.	0.0	0.0	0.0	0.0	1.9	0.2	4.0
Jul.	0.0	0.0	0.0	0.0	1.0	0.1	4.2
Aug.	0.0	0.0	0.0	0.1	1.5	0.1	5.3
Sep.	0.1	0.1	0.2	0.2	3.1	1.1	4.3
Oct.	0.3	0.4	0.4	0.6	3.7	2.8	5.1
Nov.	0.5	1.2	0.6	1.1	4.0	2.9	3.3
Dec.	0.9	1.4	0.8	1.4	4.4	3.7	3.5

Total	3.7	6.8	4.1	7.4	33.8	20.4	48.7

This dry period corresponds to July for Horta Obs. (Az.) and May for Bermuda. This features can be seen by the monthly annual rainfall rates or the annual rainfall totals per number of rain days (NRD) in mmd^{-1} for the selected weather stations and for the normal period 1981-2010 presented in Table 22.

Only for Bermuda A. the equable but with a definite wetter season (EW) is assigned to its rainfall regime but in a lightly lower percentage than SSD.

The classification of the rainfall regime suggested for S.C. Ten. (T1), Lanz. A. (A2) and El Hierro (A7) are quite different from the rest. A rainfall regime with most rain in 3 months or less (3MR) prevail in T1 (December, February and March) (with also a considerable but lower MLD characteristics being the dry period from May to September) and at A2 with some features of extreme regime (E) with almost all rain in 1-2 months. Finally in A7 an extreme regime (E) dominates with some 3MR features being December, February and November the wetter months.

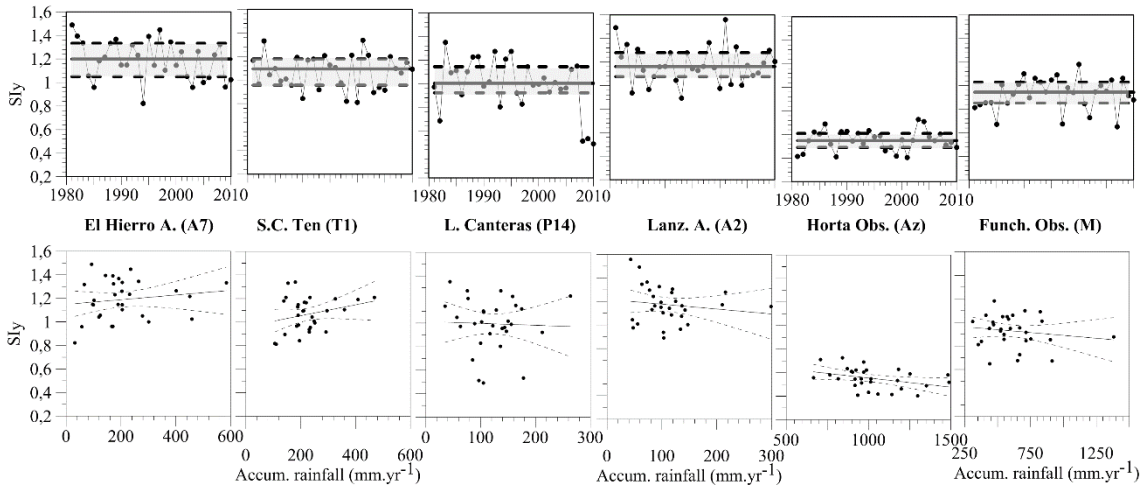

Fig.44 Variability of the annual SI_y (dots) (upper panels). The median value (solid line) as well as first and third quartiles (dashed lines) are indicated. Interquartile distance is depicted as a shadow area. Scatter diagram of SI_y versus total annual rainfall ($mmyr^{-1}$), along with best fitted line and 95% confidence intervals) (bottom panels). a) El Hierro A.

(A7), (b) S.C. Ten (T1), (c) L. Canteras (P14), (d) Lanz. A. (A2), (e) Horta Obs. (Az.), and (f) Funch. Obs. (M). Period 1981-2010. Daily data from AEMET and IPMA.

However, according to (Peña-Arencibia et al. 2010) the 100% of the analysed years and stations present a seasonal rainfall regime except El Hierro A. (A7) which presents a relative percentage of short wet season (SW) (see Table18). Therefore, the existence of a seasonality in the rainfall regime, in most of the analysed weather stations for the period 1981- 2010 can be accepted.

As represented above for Bermuda, the variability of the annual SI_y (dots) during the period 1981-2010 is shown in Fig.44 where the solid lines represent the median value, the dashed lines the third quartiles and a shadow area intervals the interquartile distance, and the scatter diagram of SI_y versus total annual precipitation (mmd^{-1}) along with best fitted line and 95% confidence for El Hierro A. (A7), S.C. Ten (T1), L. Canteras (P14), Lanz. A. (A2), Horta Obs. (Az.), and Funch. Obs. (M).

A pair of graphics are depicted for each weather station, on the upper panels the variability of the annual SI_y and on the bottom ones the scatter diagram of SI_y versus total annual precipitation.

The variability of the seasonality index (SI_y) during the normal period (1981-2010) is estimated by the interquartile range or difference between the first (Q_1=0.349mmd^{-1}) and third (Q_3=0.475mmd^{-1}) quartiles pictured by dashed lines in Fig.44.

At first glance results show a considerable inter-annual and spatial variability. The higher inter-annual variability in the rainfall regime is found in El Hierro A. (A7) with a range of 0.28mmd^{-1} and in S.C. Ten. (T1) and L. Canteras (P14), both with 0.22mmd^{-1}. The lower ones in Horta Obs. (Az.), Bermuda A. (BER1) and Funch. Obs. (M.) with ranges equal to and 0.118mmd^{-1}, 0.121mmd^{-1} and 0.176mmd^{-1}, respectively. Lanz. A.

(A2) presents an intermediate variability with a range of 0.20mmd^{-1}. Clear trends through this normal period are not present in any station, although an apparent descending trend seems to be suggested by graphics representing El Hierro A. (A7) and L. Canteras (P14). This decrease in SI_y means a tendency towards shorter dry and longer wetter seasons, but no a change in total annual precipitation.

The highest maximum interquartile SI_y value, 1.558, is reached in Lanz.A. (A2) in 2001 the lowest, 0.581, in BER1 in 1997. Additionally, the lowest minimum value is 0.201 given in BER1 for 2006 and the highest 0.892 in Lanz. A. (A2) for 1993. Therefore, it is suggested that in A2 there is a tendency towards longer dry and shorter wetter periods while the inverse situation is expected in Bermuda A. These results describe adequately the rainfall regimen in two areas immerse in completely different geographical and climatic environments. This index is not necessarily related to the total annual rainfall or the maximum daily rainfall amounts. For instead, Bermuda A. (BER1) is characterized by an increase of the wetter periods and a tendency towards shorter dry ones. However, results extracted from this work confirm that devastating rainfall is not common in this islands although sporadically daily maximum can reach 190 mmd^{-1}. See Fig.20 in the subsection 5.3, where the frequency of the daily rainfall intensity in Bermuda is analysed.

Similarly to BER1, Horta Obs. (Az.) presents also a relative low SI_y value followed by Funch. Obs. (M.) and in both high annual totals and daily maxima occur, mainly in Az. where daily maximum can be of 390 mmd^{-1}.

On the other hand, El Hierro A. (A7) and L. Canteras (P14) show relative high SI_y. In spite of having tendency towards shorter wetter periods, according to this analysis, in El Hierro A. (A7) heavy rainfall is observed and maximum daily rainfall can reach almost 300 mmd^{-1} in some occasions. However in P14 heavy rainfall does not occur. S.C. Ten. (T1) shows an intermediate SI_y with a maximum value of (1.339), in this weather

station in very brief periods devastating rainfall can be also observed. All the rainfall measurements above cited can be found in table 15.

There are not in general common years in the observations of the maximum or minimum SI_y values. Only 2001 is the year when maximum values are observed in both S. C. Ten. (T1) and Lanz. A. (A2). Results extracted from this analysis of the variability of the SI_y, confirms ones based on the frequency of dry periods in the studied area which can be found in the subsections 5.2.1. and 5.2.2. (See Table 6).

The relationship between the seasonality index (SI_y) and the annual accumulated rainfall during the normal period (1981-2010) is depicted in Fig.44.

Among all the analysed weather stations, the determination coefficient (R^2) values are lower than 0.3 indicating that there is not statistical significant correlation between both variables. Funch. Obs. (M) shows the highest (R^2) value (0.244) followed by Az. and T1. The lowest determination coefficient (R^2) are found for P14, A2 and A7. Bermuda A. (BER1) shows an intermediate value.

5.6. Episodes of heavy rainfall.

5.6.1. Bermuda

The maximum daily rainfall event in Bermuda during the selected period ($197 mmd^{-1}$) was recorded on June 1st 1996 (see Fig. 34c) and the second on August 31st 1982.

(http://www.ncdc.noaa.gov/gibbs/image/GOE-5/IR/1982-08-31-18).

These particular events were associated with convective elements embedded in quasi-stationary stalled fronts, based on satellite imagery. Satellite image (GOES-8) of June 1st 1996 is shown in Fig 45.

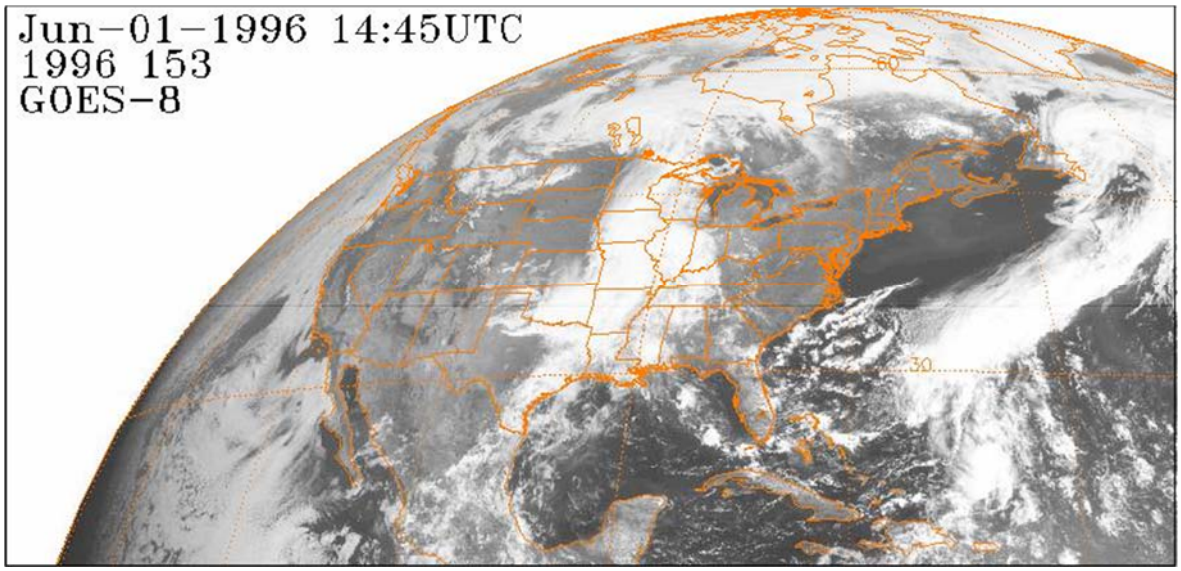

Fig.45. Satellite image (GOES-8) June 1st 1996

(http://www.ncdc.noaa.gov/gibbs/html/GOE-8/VS/1996-06-01-15)

The main rainfall records over Bermuda are represented in Table 23. All of them were associated with lots of convection except the rainfall event on October 1986 which was due to the passage of a cold front.

The highest daily rainfall associated with a tropical storm recorded at Bermuda airport during the study period occurred during the passage of Tropical Bertha on 14th July 2008, with a recorded value of 117.6 mm, on the following day 105.15 mm was recorded at S.V. (see Table 24).

(http://weather.unisys.com/hurricane/atlantic/2008H/BERTHA/track.dat)

Table 23. Records of maximum daily rainfall over Bermuda. Period 1949-2011 for BERM1 and 1974-2011 for SOM (BWS).

Main rainfall day	Max rainfall (mm)	Ind.	St.name
31/08/82	157.48	BER1	Bermuda A.
18/10/86	177.8	SOM	Somerset V.
01/06/96	197.358	BER1	Bermuda A.
	154.94	SOM	Somerset V.
01/10/07	236.22	SOM	Somerset V.

Table 24. Records of maximum daily rainfall over Bermuda associated with a tropical storm (TS Bertha). Period 1949-2011 for BER1 and 1974-2011 for SOM (BWS).

Main rainfall day	Max rainfall (mm)	Ind.	St.name
14/07/08	117.6	BER1	Bermuda A.
	8.89	SOM	Somerset V.
15/07/08	105.15	SOM	Somerset V.

The normal frequency occurrence of total number of major hurricanes (category 3 or higher on the Saffir-Simpson scale) in the North Atlantic Ocean varied from 0 to 6 over the last three decades (Molinari & Mestas-Nuñez 2003, Elsner et al. 2004).These authors have argued an increase in the number of major hurricanes occurring in the North Atlantic each year since 1995 (end of a positive NAO period) (Bates 2007).

The unusual occurrence of three tropical cyclones in the last two years affecting Bermuda is an interesting issue to further investigation about the atmospheric dynamic in this area and its relationships with atmospheric modes which clearly influence the long-term variability in rainfall or wind patterns. (Mark Guishard 2015, personal communication).

1. Tropical Storm Gabrielle (10-11th September 2013)

(*http://weather.unisys.com/hurricane/atlantic/2013H/GABRIELLE/track.dat)*

2. Hurricane Cristobal 25-28th August 2014.

(*http://weather.unisys.com/hurricane/atlantic/2014/CRISTOBAL/track.dat)*

3. Hurricane Edouard's on 15-17th September 2014.

(*http://weather.unisys.com/hurricane/atlantic/2014/EDOUARD/track.dat)*

4. Hurricane Fay (Cat.1) on 11-12th October 2014.

(*http://weather.unisys.com/hurricane/atlantic/2014/FAY/track.dat)*

5. Hurricane Gonzalo (17-18th October 2014) with easterly winds and heavy rain

(*http://weather.unisys.com/hurricane/atlantic/2014/GONZALO/track.dat)*

A detailed list of the tropical systems that have affected Bermuda during de period 1895 to 2014 including year, month and days affecting the islands, tropical system name and classification (hurricane (HR.) tropical storm (TS), subtropical storm (SS) and category (Cat.) can be found in Annexe I (Table K).

As above mentioned tropical storms in Bermuda are not commonly associated with heavy rain, an exception is the hurricane Joaquín which affected Bermuda between 4th -5th October 2015 with disruptive weather and a notable impact in terms of rainfall. However, rainfall for this month was just below the average. Rainfall totals can be found in the monthly tables at *http://weather.bm/climate.asp*

Concerning the rainfall process associated with tropical cyclones in Bermuda, there is a high degree of variability. It is not possible extracting any conclusion taking into account a single point, thus through the analysis of observed record, it would be difficult to demonstrate any significant trend (personal communication P. E. Roundy, 2015).

5.6.2. Canaries

For Canaries, daily data from all the available weather stations for the period 1957-2010 were considered. The thresholds for adverse phenomena in force in the Autonomous Community of the Canary Islands are in Table 25 including watchings or alerts (watch.) and warnings (warn.) levels 1 and 2 in case of rainfall accumulated in 12h (in mm) for the provinces of Las Palmas (LP) and Tenerife (TF). An alert means that the weather conditions are favourable for extreme adverse phenomenon to occur. A warning requires immediate action. That the occurrence of extreme weather event is imminent, occurring or may begin at any time.

Table 25. Thresholds for adverse phenomena in case of rainfall accumulated in 12h (in mm) in the Autonomous Community of the Canary Islands. Provinces of Las Palmas (LP) and Tenerife (TF).Watch. (Watching) and Warn. (Warning) Level 1 and 2. AEMET 2015.

Province	Watch.	Warn. Level 1	Warn. Level 2
LP	40	80	120
TF	60	100	180

On 24th February 1988, 590 mmd^{-1} was accumulated in San Andres (El Hierro) which represents the maximum daily rainfall during 24 hours in Canaries (see Table 26).

The analysis from ECMWF of temperature and geopotential in 500 hPa for the 24th February 1988 at 12 UTC are shown in Fig.46.

According to other studies (Departamento de producción de AEMET & Departamento de Meteorología e Clima de IMP 2012) for the period 1971-2000, the highest values were recorded at high altitudes of La Palma whereas the lowest at coastal areas of southern Tenerife and Gran Canaria and east of Fuerteventura.

Table 26. Daily rainfall maxima affecting the Canary Islands (rainfall >360 mm/24h). Rainfall episode, main rainfall day, maximum daily rainfall (mmd^{-1}), Indicative of the weather station (Ind.), Station Name (St.Name) and Elevation (Elev. (m)). Period 1957-2010. AEMET. Period 1988-2012. AEMET.

Rainfall episode	Main rainfall day	Max rainfall (mm)	Ind.	St.name (Elev.m)
10/02/78	10/02/78	399	C106U	CALDERA TABURIENTE-TABURIENTE (La Palma) (820m)
24-27/02/88	24/02/88	590	C925I	SAN ANDRES A. (El Hierro) (1030m)
			C147C	SAUCES-ESPIGON ATRAVESADO (749m)
			C925H	SAN ANDRES A. (El Hierro) (1030m)
			C925G	SAN ANDRES B. (El Hierro) (1040m)

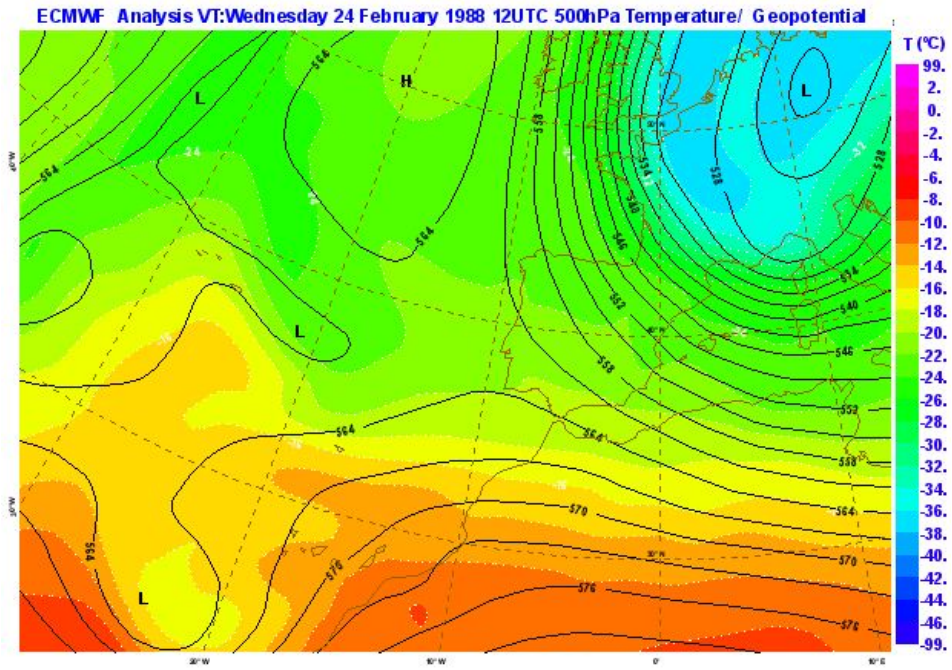

Fig.46. Temperature and geopotential in 500 hPa. 24th February 1988 at 12 UTC Analysis from ECMWF.

Table 27 resumes the most intense rainfall occurrences over the Canary Islands from daily data (rainfall between 240 and 360 mm/24h) including the date of the maximum daily rainfall, maximum daily rainfall (mmd^{-1}), Elevation (Elev. (m)), Indicative of the weather station (Ind.), Station Name (St.Name) and associated weather phenomenon in the area. (Phen.): TS (Thundersorm), SN (Snow), Hz (Haze).

Table 27. Daily rainfall maxima affecting the Canary Islands (rainfall between 240 and 360 mm/24h). Date, maximum daily rainfall (mmd-1), (Max. rainfall), Elevation (Elev. (m)), Indicative of the weather station (Ind.), Station Name (St.Name) and associated weather phenomenon in the area. (Phen.). TS (Thundersorm), SN (Snow), Hz (Haze). Period 1957-2010. AEMET.

Date	Max. rainfall (mmd^{-1})	Elev. (m)	Ind.	St.Name	Phen.
15/01/1957	250	265	C148A	SAUCES-S.ANDRES	
16/01/1957	207	265	C148A	SAUCES-S.ANDRES	
24/11/1968	297	2371	C430E	IZAÑA	
10/04/1977	290	875	C436U	ESPERANZA-C.F.	
11/04/1977	359	1435	C424E	VILAFLOR	
23/10/1987	248	600	C447R	ANAGA-CARBONERAS	
25/11/1987	309	1040	C925I	SAN ANDRES	

Date	Max. rainfall (mmd^{-1})	Elev. (m)	Ind.	St.Name	Phen.
26/11/1987	278	860	C926C	ISORA	
24/02/1988	250	860	C926C	ISORA	
27/02/1988	280	32	C929I	HIERRO/AEROPUERTO	
28/02/1988	250	553	C137F	MAZO-ROSAS	
25/10/1989	243	530	C417G	GUIA ISORA-TEJINA.COOP.AG	
24/11/1989	270	1480	C652O	SAN MATEO-LAS MESAS DE ANA LOPEZ	
04/12/1991	331	1438	C144A	SAUCES-MARCOS Y CORDERO	
05/12/1991	265	2121	C406D	CAÑADAS (BOCA TAUCE A)	
06/12/1991	295	1438	C144A	SAUCES-MARCOS Y CORDERO	
12/10/1992	254	860	C926C	ISORA	
21/10/1992	244	806	C147C	SAUCES-ESPIGON ATRAVESADO	
17/03/1993	337	2371	C430E	IZAÑA	
08/01/1999	243	1287	C454M	SANTA URSULA-MONTAÑA OVEJAS	TS,SN
12/03/2001	290	1137	C145N	GARAFIA-C.F.	
20/02/2004	249	443	C468J	GARACHICO-GENOVES.A	TS
08/11/2004	285	299	C939U	SABINOSA	TS
13/12/2004	305	30	C129E	TAZACORTE PTO. NAOS HOYAS	TS
16/01/2005	240	765	C317B	AGULO-JUEGO BOLAS	HZ,TS,SN
17/01/2005	254	15	C329F	SAN SEBASTIAN (AYUDANT.MARINA	HZ,TS,SN
27/02/2005	253	1184	C465N	TANQUE-S.JOSE DE LOS LLANOS	TS
27/01/2007	320	40	C939D	PUNTAS-CASITAS	SN
19/03/2007	312	787	C147U	GARAFIA-TRICIAS	TS,SN
23/12/2009	335	364	C145N	GARAFIA-C.F.	
01/02/2010	289	2150	C406G	CAÑADAS PARADOR	TS

An example of a cut-off low affecting the Canary Islands is the rainfall event from 5th to 8th of January 1999. Geopotential Height (Z) in m and Temperature in ºC at 500 hPa forecasted by the ECMWF on 8th of January 1999 are shown in Fig.47 and the Water Vapour channel image (METEOSAT) on 8th of January 1999 in Fig.48.

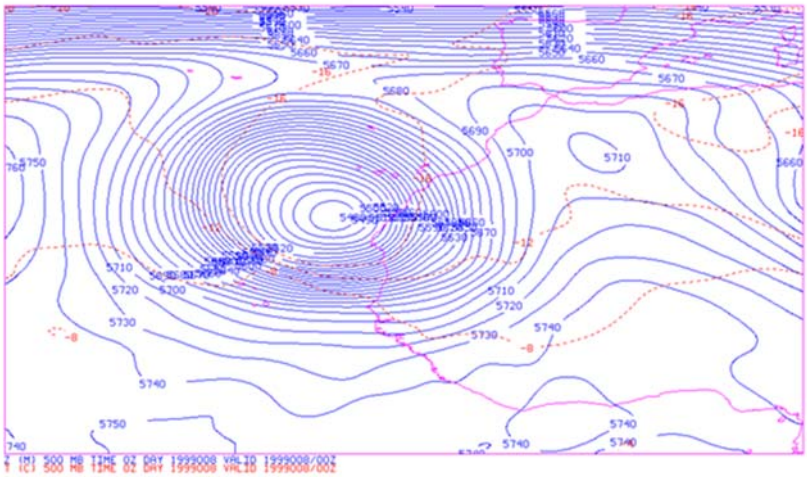

Fig. 47. Cut-off low affecting the Canary Islands. Geopotential Height (Z) in m and Temperature in ºC at 500 hPa. ECMWF (08/01/99 at 00 UTC) (AEMET).

A heavy convective rainfall event associated with a polar-subtropical cyclone affected the Canary Islands between 26th January and 4th February 2010. The previous framework was characterized by a moderate-high *El Niño*, a negative NAO (North Atlantic Oscillation) and AO (Artic Oscillation). Moreover, anomalous high precipitation water and SST (21-22ºC) were observed. These values, far from a typical tropical one, but 1.2º C warmer than usual for this time of the year for this area.

The synoptic configuration can be described as the presence of a system of high pressure at high-latitude allowing an intense cyclonic activity at low latitudes. Also, a low developed over the Atlantic Ocean as a cut-off low and a low-pressure system in the tropical or subtropical latitudes. This system had both tropical and extratropical cyclones characteristics. On 26th January 2010 the system was characterized as an extratropical cyclone, between the 30th and the 31st January experienced an extratropical-subtropical transition and on 1st February was defined as a subtropical /hybrid cyclone (Carretero et al. 2011). In particular the situation of heavy rainfall observed in early February, and more specifically between 1st and 3rd of 2010 referred to in table can be found in (Martín2010). (*http://sureste.inm.es/stapwww/fijos/casos_estudio/canaria10/indexpdf.html*)

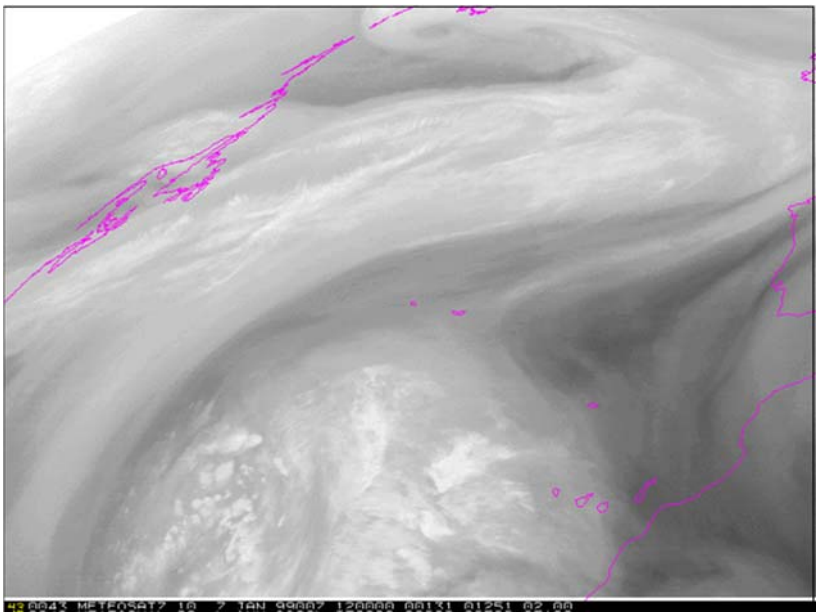

Fig.48. Cut-off low affecting the Canary Islands. (Water Vapour channel image) METEOSAT (07/01/99 AT12 UTC) (AEMET).

5.6.3. Madeira and Azores

In Horta Obs. (Az.) the maxima daily rainfall for the normal period 1981-2010 was recorded on 7th February 1995 (390 mmd^{-1}). Other records greater than 100mmd^{-1} were 206 mmd^{-1} on 1st November 1996, 142 mmd^{-1} on 24th January 2007, 128 mmd^{-1} on 7th October 1993 and 125 mmd^{-1}on 13th September 2007.

In Funch. Obs. (M), the maxima daily rainfall for this normal period was observed on 26th November 2010 (158 mmd^{-1}) followed by 119 mmd^{-1} recorded on 2nd February 2010 and 111mmd^{-1} observed on 8th April 2008.

From 2nd to 20th February 2010 the absolute rainfall records were higher than the daily records since 1949. The accumulated rainfall produced terrible floods on the 20th of February causing the loss of dozens of human lives and significant socio-economical losses (Pires et al. 2010, Miranda, 2010).

(*https://www.researchgate.net/publication/252364873_The_20_February_2010_Madeira_flash_flood).*

In Madeira as in Canaries due to the proximity of both archipelagos, as above mentioned, climate framework, the year 2010 was favourable to heavy rainfall occurrences. The winter of 2009/2010 in Madeira Island was characterized by several episodes of very intense precipitation (especially in December 2009 and February 2010)

Results extracted from this analysis during the normal period 1981- 2010 also point out the daily record of $111mmd^{-1}$ observed on 8th April 2008.

Another heavy rainfall episode in Madeira was reported on 5th November 2012, large-scale environment associated with this situation was characterized by the presence of extratropical cyclones near the island (Couto et al. 2013, Fragoso 2013, Teixeira 2014). *(https://www.researchgate.net/publication/262013258_FLASH_FLOOD_IN_MADEIRA_ISLAND_IN_AUTUMN_2012)*

The accumulated rainfall observed in the episodes associated with heavy rainfall in the Macaronesia area points out the prominent role of orography in the intensification of precipitation over the islands. The state of the terrain, due to accumulated precipitation in days and weeks before an episode of torrential rainfall is a crucial factor in the occurrence of flash floods.

5.7. Wavelet analysis

5.7.1. Discrete Wavelet Transform (DWT) applied to monthly accumulated rainfall in Bermuda

A Discrete Wavelet Transform (DWT) applied over the time series of Bermuda A. was used to explore the rainfall variability in order to extract information from this field at different frequencies. A signal decomposition corresponding to the anomaly monthly accumulated rainfall using the DWT is found in Fig.49.

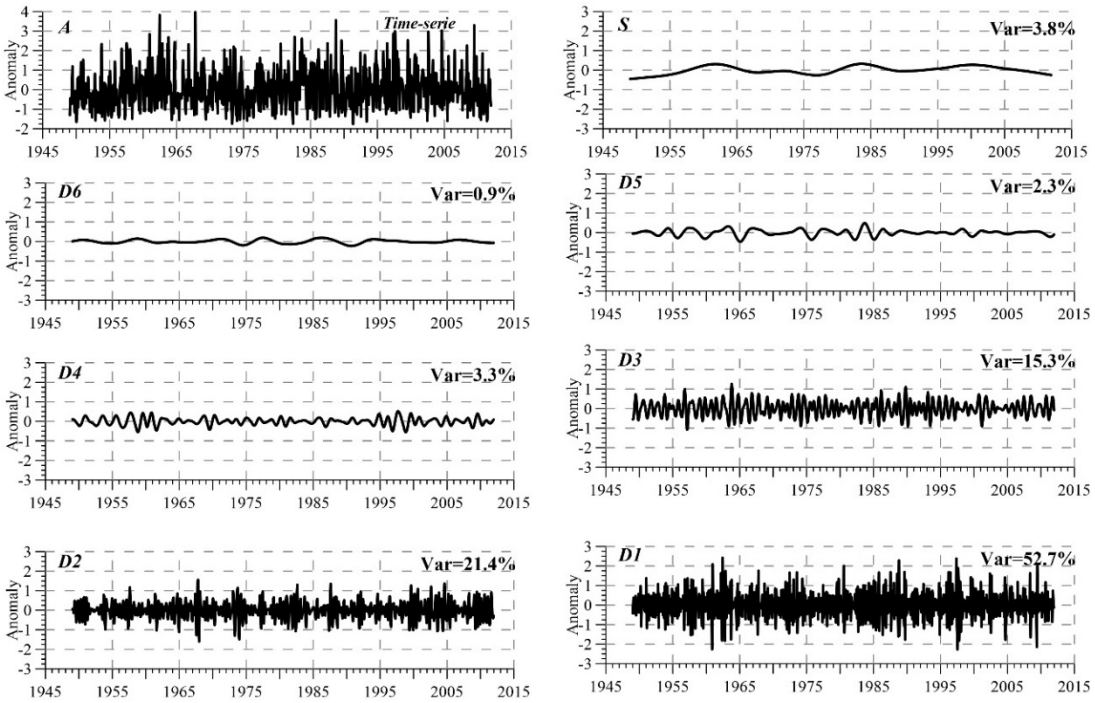

Fig.49. Wavelet decomposition (DWT) corresponding to the anomaly monthly accumulated rainfall over Bermuda A. Period 1949-2011.BWS.

At the top left panel of the figure, the original time series is represented as A. The rainfall distribution is decomposed into six details, covering long-term trends and oscillations in the signal with a period of about 63 yr. The reconstructed signals for the six intervals of time frequencies (from D1 to D6) and the smooth curve (S) were obtained using The Daubechies (Db8) type base function. The components of the decomposed time series can be divided into three groups which represent variations of the series at

different timescales. Ds indicates details processes at decreasing resolutions and S the averaged process.

In this decomposition, the first group contains the details D1, D2 and D3 with sub-annual frequencies and periods between 2 and 4 months; 4 and 8 months (seasonal) and 8 and 16 months (annual), respectively.

The second group represents the inter annual frequencies; details D4, D5 and D6 with periods between 1.3 and 2.6 years (biannual); 2.6 and 5.3 years and 5.3 and 10.6 years, respectively. QB (Quasi-Biennial) is included with a period of 1.42-3.04 yr (Segele et al. 2009) and ENSO cycles with a period of 3–6yr (Trenberth 1997). Finally, S corresponds to slow oscillations at a time scale longer than 10.6 years (decadal timescales). For each band of frequencies, the signal is reconstructed and the variance calculated as a percentage of the total variance in the original time series (Johnson 2010).

At first glance, the range variability in details from D1 to D6 is greater when the time frequency increases. The results focus on the inter-monthly variability (detail D1) as the frequency band of most contribution rainfall variance (52.7%). This filter shows marked peaks around 1961-1963, 1989, 1997 and 2009. Furthermore, change in the frequency pattern is detected close to 1985. This change in the variability is also noticeable in the filters D5, D6 and S. Irregular high-frequency spectral signals are apparent on seasonal and annual time scales (D2 and D3). Bursts of increased variability occurred repeatedly along the seasonal signal (D2). The contribution of the seasonal time scale to the variance is about 21.4% showing 1968 the highest variability. There are periods with a nearly constant periodicity, for instance between 1999 and 2006 only interrupted around 2002 and from 2009 to 2011. However, a noticeable decrease in variability is observed between 2006 and 2008. With a lower percentage (15.3%), the annual signal (represented by the detail D3) shows an almost homogenous variability

which increases slightly between 1963 and 1964. Around 1998 and 2003-2004 the variability decreases abruptly. A similar near flat oscillation is shown in QB (Quasi-Biennial) (D4) and ENSO cycles (D5). In this case, it highlights the period 1982-1983 which could be likely associated with *El Niño–La Niña* years. A lower variability is showed around 1972-1973 and 1987-1988 when another cycles of *El Niño –La Niña* are observed being 1987 a moderate and prolonged *El Niño* year.

Detail D4 reflects changes in biannual physical scales during the period 1957-1962 and another between 1996 and 2002. The filter D5 depicts a peak in the frequency in 1983. It can be distinguished as a different behaviour before 1989 with higher variability than from this year to the end of the signal, period characterized by lower peaks in the frequency. D6 shows the highest frequencies around 1977 and 1986.

The smooth signal S reflects that rainfall varies in a stable way on scales higher than 10 years. Bursts of increased variability were visible around 1961, 1983 (as in D5) and 2000. The peak around 2000 is visible in D1, D2, D3 and D4.

5.7.2. Wavelet analysis CWT (Continuous Wavelet Transform), Power spectrum of the daily rainfall in Bermuda

Quantitative identification of dominant time scales can be obtained through wavelet analysis (Fig.50) applied to the whole daily rainfall time series (Fig.50a).

The resulting wavelet spectrum or scalogram is shown in Fig.50b. Higher signal power is shown by darker areas, revealing considerable variability for periods less than one year. Lower signal in lighter areas represents higher time scales. The overall CWT power spectrum for all the scales or frequencies, that is similar to a smooth Fourier power spectrum, is obtained by averaging over time for any frequency (Fig.50c). This spectrum makes evident the predominance of the annual component. Nevertheless, whilst this is

true in general, a detailed inspection of the wavelet spectrum in the one year period band shows a remarkable intermittence of its contribution.

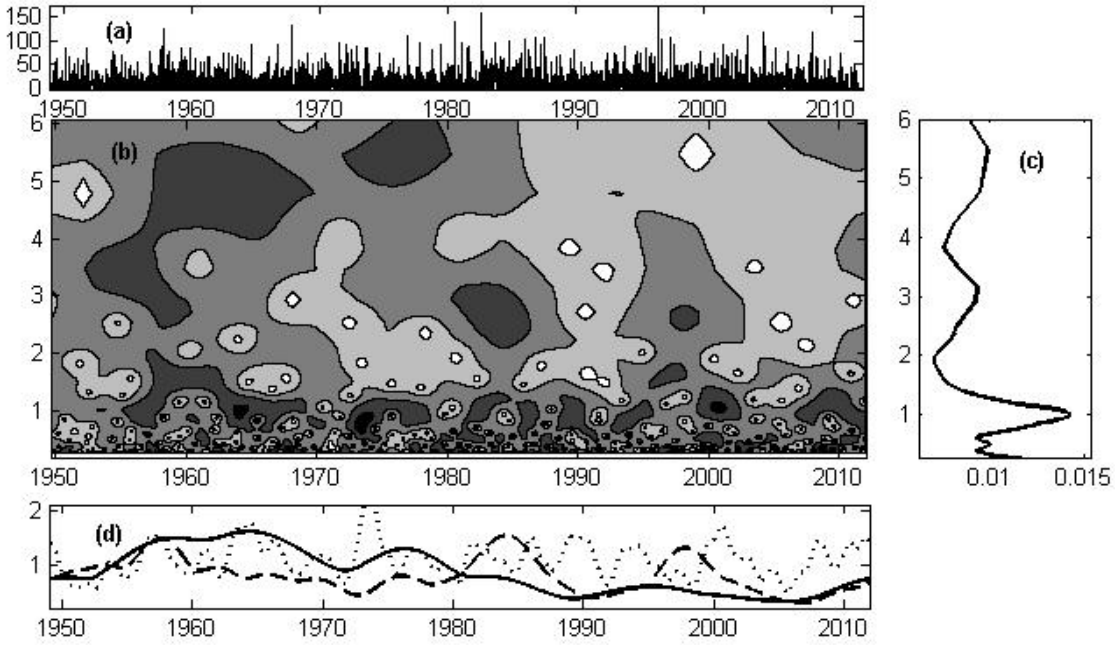

Fig.50.(a) Daily rate rainfall, (b) scalogram, (c) CWT power spectrum of the time series, and (d) instantaneous power contribution of wavelet coefficients in three period (frequency) bands: around 5 years (solid line), 3 years (dashed line) and 1 year (dotted line) (d). Bermuda A. Period 1949-2011. BWS.

This fact can be easily observed in Fig. 50d, where each curve represents the power contribution of a given frequency band to the observed process. The annual rainfall contribution (dotted line) oscillates significantly from year to year, alternating periods of weak and strong power contribution. It stands out the peak close to 1973. Something similar but not so clear happens with the semi-annual contribution, which presents a secondary peak in the low period side of the power spectrum.

Two additional notable contributions in the high period range correspond to bands around 3 and 5 years (see Fig.50d). The triennial component (dashed line) becomes relevant around 1958, 1985 and 1998. On the other hand, the quinquennial contribution (solid line) is significant from the mid-50s up to the mid-80s, gradually decreasing ever since. In light of the results derived from the wavelet spectrum, it seems reasonable to

undertake a more detailed study of the annual, intra-annual, and inter-annual variability of the rainfall regime in Bermuda.

A noteworthy phenomenon is that, in general, years with large seasonality indexes, for instance 1973, are associated with periods of prominent annual contribution in the wavelet spectrum. Whereas, periods of low contribution, such as 2006, correspond to low seasonality indexes (Fig.42a). In addition, semi-annual contribution also plays an important role in the seasonal pattern.

5.7.3. Relationship between rainfall (NRD) and NAO index in Bermuda

The relationship between the number of rainfall days (NRD) and NAO for large-scale behaviour at periods larger than 16 years is presented in Fig.51. The anomalies related to the NRD are represented by red bars and the tendency by a solid line. The NAO Index anomalies are pictured in blue bars and the tendency in a dotted line.

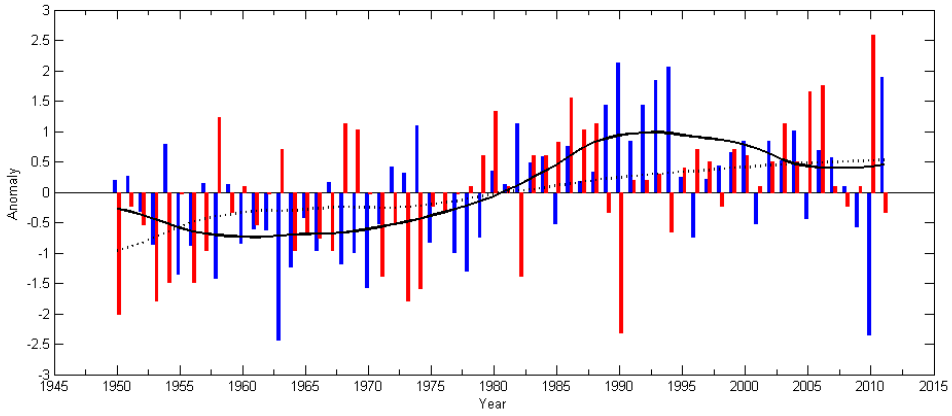

Fig.51. NAO Index anomalies (blue bars) and tendency (solid line) vs. NRD (number of rainy days) anomalies (red bars) and tendency (dotted line) during winter time (DJFM). Bermuda A. Period 1949-2011. Daily data from BWS.

Preliminary results suggest that the NRD in winter has been increasing annually and the linear trend dotted line in Fig.51 stresses it. The standardized anomaly of the winter rainfall days (NRD) (solid line) correlates negatively with the NAO index anomaly (blue

bars).The implied mechanism for this relationship is broadly consistent with a conclusion of more/less sensitivity of Bermuda rainfall events to the position and intensity of the Bermuda-Azores High in winter/summer.

Concerning the relationship between NAO and rainfall, the subtropical high experience an intensification and the Icelandic low deepens during the negative NAO phase. The resulting pressure gradient favours a decrease in the number and intensity of the storms in the subpolar region of the North Atlantic which tracks shift to the south. The moist air that moves towards the Mediterranean Sea, favours rainfall and cold temperatures to northern Europe. The eastern coast of USA experiences colder air and therefore more snow. *(http://www2.uah.es/clima/prediccion/nao.htm)*

The Pearson correlation coefficient (r) (Zou et al. 2003) has been used to measure the linear relationship between both variables. For different levels of significance and taking into account that the evaluation was made with a data set of appropriate size (69 years), results show that both variables are in general well anti-correlated. Therefore significant anti-correlation coefficient was obtained with $r = -0.408$ and p value >0.001 for the NRD. Same analysis for the accumulated rainfall was made and correlation was not found ($r = -0.129$).

The tendency of both parameters present a similar behaviour with negative anomalies values before 1980 and positive values afterward. Per to Curry & McCartney (2001), since 1989, the NAO has remained generally positive with some fluctuations. The strongest positive NAO phase period that occurred approximately between 1989 and 1995 stands out. During this period, the NRD is low with a marked negative anomaly around 1990. Similar behaviour is observed in 1974, 1982, 1998 and 2008.

However, a positive NAO phase period does not always correspond to a negative NRD anomaly. Some exceptions are the periods 1997, 1999-2000, 2002- 2004 and 2007.

On the contrary, the most negative values of NAO phase are found in 1963 and 2009-2010. During these periods a positive anomaly of NRD is observed, with the most positive value on 2009-2010. Generally for all the periods of negative NAO phases as 1985, 1996, 2001 and 2006 a positive anomaly of NRD is found. In particular, the strong negative NAO index in 1962-1963 combined with the cold air temperature anomaly was pointed out. This helps to explain the cold Eurasian winter of 1962-1963 with monthly temperature anomalies below –2º C (Hirschi & Sinha 2007).

The behaviour of both variables near the years 1900 and 2010 is similar when the study is made for the whole year. Results derived from this analysis suggest that the summer rainfall contribution is higher than the winter one, which agrees with the analysis of the seasonal variability shown in Fig.25.

A similar analysis for other meteorological parameters (standardized average temperature, Mean Sea Level Pressure (MSLP) and wind speed anomalies) during the winter time considering a period of 68 years was also made. Results reveal that temperature, MSLP appear to be closely tied to the NAO during winter time showing good correlation with r values of 0.607 and 0.463, respectively. Significant anti correlation was found for the wind speed with r= – 0.419 and $p>0.001$ for all them. These results agree with a dissertation about historical weather data from Bermuda during the period 1985-2000 (Gaurin 2008).

Wind direction is also linked to North Atlantic Oscillation (NAO), thus a positive phase of the NAO is associated with surface westerlies across the middle latitudes of the Atlantic (Hurrell & Deser 2010).

5.7.3.1. Discrete Wavelet Transform (DWT). Trend of the rainfall with NAO index for different time scale ranges

The NRD extracted from rainfall daily data series is standardized to establish whether humid or dry conditions dominate during positive or negative winter NAO phases. The components D1 to D4 represent variations of the time series at time scales from one to 16 years. Detail D1 reflects changes approximately between 1 and 2 years. Detail D2 is associated with periods between 2 and 4 years. Detail D3 corresponds to an oscillation with a period between 4 and 8 years and detail D4 reflects changes in physical scales of periods between 8 and 16 years. The decomposition in periods higher than 16 years which determinates the smooth signal is represented as a tendency in Fig.51.

The reconstructed curves by the Discrete Wavelet Transform (DWT) are shown in Fig.52. This representation evaluates the variability of the NRD compared with NAO anomalies during the winter season.

Detail D1 reflects in both NAO and NRD great variability before 1960 and in 2010. A similar feature is also visible in the signal of NRD anomalies around 1983 and 1990. For detail D2 the highest coefficients are observed approximately from 1965 to 1970 for both signals. For detail D3 the increased variability was observed from 1980 to 1995 with a peak close to 1990. There is a clear opposite behaviour in variability between NAO and NRD signals from 1970 to 1995 which is shown in detail D4 for the whole period.

A general decline of the NRD close to 1990 is noticeable in all details. This variable experiences a drop close to 1966 in the 2-4 year band (D2). During the winter time both variables are uncorrelated for all the time scales. Details D4 (8 and 16 years) with $r = -0.64$ and D1 (1- 2 years) with $r = -0.59$, show this feature clearly. For D2 (2-4 years) and D3 (4-8 years) r values are -0.32 and -0.42 respectively. However, this anti-correlation

not always is present throughout the time series, some exceptions are reflected, for example, from the beginning of the period to 1965 in detail D3.

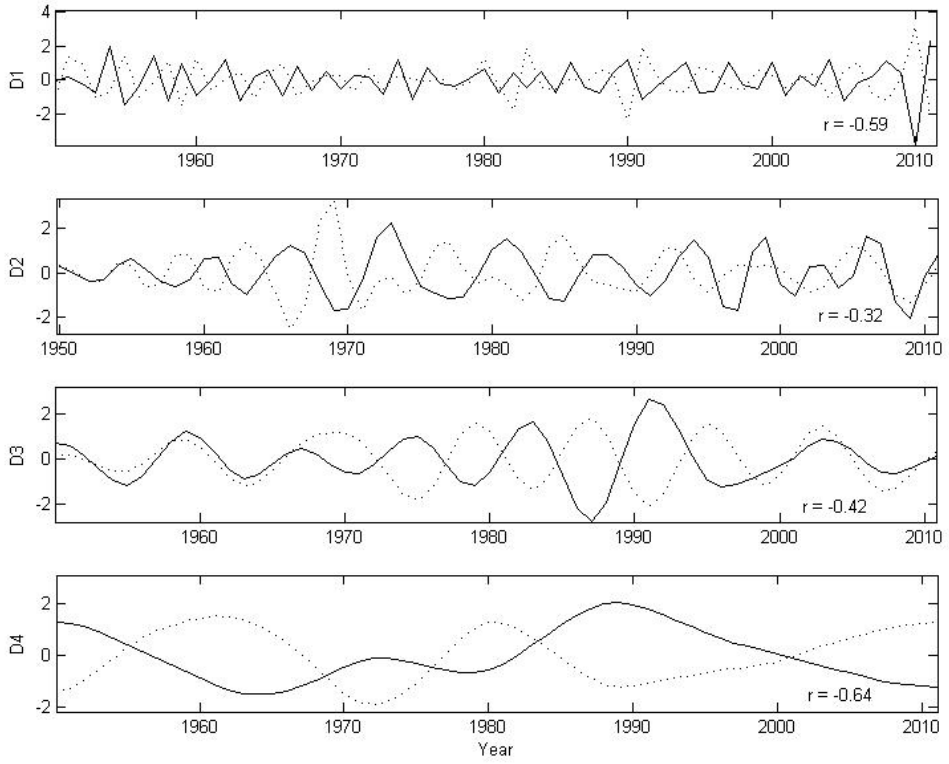

Fig.52. Discrete wavelet transform (DWT) corresponding to the variability of NRD anomalies (doted lines) compared with NAO anomalies (solid line) during winter time (DJFM). Bermuda A. Period 1949-2011. Daily data from BWS.

Same analysis made for the whole year shows that NAO and NRD are well anti-correlated in the large time scale. In this case, the best anti-correlation coefficient was obtained for D4 ($r = -0.73$) followed by D3 with $r = -0.54$. For D1 and D2 both variables are not correlated.

The results from this study may confirm other findings supporting the existence of some long-term cycles related to the NAO index. Results from section 5.5.3.1.1 (Fig. 36) show the drop in the rainfall rate and the rise of the NRD since 1990. This is coherent with the idea of the decline of the frequency of winter storms occurring in the subpolar region of the North Atlantic, since the mid-1990s (Weisse et al. 2005). Whereas, during

the strong positive state of NAO (period of 1980-1995 and 1999-2000), the Icelandic Low deepens and the Azores High is reinforced favouring strong westerlies and storms over the North Atlantic (Beersma et al. 1997, Bijl et al. 1999, Alexandersson et al. 2000, Alexander et al. 2005).

5.7.3.2. The Cross Wavelet Power (CWP) of NAO index and rainfall (annual NRD)

The Cross Wavelet Power (CWP) of the standardized NAO index and the annual rainfall rate (accumulated rainfall per NRD) are represented in Fig.53a. The CWP of NAO and the NRD during winter time (DJFM) for the period 1949-2011 are in Fig.53b. The significant regions, are in black contours, and the contour lines represent the 95% confidence level derived from (Torrence & Compo 1998) using a red-noise background spectrum. White areas do not exceed these percentages. The coefficients are reduced dividing by the scale. In the resulting wavelet spectrums, or scalograms, the signal power is stronger in darker areas, revealing the local relative phase between both time series in time frequency space and therefore considerable similarity between both.

During the winter, the strong correlation exhibited around a period of 8 years approximately from 1965 to 2000 stands out. The annual rainfall rate and NAO both show the strongest signal between 1980 and 1990 (Fig.53a). Similar behaviour occurs in this band with the NRD (Fig.53b), with marked correlation on a narrower period (1975-1985). Moreover, in the 4-6 year period significant correlation is shown close to 1995 and 2010 for the annual rainfall rate (Fig.53a) and lightly for the NRD (Fig.53b). Similarity between both patterns is also observed in the 2-4 year period band from 1949 to 1960 and 2010 for both parameters and less marked in 1965 and 2000 only for the annual rainfall rate.

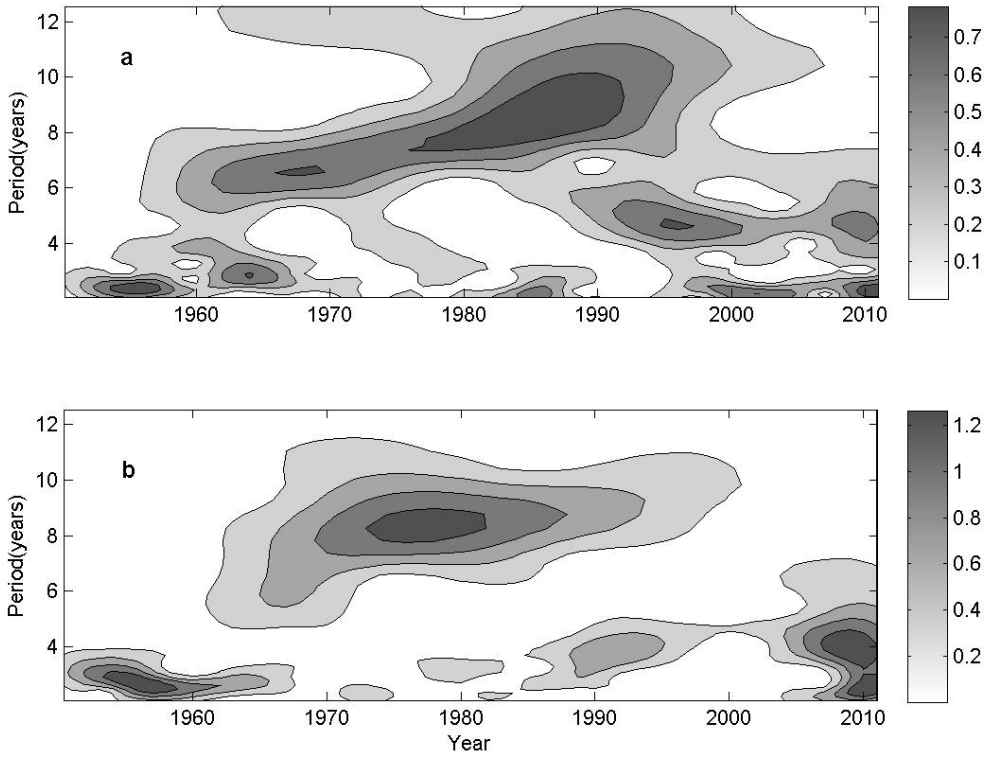

Fig.53. a) Cross Wavelet Power (CWP) of NAO and annual rainfall rate b) CWP of NAO and NRD (number of rainy days) during winter time (DJFM). Bermuda A. Period 1949-2011 Daily data from BWS.

Table 29. Coefficient of Pearson (r) for NRD (Number of annual rainy days) and annual rainfall rate versus NAO for different intervals of time frequencies (from D1 to D4) and the smooth curve (S) in Bermuda A. Period 1949-2011. Daily data from BWS.

		r		
		whole year	winter	
Details	Interval (year)	NRD vs NAO	NRD vs NAO	annual rainfall rate vs NAO
D1	1-2	-0.23	-0.59	0.02
D2	2-4	-0.13	-0.32	-0.03
D3	4-8	-0.54	-0.42	-0.50
D4	8-16	-0.73	-0.64	0.43
S	>16	-0.5	-0.40	

In general, there are clear common features in the cross wavelet analysis (CWP) of both variables between 2 and 6 years indicating large covariance at all scales in this band. Similar results (summarized in Table 29) were obtained from the DWT applied to the analysis of the correlation between NAO index and rainfall in Bermuda.

5.7.4. Wavelet spectrum and LM parameter applied to monthly rainfall and NAO index

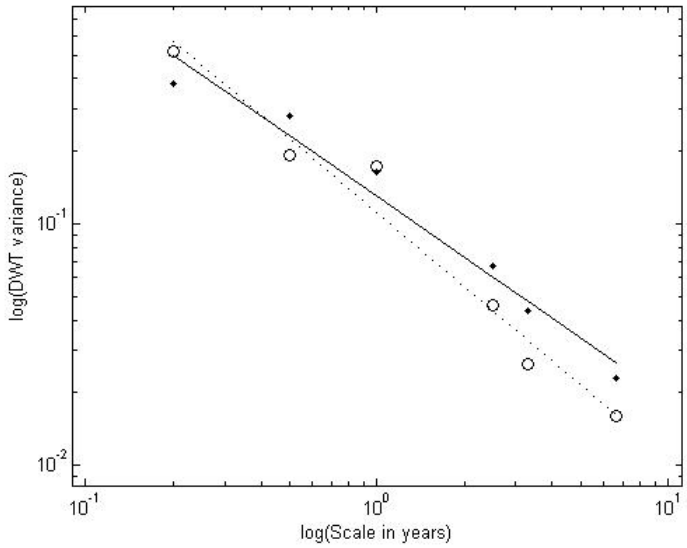

Fig.54. Discrete wavelet variance applied to monthly rainfall (circles) compared with NAO index (dots). Bermuda A. Period 1949-2011. Daily data from BWS.

The discrete wavelet variance (DWT) of monthly rainfall versus the scale in years compared with NAO is plotted on a log10–log10 plot in Fig.54. Different wavelet filters are used from D1 to D6 versus a scale of 1, 2, 4, 8 and 16 years. Circles represent the monthly rainfall and dots NAO.

The discrete wavelet variance shows linear patterns characteristic of a scaling process. The relation between wavelet variance and scale suggests Power Law behaviour which denotes scaling invariance. In logarithmic coordinates, the results are the linear fits (dotted line for monthly rainfall and a solid line for NAO).

Table 30 shows the estimates from this analysis, the slopes are calculated from the wavelet spectrum (Percival & Walden 2000). Both parameters are on a gradual declining PL trend. Values of |β| are close to 1 indicating the closeness of this process to a white noise or a random signal with a constant power spectral density higher for the monthly rainfall than for the NAO index.

Table 30. Wavelets spectrum slope (β), determination coefficient (R^2), errors variance (δ^2), p-value (p-val) and d (LM parameter) for NAO index and monthly rainfall. Bermuda A. Period 1949-2011. Daily data for BWS.

	|β|	I.C.	R^2	δ^2	p-val	d
NAO	0.84	0.21	0.97	0.05	0.0004	0.08
Rainfall	1.02	0.25	0.97	0.07	0.0004	-0.01

For the time scale near to a year, values are relatively higher and very close for both parameters showing certain seasonal component which increases the variance value. In Bermuda, the rainfall is almost homogenously distributed throughout the year. It rains nearly an average of 161.5 days per year, approximately 44%.

The estimation of the long-memory (LM) parameter of precipitation (Barbosa, 2006) may be a complementary study. However, for this analysis longer time series are required. Following the equations 5, 6 and 7 in section 4; values of the LM parameter for the NAO index and for the monthly rain are close to zero. Therefore, the data analysed cannot be described properly as a LRD (Long Range Dependence) process. However, results suggest that the NAO process implies certain long range memory whereas rain has a more random feature without a clustering trend being characterized by great unpredictability. Considerable monthly variability is observed. Thus, the timing of wetter and drier months varies from year to year. The fact that there is no month without rain during the survey period stands outs. This confirms the results achieved when the seasonal variability of rainfall was studied (see section 5.5.2).

Visualising the CWT (Continuous Wavelet Transform) power spectrum, similar to a smooth Fourier analysis, a flat spectrum is observed with the only predominance of the annual component. However, these results should be interpreted with caution since long-range analysis is complicated due to the relative short length of available time series.

5.8. Relationship between precipitation and NAO in The Canary Islands

The Canary Islands precipitation is also very sensitive to small changes in the atmospheric circulation, which has been evidenced by the presence of a significant ENSO teleconnection in the area where it had not been detected before (Gallego et al. 2001). The influence of the North Atlantic Oscillation on the rainfall in this archipelago has been studied by García-Herrera et al. 2001 and García et al. 2003. In addition, the rainy season on Canary Islands ranges from November to March when the NAO is usually most pronounced. Furthermore, the precipitation is enhanced during NAO negative years. Therefore, a negative correlation between NAO and the rainfall in this region has been found. Moreover, the NAO influence depends on the disturbance type (García Herrera, 2001).

However, there is little dependence of the rainfall over Canaries and this mode of mid-latitude atmospheric variation. The main factors that influence the relationship between rainfall and NAO are the effect of Atlantic lows which are relatively shallow disturbances when comparing with other in this subtropical region and thus poorly related to extreme precipitation and the predominant influence during the winter time. In the Canary islands winter is the rainy season , although most extreme rainfall events are associated with lots of convection which affect the archipelago mainly in autumn and spring, seasons when such relationship is not found (García-Herrera,2003).

5.9. Analysis of the complexity: Kolmogorov and Permutation Entropy

In previous section (5.2.) the scale parameters β in the case of a PL or λ when analysing a Poisson process were calculated for the analysis of the duration of consecutive dry events between rainfall events. These parameters provided a certain characterization of different areas within the studied archipelagos (Bermuda, Azores, Madeira and Canaries) related to their geographical features as elevation, geographical location and orientation which affect the distinctive rainfall pattern and climate conditions of each area. This analysis can be completed considering methods for analysing the complexity of the studied rainfall time series. One of this algorithms known as Kolmogorov complexity (KC), measures the degree of complexity of a certain sample (section 4.1.2.4.) which is a useful framework to characterize spatial-temporal patterns in non-linear systems (Kilby et al. 2014). As was explained in the methodology section, KC method estimates the degree of randomness in a time series (Lempel & Ziv 1976).

The KC method considers only strings which are composed of zeros and ones and the corresponding complexity measure is obtained by normalization. However a distinction between time series with different amplitude variations is not provided.

In order to better quantify the degree of complexity in the studied rainfall time series the Permutation Entropy method has been also used. The Kolmogorov (KV) and Permutation Entropy (PE) coefficients, for Bermuda (BER1), Funch. Obs. (M), Horta Obs. (Az.) and 18 weather stations within the Canary Islands are given in table 31 from lower to greater values.

Surrogate time series were generated and when the corresponding statistical values like means and standard deviations for them were calculated, a high correlation between both coefficients (KV and PE) and with the scale parameters (β in the case of a

PL or λ for a Poisson process) when analysing the duration of dry periods between rainfall events was found. The ranking of both complexity coefficients is very similar.

Results from the table 31 provide greater values in the case of Bermuda A. (BER1) and Horta Obs. (Az.) indicating a higher degree of randomness. The lower values, indicate less one and a greater clustering of the data in general when rainfall events occurrence.

Table 31. Acronyms for the selected weather stations, St. Name (station name), Elev. (station elevation in m), Loc. (location), Kolmogorov (KV) and Permutation Entropy (PE) coefficients, for Bermuda (BER1), Funch. Obs. (M), Horta Obs. (Az.) and 18 weather stations within the Canary Islands from lower to greater values. Period 1981-2011. Daily data from BWS, AEMET and IPMA.

St.Name	**Elev.(m)**	**Acron.**	**KV**	**St.Name**	**Elev.(m)**	**Acron.**	**PE**
S. M. Abona	642	T12	0.229	S. M. Abona	642	T12	0.545
Mogán B A.	715	P5	0.331	Mogán B A.	715	P5	0.815
Ten. S. A.	64	A5	0.365	Ten. S. A.	64	A5	0.838
Ll. Arid. B	274	T13	0.395	Ll. Arid. B	274	T13	0.978
Fuenc. Cal.	410	T14	0.410	Fuenc. Cal.	410	T14	0.997
El Hierro A.	32	A7	0.431	El Hierro A.	32	A7	1.082
L. Canteras	15	P14	0.467	L. Canteras	15	P14	1.107
Izaña	2371	T5	0.476	Izaña	2371	T5	1.162
Lanz. A.	14	A2	0.523	Lanz. A.	14	A2	1.250
G. Can. A.	24	A1	0.532	G. Can. A.	24	A1	1.284
Arucas Bañ.	50	P11	0.569	Arucas Bañ.	50	P11	1.325
S.J. Rambla	106	T2	0.573	Telde - LL.	150	P16	1.403
Telde - LL.	150	P16	0.577	S.J. Rambla	106	T2	1.414
Valseq. G.R.	540	P12	0.593	Valseq. G.R.	540	P12	1.506
Sabinosa	299	T15	0.600	Sabinosa	299	T15	1.527
S.C. Ten.	35	T1	0.628	S.C. Ten.	35	T1	1.594
Teror Dom.	630	P2	0.632	Teror Dom.	630	P2	1.599
Moya Font. C.	950	P13	0.636	Funch. Obs	58	M	1.67
Funch. Obs	58	M	0.653	Moya Font. C.	950	P13	1.672
Horta Obs	45	Az	0.918	Berm. A.	7	BERM1	2.577
Berm. A.	7	BERM1	0.976	Horta Obs	45	Az	2.886

There is a clear evidence that the rainfall process in Madeira (Funch. Obs. (M) and mainly in the Canary Islands is a more complex phenomenon than in Bermuda (BER1) and Azores (Horta Obs. (Az.)). Probably due to the combination of the influence of the Saharan desert, the Azores High, the Atlantic lows and the subtropical situations that from time to time reach this area. This peculiarity is a result of the environmental diversity (bigger area and higher elevations) and the proximity to the African continent.

In an attempt to provide an objective classification of the weather stations studied in this work under a mathematical point of view with the aim to identify similar behaviour among them, a principal components analysis based on the scale parameters used for the analysis of the duration of consecutive dry events between rainfall events together with the Kolmogorov (KV) and Permutation Entropy (PE) coefficients was made, the results are found in Fig.55.

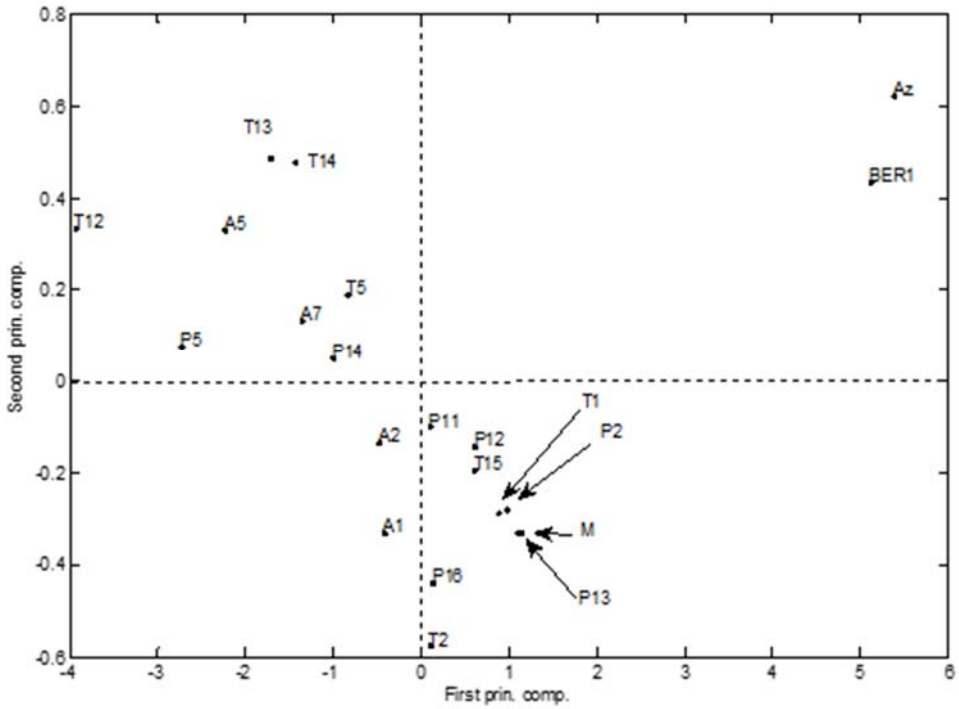

Fig. 55. Principal components analysis based on the scale parameters used for the analysis of the duration of consecutive dry events between rainfall events together with the Kolmogorov (KV) and Permutation Entropy (PE) coefficients. Period 1981-2011. Daily data from BWS, AEMET and IPMA.

This analysis provides two main components which represent the 97% and 2.5% of the variance. The statistic results are not shown since the interest of this study is only related to the classification of the studied variables. The values of these components and the associated weather stations named by its acronyms are represented.

In agreement with the results achieved when the frequency of dry period or the seasonal variability were analysed; the first component differentiates clearly Bermuda A. (BER1) and Horta Obs. (Az.). Funch. Obs. (M) together with the most of the weather stations located at northern medium elevations (Teror Dom. (P2), Valsequillo G.R. (P12), Moya Font. C. (P13)), or eastern medium ones Telde-LL. (P16), in northern windward sectors (Arucas Bañ. (P11) and S.J. Rambla (T2)) or more western locations (Sabinosa (T15)) belong to the same group. The second component separates G.Can. A (A1) and Lanz. A. (A2) with an eastern position in the Canary archipelago and in eastern coastal areas from those in low levels (L. Canteras (P14), El Hierro A. (A7)), leeward areas (Ll. Arid. B. (T13), Fuenc. Cal. (T14), S.M. Abona (T12), Mogán B. A. (P5) and Ten. S. A. (A5)) or at highest altitudes (Izaña (T5)).

6. Conclusions

6. Conclusions

- The analysis of the rainfall regime for the different archipelagos (Bermuda, Canaries, Madeira and Azores) located in the North Atlantic (subtropical) Ocean has been presented in this study around the last fifty years with emphasis in the climatic normal period 1981-2010 in order to gain a better understanding of the climate of this region.

- Non-linear models provide an adequate framework to study the rainfall variability in this region. The time passed between rain events is random and follows a negative exponential distribution, which suggests a Poissonian or random behaviour in Bermuda and Azores. Dry periods are not uniformly distributed reaching approximately a month in Bermuda. Rainfall is dispersed throughout the year where very short dry periods are observed. Therefore, the statistical probability of an increase in the number of dry spells between rain events for a given year is low.

- Some concrete patterns in terms of time ranges have been detected in Bermuda where the rainfall underlies different subjacent mechanisms which are based on the time elapsed between rain events. When less than 13 consecutive dry days are observed, the rainfall distribution follows a non-memory behaviour, indicating certain unpredictability. In addition, the occurrence of nearly 13 to 22 dry days between rainfall events indicates the break of the non-memory state and the probability of observing dry days increases when having these numbers of dry spells as well as longer durations of dry periods.

- In Canaries and Madeira these results reveal the presence of a Power Law relationship between the frequency of occurrence of dry spells and their durations. The duration of dry periods in Canaries can reach about 5 months. The northern and central sectors as well as the medium altitudes of these islands experience longer rain events when compared to those located in the southern and eastern ones. Furthermore, the occurrence of rainfall events increases from east to west. In these cases the absence of

some statistics could be inferred due to the presence of long upper tails at the end of these rainfall distributions. This behaviour responds to arid or semi-arid areas. The high probability of observing a significant number of dry days could have major social and economic consequences.

- This analysis shows that rainfall intensity in Bermuda does not follow a uniform behaviour, but its pattern changes according to time ranges and has a non-linear nature.

Moreover, rainfall intensity exhibits a high degree of randomness which denotes a high uncertainty. Summing it up, this analysis suggests that rainfall intensity trend in Bermuda is scale free, approaching a PL as well as the existence of possible transition phases and critical phenomena.

- The temporal scaling properties as well as the spatial variability of rainfall events has been also investigated for the Canary Islands. Analysis of rainfall events over these islands exhibits distributions in time that obey Power Laws. In particular, long dry periods between rainfall occurrences are observed over the study area. Scaling characteristics from the analysed records are evidence of fractal behaviour with different patterns of time clustering in the examined parameters, which are directly linked with scale-invariant processes. These results shed light upon the rainfall regime over these islands, characterised by long periods with widespread and light or moderate rainfall occurrences but occasional short episodes of torrential and localised ones. It highlights that rainfall over the Canary Islands has statistically the same irregular behaviour in terms of temporal distribution independent from the temporal scale of measurement. Comparison, of rainfall fractal characteristics from weather stations, reveals that geographical features of the selected stations like the location, orientation and elevation are crucial factors. Sites located in the northern and higher sectors of the islands have, in general, a larger fractal dimension than those in southern, eastern or flatter ones, which respond to more arid

properties. Locations affected by the cloud layer show larger fractal dimension values than those situated below and above. Furthermore, the fractal dimension increases in the archipelago from east to west.

- The rainfall occurrences in Bermuda are almost uniformly distributed throughout the year with a wetter period during the summer. The annual average rainfall pattern presents an absolute maximum around October and secondary peaks in June and January, as well as a minimum in spring. The higher monthly accumulations are mainly due to the thunderstorm activity in late summer caused by the moist unstable maritime tropical air, but not usually associated directly with tropical systems. The contribution of tropical cyclones to average annual rainfall accumulation is sporadic and it may be deemed as insignificant when compared to the contributions from frontal or convective precipitation.

On the contrary, for the rest of the archipelagos which have been the motivation for this work, the rainy season generally starts in October when the centres of high pressure move northward allowing some perturbations to reach the area. The permanent north-easterly surface flow associated with dry weather is the main feature during the summer, occurring from mid-May to the beginning of October. For Canaries the greatest monthly averages of daily rainfall are observed from November to March. In Madeira and Azores the maximum is detected in December. The lowest values are found from June to August for them all. In Azores it rains like in Bermuda throughout the year, only July can be considered a dry month. The high presence of a southerly or south-westerly surface circulation during the summer is the main generator of precipitation in Bermuda, when the Bermuda-Azores High extends westward. Southerly and easterly wind direction seems to be the most common when frontal rain and the westerlies when the convective rain due to thunderstorms is present. For the archipelagos within the Macaronesia referred to in this study, the westerly surface flow associated with the Atlantic lows causes the

heaviest rainfall. However rainfall of less intensity can be also present with trade winds. For Canaries and Madeira, northerly wind direction is the most frequent when frontal rainfall. South-westerlies, westerlies and north-westerlies affect these archipelagos when convective rainfall. Thunderstorms are mainly observed during the autumn or winter due to the passage of Atlantic lows or cut-off close to the islands. In Azores like Bermuda, easterlies are more common when frontal rainfall and westerlies when it is convective.

- When concerning the inter-annual variability, the main result extracted from Bermuda is that the annual number of rainfall days have increased during the period 1993 to 2011 while the rainfall rate has dropped.

- Spatial variability in the annual rainfall pattern has been found between archipelagos due to their different geographical location and orientation. The western islands in the Canary archipelago show similar behaviour and in at a lesser degree Madeira. They share certain features with Bermuda and Horta like the drop of rainfall accumulations close to 1990 that could be caused by changes in the atmospheric circulation. Nevertheless, the relationships between rainfall and climate modes as NAO or El Niño have not been studied enough in this work and deserve more investigation. The evaluation of the state climate mode as the ENSO or NAO and its trends entails a complex analysis including zonal wind anomaly, absolute SST (Sea Surface Temperature), nature of wind stress patterns, forcing, cooling effects, etc.… Expression of intra-seasonal variability might not necessarily reflect a real difference between past, present or future ENSO or NAO states. Moreover, comparison between past climate modes states do not always reflect a future trend (personal communication P. E. Roundy, 2015).

- Seasonal variability is generally found in the analysed region, since rainfall is not uniformly distributed throughout the year.

Nevertheless, in Bermuda this average annual pattern encloses a large variability, thus resulting in the timing of wetter and drier months which varies from year to year. The average index of seasonality indicates that the average annual rainfall regime in this archipelago belongs to a rather seasonal with a short drier season. A considerable monthly variability is observed. As a consequence, rainfall regime replicability has remained significantly low and practically unchanged during the studied period. Furthermore, it highlights that there is no month without rain in the survey period. Both, the annual seasonality index and total annual rainfall show considerable inter-annual variability. Furthermore, a lack of statistically significant correlation between seasonality index and annual rainfall has been confirmed.

- The rainfall regime in the Canary Islands is in general seasonal or has a markedly seasonal with a long drier season. However, Madeira shows generally a seasonal rainfall regime. Finally the rainfall regime in Azores is characterized as equable but with a definite wetter season. According to the index of rainfall replicability, contrary to the results obtained for Bermuda, in the selected stations within the Macaronesia there is a rather normal gradual transition from the rainiest to the driest months. The timing of the wetter and drier months is not too variable from year to year. There is a considerable homogeneity between individual annual rainfall patterns, which is equivalent to a high replicability and seasonality of the precipitation regime.

- The analysis of the interannual variability of the seasonality index during the normal period 1981-2010 shows a considerable variability for these archipelagos. The higher variability in the rainfall regime is found at The Canary Islands. The the lower one in Azores, Bermuda and Madeira. Clear trends through this normal period are not present in any station.

CONCLUSSIONS

In the Lanzarote airport there is a tendency towards longer dry and shorter wetter periods while the inverse situation is expected in Bermuda A. These results describe adequately the rainfall regime in these two areas immerse in different geographical and climatic environments.

- Seasonal analysis has allowed to bringing to light changes in the annual variability throughout the different north Atlantic archipelagos within the subtropical region. Additionally, the common length of the samples is considered very short to propose future rainfall trends. According to the trend of the distribution of accumulation daily rainfall for the five-year period, western weather stations in the Canary Islands share certain features with Bermuda, Madeira and Azores like the drop around the year 1990 caused by changes in the atmospheric circulation.

- The Discrete Wavelet Transform has been proven to be a suitable tool for the analysis of rainfall over Bermuda in order to understand their temporal variability. Results from the Discrete Wavelet Transform (DWT) corresponding to the monthly rainfall show that the components of highest frequencies are dominant. The Continuous Wavelet Transform (CWT) reveals considerable variability for the annual cycle. A noteworthy phenomenon is that, in general, years with large seasonality indexes are associated to periods of prominent annual contribution in wavelet spectrum.

- The Analysis of the relationship between the number of rainfall days and NAO index in Bermuda shows that both are negatively correlated. The implied mechanism for this relationship is broadly consistent with a conclusion of more/less sensitivity of Bermuda rainfall events to the position and intensity of the Bermuda-Azores High in winter/summer. The tendency of both parameters present a similar behaviour with negative anomalies values before 1980 and positive values afterward.

- The results from the evaluation of the variability of the number of rainfall days compared with NAO by the Discrete Wavelet Transform during the winter season could confirm other findings supporting the existence of some long-term cycles related to the NAO index. During the strongest positive NAO phase period that occurred approximately between 1989 and 1995 winter storms were enhanced in the subpolar region of the North Atlantic and appears to be reduced since the mid-1990s. The number of rainfall days in Bermuda is low with a marked negative anomaly around 1990, whereas the rainfall rate increases.

- The Cross Wavelet Power (CWP) of NAO index and annual number of rainfall days denotes clear common features of both variables between 2 and 6 years indicating large covariance at all scales in this band.

- Wavelet spectrum applied to monthly rainfall and NAO index shows linear patterns characteristic of a scaling process. A closeness of these processes to a white noise or a random signal with a constant power spectral density is found being higher for the monthly rainfall than for the NAO index. For the time scale near to a year, values are relatively higher and very close for both parameters showing certain seasonal component which increases the variance value. Long Range Dependence process has not been detected. However, results suggest that the NAO process implies certain long range memory whereas rain has a more random feature without a clustering trend being characterized by great unpredictability. The Continuous Wavelet Transform power spectrum reveals predominance of the annual component.

- The analysis of the complexity indicates a higher degree of randomness for Bermuda and Azores. There is a clear evidence that rainfall process in Madeira and mainly in the Canary Islands is a much more complex. The particular geographical location, the geological origin and the abrupt relief explain the variety of views in these

islands that go from mountains, volcanoes, snowy slopes, exuberant vegetation and forests towards desert areas, sandy beaches, dunes, rocky bays, salt marshes, cacti and xerophytic plants. Different synoptic configurations can affect the islands apart from the local effects that produce rainfall over Canaries. The proximity to the African continent makes this region in general drier than the neighbouring archipelagos within this subtropical area in the North Atlantic Ocean. This variability is also a response to a complex climatology and rainfall pattern which changes in function of the orientation and topography that causes rainfall occurrence. Results show that the rain process in the Canary Islands presents a high clustering and irregular pattern on short timescales and a more scattered structure for long ones.

- Rainfall events are less frequent than in the rest of the islands located in this subtropical region the, but produced by quite diverse factors. The different atmospheric situations that affect this area together with the orographic effects makes that the rainfall regime was quite different throughout the Canary archipelago and even in locations separate by few kilometres.

- It was also observed that the rainfall process shows an important spatial variability, which increases with altitude, as well as towards northern latitudes and western longitudes. These feature is also found in Madeira and Azores. The key role played by the topographic and orographic complexity of these islands is noteworthy.

- The combination of all these factors make the rainfall pattern in general difficult to describe and generally the attempt to homogenize rainfall time series fails. Furthermore, the accuracy of the numerical models in order to forecast rainfall episodes in this region is not precise enough to identify the heavy rainfall that in some occasions is underestimated thus this models sometimes do not reflect local effects that enhance precipitation.

- Moreover, results from the principal components analysis based on the the scale parameters used for the analysis of the duration of consecutive dry events between rainfall events together with the Kolmogorov and Permutation Entropy coefficients agree with those achieved when the frequency of dry period or the seasonal variability were studied.

Summarising the conclusions:

1. In Bermuda and Azores the distribution of the dry periods between rainfall events follows a random behavior. In Canaries and Madeira it obeys a power law which means the possible occurrence of extreme events.

2. The daily accumulated rainfall throughout the study region follows a scaling law.

3. The occurrence of rainfall events affecting Canaries has a fractal behavior with different patterns of temporal and spatial clustering.

4. The suitability of the nonlinear models to characterize the rainfall in this region has been confirmed.

5. The results from the analysis of the intrusion of dust in the Canaries give robustness to this idea.

6. The rainfall shows a seasonal nature in the Canaries and Madeira.

7. Over these islands the trade winds are predominant with frontal rain and westerlies with convective one. Over Bermuda and the Azores winds from the south and east are the most common ones when there is passage of fronts and westerlies with thunderstorms.

8. The number of rainy days in Bermuda appears to be increasing around 1995 and is well anti-correlated with the NAO index.

9. The rainfall over Bermuda and Azores has a high degree of randomness which denotes unpredictability. However in Madeira and mainly in the Canary Islands it is a more complex phenomenon.

10. Similarities between these pairs of archipelagos have been pointed out in all the results obtained in this thesis.

Finally, the results derived from this study may be useful in developing a better knowledge of the North Atlantic subtropical climate. In particular, the characterization of the dynamics of precipitation may improve the understanding of the hydrological regime in these subtropical islands, and help to define measures supporting the sustainable development of the region of study. Furthermore these findings can help to parameterize the variability of precipitation in hydrological, ecological, or other disciplines.

This thesis is the result of a joint work between Meteorological Services of Spain, Bermuda and Portugal in cooperation with the University of Las Palmas de Gran Canaria. We hope that it will encourage future inter-national and inter- regional cooperation in the field of meteorology in the subtropical North Atlantic in order to:

1. Improving the quality and delivery of services to different users, in particular emergency managers.
2. To advance in scientific research in meteorology in this region to help operational forecasting and management of water resources.

7. Future research

7. Future Research Lines

Considering that the interest to estimate changes in the probability of occurrence of rainfall extreme events has considerable impacts on society, the economy, and the environment, a future research line proposed from this study is to investigate the trend in the inter-annual and seasonal rainfall variability through an extreme analysis of daily data. Particularly, examining if the use of the POT model is a suitable framework for modelling the distribution of rainfall extreme values in this subtropical region.

8. Resumen en español

8. Resumen en español

En esta sección, se presenta un resumen en castellano de esta tesis, con especial atención en los capítulos que contienen los resultados sobre Bermudas y Canarias ya que son los archipiélagos donde se analiza en más profundidad la variable de estudio. Para obtener una información más detallada del contenido de este trabajo, el lector deberá recurrir a la versión original en inglés.

8.1. Introducción

El estudio realizado ha tenido como finalidad principal analizar el comportamiento de las series de precipitación a fin de adquirir un mayor conocimiento de la climatología de los archipiélagos de Bermudas, Canarias, Madeira y Azores. En la primera etapa del trabajo se analiza la duración de periodos secos entre eventos de lluvia en esta región del Atlántico Norte y la intensidad de la lluvia en Bermudas. En una segunda etapa se analizará el comportamiento fractal de la lluvia en Canarias. También se realizará un análisis de la variabilidad inter-anual y estacional de la precipitación sobre la zona de estudio empleando para este último un índice de estacionalidad SI (Seasonal Index).

La variabilidad en la dirección e intensidad del viento incluyendo una comparación entre lluvia de tipo convectiva y frontal también es contemplada. A continuación se estudia la evolución de la precipitación a través de las transformadas wavelet discreta (TWD), y continua (TWC). Finalmente se analiza su relación con modos climáticos que afectan a la inter-fase atmósfera-océano, tratando de establecer una relación entre el índice NAO y el número de días de anual lluvia durante el invierno. En relación a las futuras aplicaciones de los resultados previstos, destacan sus directas repercusiones socioeconómicas y medioambientales. Los resultados obtenidos podrían confirmar el empleo de este análisis para caracterizar estos fenómenos meteorológicos que en ocasiones pueden ser considerados como eventos extremos teniendo en cuenta su

impredecibilidad o incertidumbre. Estos eventos se presentan con una frecuencia relativa muy baja, motivo por el cual son considerados como eventos anómalos, raros o episódicos.

A pesar de que los archipiélagos de Bermudas y Canarias están situados a una latitud similar, unos 30ºN, y bajo la influencia del cinturón Atlántico subtropical; se ven afectados por diferentes situaciones meteorológicas. Las islas de Bermudas, altamente influenciadas por la corriente del Golfo, se encuentran con frecuencia en la trayectoria de los huracanes atlánticos. Sin embargo, las islas Canarias, al igual que Madeira y Azores, se ven afectadas directamente por los vientos alisios y el anticiclón de Azores que actúa impidiendo el paso a perturbaciones como borrascas atlánticas. Las islas Canarias, dada su situación geográfica, cercana a la costa oeste africana, en ocasiones se ven afectadas por invasiones de polvo sahariano.

Los objetivos que se persiguen en este trabajo son:

1. Descripción del comportamiento tipo duración-intensidad de los eventos de lluvia en el área de estudio.

2. Distribución temporal y cuantificación de su agrupamiento.

3. Idoneidad de los modelos no lineales para su caracterización.

4. Para el caso de Canarias, comparación con las intrusiones de polvo de origen desértico.

5. Análisis de la variabilidad espacial, estacional e interanual de la precipitación en los distintos archipiélagos que conforman esta región.

6. Estudio de la relación entre el índice NAO y los eventos de lluvia en Bermudas.

7. Determinación del grado de aleatoriedad de las series analizadas y diferenciación de zonas en función de esta variable.

Esta tesis está estructurada en siete secciones, en la primera o introducción se incluye una revisión de la literatura más relevante relacionada con estudios previos

realizados sobre la región de estudio acerca de la variable investigada. La siguiente sección presenta un marco fisiográfico y climatológico detallado de los archipiélagos de las Bermudas, las Islas Canarias, Madeira y Azores. Una descripción de los datos utilizados en el estudio se incluye en la sección 3. Los métodos de investigación como los procedimientos estadísticos utilizados se describen en la sección 4. Los principales resultados se presentan en la sección 5. Por último, las últimas secciones contienen un resumen con las principales conclusiones y una propuesta de futuras investigaciones.

8.2. Área de estudio

El área de estudio comprende los archipiélagos de Bermudas, Madeira, Canarias, y Azores ubicados en el Océano Atlántico Norte subtropical.

Bermudas es un pequeño archipiélago constituido por unas 150 islas, 6 de las cuales se consideran principales. La formación de las islas es de origen volcánico y a la vez presentan formaciones coralinas. Se caracteriza por un clima marítimo con veranos cálidos y húmedos e inviernos relativamente más fríos y también húmedos. La estación de ciclones tropicales en Bermudas se extiende desde mayo hasta noviembre. Los meses con mayor actividad son septiembre y octubre. Estas islas se localizan al norte del límite de la normal re-curvatura de los ciclones tropicales atlánticos y lejos de las trayectorias regulares de estas tormentas durante la mayor parte de la temporada de huracanes. Aunque sí se ven afectadas por vientos fuertes asociados a estas tormentas tropicales, salvo excepciones casi nunca sufren un impacto directo de huracanes. Durante el verano las islas están bajo el dominio del alta de Bermudas/Azores con una circulación débil preferentemente del sureste. A finales de marzo el alta de Bermudas empieza a migrar hacia el norte y el archipiélago queda bajo la influencia de una ligera circulación del este en niveles bajos. Cuando el alta de Bermudas bloquea la entrada de frentes fríos del norte se favorece el desarrollo de intensos sistemas de bajas presiones que desde Cuba o

Bahamas se mueven hacia el norte-nordeste pudiéndose observar en el área fuertes vientos e intensa precipitación. Tornados y trombas marinas pueden estar asociados a estas condiciones. Durante el otoño el anticiclón se debilita e inicia su migración hacia el sur favoreciendo la entrada de frentes fríos que sólo en invierno están bien definidos y seguidos de masas de aire polares frías que se pueden extender hacia los trópicos. La dirección del viento más frecuente en invierno es W/SW y la situación sinóptica se caracteriza por bajas presiones desplazándose hacia el este y pasando al sur de Nueva Escocia. Tras el paso de los frentes el viento gira a NW. El resto de las áreas incluidas en este estudio están descritas en la versión original y no se incluyen aquí debido a un general mayor conocimiento sobre ellas.

8.3. Datos

Se emplean datos diarios de precipitación para un periodo de sesenta y tres años desde 1949 a 2011 representativos del aeropuerto de Bermudas. Estos fueron comparados con los de la estación Somerset Village que representan 37 años y medio de observaciones desde 1974 hasta 2011. Para Canarias para analizar la variabilidad espacial, temporal y estacional de la precipitación, datos diarios de 38 estaciones para un periodo medio de 48 años, de enero de 1965 a diciembre de 2012, son empleados. La elección de su localización atiende a su posición geográfica, altitud y orientación; factores que contribuyen a explicar el régimen pluviométrico observado en las islas. Un listado de las mismas puede encontrarse en la tabla 4. El punto más alto analizado es Izaña con una elevación de 2371 m. La mayor parte de las estaciones consideradas están en la isla de Gran Canaria debido a su relativa posición central en el archipiélago y elevaciones intermedias. Para la comparación con otras estaciones dentro del área subtropical se emplean datos representativos del aeropuerto de Bermudas cedidos por el Centro Meteorológico de Bermudas (BWS) y Azores (Horta Observatorio) y Madeira (Funchal

Observatorio) procedentes el Centro meteorológico de Portugal. Un listado de las estaciones empleadas como fuente de datos para este trabajo también puede encontrase en las tablas incluidas en el anexo I.

Estos datos se comparan con datos de observación en superficie extraídos de METARs para algunos de los aeropuertos incluidos en la lista de referencia (tabla 4). Los siguientes aeródromos: Fuerteventura, Gran Canaria y La Palma fueron seleccionadas debido a la disponibilidad de series largas de datos y representativas de las islas. Con ellos se realiza la comparación entre el comportamiento del polvo en suspensión con procedencia desértica y la precipitación. Resultados derivados del análisis del régimen de vientos extraído de los METARs completa el estudio sobre la precipitación realizado en este trabajo. La adquisición de datos fue horaria. Los datos procedentes de G.Can. A. (A1), Lanz. A. (A) and La Palma A. (A6) se utilizaron para diferenciar entre distintos tipos de precipitación.

8.4. Metodología

Según recomendaciones de la WMO (World Meteorological Organization), 1984, para caracterizar adecuadamente el régimen de precipitación en un área específica es necesario elegir un periodo de treinta años definido como normal desde un punto de vista climatológico. Este criterio ha sido adoptado en los principales análisis realizados considerando el periodo normal 1981-2010.

Dentro del análisis matemático se emplearon tratamientos relacionados con los sistemas complejos no lineales. Entre otros se realizará un análisis de escala y fractal y se aplicarán la transformadas wavelet discreta (TWD) y continua (TWC).

8.4.1. Análisis a escala

Debido a la gran complejidad de los procesos atmosféricos, los métodos estadísticos convencionales son considerados ineficientes para describir la estructura de algunos

fenómenos como la precipitación en un amplio rango de escalas. Sin embargo, dichos procesos pueden presentar un comportamiento fractal o de escala tipo PL (Power Law) (e.g. Dickman, 2004, Mazzarella and Diodato, 2002). Es decir, que muestran propiedades estadísticas invariantes o similares respecto a un amplio rango de escalas. Los métodos de análisis utilizados para analizar las propiedades de escala están basados en la invarianza que está presente en un proceso. A través de los mismos se detecta la probabilidad de que las distribuciones tipo frecuencia-tamaño de los eventos (intensidad o duración) obedezcan a Power Laws. Este análisis ha permitido cuantificar la variabilidad de procesos como la lluvia compararla en algún caso con las intrusiones de aerosoles desérticos. Además, la detección de dichos patrones puede indicar la presencia de correlaciones de largo rango o mecanismos inusuales subyacentes como feedback loops, random network, self-organisation o phase transitions. Uno de los objetivos de este estudio consiste en analizar las propiedades a escala temporal de dichos fenómenos, en particular de la precipitación.

Por otro lado se realiza un análisis fractal. La dimensión fractal proporciona información a diferentes escalas (Malamud y Turcotte, 2006). El método empleado en este estudio es conocido como método de dust Cantor y ha sido considerado por otros autores como una herramienta adecuada para análisis no lineal como el comportamiento fractal de fenómenos meteorológicos, por ejemplo la precipitación. Se trata de un algoritmo tipo box-counting en el cual el espacio de observaciones representa la longitud total de la serie y las cajas corresponden a los intervalos de tiempo. La dimensión fractal (D) permite cuantificar el agrupamiento del fenómeno de una serie temporal de escala invariante (Mazarella y Diodato, 2002). Dicho agrupamiento aumenta cuando D se aproxima a 0. Es decir, las dimensiones fractales más pequeñas corresponden a eventos dispersos en el

tiempo (Izzo et al., 2004). Si D se aproxima a 1, los eventos están uniformemente distribuidos en el tiempo. Es decir que corresponden a una distribución más uniforme.

8.4.2. Índice de estacionalidad

El índice empleado para caracterizar la precipitación ha sido sugerido por Walsh & Lawler, 1981. Estos autores proponen un índice de estacionalidad (SI) basado en las diferencias entre la precipitación mensual observada y la esperada bajo la hipótesis de precipitación uniformemente distribuida a lo largo del año. Una versión más condensada de esta clasificación, agrupación de varias subclases, ha sido empleada por Peña-Arencibia et al. (2010).

Un método alternativo para el estudio estadístico de la estacionalidad de la lluvia en series de datos está basado en el test de Chi-cuadrado (χ^2). Cuando la precipitación durante algunos meses es significantemente mayor que durante el resto del año, no se considera la uniformidad y la estacionalidad no puede ser rechazada estadísticamente. El test de χ^2 puede ser usado para comparar distribuciones empírica y teóricamente uniformes. Se considera como hipótesis nula que la precipitación está uniformemente distribuida a lo largo del año. Para cuestionar esta hipótesis con un nivel de confidencia de un 95%, el valor crítico es $\chi^2 = 18.31$. Por tanto, cuando χ^2 es mayor que dicho valor, la hipótesis nula es rechazada y se puede concluir que existen diferencias relevantes entre los valores mensuales de precipitación y la uniformidad no puede ser aceptada, por lo que se admite la estacionalidad.

8.4.3. Análisis wavelet.

La transformada wavelet es una útil herramienta para examinar la variabilidad de un proceso en un dominio tiempo-frecuencia incluyendo estructuras multi-escalares en series temporales no estacionarias (Percival & Walden 2000). En este estudio las transformadas wavelet discreta (TWD) y continua (TWC) son aplicadas para obtener la

descomposición en tiempo-frecuencia de la lluvia a partir de una serie temporal representativa del aeropuerto de Bermudas. El algoritmo empleado está basado en el comúnmente empleado Morlet Wavelet. Detalles de esta metodología pueden encontrarse en Mallat 1999 y Percival & Walden 2000.

Como metodología general del trabajo se emplearán programas como el software MATLAB (MATrix LABoratory, The MathWorks,USA) e IDL (Interactive Data Language). Para la realización de este estudio las imágenes de satélite han constituido un apoyo fundamental.

8.5. Resultados

- Los modelos no lineales proporcionan un marco adecuado para estudiar la variabilidad de las precipitaciones en esta región.

- El tiempo transcurrido entre los eventos de lluvia es aleatorio y sigue una distribución exponencial negativa, lo que sugiere un comportamiento tipo Poisson o aleatorio en Bermudas y Azores. En cuanto a Canarias, se observa una mayor frecuencia de periodos secos de corta duración pero existe un pequeño número de largos periodos secos de una duración cercana a cinco meses que están presentes en la cola larga de la distribución. Esto sugiere un comportamiento de tipo Power Law. En Canarias y Madeira se pone de manifiesto la presencia de una relación tipo PL entre la frecuencia de ocurrencia de periodos secos y su duración, por ejemplo, al llegar a periodos de unos 5 meses sin llover en Canarias. Este tipo de patrón en algunos casos podría revelar la posibilidad de eventos extremos o sequías.

Por otro lado, este estudio muestra que la intensidad de las precipitaciones en las Bermudas sigue un comportamiento no lineal presentando un alto grado de aleatoriedad que denota al mismo tiempo un alto grado de incertidumbre. Este análisis sugiere que la

tendencia de la intensidad de las lluvias en las Bermudas es libre de escala, acercándose a un PL, así como la existencia de posibles fases de transición y fenómenos críticos.

La lluvia que afecta a Canarias tiene un comportamiento fractal y además estadísticamente un comportamiento irregular en términos de su distribución temporal independiente de la escala de medida utilizada. De la comparación de las características fractales de la lluvia registrada en las distintas estaciones seleccionadas se deduce que las características geográficas son cruciales en la distribución de la precipitación. Localidades situadas en el norte o los sectores más elevados poseen, en general, una mayor dimensión fractal (D) que aquellas orientados al sur, este o en localidades con cotas bajas o a nivel del mar lo cual responde a propiedades más áridas. Localidades afectadas por la capa de inversión muestran valores de D mayores que aquellas situadas por debajo o sobre la misma. Además, la dimensión fractal aumenta en el archipiélago de este a oeste.

Un patrón similar ha sido encontrado en el estudio sobre precipitación realizado para Madeira (de Lima and de Lima, 2009). Sin embargo los valores absolutos de la dimensión fractal son menores en Canarias. En Madeira los valores de D son aproximadamente 0.71 en zonas orientadas al norte, cercanos a 0.75 en zonas altas centrales y entre 0.53 y 0.56 en sectores sur (de Lima and de Lima, 2009). En Canarias los valores de D son en general menores y se distribuyen en un rango entre 0.29 y 0.59. Sólo algunas estaciones situadas en vertientes norte o a altitudes mayores que 1100 m muestran una D algo más similar a Madeira. Las diferencias en las propiedades fractales de ambos archipiélagos pueden ser explicadas en base a sus características geográficas y topográficas. Las islas Canarias están más expuestas a la influencia del continente africano y menos afectadas por las bajas Atlánticas que las islas portuguesas que presentan una mayor precipitación anual.

De la comparación con el análisis fractal de las invasiones de polvo se distinguen dos patrones distintos: uno con un agrupamiento moderado de los eventos de polvo que va de 1 a 8 horas, y otro que varía entre dos días y dos meses con un alto agrupamiento el cual responde a un modelo de transporte a larga escala. Del estudio de la distribución de la duración de los eventos de polvo sobre el área de Canarias se deduce que las ocurrencias de eventos de corta duración son más probables, mientras que los eventos largos son raros los cuales pueden corresponder a eventos extremos. Algunas conclusiones generales derivadas del análisis del polvo y la lluvia sobre las islas muestran que dichos fenómenos presentan distribuciones temporales que obedecen a Power Laws (PL). Esto implica la existencia de distribuciones de frecuencia con colas largas, revelando la posibilidad de eventos extremos. En particular, largos periodos secos entre ocurrencias de lluvia son observados en el área de estudio. Además, la presencia de distribuciones tipo PL también sugiere la existencia de propiedades de escala invariantes subyaciendo fenómenos críticos. Las características de escala derivadas de los datos analizados ponen en evidencia un comportamiento fractal con diferentes patrones de agrupación temporal de los parámetros estudiados, los cuales están directamente relacionados con procesos de escala invariante. Las distribuciones tipo PL sugieren la existencia de SOC (Self Organised Criticality) lo cual se pone de manifiesto en la alta diversidad del clima, topografía o características botánicas encontradas en el archipiélago. Respecto a la comparación del análisis fractal para ambos fenómenos se observa que para periodos de tiempo entre un día y una semana, La Palma y Gran Canaria presentan una mayor D para los eventos de lluvia que para los de polvo; ya que las ocurrencias de lluvia para dicha escala temporal están más uniformemente distribuidas siendo observados cortos periodos secos. La Palma presenta una dimensión fractal ligeramente más alta para el análisis de lluvia dada su localización geográfica al estar

más afectada por las bajas Atlánticas. Sin embargo, para dicha escala de tiempo, los eventos de polvo en Fuerteventura muestran un valor mayor que las ocurrencias de lluvia correspondiendo a un clima más árido. Comparando ambos fenómenos, en general, para escalas de aproximadamente un día los eventos de polvo están distribuidos más cercanos entre sí que los de lluvia. En otras palabras, el polvo es más persistente que la lluvia durante un periodo de un día. Esto implica que dichos fenómenos están afectados por procesos que actúan a diferentes escalas temporales. Como conclusiones del análisis de la precipitación en Canarias, los resultados obtenidos ayudan a definir el régimen pluviométrico sobre las islas, caracterizado por largos periodos con lluvias débiles o cierta intensidad relativamente distribuida preferentemente en vertientes norte de las islas pero cortos episodios de lluvias torrenciales en localizaciones concretas.

El régimen de lluvias en Canarias y Madeira muestra un carácter más estacional que Bermudas y Azores que presentan una corta estación seca.

Respecto al análisis del viento, en Bermudas los vientos del tercer cuadrante son los más frecuentes (la frecuencia en que soplan los vientos del sur y oeste es similar) seguidos de los procedentes del este, los del cuarto cuadrante se dan con menor frecuencia. Durante el invierno la dirección predominante es la del oeste seguido del noroeste, mientras que en verano los vientos procedentes del sur, aunque también destacan los del oeste. Los del este muestran más alta frecuencia en otoño y ligeramente entre mayo y abril. Los vientos del sur y suroeste generan en gran medida la lluvia en Bermudas.

En los archipiélagos de la Macaronesia referidos en este estudio, los vientos del oeste asociados a las bajas Atlánticas son los que causan las precipitaciones más intensas cuando la lluvia suele estar asociada a fenómenos convectivos que ocurren

preferentemente en otoño e invierno. Sin embargo, los vientos alisios producen lluvia de menor intensidad.

En cuanto a la variabilidad temporal de la precipitación, no está uniformemente distribuida a lo largo del año. El patrón de la precipitación media anual en Bermudas presenta un máximo absoluto en octubre y un pico secundario en enero, así como dos mínimos locales en noviembre-diciembre y abril-mayo. El índice medio de estacionalidad asignado a Bermudas corresponde a un régimen de precipitación que no registra grandes variaciones. No obstante, el test de χ^2 rechaza la uniformidad en la distribución de la precipitación a lo largo del año. Esta contradicción pone de manifiesto que el uso de datos medios oculta detalles sobre la variabilidad inter-anual y tiende a infra estimar la estacionalidad. Se debe tener en cuenta que el promediar los valores de precipitación correspondientes a un mes en concreto y estimar un índice de estacionalidad global puede enmascarar la real estructura estacional de la precipitación en la zona de estudio. De acuerdo con ello, el índice medio de estacionalidad calculado a partir de los valores medios de los 63 valores anuales indica que el régimen de lluvia anual media en Bermudas es más bien estacional con una corta estación seca. Se observa una considerable variabilidad mensual. De modo que, la fluctuación temporal de los meses húmedos y secos varía de año a año. Es de particular interés subrayar que cada uno de los meses del año, ha sido, al menos una vez, el más lluvioso o el más seco del año durante el periodo de estudio. Como consecuencia, el índice de replicabilidad del régimen pluviométrico permanece significantemente bajo y prácticamente invariable durante el periodo de estudio. Además, destaca que no hay un mes sin lluvia en el periodo de estudio.

El índice de estacionalidad anual en Bermudas muestra una considerable variabilidad interanual. Así, de acuerdo con Walsh & Lawler 1981 en un 52%

corresponde a un régimen pluviométrico anual estacional con una corta estación seca, mientras en un 46% a uno que no registra grandes variaciones pero una definida estación húmeda, y sólo un 2% a uno de tipo estacional. Sin embargo, de acuerdo con Peña-Arencibia et al. 2010, el 100% de los años presenta un régimen pluviométrico estacional. El test estadístico Chi-cuadrado permite aceptar con confianza la existencia de un patrón estacional en el régimen pluviométrico para cualquiera de los años analizados. A pesar de la marcada variabilidad interanual del índice de estacionalidad, el test de Mann-Kendall modificado, rechaza la existencia de tendencias positivas o negativas estadísticamente significantes. De modo similar, la precipitación total anual exhibe una notable variabilidad interanual siguiendo una normal distribución normal pero no hay evidencia estadística que soporte la existencia de ninguna tendencia significativa. Además, la falta de correlación estadísticamente significante entre el índice de estacionalidad y la lluvia anual ha sido confirmado. Para Canarias y Azores existe una estacionalidad más marcada que en Bermudas.

Análisis preliminares sobre los datos de precipitación en Bermudas indican alguna tendencia en los días de lluvia durante el invierno y una potencial relación con el índice NAO (North Atlantic Oscillation Index). En relación con la variabilidad interanual, el principal resultado extraído para Bermudas es que el número anual de días de lluvia han aumentado durante el período de 1993 a 2011, aunque la tasa de precipitación ha tendido a disminuir. Esto puede ser debido a algunos cambios en los parámetros de la circulación atmosférica en torno a 1990, ya que la frecuencia de las tormentas de invierno observadas en la región subpolar del Atlántico Norte que parece haber aumentado entre 1980 y 1995 debido a una fase de NAO positiva (Beersma et al., 1997) tienden a disminuir a partir de 1990.

8.6. Conclusiones

- Los modelos no lineales proporcionan un marco adecuado para estudiar la variabilidad de las precipitaciones en esta región.

- En Bermudas y Azores el tiempo transcurrido entre los eventos de lluvia sigue una distribución exponencial negativa, propia de un modelo de Poisson lo cual sugiere un comportamiento aleatorio. Por el contrario, en Madeira y más marcadamente en Canarias puede ser caracterizada a través de un análisis de escala o una Power Law (PL).

- Dichos comportamientos a escala o Power Low sugieren la existencia de mecanismos subyacentes relacionados con los procesos estudiados. Esto implica la existencia de colas largas al final de las distribuciones y la posible ocurrencia de eventos extremos. En estos casos algunos parámetros estadísticos como la media o varianza no pueden ser estimados.

-La intensidad de las precipitaciones en las Bermudas sigue un comportamiento aleatorio, no lineal y libre de escala, acercándose a una PL. Es sugerida la existencia de posibles fases de transición y fenómenos críticos.

- Los fenómenos de precipitación e intrusiones de polvo en Canarias tienen un carácter fractal o complejo. La dimensión fractal es mayor en los sectores del norte y centro de las islas, así como en medianías y zonas altas en comparación con las encontradas para los sectores sur y este. Por otra parte, ésta aumenta de este a oeste.

-Una marcada variabilidad espacio-temporal es encontrada al analizar las diferentes series temporales de precipitación seleccionadas.

-El régimen de lluvias en Canarias y Madeira muestra un carácter más estacional que Bermudas y Azores que presentan una corta estación seca. Las similitudes entre las estaciones mencionadas se encuentran también al analizar otros parámetros analizados en este estudio.

-El análisis de la dirección y la intensidad del viento han sido útiles en la descripción de los distintos patrones estacionales de la variable de estudio y para diferenciar entre precipitación frontal y convectiva.

-El análisis del índice de estacionalidad durante el período normal 1981-2010 muestra una mayor variabilidad en las Islas Canarias que en Azores, Bermuda Madeira.

-Con respecto al análisis de la variabilidad interanual de la precipitación en Bermudas, se puede concluir que:

1. El número de días de lluvia a partir de 1990 muestra una tendencia ascendente, pero la tasa de precipitación desciende en general. La principal contribución a este efecto parece ser el número de días de lluvia en invierno. Este hecho es consistente con la idea del carácter de la lluvia en invierno comparada con el comportamiento más estocástico de la lluvia en verano.

2. No hay variabilidad significativa entre la zona este y oeste de Bermudas. El número de días de lluvia está bien anti-correlacionado con la NAO (North Atlantic Oscillation Index).

3. No existe una significativa tendencia multi-decadal en la precipitación.

De acuerdo con la tendencia de la distribución de la lluvia acumulada para periodos de 5 años, las estaciones más occidentales en las islas Canarias mostraron ciertas características similares a Bermuda, Madeira y Azores en relación al descenso encontrado cercano al año 1990.

En resumen las principales conclusiones de esta tesis son:

RESUMEN EN ESPAÑOL

1. En Bermudas y Azores la distribución de periodos secos entre los eventos de lluvia sigue un comportamiento aleatorio. En Canarias y Madeira una ley de potencia lo que implica la posible ocurrencia de eventos extremos.

2. La lluvia acumulada diaria en toda la región de estudio sigue una ley de escala.

3. La ocurrencia de eventos de lluvia que afectan a Canarias tiene un comportamiento fractal con diferentes patrones de agrupación temporal y espacial.

4. Se confirma la idoneidad de los modelos no lineales para caracterizar la precipitación en esta región.

5. Los resultados obtenidos del análisis de las intrusiones de polvo en Canarias dan robustez a esta idea.

6. El régimen de lluvias muestra un carácter más estacional en Canarias y Madeira.

7. En estas islas el alisio predomina con lluvia frontal y el viento del oeste con convectiva. En Bermudas y Azores

los vientos del sur y este son los más frecuentes cuando hay paso de frentes y los del oeste con tormentas.

8. El número de días de lluvia en Bermudas parece estar aumentando alrededor del año 1995 y está bien anti-correlacionado con la NAO.

9. La lluvia en Bermudas y Azores presenta un alto grado de aleatoriedad lo cual denota impredictibilidad. Sin embargo en Madeira y principalmente en Canarias es un fenómeno más complejo.

10. Similitudes entre estos pares de archipiélagos se ponen de manifesto en todos los resultados obtenidos en esta tesis.

RESUMEN EN ESPAÑOL

Esta tesis es el resultado de un trabajo conjunto entre los servicios Meteorológicos de España, Bermudas y Portugal en cooperación con la Universidad de Las Palmas de Gran Canaria. Esperamos que sirva de estímulo para futuras cooperaciones internacionales e inter-regionales en el campo de la meteorología en el área subtropical del Atlántico Norte en base a:

1. Mejorar la calidad y prestación de servicios a distintos usuarios, en particular a protección civil.
2. Avanzar en la investigación científica en materia de meteorología en esta región para su aplicación en la predicción operativa y en una mejor gestión de recursos hídricos.

9. References

9. References

Abaurrea J, Cebrián AC (2002) Drought analysis based on a cluster Poisson model: distribution of the most severe drought. Climate Research 22:227-235

Addison PS (2002) The illustrated wavelet transform handbook: introductory theory and applications in science, engineering, medicine and finance, Vol. CRC press

Aguilera-Klink F, Pérez-Moriana E, Sánchez-García J (2000) The social construction of scarcity. The case of water in Tenerife (Canary Islands). Ecological Economics 34:233-245

Alexander LV, Tett SF, Jonsson T (2005) Recent observed changes in severe storms over the United Kingdom and Iceland. Geophysical Research Letters 32

Alexandersson H, Tuomenvirta H, Schmith T, Iden K (2000) Trends of storms in NW Europe derived from an updated pressure data set. Climate Research 14:71-73

Almarza C, López J, Flores C (1996) Homogeneidad y variabilidad de los registros históricos de precipitación de España. Serie Monografías, Instituto Nacional de Meteorología

Amaral LA, Ottino JM (2004) Complex networks. The European Physical Journal B-Condensed Matter and Complex Systems 38:147-162

Amigó JM, Keller K (2013) Permutation entropy: One concept, two approaches. The European Physical Journal Special Topics 222:263-273

Ayer JF, Vacher HL (1983) A numerical model describing unsteady flow in a fresh water lens. . Water Resources Bulletin 19:785-792

Báez M, Sanchez-Pinto L (1983) Islas de fuego y agua: Canarias, Azores, Madeira, Salvajes, Cabo Verde: Macronesia, Vol. Edirca

REFERENCES

Bailey K (2001) Entropy systems theory. Systems Science and Cybernetics, in Encyclopedia of Life Support Systems (EOLSS), Developed under the Auspices of the UNESCO, Eolss Publishers, Oxford, UK,[http://www eolss net]

Bak P (1996) How nature works: the science of self-organized criticality. Nature 383:772-773

Balguerías E, Quintero M, Hernandez-Gonzalez C (2000) The origin of the Saharan Bank cephalopod fishery. ICES Journal of Marine Science: Journal du Conseil 57:15-23

Bandt C, Pompe B (2002) Permutation entropy: a natural complexity measure for time series. Physical review letters 88:174102

Barabási A-L, Albert R (1999) Emergence of Scaling in Random Networks. Science 286:509-512

Barbosa S, Silva M, Fernandes M (2006) Wavelet analysis of the Lisbon and Gibraltar North Atlantic Oscillation winter indices. International Journal of Climatology 26:581-593

Barbosa S, Silva M, Fernandes M (2009) Multi-scale variability patterns in NCEP/NCAR reanalysis sea-level pressure. Theoretical and applied climatology 96:319-326

Bates NR (2001) Interannual variability of oceanic CO 2 and biogeochemical properties in the Western North Atlantic subtropical gyre. Deep Sea Research Part II: Topical Studies in Oceanography 48:1507-1528

Bates NR (2007) Interannual variability of the oceanic CO2 sink in the subtropical gyre of the North Atlantic Ocean over the last 2 decades. Journal of Geophysical Research: Oceans (1978-2012) 112

Batschelet E (1981) Circular statistics in biology, Vol III. Academic press, London

REFERENCES

Beersma J, Rider K, Komen G, Kaas E, Kharin V (1997) An analysis of extra-tropical storms in the North Atlantic region as simulated in a control and 2x CO2 time-slice experiment with a high-resolution atmospheric model. Tellus A 49:347-361

Bello N (1998) Evidence of climate change based on rainfall records in Nigeria. Weather 53:412-418

Bettencourt ML (1979) O clima dos Açores como recurso natural, especialmente em agricultura e indústria do turismo, Vol. Instituto Nacional de Meteorología e Geofísica de Portugal

Bijl W, Flather R, De Ronde J, Schmith T (1999) Changing storminess? An analysis of long-term sea level data sets. Climate Research 11:161-172

Bjerknes J (1964) Atlantic air-sea interaction. Advances in geophysics 10:82

Boettcher S, Paczuski M (1996) Ultrametricity and memory in a solvable model of self-organized criticality. Physical Review E- Phys Rev 54:1082-1095

Bojariu R (1997) Climate variability modes due to ocea-atmosphere interaction in the central Atlantic. Tellus A 49:362-370

Bourodimos EL, Oguntuase AM (1974) Cross-spectral analysis of rainfall and runoff for Raritan and Mullica river basins in New Jersey. Journal of hydrology 21:61-79

Brown S, Caesar J, Ferro CA (2008) Global changes in extreme daily temperature since 1950. Journal of Geophysical Research: Atmospheres (1984-2012) 113

Burroughs SM, and Tebbens, S.F (2001) Upper-Truncated Power Laws in Natural Systems. Pure Appl Geophys, 158:741-757

Campos PMR, Pérez SA, Agulló EC, Gómez SA, de Galisteo Marín JPO (2011) Una Climatología del Agua Precipitable en la Región Subtropical sobre la Isla de Tenerife basada en Datos de Radiosondeos.

REFERENCES

Carlson TN (1969) Some remarks on african disturbances and their progress over the tropical atlantic. Monthly Weather Review 97:716-726

Carretero O, Aguado F, Martín F (2011) A case of study of heavy convective precipitation event over the Canary Islands associated with polar- subtropical cyclone (26th January to 3rd February 2010. In: 6th European Conference on severe storm, Islas Baleares. Spain

Cassou C The north atlantic oscillation: mechanisms and spatio-temporal variability. In. Proc Iceland in the central northern atlantic: hotspot, sea currents and climate change

Cayan DR (1992) Latent and sensible heat flux anomalies over the northern oceans: The connection to monthly atmospheric circulation. Journal of Climate 5:354-369

Cebrián AC, Abaurrea J (2006) Drought Analysis Based on a Marked Cluster Poisson Model. Journal of Hydrometeorology 7

Cello G, Malamud BD (2006) Fractal analysis for natural hazards, Vol, London

Clauset A, Shalizi, C.R and Newman, M.E.J. (2009) Power-law distributions in empirical data *SIAM review*/ SIAM Rev 51:661-703

Coates KA, Fourqurean JW, Kenworthy WJ, Logan A, Manuel SA, Smith SR (2013) Introduction to Bermuda: Geology, Oceanography and Climate. In: Coral Reefs of the United Kingdom Overseas Territories. Springer

Coates L (1996) An overview of fatalities from some natural hazards in Australia. Proceedings NDR96 Conference on Natural Disaster Reduction, Institute of Engineers Australia,Canberra:49-54.

Conover W (1980) Practical nonparametric statistics. Hoboken, NJ: John Wiley & Sons, Inc

REFERENCES

Consul P, Famoye F (1992) Generalized Poisson regression model. Communications in Statistics-Theory and Methods 21:89-109

Consul PC, Jain GC (1973) A generalization of the Poisson distribution. Technometrics 15:791-799

Couto F, Salgado R, Costa MJ (2013) Flash flood in Madeira Island in autumn 2012. In: 7th European Conference on Severe Storms (ECSS2013), Helsinki, Finland

Curry RG, McCartney MS (2001) Ocean Gyre Circulation Changes Associated with the North Atlantic Oscillation*. Journal of Physical Oceanography 31:3374-3400

Custodio E (2002) Aquifer overexploitation: What does it mean? Hydrogeol Journal /Hydrogeol J, **10**:254-277

Chapa SR, Rao VB, Prasad GSSD (1998) Application of wavelet transform to Meteosat-derived cold cloud index data over South America. Monthly Weather Review 126:2466-2481

Charpentier É, Lesne A, Nikolski N (2007) Kolmogorov's heritage in mathematics, Vol. Springer Science & Business Media

Chen D, Li X (2004) Scale-dependent relationship between maximum ice extent in the Baltic Sea and atmospheric circulation. Global and Planetary Change 41:275-283

Chen K, Fu I, Su S, Liu C (1995) Wavelet analysis on transient behavior of wind fluctuations observed by MST radar. Radio science 30:1111-1123

Chen Y-C, Sung Q.-C., Yu T.T., and Sun, R.J. (2003) Earthquake time series analysis by Cantor set model in Taiwan. Terrestrial, Atmospheric and Oceanic Sciences/Terr, Atmos OceanSci, 14:85-98

Chow KV, Denning KC (1993) A simple multiple variance ratio test. Journal of Econometrics 58:385-401

REFERENCES

Dalelane C, Deutschländer T (2013) A robust estimator for the intensity of the Poisson point process of extreme weather events. Weather and Climate Extremes 1:69-76

Datsenko N, Shabalova M, Sonechkin D (2001) Seasonality of multidecadal and centennial variability in European temperatures: The wavelet approach. Journal of Geophysical Research: Atmospheres (1984-2012) 106:12449-12461

Daubechies I (1992) Ten lectures on wavelets, Vol 61. SIAM

Davidowitz G (2002) Does precipitation variability increase from mesic to xeric biomes? Global Ecology and Biogeography 11:143-154

Davies JR, Rowell DP, Folland CK (1997) North Atlantic and European seasonal predictability using an ensemble of multidecadal atmospheric GCM simulations. International Journal of Climatology 17:1263-1284

de Azevedo EB, Pereira LS, Itier B (1999) Simulation of local climate in islands environments using a GIS integrated model. In: Second Inter-regional conference on Envyronment-Water 99, Lausanne, Switzerland

De Lima MPI, De Lima JLMP (2009) Investigating the multifractality of point precipitation in the Madeira archipelago. Nonlinear Processes Geophysics 16:299-311,

De Lùis MD, Raventós J, Gonzalez-Hidalgo J, Sanchez J, Cortina J (2000) Spatial analysis of rainfall trends in the region of Valencia (East Spain). Int J Climatol 20:1451-1469

De USaK, M.and Dandekar, M. M.: (2004) Natural Hazards Associated with Meteorological Extreme Events. Natural Hazards 31:487-497

Deb P, Sefton M (1996) The distribution of a Lagrange multiplier test of normality. Economics Letters 51:123-130

REFERENCES

Departamento de producción de AEMET, Departamento de Meteorología e Clima de IMP (2012) Atlas climático de los archipiélagos de Canarias, Madeira y Azores. Temperatura del aire y precipitación (1971-2000). Agencia estatal de Meteorología y Servicios Meteorologícos de Portugal:80

Diaz HF, Carlson TN, Prospero JM (1976) A study of the structure and dynamics of the Saharan air layer over the northern equatorial Atlantic during BOMEX.

Díaz JP, Expósito FJ, Torres CJ, Herrera F, Prospero JM, Romero MC (2001) Radiative properties of aerosols in Saharan dust outbreaks using groundâ€ based and satellite data: Applications to radiative forcing. Journal of Geophysical Research/ J GeophysRes Atmospheres (1984-2012) 106:18403-18416

Dickman R (2004) Fractal rain distributions and chaotic advection. Brazilian Journal of Physics/Brazilian J Phys, 34:337-346

Dickson R, Osborn T, Hurrell J, Meincke J, Blindheim J, Adlandsvik B, Vinje T, Alekseev G, Maslowski W (2000) The Arctic ocean response to the North Atlantic oscillation. Journal of climate 13:2671-2696

Drinkwater KF, Belgrano A, Borja A, Conversi A, Edwards M, Greene CH, Ottersen G, Pershing AJ, Walker H (2003) The response of marine ecosystems to climate variability associated with the North Atlantic Oscillation. The North Atlantic Oscillation: climatic significance and environmental impact:211-234

Dubois J, Cheminee JL (1991) Fractal analysis of eruptive activity of some basaltic volcanoes. Journal of Volcanology and Geothermal Research/J Volcanol Geoth Res, 45:197-208

Dunion JP, Velden CS (2004) The impact of the Saharan air layer on Atlantic tropical cyclone activity. Bulletin of the American Meteorological Society 85:353-365

Durand B, Zvonkin A (2007) Kolmogorov complexity, Vol. Springer

REFERENCES

Elizaga F, Rus C, Bustos JJ, Marrero C, Sanz R, Calbet X, Rípodas P, Alejo CJ, Martín F, San Ambrosio I, Del río P (2003) Situación de lluvias torrenciales en Santa Cruz de Tenerife (31 de Marzo de 2002). Nota técnica del Instituto Nacional de Meteorología

Elsner J, Kara A, Owens M (1999) Fluctuations in North Atlantic hurricane frequency. Journal of Climate 12:427-437

Elsner JB, Kara AB (1999) Hurricanes of the North Atlantic: Climate and society, Vol. Oxford University Press

Elsner JB, Niu X, Jagger TH (2004) Detecting shifts in hurricane rates using a Markov chain Monte Carlo approach. Journal of Climate 17:2652-2666

Emery WJ, Thompson RE (2001) Data Analysis Methods in Physical Oceanography, Vol. Elsevier

Enfield DB, Mayer DA (1997) Tropical Atlantic sea surface temperature variability. Journal of Geophysical Research 102:929-945

Fang J, Chen A, Peng C, Zhao S, Ci L (2001) Changes in forest biomass carbon storage in China between 1949 and 1998. Science 292:2320-2322

Farge M (1992) Wavelet transforms and their applications to turbulence. Annual Review of Fluid Mechanics 24:395-458

Fatichi S, Caporali E (2009) A comprehensive analysis of changes in precipitation regime in Tuscany. International Journal of Climatology 29:1883-1893

Fatichi S, Ivanov VY, Caporali E (2012) Investigating Interannual Variability of Precipitation at the Global Scale: Is There a Connection with Seasonality? Journal of Climate 25:5512-5523

Fedoseev A (1970) Geostrophic circulation of surface waters on the shelf of north-west Africa. Rapp PV Reun Cons Int Explor Mer 159:32-37

REFERENCES

Ferbus-Zanda M, Grigorieff S (2010) Kolmogorov Complexity in perspective. Part I: Information Theory and Randomnes. arXiv preprint arXiv:10103201

Fernandopullé D (1976) Climatic characteristics of the Canary Islands. In: Biogeography and ecology in the Canary Islands. Springer

Font Tullot I (1956) El tiempo atmosférico en las Islas Canarias, Vol. Servicio Meteorológico Nacional, Sección de Predicción

Fontaine B, Janicot S, Moron V (1995) Rainfall anomaly patterns and wind field signals over West Africa in August (1958-1989). Journal of Climate 8:1503-1510

Fragoso M, Trigo R, Pinto J, Lopes S, Lopes A, Ulbrich S, Magro C (2012) The 20 February 2010 Madeira flash-floods: synoptic analysis and extreme rainfall assessment. Natural Hazards and Earth System Science 12:715-730

Fujita K (2008) Effect of precipitation seasonality on climatic sensitivity of glacier mass balance. Earth and Planetary Science Letters 276:14-19

Gamage N, Blumen W (1993) Comparative analysis of low-level cold fronts: wavelet, Fourier, and empirical orthogonal function decompositions. Monthly Weather Review 121:2867-2878

Gao S, Wu Q (2015) Period analysis and trend forecast for soil temperature in the Qinghai-Xizang Highway by wavelet transformation. Environmental Earth Sciences 74:2883-2891

Gao W, Li B (1993) Wavelet analysis of coherent structures at the atmosphere-forest interface. Journal of Applied Meteorology 32:1717-1725

García-Herrera R, Gallego D, Hernández E, Gimeno L, Ribera P, Calvo N (2003) Precipitation trends in the Canary Islands. International Journal of Climatology/ Int J Climatol, 23:235-241

REFERENCES

García-Herrera R, Puyol DG, Martín EH, Presa LG, Rodríguez PR (2001) Influence of the North Atlantic oscillation on the Canary Islands precipitation. Journal of climate /J Climate 14:3889-3903

Gaurin SE North Atlantic Climate Variability Over the Holocene: Preliminary Analysis of Bermuda Historical Weather Data and Stable Isotope Time Series from Bermuda Stalagmites. In. Proc 2008 Joint Meeting of The Geological Society of America, Soil Science Society of America, American Society of Agronomy, Crop Science Society of America, Gulf Coast Association of Geological Societies with the Gulf Coast Section of SEPM

Goodwin BC (1994) How the leopard changed its spots: The evolution of complexity, Vol. Princeton University Press

Grinsted A, Moore JC, Jevrejeva S (2004) Application of the cross wavelet transform and wavelet coherence to geophysical time series. Nonlinear processes in geophysics 11:561-566

Grossmann A, Morlet J (1984) Decomposition of Hardy functions into square integrable wavelets of constant shape. SIAM journal on mathematical analysis 15:723-736

Guerra JL (1989) Plan Hidrológico de Gran Canaria. Avance: Estudio de Pluviometría. In. Gobierno de España

Guijarro JA, Jiménez de Mingo. A (2013) Series de precipitación mensual 1981-2010, Vol. Agencia Estatal de Meteorología, Madrid

Guishard MP, Nelson EA, Evans JL, Hart RE, O'Connell DG (2007) Bermuda subtropical storms. Meteorology and Atmospheric Physics 97:239-253

Hirsch RM, Slack JR (1984) A nonparametric trend test for seasonal data with serial dependence. Water Resources Research 20:727-732

REFERENCES

Hirschi JlJM, Sinha B (2007) Negative NAO and cold Eurasian winters: how exceptional was the winter of 1962/1963? Weather 62:43-48

Holton JR, Dmowska R, Philander SG (1989) El Niño, La Niña, and the southern oscillation, Vol 46. Academic press

Huang J, Higuchi K, Shabbar A (1998) The relationship between the North Atlantic Oscillation and El Niño-Southern Oscillation. Geophysical Research Letters 25:2707-2710

Hurrell JW (1995) Decadal trends in the North Atlantic oscillation. Science 269:676-679

Hurrell JW, Deser C (2001) North Atlantic climate variability: the role of the North Atlantic Oscillation. Journal of Marine Systems 79:231-244

Hurrell JW, Deser C (2004) North Atlantic climate variability: the role of the North Atlantic Oscillation. Journal of Marine Systems 79:231-244

Hurrell JW, Deser C (2010) North Atlantic climate variability: the role of the North Atlantic Oscillation. Journal of Marine Systems 79:231-244

Hurrell JW, Kushnir Y, Ottersen G, Visbeck M (2003) An overview of the North Atlantic oscillation, Vol. Wiley Online Library

Hurrell JW, Van Loon H (1997) Decadal variations in climate associated with the North Atlantic Oscillation. In: Climatic Change at High Elevation Sites. Springer

Izzo M, Aucelli PP, Mazzarella A (2004) Recent changes in rainfalland air temperature at Agnone (Molise-Central Italy). Annals of Geophysics/Ann Geophys, 47:1689-1698

Jaagus J (2006) Climatic changes in Estonia during the second half of the 20th century in relationship with changes in large-scale atmospheric circulation. Theoretical and Applied Climatology 83:77-88

REFERENCES

Jarque CM, Bera AK (1987) A test for normality of observations and regression residuals. International Statistical Review/Revue Internationale de Statistique:163-172

Jiang J, Zhang De, Fraedrich K (1997) Historic climate variability of wetness in East China(960â€“1992): a wavelet analysis. International Journal of Climatology 17:969-981

Johnson F, Westra S, Sharma A, Pitman AJ (2011) An assessment of GCM skill in simulating persistence across multiple time scales. Journal of Climate 24:3609-3623

Johnson RW (2010) Edge adapted wavelets, solar magnetic activity, and climate change. Astrophysics and Space Science 326:181-189

Jones CG, Thorncroft CD (1998) The role of El Niño in Atlantic tropical cyclone activity. Weather 53:324-336

Jones P, Conway D (1997) Precipitation in the British Isles: an analysis of area-average data updated to 1995. International Journal of Climatology 17:427-438

Juan C, Emerson BC, Oromí P, Hewitt GM (2000) Colonization and diversification: towards a phylogeographic synthesis for the Canary Islands. Trends in Ecology & Evolution 15:104-109

Kendall K (1975) Thin-film peeling-the elastic term. Journal of Physics D: Applied Physics 8:1449

Kilby MC, Slobounov SM, Newell KM (2014) Postural instability detection: aging and the complexity of spatial-temporal distributional patterns for virtually contacting the stability boundary in human stance.

Kleissl J, Honrath RE, Dziobak MP, Tanner D, Val Martín M, Owen R, Helmig D (2007) Occurrence of upslope flows at the Pico mountaintop observatory: A case study

of orographic flows on a small, volcanic island. Journal of Geophysical Research: Atmospheres (1984-2012) 112

Knapp AK, Smith MD (2001) Variation among biomes in temporal dynamics of aboveground primary production. Science 291:481-484

Koppen W (1936) Das geographische system der klimate, Handbuch der Kliatologie. Ed W Koppen and R Geiger 1

Koutsoyiannis D (2006) An entropic- stochastic representation of rainfall intermittency: The origin of clustering and persistence. Water Resources Research 42

Kumar P, Foufoula-Georgiou E (1993) A multicomponent decomposition of spatial rainfall fields: 1. Segregation of large and small scale features using wavelet transforms. Water Resources Research 29:2515-2532

Kumar P, Foufoula-Georgiou E (1997) Wavelet analysis for geophysical applications. Reviews of Geophysics 35:385-412

Labat D, Ababou R, Mangin A (2001) Introduction of Wavelet Analyses to Rainfall/Runoffs Relationship for a Karstic Basin: The Case of Licq-Atherey Karstic System (France). Groundwater 39:605-615

Laherrere J, Sornette D (1998) Stretched exponential distributions in nature and economy: 'fat tails' with characteristic scales. The European Physical Journal B-Condensed Matter and Complex Systems 2:525-539

Lare AR, Nicholson SE (1994) Contrasting Conditions of Surface Water Balance in Wet Years and Dry Years as a Possible Land Surface-Atmosphere Feedback Mechanism in the West African Sahel. Journal of Climate 7:653-668

Lau K, Weng H (1999) Interannual, decadal-interdecadal, and global warming signals in sea surface temperature during 1955-97. Journal of Climate 12:1257-1267

REFERENCES

Lau N-C, Philander S, Nath MJ (1992) Simulation of ENSO-like phenomena with a law-resolution coupled GCM of the global ocean and atmosphere. Journal of Climate 5:284-307

Lee SK, Enfield D, Wang C (2008) Why do some El Niños have no impact on tropical North Atlantic SST? Geophysical Research Letters 35

Lempel A, Ziv J (1976) On the complexity of finite sequences. Information Theory, IEEE Transactions on 22:75-81

Li C, Ma T, Zhu X, Li W (2011) The power-law relationship between landslide occurrence and rainfall level. Geomorphology 130:221-229

Li Y, Xue H, Bane JM (2002) Air-sea interactions during the passage of a winter storm over the Gulf Stream: A three-dimensional coupled atmosphere-ocean model study. Journal of Geophysical Research: Oceans (1978-2012) 107:21-21-21-13

Lilliefors HW (1967) On the Kolmogorov-Smirnov test for normality with mean and variance unknown. Journal of the American Statistical Association 62:399-402

Lilliefors HW (1969) On the Kolmogorov-Smirnov test for the exponential distribution with mean unknown. Journal of the American Statistical Association 64:387-389

Liu PC, Miller GS (1996) Wavelet Transforms and Ocean Current Data Analysis. Journal of Atmospheric and Oceanic Technology 13:1090-1099

Livada I, Asimakopoulos D (2005) Individual seasonality index of rainfall regimes in Greece. Climate Res 28:155-161

Lovejoy S, Schertzer D, Tsonis A (1987) Functional box-counting and multiple elliptical dimensions in rain. Science 235:1036-1038

Lumley S, Grimes R, Murphy S, Burr P, Chroneos A, Chard-Tuckey P, Wenman M (2014) The thermodynamics of hydride precipitation: The importance of entropy, enthalpy and disorder. Acta Materialia 79:351-362

REFERENCES

Lundstedt H, Liszka L, Lundin R Solar activity explored with new wavelet methods. In. Proc Annales Geophysicae. Copernicus GmbH

Luongo G, Mazzarella A (2003) On the time-scale invariance of the eruptive activity of Vesuvius. Journal of Volcanology and Geothermal Research 120:311-313

Lütkepohl H (2005) New introduction to multiple time series analysis, Vol. Springer Science & Business Media

Macky WA (1946) The Rainfall and Water Supply of Bermuda, Vol. Bermuda Met. Station

Macky WA (1947) Gales in Bermuda. In. Bermuda Met. Station, Hamilton

Macky WA (1948) Bermuda Temperatures, Vol. Bermuda Met. Station

Macky WA (1952) Sunshine in Bermuda, Vol. Meteorological Office

Macky WA (1956) The Surface Wind in Bermuda. In. Bermuda Met. Office, Hamilton

Macky WA (1957) The Rainfall of Bermuda, Vol. Bermuda Met. Office

Mahrt L (1991) Eddy asymmetry in the sheared heated boundary layer. J Atmos Sci 48:472-492

Malamud BD, Turcotte DL (2006) The applicability of power-law frequency statistics to floods. Journal of Hydrology/J Hydrol, 322:168-180

Mallat S (1998) A Wavelet Tour of Signal Processing Academic. New York 16

Mallat S (1999) A wavelet tour of signal processing, Vol. Academic press, New York

Mallat SG (1989) A theory for multiresolution signal decomposition: the wavelet representation. Pattern Analysis and Machine Intelligence, IEEE Transactions on 11:674-693

Mandelbrot BB (1983) The fractal geometry of nature. New York, WH Freeman and Co 1:495

REFERENCES

Mann HB (1945) Nonparametric tests against trend. Econometrica: Journal of the Econometric Society:245-259

Maraun D, Kurths J (2004) Cross wavelet analysis: significance testing and pitfalls. Nonlinear Processes in Geophysics 11:505-514

Marshall J, Kushnir Y, Battisti D, Chang P, Czaja A, Dickson R, Hurrell J, McCARTNEY M, Saravanan R, Visbeck M (2001) North Atlantic climate variability: phenomena, impacts and mechanisms. International Journal of Climatology 21:1863-1898

Marticorena B, Cairo F (2006) EOP/LOP Aerosols Monitoring and Radiation (TT2b). AMMA International Implementation Plan-Version 2:2-15

Martiín F, Alejo CJ, Bustos JJ, Calvo FJ, San Ambrosio I, Sánchez-Laulhé JM, Santos D (2007) Estudio de la tormenta tropical "Delta" y su transición extratropical: efectos meteorológicos en Canarias (27-29 de noviembre de 2005). Nota técnica del Instituto Nacional de Meteorología

Martín-León F (2003) Las gotas frías/ DANAs: ideas y conceptos básicos, Vol. Instituto Nacional de Meteorología. Ministerio de Medio Ambiente, Madrid

Martín F (2010) Estudio de dos situaciones de precipitaciones intensas y viento huracanados del invierno de 2010 en Canarias, Vol. AEMET. Ministerio de Medio Ambiente, Madrid

Martin F, Alejo CJ, Bustos JJ, Calvo FJ, San Ambrosio I, Sánchez-Laulhé JM, Santos D (2007) Estudio de la tormenta tropical "Delta" y su transición extratropical: efectos meteorológicos en Canarias (27-29 de noviembre de 2005), Vol. Instituto Nacional de Meteorología, Madrid

REFERENCES

Masseti M (2010) Mammals of the Macaronesian islands (the Azores, Madeira, the Canary and Cape Verde islands): redefinition of the ecological equilibrium. mammalia 74:3-34

Mayer L (1992) Fractal characteristics of desert storm sequences and implications for geomorphic studies. Geomorphology 5:167-183

Máyer P (2003) Lluvias e inundaciones en la ciudad de Las Palmas de Gran Canaria (1869-1999). Universidad de Las Palmas de Gran Canaria y Ayuntamiento de Las Palmas de Gran Canaria Las Palmas de Gran Canaria

Mazzarella A (1998) The time clustering of floodings in Venice and the Cantor dust method. Theoretical and applied climatology 59:147-150

Mazzarella A (1999) Multifractal dynamic rainfall processes in Italy. Theoretical and applied climatology 63:73-78

Mazzarella A, Diodato N (2002) The alluvial events in the last two centuries at Sarno, southern Italy: their classification and power-law time-occurrence. Theoretical and applied climatology 72:75-84

Mazzarella A, Giuliacci A (2009) The El Niño events: their classification and scale-invariance laws. Annals of Geophysics/Ann Geophys, 52:517-522

Mazzarella A, Rapetti F (2004) Scale-invariance laws in the recurrence interval of extreme floods: an application to the upper Po river valley (northern Italy). Journal of Hydrology/ JHydrol 288:264-271

McGarry T, Anderson DI, Wallace SA, Hughes MD, Franks IM (2002) Sport competition as a dynamical self-organizing system. Journal of Sports Sciences 20:771-781

Meals DW SJ, Dressing S A, and Harcum J B. (2011) Statistical Analysis for Monotonic Trends. National Nonpoint Source Monitoring Program Tech. note 6

Mega MS, Allegrini P, Grigolini P, Latora V, Palatella L, Rapisarda A, Vinciguerra S (2003) Power-law time distribution of large earthquakes. Physical Review Letters 90:188501

Meyer Y, Salinger DH (1992) Wavelets and operators, Vol 37. Cambridge Univ Press

Meyers SD, Kelly BG, O'Brien JJ (1993) An introduction to wavelet analysis in oceanography and meteorology: With application to the dispersion of Yanai waves. Monthly Weather Review 121:2858-2866

Michaels AF, Knap AH, Dow RL, Gundersen K, Johnson RJ, Sorensen J, Close A, Knauer GA, Lohrenz SE, Asper VA (1994) Seasonal patterns of ocean biogeochemistry at the US JGOFS Bermuda Atlantic Time-series Study site. Deep Sea Research Part I: Oceanographic Research Papers 41:1013-1038

Miranda P, Tomé R, Azevedo E, Cardoso R The 20 February 2010 Madeira flash flood. In. Proc 10th EMS Annual Meeting, 10th European Conference on Applications of Meteorology (ECAM)

Mitzenmacher M (2004) A brief history of generative models for power law and lognormal distributions. Internet mathematics/Internet Math 1:226-251

Molinari RL, Mestas-Nuñez AM (2003) North Atlantic decadal variability and the formation of tropical storms and hurricanes. Geophysical Research Letters 30

Morata A, Martin M, Luna M, Valero F (2006) Self-similarity patterns of precipitation in the Iberian Peninsula. Theoretical and applied climatology 85:41-59

Morlet J, Arens G, Fourgeau E, Glard D (1982) Wave propagation and sampling theory-Part I: Complex signal and scattering in multilayered media. Geophysics 47:203-221

Newman M, Barabási A-L, Watts DJ (2006) The structure and dynamics of networks, Vol. Princeton University Press

REFERENCES

Newman ME (2005) Power laws, Pareto distributions and Zipf's law. Contemporary physics 46:323-351

Olsson J, Niemczynowicz J, Berndtsson R (1993) Fractal analysis of high-resolution rainfall time series. Journal of Geophysical Research/J Geophys Res: Atmospheres (1984-2012) 98:23265-23274

Olsson J, Niemczynowicz J, Berndtsson R, Larson M (1992) An analysis of the rainfall time structure by box counting-some practical implications. Journal of Hydrology/J Hydrol, 137:261-277

Onof C, Chandler R, Kakou A, Northrop P, Wheater H, Isham V (2000) Rainfall modelling using Poisson-cluster processes: a review of developments. Stochastic Environmental Research and Risk Assessment 14:384-411

Onorato M, Salvetti M, Buresti G, Petagna P (1997) Application of a wavelet cross-correlation analysis to DNS velocity signals. EUROPEAN JOURNAL OF MECHANICS SERIES B FLUIDS 16:575-597

Ouyang G, Li J, Liu X, Li X (2013) Dynamic characteristics of absence EEG recordings with multiscale permutation entropy analysis. Epilepsy research 104:246-252

Pal S, Devara P (2012) A wavelet-based spectral analysis of long-term time series of optical properties of aerosols obtained by lidar and radiometer measurements over an urban station in Western India. Journal of Atmospheric and Solar-Terrestrial Physics 84:75-87

Pelletier JD (2007) Cantor set model of eolian dust deposits on desert alluvial fan terraces. Geology 35:439-442

Penland Cc, Matrosova L (1998) Prediction of tropical Atlantic sea surface temperatures using linear inverse modeling. Journal of Climate 11:483-496

Peña-Arencibia J, Van Dijk A, Mulligan M, Bruijnzeel LA (2010) The role of climatic and terrain attributes in estimating baseflow recession in tropical catchments. Hydrology and Earth System Sciences 14:2193-2205

Peñate I, Martín-González JM, Rodríguez G, Cianca A (2013) Scaling properties of rainfall and desert dust in the Canary Islands. Nonlin Processes Geophys 20:1079-1094

Percival DB, Walden AT (2000) Wavelet Methods for Time Series Analysis (Cambridge Series in Statistical and Probabilistic Mathematics).

Perica S, Foufoula-Georgiou E (1996) Model for multiscale disaggregation of spatial rainfall based on coupling meteorological and scaling descriptions. Journal of Geophysical Research: Atmospheres (1984-2012) 101:26347-26361

Pirazzoli PA (2005) Recent changes in surface air pressure and wind activity on the Atlantic coasts of France and Ireland. Journal of Coastal Research:236-252

Pirazzoli PA, Tomasin A (2003) Recent near- surface wind changes in the central Mediterranean and Adriatic areas. International Journal of Climatology 23:963-973

Pires V, Marques J, Silva A Madeira Extreme Floods: 2009/2010 Winter. Case study-2nd and 20th of February. In. Proc 10th EMS Annual Meeting, 10th European Conference on Applications of Meteorology (ECAM)

Potter TD, Colman BR (2003) Handbook of Weather, Climate, and Water: Atmospheric Chemistry, Hydrology, and Societal Impacts, Vol 1. Wiley-Interscience, Michigan

Pozo-Vazquez D, Esteban-Parra M, Rodrigo F, Castro-Diez Y (2001) A study of NAO variability and its possible non-linear influences on European surface temperature. Climate dynamics 17:701-715

Prada SLRN (2000) Geologia e recursos hídricos subterráneos da ilha da Madeira. Universidade da Madeira,

Prospero JM, Blades E, Mathison G, Naidu R (2005) Interhemispheric transport of viable fungi and bacteria from Africa to the Caribbean with soil dust. Aerobiologia 21:1-19

Pryor S, Schoof JT (2008) Changes in the seasonality of precipitation over the contiguous USA. Journal of Geophysical Research: Atmospheres (1984-2012) 113

Puyol DG, García-Herrera R, Hernández AMM, Martín EH (2004) Reconstrucciones climáticas. El ejemplo de la Oscilación del Atlántico Norte. Física de la Tierra 16:83-92

Puyol DG, Herrera RG, Martín EH, Presa LG, Rodríguez PR (2002) Major influences on precipitation in the Canary Islands. Adv Glob Change Res 10:57-73

Radermacher C, Tomassini L (2012) Thermodynamic Causes for Future Trends in Heavy Precipitation over Europe Based on an Ensemble of Regional Climate Model Simulations. Journal of climate 25

Riedl M, Müller A, Wessel N (2013) Practical considerations of permutation entropy. The European Physical Journal Special Topics 222:249-262

Rodwell MJ, Rowell DP, Folland CK (1999) Oceanic forcing of the wintertime North Atlantic Oscillation and European climate. Nature 398:320-323

Rogers JC (1984) The association between the North Atlantic Oscillation and the Southern Oscillation in the northern hemisphere. Monthly Weather Review 112:1999-2015

Rogers JC, Van Loon H (1979) The seesaw in winter temperatures between Greenland and northern Europe. Part II: some oceanic and atmospheric effects in middle and high latitudes. Monthly Weather Review 107:509-519

Rowe MP (1984) The freshwater "Central Lens" of Bermuda. Journal of Hydrology 73:165-176

Rowe MP (2011) Rain Water Harvesting in Bermuda1. JAWRA Journal of the American Water Resources Association 47:1219-1227

Rowe MP, Bristow CS (2012) Landward-advancing quaternary eolianites of Bermuda. Aeolian Research

Saco PM, Carpi LC, Figliola A, Serrano E, Rosso OA (2010) Entropy analysis of the dynamics of El Niño/Southern Oscillation during the Holocene. Physica A: Statistical Mechanics and its Applications 389:5022-5027

Saenz-Oiza J (1975) Estudio científico de los recursos de agua de las islas Canarias. MOPPNUD-UNESCO

Santos N, Israelian G, Mayor M (2001) The metal-rich nature of stars with planets. Arxiv preprint astro-ph/0105216

Savaglio S, Carbone V (2000) Human performance: Scaling in athletic world records. Nature 404:244-244

Scheffer M, Bascompte J, Brock WA, Brovkin V, Carpenter SR, Dakos V, Held H, Van Nes EH, Rietkerk M, Sugihara G (2009) Early-warning signals for critical transitions. Nature 461:53-59

Schroeder M (1991) Fractals, chaos, power laws: minutes from an infinite paradise, Vol 44. W.H. Freeman Co., New York

Segele ZT, Lamb PJ, Leslie LM (2009) Large- scale atmospheric circulation and global sea surface temperature associations with Horn of Africa June- September rainfall. International Journal of Climatology 29:1075-1100

REFERENCES

Servicio de desarrollo climatológico (2002) Valores normales y estadísticos de observatorios meteorológicos principales 1971- 2000, Vol 6. Centro de Publicaciones del Instituto Nacional de Meteorología, Secretaria General técnica, Ministerio de Medio Ambiente, Madrid

Sicard M, Reba MNM, Tomás S, Comerón A, Batet O, Muñoz-Porcar C, Rodríguez A, Rocadenbosch F, Muñoz-Tuñón C, Fuensalida JJ (2010) Results of site testing using an aerosol, backscatter lidar at the Roque de los Muchachos Observatory. Monthly Notices of the Royal Astronomical Society 405:129-142

Smalley R, Chatelain J-L, Turcotte D, Prévot R (1987) A fractal approach to the clustering of earthquakes: applications to the seismicity of the New Hebrides. Bulletin of the Seismological Society of America/ B Seismol Soc Am 77:1368-1381

Sornette D (2004) Critical phenomena in natural sciences: chaos, fractals, self-organization, and disorder: concepts and tools, Vol. Springer -Verlag Heidelberg

Sornette D (2006) Critical phenomena in natural sciences: chaos, fractals, selforganization and disorder: concepts and tools, Vol. Taylor & Francis US

Spedding G, Browand F, Huang N, Long S (1993) A 2-D complex wavelet analysis of an unsteady wind-generated surface wave field. Dynamics of atmospheres and oceans 20:55-77

Sperling FN, Washington R, Whittaker RJ (2004) Future climate change of the subtropical North Atlantic: implications for the cloud forests of tenerife. Climatic change 65:103-123

Stumpf MP, Porter MA (2012) Critical truths about power laws. Science 335:665-666

Sultan B, Janicot S (2003) The West African monsoon dynamics. Part II: The â€œpreonsetâ€ and â€œonsetâ€ of the summer monsoon. Journal of Climate 16:3407-3427

Sumner G, Homar V, Ramis C (2001) Precipitation seasonality in eastern and southern coastal Spain. International Journal of Climatology 21:219-247

Sundseth K (2009) Natura 2000 in the Macaronesian region.

Sutton R, Hodson D (2003) Influence of the ocean on North Atlantic climate variability 1871-1999. Journal of climate 16:3296-3313

Suyal V, Prasad A, Singh H (2012) Hysteresis in a Solar Activity Cycle. Solar Physics 276:407-414

Tabari H, Marofi S, Aeini A, Talaee PH, Mohammadi K (2011a) Trend analysis of reference evapotranspiration in the western half of Iran. Agricultural and Forest Meteorology 151:128-136

Tabari H, Somee BS, Zadeh MR (2011b) Testing for long-term trends in climatic variables in Iran. Atmospheric Research 100:132-140

Takayasu H (1990) Fractals in the Physical Science, Vol, New York

Tapiador F (2007) A maximum entropy analysis of global monthly series of rainfall from merged satellite data. International Journal of Remote Sensing 28:1113-1121

Taylor AH, Jordan MB, Stephens JA (1998) Gulf Stream shifts following ENSO events. Nature 393:638-638

Taylor AH, Stephens JA (1998) The North Atlantic oscillation and the latitude of the Gulf Stream. Tellus A 50:134-142

Teixeira J, Carvalho A, Carvalho M, Luna T, Rocha A (2014) Sensitivity of the WRF model to the lower boundary in an extreme precipitation event-Madeira island case study. Natural Hazards and Earth System Science 14:2009-2025

Terradellas E, Morales G, Cuxart J, YagÃ¼e C (2001) Wavelet methods: application to the study of the stable atmospheric boundary layer under non-stationary conditions. Dynamics of Atmospheres and Oceans 34:225-244

Thomson JA (1989) Modeling Ground-Water Management Options for Small Limestone Islands: the Bermuda Example. Ground Water 27:147-154

Timmermann A (1999) Detecting the nonstationary response of ENSO to greenhouse warming. Journal of the Atmospheric Sciences 56:2313-2325

Tomassini L, Jacob D (2009) Spatial analysis of trends in extreme precipitation events in high-resolution climate model results and observations for Germany. Journal of Geophysical Research: Atmospheres (1984-2012) 114

Torrence C, Compo GP (1998) A practical guide to wavelet analysis. Bulletin of the American Meteorological Society 79:61-78

Torres C, Cuevas E, Guerra J, Carreño V (2001) Caracterización de las masas de aire en la región subtropical. Libro de comunicaciones del V Simposio Nacional de Predicción. Available (in Spanish). Instituto Nacional de Meteorología, Madrid. In. ISBN 84-8320-192-5

Trigo RM, Osborn TJ, Corte-Real JoM (2002) The North Atlantic Oscillation influence on Europe: climate impacts and associated physical mechanisms. Climate Research 20:9-17

Trigo RM, Pozo Vázquez D, Osborn TJ, Castro Díez Y, Gamiz Fortis S, Esteban Parra MJ (2004) North Atlantic Oscillation influence on precipitation, river flow and water resources in the Iberian Peninsula. International Journal of Climatology 24:925-944

Tsallis C (2009) Introduction to nonextensive statistical mechanics: approaching a complex world, Vol. Springer, New York

Tucker T (1972) Beware the Hurricane!: The Story of the Cyclonic Tropical Storms that Have Struck Bermuda and the Islanders' Folk-lore Regarding Them, Vol. Island Press

Tucker T (1982) Beware of the hurricane!, the history of the cyclonic tropical storms that have struck Bermuda, 1609-1982. In. Island Press Limited, Hamilton, Bermuda

Tuenter HJ (2000) On the generalized Poisson distribution. Statistica Neerlandica 54:374-376

Turcotte D, Greene L (1993) A scale-invariant approach to flood-frequency analysis. Stochastic hydrology and hydraulics 7:33-40

Turcotte DL (1997) Fractals and chaos in geology and geophysics, Vol. Cambridge university press, New York

Vacher H, Rowe MP (1997) Geology and hydrogeology of Bermuda. Geology and hydrogeology of carbonate islands Amsterdam, Netherlands7 Elsevier:35-90

Vacher H, Rowe MP (2004) Geology and hydrogeology of Bermuda. Developments in Sedimentology 54:35-90

Vacher HL, Ayers JF (1980) Hydrology of small oceanic islands-Utility of an estimate of recharge inferred from the chloride concentration of the freshwater lenses. Journal of Hydrology 45:21-37

Vacher HL, Wallis T (1992) Comparative Hydrogeology of Fresh Water Lenses of Bermuda and Great Exuma Island, Bahamas. Groundwater 30:15-20

Van Camp L, Nykjaer L, Mittelstaedt E, Schlittenhardt P (1991) Upwelling and boundary circulation off Northwest Africa as depicted by infrared and visible satellite observations. Progress in Oceanography 26:357-402

Van den Hurk BJ, Viterbo P, Los SO (2003) Impact of leaf area index seasonality on the annual land surface evaporation in a global circulation model. Journal of Geophysical Research: Atmospheres (1984-2012) 108

Vandever MR, Pearson DS (1994) Forecaster's handbook for Bermuda. . Naval Atlantic Meteorology and Oceanography Facility, Bermuda,:101

REFERENCES

Varela A, Bertolin C, Muñoz-Tuñón C, Ortolani S, Fuensalida J (2008) Astronomical site selection: on the use of satellite data for aerosol content monitoring. Monthly Notices of the Royal Astronomical Society 391:507-520

Varela AM, Muñoz-Tuñon C, Espinosa JMR, Garcia-Lorenzo B, Cuevas E Non-correlation between atmospheric extinction coefficient and TOMS aerosol index at the Canarian Observatories. In. Proc Remote Sensing. International Society for Optics and Photonics

Vargas P (2007) Are Macaronesian islands refugia of relict plant lineages?: a molecular survey. In: Phylogeography of southern European refugia. Springer

Veza JM (2001) Desalination in the Canary Islands: an update. Desalination 133:259-270

Virkar Y, Clauset A (2012) Power-law distributions in binned empirical data.

Visbeck M, Chassignet EP, Curry RG, Delworth TL, Dickson RR, Krahmann G (2003) The ocean's response to North Atlantic Oscillation variability. The North Atlantic Oscillation: climatic significance and environmental impact:113-145

Walsh R, Lawler D (1981) Rainfall seasonality: description, spatial patterns and change through time. Weather 36:201-208

Wang N, Lu C (2010) Two-dimensional continuous wavelet analysis and its application to meteorological data. Journal of Atmospheric and Oceanic Technology 27:652-666

Weiguo S, Jian W, Kohyu S, Weicheng F (2006) Three types of power-law distribution of forest fires in Japan. Ecological Modelling 196:527-532

Weisse R, von Storch H, Feser F (2005) Northeast Atlantic and North Sea storminess as simulated by a regional climate model during 1958-2001 and comparison with observations. Journal of Climate 18:465-479

Weng H, Lau K (1994) Wavelets, period doubling, and time-frequency localization with application to organization of convection over the tropical western Pacific. Journal of the Atmospheric Sciences 51:2523-2541

West GB, Brown JH, Enquist BJ (1997) A general model for the origin of allometric scaling laws in biology. Science 276:122-126

Westra S, Sharma A (2006) Dominant modes of interannual variability in Australian rainfall analyzed using wavelets. Journal of Geophysical Research: Atmospheres (1984-2012) 111

White EP, Enquist BJ, Green JL (2008) On estimating the exponent of power-law frequency distributions. Ecology 89:905-912

Wiegand T, A Moloney K (2004) Rings, circles, and nullâ€ models for point pattern analysis in ecology. Oikos 104:209-229

Wilks DS (2006) Comparison of ensemble-MOS methods in the Lorenz'96 setting. Meteorological Applications 13:243-256

WMO (1984) Technical regulations. WMO Publ 49:5044

Wooster W, Bakun A, McLain D (1976) The seasonal upwelling cycle along the eastern boundary of the North Atlantic. J mar Res 34:130-141

Yang Y, Fang J, Ma W, Wang W (2008) Relationship between variability in aboveground net primary production and precipitation in global grasslands. Geophysical Research Letters 35

Yi H, Shu H (2012) The improvement of the Morlet wavelet for multi-period analysis of climate data. Comptes Rendus Geoscience 344:483-497

Yost D, Jones R, Rowe C, Mitchelmore CL (2012) Quantification of total and particulate dimethylsulfoniopropionate (DMSP) in five Bermudian coral species across a depth gradient. Coral reefs 31:561-570

Zhang M, Cess R, Xie S (1996) Relationship between cloud radiative forcing and sea surface temperatures over the entire tropical oceans. Journal of Climate 9:1374-1384

Zhang Z, Moore JC, Grinsted A (2014) Haar wavelet analysis of climatic time series. International Journal of Wavelets, Multiresolution and Information Processing 12:1450020

Zou KH, Tuncali K, Silverman SG (2003) Correlation and Simple Linear Regression1. Radiology 227:617-628

10. Annexes

ANNEXE

Table A. Data availability with a percentage higher than 95% in La Palma (LPa), La Gomera (G) and El Hierro (EH) .Code of station (Ind.), station name (St.name), orientation (North N (1) /South S (2)) , elevation (Elev.(m), latitude (Lat.(deg.)), longitude (Lon.(deg.)), number of dates with -4 (N(-4)), number of dates with negligible rainfall (N(-3)), number of zeros (N(0)), number of values (N(>0)), the number of data coded by -9999 or not data (N(-9999)), the number of blank spaces or no data (N (B)), number of real data (N R), percentage of data (data %), initial year (Ini.yr.), last year (Last yr.) and total number of years (N.yrs.) AEMET.

Ind.	St.name	N(1)/S(2)	Elev.(m)	Lat.(deg.)	Lon.(deg.)	N(-4)	N(-3)	N(0)	N(>0)	N(-9999)	N(B)	N (R)	Data %	Ini.yr.	Last yr.	N.yrs.
C937M	FRONTERA-RASO	2	620	27,74	18,02	896	0	1141	154	0	0	2191	100,0	1989	1994	6
C125C	PASO-ALTOS ERMITA	1	1050	28,66	17,83	1721	0	408	62	0	0	2191	100,0	1981	1986	6
C319E	VALLEHERMOSO	2	212	28,18	17,26	120	105	2901	526	0	0	3652	100,0	1981	1990	10
C929I	HIERRO/AEROPUERTO	2	32	27,82	17,89	0	336	9461	1160	0	0	10957	100,0	1981	2010	30
C139E	LA PALMA/AEROPUERTO	1	33	28,63	17,75	0	278	8588	2062	29	0	10928	99,7	1981	2010	30
C128B	LLANOS ARIDANE-B	1	410	28,66	17,91	0	134	9720	1041	0	62	10895	99,4	1981	2010	30
C315I	VALLE GRAN REY-HAYAS	2	1007	28,13	17,29	1251	0	3468	364	0	31	5083	99,4	1984	1997	14
C127E	PASO-MANCHAS	1	620	28,60	17,88	0	0	4517	565	0	31	5082	99,4	1981	1994	14
C134K	CUMBRE NUEVA-LOMO SARGENTA	1	1375	28,65	17,82	2641	0	1253	92	0	31	3986	99,2	1985	1995	11
C127C	PASO-FATIMA A	1	735	28,66	17,88	1	10	7518	780	0	92	8309	98,9	1986	2008	23
C127U	FUENCALIENTE-CALETAS	1	498	28,50	17,83	1	67	9598	1168	0	123	10834	98,9	1981	2010	30
C127F	PASO-MANCHAS A	1	676	28,60	17,88	0	39	8271	1063	0	123	9373	98,7	1985	2010	26
C138N	BREÑA ALTA-BOTAZO	1	523	28,67	17,79	37	248	6858	1500	0	123	8643	98,6	1987	2010	24
C326C	ALAJERO	2	855	28,06	17,24	55	38	9755	955	0	154	10803	98,6	1981	2010	30
C145U	GARAFIA-MONTE TRICIAS	1	1209	28,77	17,95	3997	0	1984	136	0	92	6117	98,5	1985	2001	17
C917A	SABINAR-TAJUTANTA	2	570	27,75	18,13	1750	0	5844	319	0	122	7913	98,5	1981	2002	22
C319X	VALLEHERMOSO-DAMA	2	250	28,06	17,30	0	18	10208	549	0	182	10775	98,3	1981	2010	30
C939U	SABINOSA	2	299	27,75	18,10	1	373	8468	1930	0	185	10772	98,3	1981	2010	30
C113C	PUNTAGORDA-REVENTON	1	1525	28,75	17,93	3410	0	2560	116	0	123	6086	98,0	1985	2001	17
C316L	VALLE GRAN REY-ARURE ACARDECE	2	840	28,14	17,31	568	34	4484	636	0	122	5722	97,9	1981	1996	16
C139R	SANTA C.PALMA-MIRCA	1	199	28,70	17,76	0	279	7588	2454	0	271	10321	97,4	1982	2010	29
C317B	AGULO-JUEGO BOLAS	2	765	28,18	17,21	3248	4	5030	961	40	213	9243	97,3	1985	2010	26
C915I	DEHESA-MIRADOR SERRADOR	2	1130	27,73	18,10	2307	0	3722	364	0	181	6393	97,2	1985	2002	18

ANNEXE

Ind.	St.name	N(1)/S(2)	Elev.(m)	Lat.(deg.)	Lon.(deg.)	N(-4)	N(-3)	N(0)	N(>0)	N(-9999)	N(B)	N (R)	Data %	Ini.yr.	Last yr.	N.yrs.
C129A	TAZACORTE	1	164	28,64	17,93	31	0	9819	770	0	337	10620	96,9	1981	2010	30
C126L	FUENCALIENTE-CHARCO A	1	875	28,56	17,87	212	61	7778	1506	0	305	9557	96,9	1984	2010	27
C147F	BARLOVENTO-C.F.	1	580	28,82	17,80	15	868	4295	2236	11	245	7414	96,7	1981	2001	21
C328T	HERMIGUA-VALL.ALTO CORRALETE	2	375	28,16	17,20	148	63	7589	663	0	303	8463	96,5	1987	2010	24
C115Z	TIJARAFE-TIME	1	1220	28,69	17,92	3766	0	2100	128	0	215	5994	96,5	1985	2001	17
C916S	PINAR ROQUE	2	859	27,70	17,98	14	0	6515	864	3	274	7393	96,4	1990	2010	21
C318F	VALLEHERMOSO-MACAYO ROQUILLO	2	410	28,17	17,27	488	209	6509	1225	0	335	8431	96,2	1981	2004	24
C316B	AGULO-FUENSANTA	2	995	28,15	17,25	6745	6	1322	331	0	362	8404	95,9	1984	2007	24
C917T	PINAR-LLANOS	2	720	27,69	17,98	23	0	7155	525	0	332	7703	95,9	1985	2006	22
C128D	LLANOS ARIDANE-HERMOSILLA	1	494	28,66	17,90	1	255	8536	1009	0	426	9801	95,8	1983	2010	28
C316M	VALLE GRAN REY-HOYA JUAN DIAZ	2	980	28,14	17,30	853	2	2369	276	0	153	3500	95,8	1987	1996	10
C927U	GUARAZOCA	2	585	27,81	17,97	206	34	8265	928	0	428	9433	95,7	1981	2007	27
C148M	GARAFIA-JUAN ADALID	1	290	28,84	17,90	108	5	7412	508	0	367	8033	95,6	1985	2007	23
C319I	VALLEHERMOSO-ALOJERA LOMADAS	2	125	28,17	17,32	529	0	3765	242	0	212	4536	95,5	1985	1997	13
C317H	VALLEHERMOSO-DEGOLLADA ASNOS	2	752	28,08	17,28	968	4	6935	464	0	395	8371	95,5	1987	2010	24
C326I	SAN SEBASTIAN-VEGAIPALA	2	900	28,10	17,19	0	0	2191	244	0	121	2435	95,3	1985	1991	7
C329E	SAN SEBASTIAN-PLAYA CABRITO	2	41	28,07	17,14	2	1	7488	512	0	398	8003	95,3	1988	2010	23
C319L	VALLE GRAN REY-TAGULUCHE	2	306	28,14	17,33	58	1	8541	442	0	454	9042	95,2	1985	2010	26
C925C	VALVERDE-MÑA.FRAILE	2	1160	27,74	17,97	1958	12	1935	266	0	212	4171	95,2	1983	1994	12
C317E	VALLEHERMOSO-CAÑADA TORIL	2	580	28,16	17,25	4136	46	4332	520	5	457	9034	95,1	1985	2010	26
C145J	BARLOVENTO-REFUGIO GALLEGOS	1	1200	28,80	17,84	5421	9	218	256	0	305	5904	95,1	1985	2001	17

ANNEXE

Table B. Data availability with a percentage higher than 95% in Tenerife (Ten.) Code of station (Ind.), station name (St.name), orientation (North N (1) /South S (2)) , elevation (Elev.(m), latitude (Lat.(deg.)), longitude (Lon.(deg.)), number of dates with -4 (N(-4)), number of dates with negligible rainfall (N(-3)), number of zeros (N(0)), number of values (N(>0)), the number of data coded by -9999 or not data (N(-9999)), the number of blank spaces or no data (N (B)), number of real data (N R), percentage of data (data %), initial year (Ini.yr.), last year (Last yr.) and total number of years (N.yrs.) AEMET.

Ind.	St.name	N(1)/S(2)	Elev.(m)	Lat.(deg.)	Lon.(deg.)	N(-4)	N(-3)	N(0)	N(>0)	N(-9999)	N(B)	N (R)	Data %	Ini.yr.	Last yr.	N.yrs.
C418O	ADEJE-MENORES	2	300	28,14	16,76	0	0	347	18	0	0	365	100,0	1989	1989	1
C466K	ICOD-CERRO GORDO	1	920	28,34	16,73	0	0	325	41	0	0	366	100,0	1988	1988	1
C458K	OROTAVA-BARROS	1	340	28,38	16,51	0	0	332	34	0	0	366	100,0	1988	1988	1
C458E	SAUZAL	1	455	28,47	16,43	0	23	842	230	0	0	1095	100,0	1981	1983	3
C449C	STA.CRUZ DE TENERIFE	1	35	28,46	16,26	0	701	8472	1784	0	0	10957	100,0	1981	2010	30
C429I	TENERIFE/SUR	2	64	28,05	16,56	0	228	10009	717	3	0	10954	100,0	1981	2010	30
C468A	GUANCHA (ASOMADA)	1	572	28,37	16,65	0	223	8912	1762	0	60	10897	99,5	1981	2010	30
C469A	SAN JUAN DE LA RAMBLA	1	106	28,39	16,65	0	614	8693	1527	0	123	10834	98,9	1981	2010	30
C428E	ARONA-BUZANADA	2	280	28,06	16,65	116	0	2337	73	0	31	2526	98,8	1988	1994	7
C428J	GRANADILLA-YACO	2	375	28,08	16,56	1056	0	1434	36	0	31	2526	98,8	1988	1994	7
C412C	GUIA ISORA-SAMARA	2	1958	28,27	16,72	4569	11	4579	181	1	155	9340	98,4	1985	2010	26
C446R	TEGUESTE-PEDRO ALVAREZ A	1	625	28,53	16,31	14	0	5929	1241	1	120	7184	98,3	1986	2005	20
C451U	REALEJOS-PORTILLO	1	2137	28,30	16,57	140	1	10172	460	0	184	10773	98,3	1981	2010	30
C438I	ARAFO	1	499	28,34	16,42	0	351	9389	1031	0	186	10771	98,3	1981	2010	30
C406A	CAÑADAS-UCANCA LLANO	2	2051	28,21	16,65	3571	9	4890	147	0	149	8617	98,3	1987	2010	24
C428F	ARONA-CAMELLA MORRO NEGRO	2	503	28,09	16,69	0	101	7529	616	1	154	8246	98,2	1988	2010	23
C406C	CAÑADAS-ENCERRADERO	2	2155	28,24	16,70	4222	5	5254	196	0	185	9677	98,1	1984	2010	27
C447A	TENERIFE/LOS RODEOS	1	632	28,48	16,33	0	724	7223	2799	0	211	10746	98,1	1981	2010	30
C424E	VILAFLOR	2	1435	28,15	16,64	21	3	10088	630	0	215	10742	98,0	1981	2010	30
C412M	GUIA ISORA-CHAVAO	2	1998	28,22	16,70	4534	7	4580	162	0	213	9283	97,8	1985	2010	26
C457C	TACORONTE	1	564	28,48	16,41	0	371	7859	2481	0	246	10711	97,8	1981	2010	30
C414O	ADEJE-CEDRO FYFFES	2	1350	28,19	16,71	4521	8	3877	146	0	214	8552	97,6	1987	2010	24
C463H	ICOD-BARRENOS	1	1510	28,30	16,71	4241	0	2714	167	0	183	7122	97,5	1987	2006	20

ANNEXE

Ind.	St.name	N(1)/S(2)	Elev.(m)	Lat.(deg.)	Lon.(deg.)	N(-4)	N(-3)	N(0)	N(>0)	N(-9999)	N(B)	N (R)	Data %	Ini.yr.	Last yr.	N.yrs.
C448S	TEGUESTE	1	435	28,52	16,34	0	17	9177	1488	0	275	10682	97,5	1981	2010	30
C427E	SAN MIGUEL ABONA	2	642	28,10	16,62	0	0	10234	447	0	276	10681	97,5	1981	2010	30
C448L	ANAGA-CAMPANARIO	1	330	28,56	16,20	148	0	7927	1175	0	246	9250	97,4	1985	2010	26
C458L	SANTA URSULA	1	344	28,42	16,49	31	22	7435	1399	28	216	8887	97,3	1986	2010	25
C440J	SANTA C. TFE-DEPURADORA	1	85	28,45	16,27	536	0	1495	101	0	59	2132	97,3	1990	1995	6
C438H	GUIMAR-CASINO	1	358	28,32	16,41	23	0	7761	368	4	245	8152	97,0	1988	2010	23
C433K	CANDELARIA-BOCA DEL VALLE	1	1565	28,38	16,41	3342	2	2184	134	0	182	5662	96,9	1988	2003	16
C448O	ANAGA-TAGANANA FAJANETAS	1	402	28,55	16,21	78	58	9053	1371	0	397	10560	96,4	1981	2010	30
C467T	BUENAVISTA-PORTELAS	1	690	28,32	16,84	30	0	3401	436	0	151	3867	96,2	1983	1993	11
C468H	ICOD-PIE DE LAS LAJAS	1	350	28,37	16,70	167	0	6694	869	0	306	7730	96,2	1984	2005	22
C416O	ADEJE-TAUCHO	2	910	28,15	16,73	3381	9	6126	316	0	395	9832	96,1	1983	2010	28
C455F	TACORONTE-PARCELA	1	1010	28,44	16,39	3290	8	1109	157	0	184	4564	96,1	1985	1997	13
C416A	SANTIAGO DEL TEIDE	1	902	28,30	16,82	59	0	8338	1433	0	397	9830	96,1	1983	2010	28
C466Q	SILOS-MONTE DEL AGUA	1	900	28,32	16,81	4760	0	1042	164	0	244	5966	96,1	1984	2000	17
C467A	GUANCHA-C.F.	1	580	28,36	16,61	4	0	4765	831	0	244	5600	95,8	1983	1998	16
C459S	REALEJOS-SAN AGUSTIN	1	312	28,39	16,59	0	0	8440	996	0	426	9436	95,7	1984	2010	27
C434M	CANDELARIA-CHIVISAYA	1	1300	28,37	16,42	5622	11	2213	186	0	368	8032	95,6	1985	2007	23
C468F	ICOD-SANTA BARBARA	1	468	28,37	16,69	30	304	6967	1069	0	396	8370	95,5	1987	2010	24
C447V	LAGUNA (MONTAÑA GILES)	1	535	28,46	16,32	2615	0	430	89	0	153	3134	95,3	1991	1999	9
C458P	OROTAVA-RAMAL	1	268	28,39	16,51	59	0	2825	250	0	153	3134	95,3	1981	1989	9
C437L	ARAFO-BARRANCO AFOÑA	1	610	28,35	16,40	5447	15	2361	180	0	397	8003	95,3	1985	2007	23
C430E	IZAÑA	1	2371	28,31	16,50	0	235	8979	1220	5	518	10434	95,2	1981	2010	30
C448X	TEGUESTE-DRAGO	1	417	28,51	16,36	32	208	6558	1540	0	428	8338	95,1	1987	2010	24
C457R	REALEJOS-PALO BLANCO	1	675	28,36	16,57	27	1	6583	1030	0	395	7641	95,1	1984	2005	22
C447I	LAGUNA-CERCADO MESA	1	510	28,48	16,32	235	17	1218	266	0	90	1736	95,1	1987	1991	5
C459G	SAUZAL-NARANJOS	1	260	28,47	16,45	129	152	4983	1676	0	365	6940	95,0	1991	2010	20

ANNEXE

Table C. Data availability with a percentage higher than 95% in Canaria (GC). Code of station (Ind.), station name (St.name), orientation (North N (1) /South S (2)) , elevation (Elev.(m), latitude (Lat.(deg.)), longitude (Lon.(deg.)), number of dates with -4 (N(-4)), number of dates with negligible rainfall (N(-3)), number of zeros (N(0)), number of values (N(>0)), the number of data coded by -9999 or not data (N(-9999)), the number of blank spaces or no data (N (B)), number of real data (N R), percentage of data (data %), initial year (Ini.yr.), last year (Last yr.) and total number of years (N.yrs.)AEMET.

Ind.	St.name	N(1)/S(2)	Elev.(m)	Lat.(deg.)	Lon.(deg.)	N(-4)	N(-3)	N(0)	N(>0)	N(-9999)	N(B)	N (R)	Data %	Ini.yr.	Last yr.	N.yrs.
C658N	LAS PALMAS DE G.C. (JARDIN CANARIO II)	1	260	28,06	15,46	238	72	5923	1072	0	0	7305	100,0	1991	2010	20
C659Q	LAS PALMAS DE G.C.-LAS CANTERAS	1	15	28,10	15,43	0	9	9689	1259	0	0	10957	100,0	1981	2010	30
C649I	GRAN CANARIA/AEROPUERTO	2	24	27,92	15,39	0	569	9205	1177	6	0	10951	99,9	1981	2010	30
C658L	LAS PALMAS DE G.C. (TAFIRA CMT)	1	269	28,08	15,45	0	126	5206	1221	21	0	6553	99,7	1993	2010	18
C665M	VALLESECO-EL CASERON	1	890	28,06	15,57	3	0	5982	2019	0	31	8004	99,6	1989	2010	22
C656J	SANTA BRIGIDA-FINCA MADROÑAL	1	700	28,02	15,52	19	52	5069	1038	0	31	6178	99,5	1994	2010	17
C659B	TELDE-JINAMAR	1	95	28,03	15,42	0	387	4212	849	0	31	5448	99,4	1996	2010	15
C649U	TELDE-LOS LLANOS	2	150	28,00	15,42	0	327	8894	1644	0	92	10865	99,2	1981	2010	30
C656U	TEROR-DOMINICAS	1	630	28,07	15,54	2	3	8526	2333	0	93	10864	99,2	1981	2010	30
C647O	VALSEQUILLO-GRANJA LAS ROSAS	2	540	27,99	15,49	13	367	8568	1875	11	123	10823	98,8	1981	2010	30
C649W	TELDE-LA PARDILLA	1	50	28,01	15,39	4	85	9376	1337	0	155	10802	98,6	1981	2010	30
C669A	ARUCAS (BAÑADEROS)	1	50	28,15	15,53	21	528	9259	967	0	182	10775	98,3	1981	2010	30
C658P	LAS PALMAS DE G.C.-TAMARACEITE	1	200	28,10	15,47	5	0	8946	1823	0	183	10774	98,3	1981	2010	30
C668A	ARUCAS-HEREDAD	1	250	28,12	15,52	243	33	9002	1493	0	186	10771	98,3	1981	2010	30
C654O	SAN MATEO-LOMO ALJORRADERO	2	1070	28,00	15,55	0	48	8429	2294	0	186	10771	98,3	1981	2010	30
C658K	SANTA BRIGIDA-EL TEJAR	1	390	28,04	15,50	1	222	7992	2529	0	213	10744	98,1	1981	2010	30
C648T	TELDE-CAPELLANIA	2	260	27,98	15,43	165	52	6203	734	0	151	7154	97,9	1991	2010	20
C652I	SAN MATEO-HOYA GAMONAL	2	1480	27,97	15,56	0	1	8480	2231	0	245	10712	97,8	1981	2010	30
C626E	MOGAN-BARRANQUILLO ANDRES	2	715	27,89	15,68	79	291	9511	799	3	274	10680	97,5	1981	2010	30
C613E	AGAETE-PINAR DE TAMADABA	1	1255	28,05	15,69	11	3	8250	2048	3	277	10312	97,4	1981	2009	29

ANNEXE

Ind.	St.name	N(1)/S(2)	Elev.(m)	Lat.(deg.)	Lon.(deg.)	N(-4)	N(-3)	N(0)	N(>0)	N(-9999)	N(B)	N (R)	Data %	Ini.yr.	Last yr.	N.yrs.
C653O	SAN MATEO-CUEVA GRANDE	2	1380	27,99	15,57	1	29	8718	1904	0	305	10652	97,2	1981	2010	30
C668O	GUIA-PRESA JIMENEZ	1	240	28,13	15,63	3	45	8651	1925	0	333	10624	97,0	1981	2010	30
C646O	VALSEQUILLO-HACIENDA LOS MOCANES	2	620	27,98	15,49	0	234	8820	1569	0	334	10623	97,0	1981	2010	30
C667K	MOYA-HEREDAD	1	460	28,11	15,58	18	0	9011	1593	0	335	10622	96,9	1981	2010	30
C658J	LAS PALMAS DE G.C.-JARDIN CANARIO I	1	270	28,06	15,46	15	18	8735	1851	0	338	10619	96,9	1981	2010	30
C657E	SANTA BRIGIDA-CAMPO DE GOLF BANDAMA	1	450	28,03	15,46	4	473	8228	1890	0	362	10595	96,7	1981	2010	30
C659U	LAS PALMAS DE G.C.-TENOYA	1	160	28,11	15,49	13	88	9238	1252	0	366	10591	96,7	1981	2010	30
C662I	VALLESECO-LA RETAMILLA	1	1400	28,03	15,60	13	0	8328	2250	0	366	10591	96,7	1981	2010	30
C665O	MOYA-LOMO LA MAJADILLA	1	980	28,07	15,62	21	0	8460	2109	3	364	10590	96,7	1981	2010	30
C658O	LAS PALMAS DE G.C.-SAN LORENZO	1	220	28,08	15,48	29	0	8700	1500	0	363	10229	96,6	1982	2010	29
C646E	AGUIMES-TEMISAS	2	690	27,91	15,51	4	4	9693	857	0	399	10558	96,4	1981	2010	30
C657K	SANTA BRIGIDA (MONTE COELLO)	1	460	28,05	15,47	17	97	5039	1181	0	240	6334	96,3	1993	2010	18
C659J	LAS PALMAS DE G.C.-MAYORAZGO	1	60	28,10	15,43	3	676	8479	1397	0	402	10555	96,3	1981	2010	30
C658V	LAS PALMAS DE G.C.-EL TOSCON	1	310	28,09	15,51	46	36	8769	1679	1	426	10530	96,1	1981	2010	30
C624E	TEJEDA-VIVERO DE ÑAMERITAS	2	1040	27,93	15,68	96	161	9302	969	0	429	10528	96,1	1981	2010	30
C652O	SAN MATEO-LAS MESAS DE ANA LOPEZ	2	1480	27,99	15,58	33	0	8585	1909	1	429	10527	96,1	1981	2010	30
C614I	TEJEDA-PINAR DE PAJONALES	2	1190	27,95	15,66	99	163	9243	993	0	459	10498	95,8	1981	2010	30
C619O	SAN NICOLAS TOLENTINO-CASCO	2	80	27,98	15,78	2	338	9498	632	0	487	10470	95,6	1981	2010	30
C667J	VALLESECO-LAS MADRES	1	560	28,07	15,58	244	15	8349	1862	0	487	10470	95,6	1981	2010	30
C649F	AGUIMES-PILETAS	2	100	27,88	15,45	3	2	9574	889	0	489	10468	95,5	1981	2010	30
C655P	SAN MATEO-LA SOLANA	1	780	28,03	15,53	2	0	6413	1592	0	394	8007	95,3	1988	2010	23
C625A	MOGAN (INAGUA)	2	950	27,93	15,74	221	211	9209	796	28	492	10437	95,3	1981	2010	30
C614G	TEJEDA-LA CULATA	2	1180	27,98	15,60	2	0	9088	1347	0	520	10437	95,3	1981	2010	30
C614E	TEJEDA-RINCON DE TEJEDA	1	1090	28,00	15,61	1	0	8969	1465	0	522	10435	95,2	1981	2010	30
C665L	MOYA-FONTANALES CISTERNA	1	950	28,06	15,60	2	1	7844	2586	1	523	10433	95,2	1981	2010	30

ANNEXE

Table D. Data availability with a percentage higher than 95% in Lanzarote (Lz) and Fuerteventura (Fv). Code of station (Ind.), station name (St.name), orientation (North N (1) /South S (2)) , elevation (Elev.(m), latitude (Lat.(deg.)), longitude (Lon.(deg.)), number of dates with -4 (N(-4)), number of dates with negligible rainfall (N(-3)), number of zeros (N(0)), number of values (N(>0)), the number of data coded by -9999 or not data (N(-9999)), the number of blank spaces or no data (N (B)), number of real data (N R), percentage of data (data %), initial year (Ini.yr.), last year (Last yr.) and total number of years (N.yrs.) AEMET.

Ind.	St.name	N(1)/S(2)	Elev.(m)	Lat.(deg.)	Lon.(deg.)	N(-4)	N(-3)	N(0)	N(>0)	N(-9999)	N(B)	N (R)	Data %	Ini.yr.	Last yr.	N.yrs.
C038P	HARIA-CASCO	1	270	29,15	13,50	91	0	7137	807	0	0	8035	100,0	1989	2010	22
C249I	FUERTEVENTURA/AEROPUERTO	1	25	28,44	13,86	0	259	9843	855	0	0	10957	100,0	1981	2010	30
C029O	LANZAROTE/AEROPUERTO	1	14	28,95	13,60	0	454	9340	1163	0	0	10957	100,0	1981	2010	30
C029R	ARRECIFE (GRANJA CABILDO)	1	110	29,00	13,56	0	7	6160	760	13	0	6927	99,8	1992	2010	19
C039J	HARIA-ARRIETA	1	30	29,14	13,45	12	0	7152	842	0	29	8006	99,6	1989	2010	22
C039I	HARIA-MALA	1	40	29,09	13,47	2	55	7266	682	0	30	8005	99,6	1989	2010	22
C049U	TINAJO-CASCO	1	180	29,07	13,68	2	441	6599	961	1	31	8003	99,6	1989	2010	22
C018L	YAIZA-LA GERIA	1	310	28,98	13,71	1	212	5624	1072	0	31	6909	99,6	1992	2010	19
C038V	HARIA-GUINATE	1	370	29,18	13,49	0	232	7001	740	1	61	7973	99,2	1989	2010	22
C028I	TIAS-LA ASOMADA	1	240	28,95	13,69	0	0	3962	362	0	59	4324	98,7	1981	1992	12
C039U	HARIA-ORZOLA	1	40	29,21	13,45	0	0	9910	899	0	148	10809	98,6	1981	2010	30
C028K	TIAS-MASDACHE	1	320	28,99	13,66	2	200	6120	881	10	92	7203	98,6	1991	2010	20
C239E	TUINEJE-TARAJALEJO	2	30	28,20	14,12	10	51	7564	253	3	154	7878	98,0	1989	2010	22
C037I	HARIA-MONTAÑA DE HARIA	1	580	29,13	13,51	1	0	8957	1059	0	210	10017	97,9	1983	2010	28
C239O	TUINEJE-GRAN TARAJAL	2	130	28,25	14,02	24	51	7538	238	0	184	7851	97,7	1989	2010	22
C239P	TUINEJE-CASCO	1	190	28,32	14,04	3	0	7371	449	0	212	7823	97,4	1989	2010	22
C019I	YAIZA-CASCO	1	150	28,95	13,77	0	0	9064	1193	1	334	10257	96,8	1982	2010	29
C029V	TEGUISE-CAMPO DE GOLF	1	110	29,01	13,52	1	86	5726	546	0	215	6359	96,7	1993	2010	18
C259C	LA OLIVA-ISLA DE LOBOS	1	14	28,74	13,82	6	0	6894	164	0	241	7064	96,7	1991	2010	20
C018O	YAIZA-FEMES	1	360	28,91	13,78	13	0	7085	638	0	299	7736	96,3	1989	2010	22
C217E	BETANCURIA-CASTILLO DE LARA	1	470	28,41	14,06	3	102	9206	1200	27	419	10511	95,9	1981	2010	30
C239F	TUINEJE-TESEJERAGUE	1	120	28,28	14,11	0	1	7226	444	0	364	7671	95,5	1989	2010	22

ANNEXE

Ind.	St.name	N(1)/S(2)	Elev.(m)	Lat.(deg.)	Lon.(deg.)	N(-4)	N(-3)	N(0)	N(>0)	N(-9999)	N(B)	N (R)	Data %	Ini.yr.	Last yr.	N.yrs.
C028J	TIAS (CASCO)	1	210	28,95	13,65	1	21	9656	769	1	509	10447	95,3	1981	2010	30
C248A	ANTIGUA-AGUA DE BUEYES	1	280	28,38	14,02	21	317	9384	715	0	520	10437	95,3	1981	2010	30
C038E	TEGUISE-CHIMIDAS	1	300	29,07	13,56	6	32	6887	713	0	397	7638	95,1	1989	2010	22

ANNEXE

Table E. Monthly NRD (Numer of rainfall days) (days month $^{-1}$). Daily rainfall data from weather automated and not automated stations. Canary,

, Madeira and Bermuda Islands. Period 1981-2010. Daily data from AEMET/IPMA/BWS.

Month	A1	A2	A5	A7	P2	P13	P14	P15	T1	T2	T5	T12	T13	T14	T15	Az	M	BER1	Total
Jan.	233	223	104	175	290	316	177	309	294	259	173	41	137	147	280	664	297	526	5344
Feb.	200	193	131	169	253	285	133	266	273	241	186	77	140	141	252	584	286	478	4723
Mar.	185	179	109	161	225	272	118	250	262	247	156	52	138	124	233	607	255	457	1199
Abr.	149	146	74	120	244	262	102	225	243	217	130	30	108	110	215	530	238	368	4030
May	83	85	37	79	168	201	52	151	178	148	72	11	54	58	138	523	165	299	4645
Jun.	40	28	16	44	90	124	35	53	80	91	19	2	22	39	79	448	75	334	4288
Jul.	32	13	3	23	52	56	30	23	41	34	12	2	6	8	36	408	26	394	3511
Aug.	22	20	16	28	45	53	22	39	55	49	30	2	18	12	42	415	52	470	4074
Sep.	100	75	53	58	126	135	66	109	142	115	92	16	57	59	124	501	175	428	1619
Oct.	201	167	104	174	252	231	133	223	250	212	171	54	133	137	258	631	283	460	2431
Nov.	244	229	128	201	284	305	196	308	326	273	185	69	159	191	308	605	303	409	2502
Dec.	257	259	170	264	307	347	204	355	341	255	229	91	203	209	338	668	389	458	1390
Total	1746	1617	945	1496	2336	2587	1268	2311	2485	2141	1455	447	1175	1235	2303	6584	2544	5081	39756

ANNEXE

Table F. Monthly accumulated rainfall (mm month^{-1}). Daily rainfall data from weather automated and not automated stations. Canary, Azores, Madeira and Bermuda Islands. Period 1981-2010. Daily data from AEMET/IPMA/BWS.

Month	A1	A2	A5	A7	P2	P13	P14	P15	T1	T2	T5	T12	T13	T14	T15	Az	M	BER1	Total
Jan.	755	496	499	834	2419	2939	593	2499	944	1274	1422	601	1476	2114	1377	2953	2176	4139	29510
Feb.	732	547	596	1136	1981	2550	651	2631	1063	1110	1934	1180	1865	2107	1317	3247	2459	3682	30788
Mar.	376	374	440	750	1394	1967	365	1719	1134	1182	1676	720	1371	1555	1184	2674	1790	3566	24237
Abr.	177	157	221	382	1039	1146	147	851	347	600	523	280	702	887	593	1961	1305	3161	14479
May	33	47	32	68	541	625	59	291	107	249	213	55	259	382	218	2079	838	2668	8764
Jun.	10	4	3	32	228	267	23	61	28	187	15	23	27	100	119	1729	216	3566	6638
Jul.	2	0	2	4	129	123	14	19	2	23	13	3	8	66	32	885	48	3951	5324
Aug.	12	16	38	20	148	160	32	72	62	82	144	46	33	40	84	1356	58	4898	7301
Sep.	272	65	108	97	524	657	144	479	204	156	368	202	252	473	240	2763	984	3859	11847
Oct.	479	296	344	416	1479	1709	362	1454	560	1036	1034	731	1169	1647	957	3408	2645	4788	24514
Nov.	653	440	789	1104	2416	2936	538	2569	1023	1596	1455	1148	1917	2556	2268	3620	2583	2940	32551
Dec.	938	879	908	1332	2533	3118	758	3601	1296	1286	1682	1701	2900	3304	2267	4065	3435	3277	39280
Total	4439	3321	3980	6175	14831	18197	3686	16246	6770	8781	10479	6690	11979	15231	10656	30740	18537	44495	

ANNEXE

Table G. Monthly daily rainfall maxima (mm month^{-1}). Data from weather automated and not automated stations. Canaries, Azores, Madeira (rainfall ≥ 0.05 mm) and Bermuda (rainfall ≥ 0.25 mm d^{-1}). Period 1981-2010. Daily data from AEMET/IPMA/BWS.

Month	A1	A2	A5	A7	P2	P13	P14	P15	T1	T2	T5	T12	T13	T14	T15	Az	M	BER1	Max	
Jan.	75	22	46	79	115	166	23	156	65	37	145	80	123	119	73	142	90	101	166	P13
Feb.	65	55	61	280	75	103	112	129	104	58	158	105	107	160	79	391	120	97	391	Az
Mar.	52	39	53	70	51	106	33	120	233	87	337	70	79	162	75	84	65	92	337	T5
Abr.	21	16	20	121	75	53	19	58	23	23	74	40	61	79	45	43	111	70	121	A7
May	5	6	7	9	28	26	5	21	13	14	24	11	35	35	31	62	61	105	105	BER1
Jun.	3	1	1	14	17	14	2	6	7	35	5	18	5	15	33	59	43	197	197	BER1
Jul.	1	0	2	2	12	10	3	4	1	6	8	3	6	27	10	37	7	118	118	BER1
Aug.	4	7	19	5	16	20	18	9	26	14	29	46	10	8	24	52	8	157	157	BER1
Sep.	85	11	14	29	26	38	20	37	35	25	44	38	60	48	39	125	98	94	125	Az
Oct.	73	24	47	30	106	97	54	83	46	80	80	80	55	110	68	128	94	107	128	Az
Nov.	39	49	136	153	81	114	52	122	68	64	103	90	108	143	285	206	159	97	285	T15
Dec.	74	51	45	136	101	135	33	126	83	49	102	130	103	138	73	91	72	73	138	T14
Max	85	55	136	280	115	166	112	156	233	87	337	130	123	162	285	391	159	197	391	Az
	Sep.	Feb.	Nov.	Feb.	Jan.	Jan.	Feb.	Jan.	Mar.	Mar.	Mar.	Dec.	Jan.	Mar.	Nov.	Feb.	Nov.	Jun.		

ANNEXE

Table H. Inter-annual NRD (Number of rainfall days). (days. month^{-1}) Daily rainfall data from weather automated and not automated stations. Canaries, Azores, Madeira (rainfall ≥ 0.05 mm) and Bermuda (rainfall ≥ 0.25 mm). Period 1981-2010. Daily data from AEMET/IPMA/BWS.

Year	A1	A2	A5	A7	P2	P13	P14	P15	T1	T2	T5	T12	T13	T14	T15	Az	M	BER1	total
1981	51	43	30	14	56	52	21	54	98	63	64	15	43	27	65	222	93	159	1170
1982	73	54	32	20	86	71	32	55	108	70	49	14	44	38	89	253	60	158	1306
1983	62	51	34	32	44	49	17	36	79	60	43	20	45	27	87	234	99	177	1196
1984	81	62	39	24	87	54	31	70	115	86	52	24	51	44	110	222	80	158	1390
1985	65	62	20	27	79	81	30	58	84	87	45	9	41	37	88	206	103	171	1293
1986	68	65	27	18	79	83	30	66	92	78	40	11	34	33	84	197	56	170	1231
1987	55	62	44	39	66	60	30	47	84	75	53	29	60	48	103	257	95	164	1371
1988	53	57	35	40	66	84	38	49	89	72	47	24	42	51	97	253	85	167	1349
1989	71	67	35	53	75	99	57	58	87	81	62	16	55	45	93	241	99	157	1451
1990	78	50	35	44	84	34	57	60	93	76	57	15	45	41	71	238	95	132	1305
1991	69	58	22	45	65	92	37	61	83	64	49	12	37	38	66	209	81	139	1227
1992	47	48	23	52	73	95	39	64	76	77	42	12	28	28	71	210	84	177	1246
1993	60	54	25	59	84	124	53	73	75	82	58	13	34	33	84	245	83	159	1398
1994	42	45	12	38	56	68	38	39	49	43	35	8	17	19	46	221	60	165	1001
1995	45	42	23	50	49	66	37	46	56	53	62	13	29	27	60	227	80	168	1133
1996	68	77	43	91	83	93	57	98	99	90	71	18	53	42	92	262	107	171	1615
1997	47	53	24	59	73	95	57	82	79	70	47	8	30	28	68	252	109	185	1366
1998	39	35	20	48	64	82	26	75	62	62	39	7	29	27	56	216	68	178	1133
1999	72	50	24	48	93	98	54	111	98	69	33	9	24	30	66	217	75	185	1356
2000	34	46	27	38	62	76	35	77	77	43	43	8	28	28	60	221	75	191	1169
2001	62	31	32	53	69	97	29	96	75	63	15	17	33	24	73	248	98	167	1282
2002	78	60	32	80	86	102	65	103	84	78	0	13	36	28	99	217	89	182	1432

ANNEXE

Year	A1	A2	A5	A7	P2	P13	P14	P15	T1	T2	T5	T12	T13	T14	T15	Az	M	BER1	total
2003	70	51	25	63	74	105	54	98	78	78	50	9	21	28	70	207	84	177	1342
2004	93	63	36	65	105	124	60	118	90	67	75	18	38	46	64	176	73	166	1477
2005	66	54	43	65	69	81	44	85	73	61	60	20	51	61	71	175	93	183	1355
2006	64	56	39	61	106	105	47	115	78	77	57	19	38	67	72	195	85	182	1463
2007	33	44	34	49	106	90	49	94	79	64	46	8	36	57	51	160	70	167	1237
2008	40	59	35	67	107	113	48	122	87	84	63	17	38	75	72	186	73	167	1453
2009	34	60	33	68	114	128	55	112	90	88	48	17	44	78	102	215	92	179	1557
2010	26	58	62	86	76	88	41	89	68	80	50	24	71	80	74	202	100	180	1455
Total	1746	1617	945	1496	2338	2587	1268	2311	2485	2141	1455	447	1175	1235	2303	6584	2544	5081	

ANNEXE

Table I. Interannual accumulated rainfall (mm.yr^{-1}). Daily rainfall data from weather automated and not automated stations. Canaries, Azores, Madeira (rainfall ≥ 0.05 mm) and Bermuda (rainfall ≥ 0.25 mmd^{-1}). Period 1981-2010. Daily data from AEMET/IPMA/BWS.

Year	A1	A2	A5	A7	P2	P13	P14	P15	T1	T2	T5	T12	T13	T14	T15	Az	M	BER1	Total
1981	81	58	64	92	393	404	63	469	218	257	413	113	243	427	210	1143	354	1376	6378
1982	112	83	92	144	549	880	85	588	182	231	406	120	349	550	289	999	376	1347	7382
1983	47	63	251	204	221	299	44	166	152	209	335	204	434	522	426	957	550	1877	6961
1984	195	102	154	124	599	426	105	660	238	288	447	224	495	596	344	962	753	1560	8272
1985	114	118	60	165	490	648	129	378	210	363	335	73	301	454	297	972	915	1594	7616
1986	119	80	51	102	565	702	117	579	251	293	352	89	111	458	155	971	311	1748	7054
1987	206	133	145	450	480	518	105	371	248	420	557	331	789	974	508	1490	900	1402	10027
1988	186	143	107	583	477	546	177	419	239	392	622	181	472	836	482	936	527	1689	9014
1989	240	298	266	191	666	937	263	758	409	500	739	365	610	729	496	989	838	1284	10578
1990	141	136	135	96	440	283	122	479	195	295	535	293	306	534	353	1182	707	1095	7327
1991	220	215	100	189	510	639	150	722	212	285	285	208	537	569	387	917	547	1141	7833
1992	78	46	85	65	538	594	137	422	138	250	165	136	251	424	269	899	415	1434	6346
1993	240	103	146	177	671	963	136	859	231	303	639	167	326	520	307	1014	583	1515	8900
1994	135	118	29	31	339	414	77	367	146	191	105	109	133	172	157	872	438	1628	5461
1995	164	113	130	170	286	349	76	389	189	233	249	188	240	326	279	1483	539	1479	6882
1996	205	141	210	204	588	836	213	566	359	375	321	378	646	588	441	1263	824	1423	9581
1997	102	86	92	235	393	482	100	259	191	342	286	171	288	382	233	1200	653	1768	7263
1998	82	73	76	205	303	380	35	312	105	184	107	134	287	399	293	918	471	1524	5888
1999	114	98	37	263	676	789	156	644	232	331	159	148	381	670	297	1058	525	1453	8031
2000	86	47	84	99	341	375	89	284	110	181	285	91	296	366	257	666	474	1763	5894
2001	138	43	83	203	339	568	57	553	179	228	49	243	450	440	426	1299	714	1526	7538
2002	184	55	216	277	563	684	147	635	468	288	0	390	427	482	549	1016	669	1540	8590
2003	118	95	70	56	509	679	102	468	141	384	184	117	169	344	247	841	598	1504	6626
2004	131	147	162	401	557	665	139	714	230	304	316	321	541	557	629	722	464	1428	8428

ANNEXE

Year	A1	A2	A5	A7	P2	P13	P14	P15	T1	T2	T5	T12	T13	T14	T15	Az	M	BER1	Total
2005	213	210	251	300	483	705	144	860	291	289	561	431	644	576	470	765	667	1399	9259
2006	308	117	348	118	519	725	175	649	325	327	524	406	337	574	237	816	573	1544	8622
2007	136	102	118	230	526	504	164	473	295	238	477	97	367	309	372	903	442	1436	7189
2008	100	98	102	172	527	849	97	760	190	238	256	217	347	316	234	959	616	1418	7496
2009	68	77	60	169	723	737	178	565	189	289	210	184	382	489	427	1177	715	1422	8061
2010	175	124	254	458	562	618	105	868	207	271	560	566	821	657	588	1352	1381	1176	10743
Total	4438	3322	3978	6173	14833	18198	3687	16246	6770	8779	10479	6695	11980	15240	10659	307401	18539	44495	

ANNEXE

Table J. Interannual daily rainfall maxima (mm.yr^{-1}). Data from weather automated and not automated stations. Canaries, Azores, Madeira (rainfall ≥ 0.05 mm) and Bermuda (rainfall ≥ 0.25 mm). Period 1981-2011. Daily data from AEMET/IPMA/BWS.

Year	A1	A2	A5	A7	P2	P13	P14	P15	T1	T2	T5	T12	T13	T14	T15	Az	M	BER1	Max
1981	23	33	19	18	46	40	17	60	46	36	61	30	44	95	29	52	35	97	97
1982	25	16	23	53	39	106	9	88	32	42	108	38	61	53	45	49	42	157	157
1983	15	15	136	50	38	52	17	31	68	45	103	76	73	123	81	51	36	94	136
1984	35	25	45	18	52	80	21	83	43	37	41	53	79	78	56	75	73	97	97
1985	28	22	10	34	35	40	20	39	23	27	62	20	48	67	39	35	56	72	72
1986	23	14	17	38	75	62	15	60	51	37	66	24	27	79	18	95	45	107	107
1987	85	21	38	146	51	48	30	67	33	80	80	54	123	143	57	99	92	105	146
1988	53	17	31	280	66	69	35	51	27	38	102	26	46	160	73	71	47	71	280
1989	65	55	97	77	75	85	112	115	83	49	75	90	108	86	102	73	98	81	112
1990	22	32	20	34	41	45	18	45	31	38	141	41	77	162	51	57	72	55	162
1991	61	51	28	38	57	90	33	120	34	36	42	53	103	138	73	91	56	57	138
1992	14	14	26	10	106	97	19	83	13	23	22	30	49	53	46	77	30	73	106
1993	50	14	53	30	101	135	31	120	23	38	337	50	44	100	26	128	89	89	135
1994	18	16	14	11	24	31	15	38	19	43	24	40	40	41	54	52	61	77	77
1995	52	39	32	43	30	31	20	46	49	32	38	58	54	47	65	391	95	83	391
1996	55	13	61	23	41	57	37	47	104	39	33	70	45	57	66	206	67	197	206
1997	29	9	20	121	57	63	16	54	33	35	41	35	55	110	20	79	68	105	121
1998	32	22	20	36	77	55	6	55	15	35	17	36	35	52	33	48	67	54	77
1999	10	24	10	136	110	166	15	156	32	37	33	56	101	85	27	69	53	78	166
2000	21	6	16	14	23	36	29	29	25	29	109	23	40	34	31	32	38	75	109
2001	39	22	14	25	33	72	12	85	39	44	20	55	76	55	75	47	91	92	92
2002	74	11	42	75	47	55	22	126	233	26	0	130	45	60	68	49	78	81	233
2003	24	24	19	6	35	54	9	39	15	40	26	43	29	68	30	61	65	111	111
2004	29	30	30	153	45	60	30	100	35	35	38	105	107	100	285	69	59	118	285

2005	27	44	57	79	63	103	20	94	53	40	77	87	72	62	69	49	44	83	103
2006	75	25	81	19	67	114	54	72	65	64	74	80	49	93	32	64	46	77	114
2007	47	16	46	74	115	80	33	140	74	87	145	31	61	56	73	142	64	68	142
2008	15	32	30	51	37	54	13	54	33	58	54	87	79	58	35	74	111	118	118
2009	9	11	10	29	51	46	52	48	33	38	26	32	77	122	44	55	82	65	122
2010	53	43	48	82	81	74	22	129	82	25	158	80	65	91	87	66	159	73	159
Max	85	55	136	280	115	166	112	156	233	87	337	130	123	162	285	391	159	197	

ANNEXE

Table K. Tropical systems that have affected Bermuda. Year, month and days affecting the islands, tropical system name and classification (hurricane (HR.) tropical storm (TS), subtropical storm (SS) and category (Cat.). Period 1895 to 2014. BWS.

Year	month	days	Name	Classif.
1895	10	24		HRCat.2
1899	9	04-05		HRCat.2
1899	9	12-13		HRCat.3
1900	9	17		HRCat.2
1903	9	28		HRCat.2
1906	9	09		TS
1910	9	25		HR
1915	9	03-04		HRCat. 3
1916	9	23		HRCat. 3
1917	9	04		HRCat. 3
1918	9	04		HRCat.2
1918	9	05		HRCat.2
1921	9	15		HRCat. 3
1922	9	21		HRCat. 3
1923	9	30		HRCat. 3
1926	8	06	unnamed	HRCat.2
1926	10	22	unnamed	HRCat.2
1932	11	12	unnamed	HRCat.2
1939	10	16	unnamed	HRCat. 4
1947	10	20	unnamed	HRCat. 3
1948	9	13	unnamed	HRCat. 3
1948	10	07	unnamed	HRCat.2
1949	9	08	unnamed	HRCat.3
1950	9	08	Dog	HR
1950	10	02	George	HRCat.1
1952	9	27	Charlie	HR
1953	9	05	Carol	HRCat.3
1953	9	12	Dolly	TS
1953	9	17	Edna	HR
1958	9	28	Ilsa	HRCat.2
1961	10	06-07	Frances	hur.Cat.3
1962	10	06	Daisy	HR.Cat2
1963	8	09	Arlene	HRCat.1
1964	9	13	Ethel	HRCat.2
1966	8	31	faith	HRCat.2
1970	10	16	unnamed HR	HR
1973	7	03-04	Alice	HRCat.1
1975	9	26	Faye	HR
1977	9	27	Dorothy	HR

ANNEXE

Year	month	days	Name	Classif.
1981	9	02-03	Emily	HR
1981	9	08	Floyd	HR
1982	9	15	Debby	HR
1987	8	13	Arlene	TS
1987	9	25	Emily	HR
1989	8	06	Dean	HR
1991	10	27-29	Grace	HRCat.1
1995	8	14	Felix	HR
1996	10	20	Lili	HRCat.2
1997	10	08-09	Erika	HRCat.3
1998	9	02-03	Danielle	HR
1998	11	06	Mitch	HR
1999	9	21	Gert	HR
2000	9	16	Florence	HRCat.1
2001	9	09	Erin	HRCat.3
2001	10	11	Karen	TS
2001	11	07	Michelle	HR
2002	9	30	Kyle	HR
2003	4	18-21	Ana	SS
2003	9	05-06	Fabian	Majo rHRcat3
2003	9	26	Juan	HR
2004	10	09-10	Nicole	SS
2005	8	03-04	Harvey	TS
2005	9	08-09	Nate	HR
2005	10	25	Wilma	Major HR
2006	9	10-11	Florence	HRcat1
2007	11	02	Noel	HRcat1
2008	7	14	Bertha	TS
2008	7	15	Bertha	HR
2008	9	27-28	Kyle	TS
2009	8	21	Bill	HR
2010	8	05-08	Colin	TS
2010	9	01-04	Fiona	TS
2010	9	16-17	Igor	HRcat3
2010	9	18-19	Igor	HRcat2
2010	9	20	Igor	HRcat1
2010	10	29	Shary	HR
2011	8	14-15	Gert	TS
2011	8	28	Jose	TS
2011	9	08	Katia	HR
2011	9	13-15	Maria	TS
2011	9	30	Ophelia	HRCat.4

ANNEXE

Year	month	days	Name	Classif.
2011	11	08-11	Sean	SS
2012	6	17		Tdisturbance
2012	6	29	Debby	TS
2012	9	09	Leslie	HR
2012	10	16-17	Rafael	HR Cat1
2012	10	27-29	Sandy	HR
2013	9	10-11	Gabrielle	TS
2014	8	25-28	Cristobal	HR
2014	7	15-17	Edouard's	HR Cat3
2014	8	25-28	Cristobal	HR
2014	10	11-12	Fay	HR Cat1
2014	10	17-18	Gonzalo	HR Cat2-3

Table 4. Weather stations selected for the analysis of all the records used in this study. N (number of station in the work), Ind. (station code), St. Name (station name), Prov. (province: LP (Las Palmas) and TF (Sta. Cruz de Tenerife)), Acr. (Acronym used in the study), Elev. (station elevation in m), Loc. (location), geographical coordinates (Lat.N and Log.W: latitude North and longitude W respectively in sexagesimal format), Period, N.yr (number of years considered in the data analysis) and Obs. (type of observation: D (daily) or/and H (hourly)).

N	Ind.	St. name	Prov.	Acr.	Elev.(m)	Loc.	Lat.N	Long.W	Period	N.yr.	Obs.
1	C649I	G. Can. A.	LP	A1	24	E	27 55 21	15 23 22	1951-2012	62	D/H
2	C029O	Lanz. A.	LP	A2	14	SE	28 57 07	13 36 01	1972-2012	41	D/H
3	C249I	Fuert. A.	LP	A3	25	E	28 26 41	13 51 47	1969-2012	46	D/H
4	C447A	Ten. N. A.	TF	A4	632	NE	28 28 39	16 19 46	1960-2012	62	D/H
5	C429I	Ten. S. A.	TF	A5	64	S	28 02 51	16 33 39	1980-2012	33	D/H
6	C139E	La Palma A	TF	A6	33	E	28 37 59	17 45 18	1970-2012	43	D/H
7	C929I	El Hierro A.	TF	A7	32	NE	27 49 08	17 53 20	1973-2012	40	D/H
8	C689E	Masp.	LP	P1	6	SW	27 44 08	15 35 53	1997-2012	16	D
9	C656U	Teror Dom.	LP	P2	630	N	28 03 59	15 32 38	1963-2012	50	D
10	C662I	Valleseco R.	LP	P3	1400	N	28 01 44	15 36 12	1965-2012	48	D
11	C654Q	S. Mat. Lag.	LP	P4	1160	C	28 00 18	15 34 49	1965-2012	48	D
12	C626E	Mogán B A.	LP	P5	715	SW	27 53 35	15 40 45	1964-2012	49	D
13	C624E	Tejeda V.Ñ.	LP	P6	1040	C	27 55 55	15 40 30	1964-2010	47	D
14	C637A	S.B. Tir. P.	LP	P7	570	S	27 50 20	15 38 10	1965-2012	48	D
15	C625O	S.B.Tir.L.P.A.	LP	P8	806	S	27 51 24	15 38 41	1965-2012	48	D

ANNEXE

N	Ind.	St. name	Prov.	Acr.	Elev.(m)	Loc.	Lat.N	Long.W	Period	N.yr.	Obs.
16	C625A	Mogán Inag.	LP	P9	950	W	27 55 52	15 4415	1952-2010	59	D
17	C627A	S. Nic. T.T.	LP	P10	420	SW	27 55 12	15 45 47	1965-2009	45	D
18	C669A	Arucas Bañ.	LP	P11	50	N	28 08 47	15 32 01	1965-2012	48	D
19	C647O	Valseq. G.R.	LP	P12	540	C	27 59 30	15 29 38	1965-2012	48	D
20	C665L	Moya Font. C.	LP	P13	950	N	28 03 25	15 36 15	1965-2012	48	D
21	C659Q	L. Canteras	LP	P14	15	N	28 08 26	15 26 02	1965-2012	48	D
22		L. Alhorr.	LP	P15	1100	C	27 59 57	15 33 13	1924-2012	89	D
23	C649U	Telde - LL.	LP	P16	150	E	27 59 43	15 25 09	1965-2012	48	D
24	C449C	S.C. Ten.	TF	T1	35	NE	28 27 47	16 1519	1960-2012	62	D
25	C469A	S.J. Rambla	TF	T2	106	N	28 23 38	16 39 02	1948-2012	62	D
26	C129C	Tazac. M.T.	TF	T3	274	W	28 36 42	17 54 54	1984-2012	29	D
27	C457C	Tacoronte	TF	T4	564	NE	28 28 55	16 24 35	1945-2012	62	D
28	C430E	Izaña	TF	T5	2371	C	28 18 32	16 29 58	1933-2012	62	D
29	C419X	Adeje Cal. B	TF	T6	130	SW	28 04 53	16 42 39	1988-2011	23	D
30	C126A	El Paso C.F.	TF	T7	844	W	28 39 14	17 51 11	1986-2012	27	D
31	C117A	Puntagorda	TF	T8	684	NW	28 45 38	17 59 08	1986-2012	27	D
32	C329Z	S. S. Gomera	TF	T9	15	E	28 05 23	17 06 41	1995-2012	18	D
33	C317B	Agulo J.B.	TF	T10	765	NW	28 10 44	17 12 47	1986-2012	27	D
34	C315P	Valleher. Ch.	TF	T11	1242	W	28 06 38	17 15 47	1986-2012	27	D
35	C427E	S. M. Abona	TF	T12	642	S	28 05 48	16 36 57	1952-2012	61	D
36	C128B	Ll. Arid. B	TF	T13	410	W	28 39 32	17 54 37	1978-2012	35	D
37	C127U	Fuenc. Cal.	TF	T14	498	S	28 29 42	17 49 43	1946-2012	67	D
38	C939U	Sabinosa	TF	T15	299	W	27 44 51	18 05 45	1978-2012	35	D
39		Berm. A.		BER1	7	NE	32 21 50	64 40 01	1949-2011	63	D
40	505	Horta Obs.		Az.	45	SE	38 31 16	28 42 50	1970-2011	42	D
41	522	Funch. Obs.		M	58	S	32 38 51	16 5 333	1970-2011	42	D

Fig.11. Weather stations used for this studyd B) The Canary Islands (Lanzarote, Fuerteventura, Gran Canaria, Tenerife, La Palma, La Gomera and El Hierro).

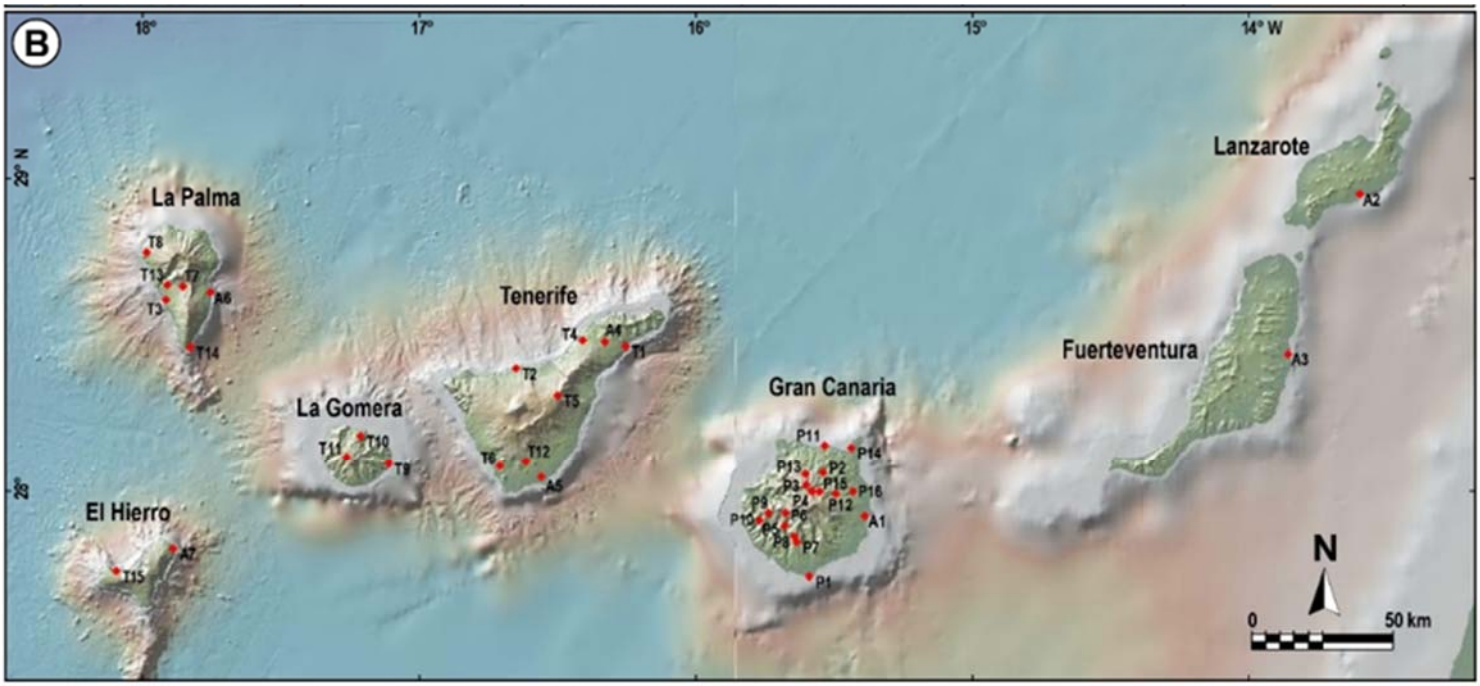

ANNEXE

List of Tables and Figures

Tables:

ANNEXE

Table 9. Acronyms for the weather stations used in the study (Acr.), fractal dimensions (D), station elevation in m (Elev.), location (Loc.) and percentage of the annual number of rainfall days (NRD yr^{-1} (%). Period 1969-2010. Daily rainfall data from automated and not automated stations. AEMET.

Table 10. Fractal dimensions (D), station elevation in m (Elev.), location (Loc.) and percentage of the annual number of rainfall days (NRD yr-1 (%). Period 1969-2010. Daily rainfall data from automated and not automated stations. AEMET.

Table 11. Acronyms for the selected weather stations, total accumulated daily rainfall (CUM) in mm, average rainfall (AVR) in mm, standard deviation (STD) in mm, daily maxima (MAX) in mmd^{-1}, number of rainfall days (NRD) in d, the rainfall rate (Rate) in mm and the total number of data (Ndata) for the whole period 1981-2010. Daily rainfall data from BWS, AEMET & IPMA whole period 1981-2010. Daily rainfall data from BWS, AEMET & IPMA.

Table12. Month, lower annual daily maxima rainfall (Max (mmd^{-1})), higher annual daily maxima rainfall, acronyms for the weather stations used in the analysis (Acr.), and station names (St. name). Period 1981-2010. Daily rainfall data from AEMET, BWS and IPMA.

Table 13. Records of maximum sustained wind speed (km/h) over Bermuda A. Mean Sea Level Pressure (MSLP) (hPa), wind direction (Wind. Dir.), wind speed (Wnd. Spd.), wind gust (Wnd. Gust) and type of tropical system. (Hurricane (HR). Period (1942-2011). Daily data BWS.

Table 14. Range (RNG), minimum (MIN), maximum (MAX), average (AVG), standard error (SE) and 95% confidence interval (CI) of total daily accumulated rainfall (CUM), ($mmyr^{-1}$), daily average rainfall (AVG) (mmd^{-1}) , daily maxima rainfall (MAX) (mmd^{-1}) and number of rain days (NRD) (dyr^{-1}). Bermuda A. Period 1949-2011. Daily rainfall data from BWS.

Table 15. Range (RNG), years with minimum (MIN) and maximum (MAX) values, average (AVG), standard deviation (SD) and 95% confidence interval (CI) for the total cumulative daily rainfall in $mmyr^{-1}$ (CUM), daily maxima rainfall in mmd^{-1} (MAX) and number of rainfall days in dyr^{-1} (NRD). Bermuda (BER1), M (Funch. Obs.), Az (Horta Obs.), CAN (Canaries average values of the 15 stations), A2 (Lanzarote A.), A7 (El Hierro A.), T1 (S. C.Ten.) and P14 (L.Canteras). Period 1981-2011. Daily data from BWS, AEMET and IPMA.

Table 16. Acronym (Acron.), Station name (St. name), h (value related to the test decision for the null hypothesis that the data comes from a normal distribution), the scalar value *p-value* and the non-negative scalar value *kstat*.for Bermuda A.(BER1), M (Funch. Obs.), Az (Horta Obs.), A2 (Lanzarote A.), A7 (El Hierro A.), T1(S. C.Ten.) and P14 (L.Canteras). Period 1981-2011. Daily data from BWS, AEMET and IPMA.

Table 17. Seasonality Index (SI), long-term mean value of the seasonality index ($\overline{SI}$) and index of rainfall replicability *(RI)* according to Walsh & Lawler (1981) for the whole study period 1981-2010 and normal sub-periods for Bermuda A. (BER1). Daily rainfall data from BWS.

ANNEXE

Table 18. Global average and long-term mean seasonality indexes, and replicability index for the whole study period (1949-2011) and normal sub-periods for El Hierro A. (A7), (b) S.C. Ten (T1), (c) L. Canteras (P14), (d) Lanz. A. (A2), (e) Horta Obs. (Az), and (f) Funch. Obs. (M). Daily rainfall data from AEMET and IPMA.

Table 19. Seasonality Index (SI), long-term mean value of the seasonality index ($\overline{SI}$) and index of rainfall replicability *(RI)* according to Walsh & Lawler (1981) for the whole study period 1981-2010 and normal sub-periods for El Hierro A. (A7), S.C. Ten (T1), L. Canteras (P14), Lanz. A. (A2), Funch. Obs. (M) and Horta Obs. (Az.). Daily rainfall data from AEMET and IPMA.

Table 20. St. name (station name), Acr. (acronyms), and Chi^2 value for Bermuda A.(BER1), M (Funch. Obs.), Az (Horta Obs.), A2 (Lanzarote A.), A7 (El Hierro A.), T1(S. C.Ten.) and P14 (L.Canteras). Period 1981-2011. Daily data from BWS, AEMET and IPMA.

Table 21. Percentages corresponding to each class rainfall regime in terms of the values of the SI_y (Seasonality Index (SI) for a given year) according to Walsh & Lawler (1981) : very equable (VE), rather seasonal with a short drier season (SSD), equable but with a definite wetter season (EW), seasonal (S), markedly seasonal with a long drier season (MLD), most rain in 3 months or less (3MR), extreme, almost all rain in 1-2 months (E) or short wet season (SW), the determination coefficients (R^2), of the SI_y versus the total annual rainfall , the years with minimum and maximum (MIN/MAX) interquartile values and the interquartile range (RNG) for El Hierro A. (A7), (b) S.C. Ten (T1), (c) L. Canteras (P14), (d) Lanz. A. (A2), (e) Horta Obs. (Az), and (f) Funch. Obs. (M). Period 1981-2010. Daily rainfall data from BWS, AEMET and IPMA.

Table 22. Monthly annual rainfall rate (annual rainfall totals per number of rain days (NRD) in mmd^{-1}) for El Hierro A. (A7), (b) S.C. Ten (T1), (c) L. Canteras (P14), (d) Lanz. A. (A2), (e) Horta Obs. (Az), and (f) Funch. Obs. (M). Period 1981-2010. Daily rainfall data from BWS, AEMET and IPMA.

Table 23. Records of maximum daily rainfall over Bermuda. Period 1949-2011 for BERM1 and 1974-2011 for SOM (BWS).

Table 24. Records of maximum daily rainfall over Bermuda associated with a tropical storm (TS Bertha). Period 1949-2011 for BER1 and 1974-2011 for SOM (BWS).

Table 25. Thresholds for adverse phenomena in case of rainfall accumulated in 12h (in mm) in the Autonomous Community of the Canary Islands. Provinces of Las Palmas (LP) and Tenerife (TF).Watch. (Watching) and Warn. (Warning) Level 1 and 2. AEMET 2015.

Table 26. Daily rainfall maxima affecting the Canary Islands (rainfall >360 mm/24h). Rainfall episode, main rainfall day, maximum daily rainfall (mmd^{-1}), Indicative of the weather station (Ind.), Station Name (St.Name) and Elevation (Elev. (m)). Period 1957-2010. AEMET. Period 1988-2012. AEMET.

Table 27. Daily rainfall maxima affecting the Canary Islands (rainfall between 240 and 360 mm/24h). Date, maximum daily rainfall (mmd^{-1}), (Max. rainfall), Elevation (Elev. (m)), Indicative of the weather station (Ind.), Station Name (St.Name) and associated

weather phenomenon in the area. (Phen.). TS (Thundersorm), SN (Snow), Hz (Haze). Period 1957-2010. AEMET.

Table 28. Acronyms for the selected weather stations, wavelets spectrum slope |β|, confidence interval (C.I.) determination coefficient of linear regression R^2 , p-value and error variance (δ^2) for Bermuda (BER1), M (Funch. Obs.), Az (Horta Obs.), CAN (Canaries average values of the 15 stations), A2 (Lanzarote A.), A7 (El Hierro A.), T1 (S. C.Ten.) and P14 (L.Canteras). Period 1981-2011. Daily data from BWS, AEMET and IPMA.

Table 29. Coefficient of Pearson (r) for NRD (Number of annual rainy days) and annual rate rainfall versus NAO for different intervals of time frequencies (from D1 to D4) and the smooth curve (S) in Bermuda A. Period 1949-2011. Daily data from BWS.

Table 30. Wavelets spectrum slopes (β), determination coefficients (R2), error variance (δ^2), p-values (p-val) and d (LM parameters) for NAO index and monthly rainfall. Bermuda A. Period 1949-2011. Daily data for BWS.

Table 31. Acronyms for the selected weather stations, St. Name (station name), Elev. (station elevation in m), Loc. (location), Kolmogorov (KV) and Permutation Entropy (PE) coefficients, for Bermuda (BER1), Funch. Obs. (M), Horta Obs. (Az.) and 18 weather stations within the Canary Islands from lower to greater values. Period 1981-2011. Daily data from BWS, AEMET and IPMA.

Figures:

Fig.1. Location of the subtropical area.

(https://upload.wikimedia.org/wikipedia/commons/b/b0/World_map_indicating_tropics_and_subtropics.png).

Fig.2. Bermuda topographic map. Inset indicates geographic location of the archipelago in the North Atlantic Ocean (Eric Gaba-Wikipedia Commons) *(http://mapsof.net/map/bermuda-topographic-map).*

Fig.3. Sea level pressure (mb) Dec-Jan-Feb composite mean for the winters in the recent climate (1981-2010) representing typical winter synoptic situation over Bermuda (NCEP (National Center for Environmental Prediction) /NCAR (National Center for Atmospheric Research) reanalysis).

Fig.4. Location of the warm and cold currents in the North Atlantic Ocean. *(https://www.britannica.com/place/Gulf-Stream/images-videos).*

Fig.5. Location of the Azores, Madeira and Canary archipelagos (Morton, B., et. al., 1998).

Fig.6. Layout of the archipelago of The Canary Islands (AEMET & IP 2012).

ANNEXE

Fig.7. Seasonal migration of the Inter-Tropical Convergence Zone (ITCZ).

(http://www.geography.hunter.cuny.edu/~tbw/wc.notes/15.climates.veg/climate/A/seasonal.migration.ITCZ.jpg).

Fig.8. Typical synoptic pattern in the Canary Islands and Bermuda during the summer. 06 July 2011. Surface Analysis (BWS).

Fig.9. Track of the extra tropical depression Delta (27th -29th November 2005) (Best Track NHC).

Fig.10. Layout of the archipelago of the Madeira and Azores Islands. (AEMET & IP 2012).

Fig.11. Weather stations used for this study. A) North Atlantic Ocean (Bermuda, Madeira, Azores and the Canary Islands) and B) The Canary Islands (Lanzarote, Fuerteventura, Gran Canaria, Tenerife, La Palma, La Gomera and El Hierro). (This figure can be found in a larger size in the Annexe I).

Fig.12. Weather stations on Bermuda used for this study: .B1 (Naval Air Station), B2 (Bermuda Airport), B3 (Somerset Village), B4 (Dept. of Agriculture and Fisheries).

Fig.13. Topographic map and geographic location of measurement stations in Gran Canaria.

Fig.14. Distribution of the rainfall Time series in La Palma (LPa), La Gomera (G) , El Hierro (EH), Tenerife (Ten), Gran Canaria (GC) Lanzarote (Lz) and Fuerteventura (Fv) through the number of years. (a) Rainfall data coverage for the period 1951-2012. Light blue for 0 to less than 30 years and dark blue for 30 or more years. (b) Rainfall data coverage for the period 1981-2010. Light blue for 0 to less than 30 years and dark blue for 30 years. (c) The percentage of the number of station according to its quality. Daily data from AEMET.

Fig.15. Representation of the permutations for m = 3 and its frequencies in a signal (Riedl et al. (2013).

Fig. 16. Seasonal distribution of rainfall at Bermuda A. (a) Daily rainfall average for each day of the year in mmd^{-1} (AVG) (b) maximum daily rainfall for each day of the year (MAX) in mmd^{-1} (c), number of rainfall days (NRD) (%) and (d) daily rainfall accumulation (CUM) (%) at Bermuda A. (red dots) and Somerset V. (blue dots). Period 1981-2010. Daily data from BWS.

Fig.17. Histogram of the number of dry days between successive rainfall events. Inset figure the semi-log plot of the frequency with fitted straight. Bermuda A. Period 1949-2011. Daily data from BWS.

Fig.18. Histogram of time intervals (in days) between rain events for G. Canaria A. and log–log representation with fitted straight line (inset figure). Period 1989-2010. Hourly data (METARs) from AEMET.

Fig.19. Log–log plot with fitted straight line of the frequency of dry periods versus the number of consecutive dry days between rain events when values of daily rainfall are

greater than or equal to 0.1 mmd^{-1} (circles), greater than 1 mmd^{-1} (red crosses) and greater than 5 mmd^{-1} (red dots) the frequency of dry periods versus the number of days for S.C. Ten. (T1), Ten. S. (A5), Bermuda A. (BER1) and Horta Obs. (Az.). Period 1989-2010. Daily data from AEMET, BWS and IMPA.

Fig.20. Histogram of daily rainfall intensity or daily accumulated rainfall (mmd^{-1}) and log-log representation with fitted straight (inset figure).Bermuda A. Period 1949-2011. Daily data from BWS.

Fig.21. Box-counting log–log plots and slopes, D, for the rainfall (asterisks) and dust event (dots) data series at Gran Canaria airport. The non-overlapping segments of a characteristic size, s, (1/2h) in which the time interval is divided versus the number N(s) of intervals of length s (1/2 hour) occupied by the rain or dust events. Data from METARs for the period 1989–2010.AEMET.

Fig.22. Spatial variability of rainfall fractal dimension over Canaries. Daily data from AEMET.

Fig.23. Seasonal and inter-annual variability of rainfall in Bermuda (a) Daily rainfall corresponding to a certain day of a given year and its intensity given by a colour indicated in a colour-bar in mmd^{-1} .(b) Inter-annual variability of accumulated rainfall (anomaly) (c) Seasonal variability of rainfall accumulated (anomaly) and 31 days- running mean in red line. Bermuda A. Period 1949-2011. Daily data from BWS.

Fig.24. Seasonal variability of daily rainfall corresponding to a certain day of a given year and its intensity given by a colour indicated in a colour-bar in mmd^{-1}, in El Hierro A. (A6), S.C. Ten (T1), L. Canteras (P14), Lanz.A.(A2), Berm. A. (BER1), Horta Obs. (Az) and Funch. Obs. (M). Period 1981-2010. Daily data from AEMET, BWS and IPMA.

Fig.25 .Monthly average of daily rainfall variability in mmd^{-1} (red line) with the 99% confidence intervals (dash blue lines) and the expected total rainfall in mm considering uniform rainfall through the year (green line). Bermuda A. Period 1949-2011. Daily data from BWS.

Fig.26. Monthly average of daily rainfall variability in mmd^{-1} comparing data from 1973 (red line) and data from 2006 (blue line). Bermuda A. Period 1949-2011. Daily data from BWS.

Fig.27 .Monthly average of daily rainfall variability in mmd^{-1} (red line) with the 99% confidence intervals (dash blue lines) and the expected total rainfall in mm considering uniform rainfall through the year (green line). a) El Hierro A. (A7), (b) S.C. Ten (T1), (c) L. Canteras (P14), (d) Lanz. A. (A2), (e) Horta Obs. (Az), and (f) Funch. Obs. (M). Period 1981-2010. Daily data from AEMET and IPMA.

Fig.28. Comparison of the seasonal distribution of rainfall in the Canary Islands (Las Canteras (blue), S. C. Ten. (red), El Hierro A. (green) and Fuer. A. (yellow) on the left side with Berm. A. (red), Horta Obs. (Az.) (blue) and Funch. Obs. (M) (green) on the right side. (a /b) Daily rainfall average for each day of the year in mmd^{-1} (AVG); (c/d) maximum daily rainfall for each day of the year in mmd^{-1}(MAX); (e/f) number of rainfall days (NRD) (%) and (g/h) daily rainfall accumulation (%) (CUM). Period 1981-2010. Daily data from AEMET, BWS and IPMA.

ANNEXE

Fig.29. In left side, seasonal variability of rainfall daily average (mm) and 31 days-running mean in red line. In right side, seasonal variability of number of rain days (anomaly) and 31 days- running mean in red line. Bermuda (BER1), Horta Obs. (Az), Funch. Obs. (M), El Hierro A. (A6), S.C. Ten (T1), L. Canteras (P14) and Lanz. A. (A2). Period 1981-2010. Daily data from AEMET, BWS and IPMA.

Fig.30. Wind roses representing seasonal wind direction (Wnd. Dir.) and wind speed (Wnd. Sp.) during a) winter b) spring c) summer and d) autumn. Bermuda A. Period 1942-2011. Hourly data from BWS.

Fig.31. Wind roses representing wind direction (Wnd. Dir.) and wind speed (Wnd. Sp.) when a) frontal rain (RA) and b) convective rain (TS) .Bermuda A., Period. 1942-2011. Hourly data from BWS.

Fig.32. Wind roses representing wind direction (Wnd. Dir.) and wind speed (Wnd. Sp.) when a) frontal rain (RA) and b) convective rain (TS). Lanz. A., G.Can. A. and La Palma A. Period. 1998-2014. Hourly data from AEMET.

Fig.33. Wind roses representing wind direction (Wnd. Dir.) and wind speed (Wnd. Sp.) when a) frontal rain (RA) and b) convective rain (TS). Horta airport and Funchal airport. Period. 2003-2014. Hourly data from IPMA.

Fig.34. Interannual daily rainfall variability. (a) Annual accumulated rainfall (mm yr^{-1}), (b) NRD (number of rainfall days) per year. (c) Maxima daily rainfall in mmd^{-1}. (d) Rainfall rate (annual accumulated rainfall / NRD) in mmd^{-1}.Bermuda A. Period 1949-2011. Daily data from BWS.

Fig.35. Associated empirical probability density function in terms of relative frequency of annual total rainfall ($mmyr^{-1}$). Bermuda A. Period 1949-2011. Daily data from BWS.

Fig.36. NRD (Number of Rain Days) anomaly per year (red bars) and tendency (solid line) vs. the annual rainfall rate (annual rainfall totals per number of rain days in mmd^{-1}) anomaly (blue bars) and tendency (dotted line). Bermuda A. Period 1949-2011. Daily data from BWS.

Fig.37. Accumulation rainfall in annual, bi-annual, five-year period and ten-year period (decadal). Bermuda A. Period 1949-2011. Daily data from BWS.

Fig.38. In the left side Inter-annual variability of annual accumulated rainfall ($mmyr^{-1}$).I n the right side Inter-annual variability of number of rain days (NRD)(dyr^{-1}). Bermuda (BER1), Horta Obs. (Az), Funch. Obs. (M), El Hierro A. (A7), S.C. Ten (T1), L. Canteras (P14) and Lanz. A. (A2).Period 1981-2010. Daily data from AEMET, BWS and IPMA.

Fig.39. Associated empirical probability density function in terms of relative frequency of annual total rainfall ($mmyr^{-1}$) for Bermuda (Berm. A.) Azores (Horta Obs.), Madeira (Funch. Obs.) and Canaries (El Hierro A., S. C. Ten., L.Canteras and Lanzarote A.) Period 1949-2011. Daily data from BWS, AEMET and IPMA.

Fig.40. Five-year period acccumulation rainfall (mm). Bermuda (BER1), Horta Obs. (Az), Funch. Obs. (M), El Hierro A. (A7), S.C. Ten (T1), L. Canteras (P14) and Lanz. A. (A2). Period 1949-2011. Daily data from BWS, AEMET and IPMA.

ANNEXE

Fig.41. Ranking of months within any year in terms of accumulated rainfall. Lighter (darker) tones correspond to drier (wetter) months. Colour bar legend. Bermuda A. Period 1949-2011. Daily data from BWS.

Fig.42 a) Variability of the annual SI_y (dots). The median value (solid line) as well as first and third quartiles (dashed lines) are indicated. Interquartile distance is depicted as a shadow area. b) Scatter diagram of SI_y versus total annual rainfall ($mmyr^{-1}$), along with best fitted line and 95% confidence intervals. Bermuda A. Period 1949-2011. Daily data from BWS.

Fig.43. Ranking of months within any year in terms of daily accumulated rainfall. Lighter (darker) tones correspond to drier (wetter) months. Colour bar legend. a) El Hierro A. (A7), (b) S.C. Ten (T1), (c) L. Canteras (P14), (d) Lanz. A. (A2), (e) Horta Obs. (Az), and (f) Funch. Obs. (M). Period 1981-2010. Daily data from AEMET and IPMA.

Fig.44. Variability of the annual SI_y (dots) (upper panels). The median value (solid line) as well as first and third quartiles (dashed lines) are indicated. Interquartile distance is depicted as a shadow area. Scatter diagram of SI_y versus total annual rainfall ($mmyr^{-1}$), along with best fitted line and 95% confidence intervals) (bottom panels). a) El Hierro A. (A7), (b) S.C. Ten (T1), (c) L. Canteras (P14), (d) Lanz. A. (A2), (e) Horta Obs. (Az), and (f) Funch. Obs. (M). Period 1981-2010. Daily data from AEMET and IPMA.

Fig.45. Satellite image (GOES-8) June 1st 1996.

(http://www.ncdc.noaa.gov/gibbs/html/GOE-8/VS/1996-06-01-15).

Fig.46. Temperature and geopotential in 500 hPa. 24th February 1988 at 12 UTC Analysis from ECMWF.

Fig.47. Cut-off low affecting the Canary Islands. Geopotential Height (Z) in m and Temperature in ºC at 500 hPa. ECMWF (08/01/99 at 00 UTC (AEMET).

Fig.48. Cut-off low affecting the Canary Islands. (Water Vapour channel image) METEOSAT (07/01/99 AT12 UTC) (AEMET).

Fig.49. Wavevet decomposition (DWT) corresponding to the anomaly monthly accumulated rainfall. Bermuda A. Period 1949-2011.BWS.

Fig.50. (a) Daily rate rainfall, (b) scalogram, (c) CWT power spectrum of the time series, and (d) instantaneous power contribution of wavelet coefficients in three period (frequency) bands: around 5 years (solid line), 3 years (dashed line) and 1 year (dotted line) (d). Bermuda A. Period 1949-2011. BWS.

Fig.51. NAO Index anomalies (blue bars) and tendency (solid line) vs. NRD (number of rainy days) anomalies (red bars) and tendency (dotted line) during winter time (DJFM).Bermuda A. Period 1949-2011. Daily data from BWS.

Fig.52. Discrete wavelet transform (DWT) corresponding to the variability of NRD anomalies (doted lines) compared with NAO anomalies (solid line) during winter time (DJFM). Bermuda A. Period 1949-2011. Daily data from BWS.

Fig.53. a) Cross Wavelet Power (CWP) of NAO and annual rate rainfall b) CWP of NAO and NRD (number of rainy days) during winter time (DJFM). Bermuda A. Period 1949-2011. Daily data from BWS.

Fig.54. Discrete wavelet variance applied to monthly rainfall (circles) compared with NAO index (dots) Bermuda A. Period 1949-2011. Daily data from BWS.

Fig.55. Principal components analysis based on the the scale parameters used for the analysis of the duration of consecutive dry events between rainfall events together with the Kolmogorov (KV) and Permutation Entropy (PE) coefficients. Period 1981-2011. Daily data from BWS, AEMET and IPMA.

ACRONYMS:

A1: Gran Canaria airport

A2: Lanzarote airport

A3: Fuerteventura airport

A4: Tenerife North airport

A5: Tenerife South airport

A6: La Palma airport

A7: El Hierro airport

A&F (D. Agric. & Fish.): Department of Agriculture and Fisheries

AEJ: African Easterly Jet

AEMET: Agencia Estatal de Meteorología

AERONET: Aerosol Robotic NETwork

AEW:African Easterly Waves

AO: Artic Oscillation

AOD: Aerosol Column Optical Depth

AVG: Daily rainfall average

Az: Azores

ANNEXE

BA: Bermuda A.:Bermuda Airport,

BAS: Bermuda Aviation Services

BER1: Time series 1. Bermuda airport

BER2: Time series 3

BLDU: blowing dust

BWS: Bermuda Weather Service

Cat: Category

CMT: Carlsberg Meridian Telescope

CREPAD: Centro de Recepción, Proceso, Archivo y Distribución de Datos de Observación de la Tierra

CUM: daily rainfall accumulation

CWP: Cross Wavelet Power

CWT: Continuous Wavelet Transform

D: Fractal Dimension

DRDU: drifting dust raised by wind at or near the station at the time of

DS: dust storm

DU: widespread dust in suspension in the air

DWT: Discrete Wavelet Transform

DZ: drizzle

E: extreme, almost all rain in 1-2 months

ECMWF: European Centre for Medium-Range Weather Forecasts

EH: El Hierro

ENSO: El Niño Southern Oscillation

EP: Earth Probe

ERA 40: ECMWF re-analysis

ESRL:Earth System Research Laboratory

EW: equable but with a definite wetter season

FEMA: Federal Emergency Management Agency

Fv: Fuerteventura

G: La Gomera

GC: Gran Canaria

HIRLAM: High Resolution Limited Area Modelling

HR: hurricane

HZ: haze

ICAO: International Civil Aviation Organization

IDL: Interactive Data Language

IMP: Instituto Meteorológico de Portugal

INTA: Instituto Nacional de Técnica Aeroespacial

INM: Instituto Nacional de Meteorología

IPMA: Instituto Portugues do Mar e Atmosfera

ITCZ: Intertropical Convergence Zone

ITF: Intertropical Front

J-B: Jarque-Bera

KC: Kolmogorov complexity

L: Lillie tests

LM: Long Memory

LRD: Long Range Dependence

LPa: La Palma

LP: Las Palmas

Lz: Lanzarote

LZC: Lempel-Ziv

M: Madeira

MARS: Meteorological Archival and Retrieval System

MATLAB: MATrix LABoratory

MAX: maximum daily rainfall

METARs: METeorological Aerodrome Reports

MK: Mann-Kendall

MLD: markedly seasonal with a long drier season

MML: maritime mixing layer

MODIS: Moderate-Resolution Imaging Spectroradiometer

3MR: most rain in 3 months or less

MSG: Meteosat Second Generation

MSLP: Mean Sea-Level Pressures

NAS: Naval Air St.: Naval Air Station

NASA**:** National Aeronautics and Space Administration

NAO: North Atlantic Oscillation

NCAR: National Center for Atmospheric Research

NCEP: National Center for Environmental Prediction

NDD: number of dry days

NHC: National Hurricane Centre

NNSMP: National Nonpoint Source Monitoring Programme

NOAA: National Oceanic and Atmospheric Administration

NRD: Number of Rainy Days

NSF: National Science Foundation

N7: Nimbus-7

OAI: Izaña Atmospheric Observatory

OMI: Ozone Monitoring Instrument

OMTO3: OMI total column ozone

OPTICON: Optical Infrared Coordination Network for Astronomy

ORM: Roque de Los Muchachos Observatory

ANNEXE

OT: Teide Observatory

P1: Maspalomas

P2: Teror-Dominicas

P3: Valleseco-La Retamilla

P4: San Mateo-Las Lagunetas

P5: Mogán- Barranquillo Andrés

P6: Tejeda-Vivero de Ñameritas

P7: San Bartolomé de Tirajana-Palomas

P8: San Bartolomé de Tirajana-Lomo Pedro Alfonso

P9: Mogán (Inagua)

P10: San Nicolás de Tolentino-Tasarte

P11: Arucas (Bañaderos

P12: Valsequillo-Granja Las Rosas

P13: Moya-Fontanales Cisterna

P14: Las Palmas de G.C.-Las Canteras

P15: Lomo Alhorradero

P16: Telde Los Llanos

PCI: Precipitation Concentration Index

PE: Permutation Entropy

P.L.: Power Law

PM: Post Meridian

Q: quartil

RA: rain

Rep.: replicability

RI :replicability index

RMSE: root mean square error

S: seasonal

SAL: Saharan Air Layer

SCI: Seasonality Concentration Index

SeaWIFS: Sea-viewing Wide Field-of-view Sensor

SHRA: shower

SI: Seasonality Index

$\overline{SI}$: average index of seasonality

SOC: Self-Organized Criticality

SOI: Southern Oscillation Index

SOM: SV: Somerset V.: Somerset Village

SSD: rather seasonal with a short drier season

SST: Surface Sea Temperature

SW:short wet season

T1: Santa Cruz de Tenerife

T2: San Juan de La Rambla

T3: Tazacorte-Mña Todoque

T4: Tacoronte

T5: Izaña

T6: Adeje-Caldera B

T7: El Paso C.F.

T8: Puntagorda

T9: San Sebastián de La Gomera

T10: Agulo-Juego Bolas

T11: Vallerhermoso-Chipude

T12: San Miguel de Abona

T13: Llanos de Aridane

T14: Fuencaliente-Caletas

TF: Sta. Cruz de Tenerife

TS: thunderstorm

Terra: Earth Observing System Anti Meridian (AM)

TL: troposphere layer

TOMS: Total Ozone Mapping Spectrometer

TWC: transformadas wavelet continua

TWD: transformadas wavelet discreta

UTC: Coordinated Universal Time

UV: ultraviolet

VE: very equable

Wnd. Spd: wind speed

Wnd. Gust: wind gust

WMA: Wavelet Multi-resolution Analysis

WMO: World Meteorological Organization

WT: Wavelet transform

Z: Geopotential Height